

**The Production of Fluid Fuels
From Biomass**

Ryan E. Katofsky

PU/CEES Report No. 279

June 1993

Submitted in partial fulfillment of the requirements for the degree
of Master of Science in Engineering from Princeton University, 1993.

*Center for Energy and Environmental Studies
The Engineering Quadrangle
Princeton University
Princeton, New Jersey 08544*

Financial support for this research was provided by the Air and Energy Engineering Laboratory of the US Environmental Protection Agency, the Energy Foundation, the W. Alton Jones Foundation, the Geraldine R. Dodge Foundation, the John Merck Fund, and the Mobil Oil Company.



THE PRODUCTION OF FLUID FUELS FROM BIOMASS

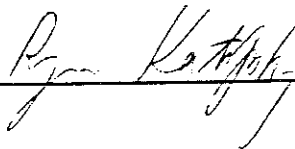
by

Ryan E. Katofsky

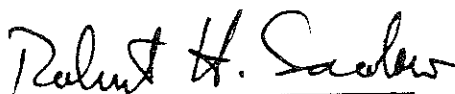
Princeton University
School of Engineering and Applied Science
Department of Mechanical and Aerospace Engineering
Center for Energy and Environmental Studies

Submitted in partial fulfillment of the requirements for the degree
of Master of Science in Engineering from Princeton University, 1993


Prepared by:



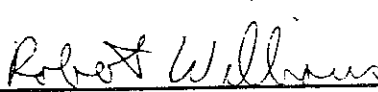
Approved by:



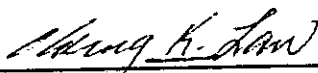
Professor Robert Socolow
Thesis Advisor



Dr. Eric Larson
Co-Advisor



Dr. Robert Williams
Co-Advisor



Professor C.K. Law
Thesis Reader

June 1993

© Copyright by Ryan Ezra Katofsky, 1993. All rights reserved.

Abstract

This thesis assesses the technology and economics of methanol and hydrogen production from biomass for use in fuel cell electric vehicles (FCEVs). Urban air pollution and net carbon dioxide (CO₂) emissions resulting from the use of gasoline powered internal combustion engine vehicles (ICEVs) could be sharply reduced because FCEVs would emit virtually no pollutants and because biomass is a renewable resource. Using FCEVs, US dependence on imported oil could be reduced by more than 50%, because enough biomass could be grown domestically to fuel the entire US light duty vehicle fleet.

Methanol and hydrogen can be produced from biomass, coal and natural gas. Biomass offers the greatest environmental benefits. This thesis is perhaps the most comprehensive assessment of all three feedstocks within a consistent analytical framework, and utilizes advanced chemical-process simulation software and pinch analysis techniques. In all cases, methanol and hydrogen production starts with syngas generation, followed by chemical synthesis. Natural gas processes are commercially available. Coal and biomass are not, but could be commercialized quickly. Based on the technologies studied here, the achievable efficiencies of producing methanol from biomass, coal and natural gas are 63%, 62% and 72% respectively (higher heating value basis). Hydrogen production would be more efficient, with achievable efficiencies of 69%, 63% and 85% respectively.

Using advanced, low cost biomass gasification technologies, the unit production costs of methanol and hydrogen from biomass would be comparable to the costs from coal, even though coal would cost significantly less than biomass and coal facilities would

be much larger than biomass facilities. Due to lower capital costs and higher efficiencies, methanol and hydrogen production from natural gas would be less costly at today's prices. However, if present projections of increased natural gas prices materialize, coal and biomass would become economical early in the next century. Quantifying environmental externalities would further favor the use of biomass.

Due to the high efficiencies of FCEVs, the levelized costs (\$ per km) of driving FCEVs that use methanol or hydrogen derived from biomass would be lower than the costs of driving comparable gasoline ICEVs, even though the delivered costs of these renewable fuels would be up to 50% higher than today's cost of gasoline.

Acknowledgements

There are many people to thank who have been helpful throughout the various stages of my research.

First of all, I am grateful for having been given the opportunity to tackle such an important and timely issue. I have learned a great deal during the course of my research, and I hope that I have made a valuable contribution. I will look back fondly at the time I spent at the Center for Energy and Environmental Studies.

I thoroughly enjoyed working with and learning from Dr. Eric Larson, who was my direct supervisor throughout my research. The thoughtful and careful reviews of my work by Dr. Robert Williams resulted in a much improved thesis. Professor Robert Socolow's insight was very helpful in defining the scope and direction of my research. His critical review of the first draft of this thesis was also very helpful, in addition to his later comments. Many thanks go to Professor C.K. Law, my Thesis Reader, for his valuable comments.

I would also like to thank Dr. Joan Ogden for her comments on an early draft. Graduate student Mike Luyben from the Chemical Engineering Department deserves thanks for helping me with chemical process simulation software early on in my research.

Outside of Princeton University, I received the help and advice of many professionals, including Mark Paisley from Battelle Columbus Laboratory, Dr. Durai-Swamy from Manufacturing and Technology Conversion International, Dr. James Kuo from Mobil Research & Development, Dr. Richard Bain from the National Renewable Energy Laboratory, and the technical support people at Aspen Technology. Mr. Paisley was also kind enough to review the final draft of my thesis, for which I am especially grateful.

Finally, I would like to thank the following people for the following things, which made my time in Princeton a time to remember. The people: Greg Terzian, Chris Marrison, Vicky Kaspi, Peter Ozsvath, and Ruth Smolash. The things (in no particular order): Good home cookin', good conversation, friendship, love, good wine, evenings at the D-bar, and trips to Quaker Bridge Mall.

This thesis carries the identification 1973-T in the records of the Department of Mechanical and Aerospace Engineering.



Table of Contents

Abstract	iii
Glossary	xiv
List of Symbols	xvii
Chapter 1: Introduction	1
1.1 Introduction	1
1.2 The Challenges Facing the US Transportation Sector	2
1.3 The Motivations for Producing Transportation Fuels from Biomass ...	5
1.4 Additional Benefits of Biomass Energy Use	11
1.5 Scope of this Study	12
Figures	16
References	17
Chapter 2: Literature Review	19
2.1 Introduction	19
2.2 Reasons Why Biomass Energy has not Been Considered Seriously to Date	19
2.3 Previous Assessments of Methanol and Hydrogen Production	26
2.4 Conclusions	32
References	33
Chapter 3: Biomass Gasification	35
3.1 Introduction	35
3.2 Physical and Chemical Properties of Biomass	35
3.3 Fundamentals of Biomass Conversion	39
3.4 Gasifier Types	59
3.5 Summary	78
Figures	80
References	97
Appendix 3A: Equilibrium Modeling of Entrained-Bed Biomass Gasification	102
Chapter 4: Gas Processing Technology: Fundamental and Practical Considerations	110
4.1 Introduction	110
4.2 Basic Process Configurations for Producing Fluid Fuels from Biomass	110
4.3 Some General Considerations for Chemical Reactors	113
4.4 Gas Cleanup Technologies	117
4.5 Methane Reforming	121
4.6 The Water-Gas Shift Reaction	133

4.7 Methanol Synthesis	135
4.8 Acid Gas Removal	142
4.9 Hydrogen Separation and Purification Technologies	143
Figures	149
References	168
Chapter 5: Modeling Methanol and Hydrogen Production	172
5.1 Introduction	172
5.2 General Thermodynamic Considerations	172
5.3 Heat Integration Using Pinch Analysis	177
5.4 Gasifier Performance Estimation	186
5.5 Chemical Process Simulation	187
5.6 Modeling Unit Operations	189
Figures	196
References	201
Chapter 6: The Technology of Methanol and Hydrogen Production	203
6.1 Introduction	203
6.2 Defining the Framework for Evaluating Thermodynamic Performance	204
6.3 Natural Gas Processes	212
6.4 Summary of Results for Biomass and Coal Gasification	220
6.5 Prospects for Technological Improvements	234
6.6 Conclusions	236
Figures	238
References	243
Appendix 6A: Process Configurations, Stream Summaries and Pinch Analyses for Chapter 6	245
Chapter 7: The Economics of Methanol and Hydrogen Production	284
7.1 Introduction	284
7.2 Feedstock Costs	285
7.3 Baseline Production Cost Estimates	290
7.4 Hydrogen and Methanol Use in the Transportation Sector	300
7.5 A Scenario for Using Biomass Derived Fuels	308
7.6 Policy Implication	309
7.7 Summary	311
Figures	313
References	318
Chapter 8: Conclusions	321
8.1 General Conclusions	321
8.2 Summary of Specific Results	324
8.3 Suggestions for Future Work	327

List of Figures

Figure 1-1: Normalized pollutant emissions from all mobile sources in the United States.	16
Figure 3-1: The chemical structures of cellulose (top) and three different types of hemicellulose, two of the main components of biomass	80
Figure 3-2: The chemical structure of lignin, a main component of wood	81
Figure 3-3: Comparison of coal and cellulose pyrolysis	82
Figure 3-4: Comparison of the reactivity of coal and biomass chars.	82
Figure 3-5: Simplified schematic representation of biomass gasification.	83
Figure 3-6: Schematic representations of cellulose and lignin pyrolysis	84
Figure 3-7: Schematic representations of directly heated gasifiers.	85
Figure 3-8: Effect of oxygen consumption on synthesis gas production and temperature for oxygen blown biomass gasification, assuming chemical equilibrium.	86
Figure 3-9: Effect of steam rate on synthesis gas production and temperature for oxygen blown biomass gasification, assuming chemical equilibrium.	87
Figure 3-10: Effect of temperature on synthesis gas production for biomass gasification, assuming chemical equilibrium and a fixed C:H:O ratio.	88
Figure 3-11: Effect of pressure on synthesis gas production and temperature for oxygen blown biomass gasification, assuming chemical equilibrium and a fixed level of oxygen consumption.	89
Figure 3-12: The Lurgi fixed-bed coal gasifier	90
Figure 3-13: The Institute of Gas Technology RENUGAS™ fluidized-bed oxygen-blown biomass gasifier	91
Figure 3-14: Current status of directly heated fluidized-bed biomass gasifiers	92
Figure 3-15: Schematic representations of the various heat transfer methods of indirectly heated gasifiers.	93
Figure 3-16: Schematic representation of the Battelle-Columbus Laboratory (BCL) indirectly heated gasifier	94

Figure 3-17: Schematic representation of the Manufacturing and Technology Conversion International (MTCI) pulse-enhanced indirectly heated gasifier	95
Figure 3-18: Schematic representation of the Wright-Malta (WM) indirectly heated gasifier	96
Figure 4-1: Block diagram of the process configurations for the production of methanol or hydrogen from biomass	149
Figure 4-2: Chemical equilibrium modeling showing the conditions necessary for carbon formation at a pressure of 1 MPa, for mixtures containing H ₂ , CO, CO ₂ , CH ₄ , H ₂ O and C _(s) at different C:H:O ratios.	150
Figure 4-3: Chemical equilibrium composition as a function of temperature for the water-gas shift reaction.	151
Figure 4-4: Methanol synthesis reaction rate as a function of temperature for the Imperial Chemical Industries (ICI) catalyst	152
Figure 4-5: Chemical equilibrium composition as a function of temperature for steam reforming of the BCL product gas.	153
Figure 4-6: Chemical equilibrium concentrations of ethane and ethylene in the reformer product gas using the product gas of the BCL gasifier as the feed	154
Figure 4-7: Chemical equilibrium composition as a function of pressure for steam reforming of the product gas from the BCL gasifier	155
Figure 4-8: Chemical equilibrium composition as a function of steam:hydrocarbon ratio for steam reforming of the BCL synthesis gas	156
Figure 4-9: Schematic representation of a steam reformer	157
Figure 4-10: Schematic representation of a catalytic autothermal reformer	158
Figure 4-11: The effect of the steam:hydrocarbon ratio on the equilibrium composition of the gas produced via catalytic autothermal reforming using the product gas of the IGT gasifier as the feed	159
Figure 4-12: The effect of temperature on the equilibrium composition of the gas produced via catalytic autothermal reforming using the IGT gasifier	160

Figure 4-13: A comparison of syngas production for conventional steam reforming and catalytic autothermal reforming using the product gas of the IGT gasifier as the feed.	161
Figure 4-14: Equilibrium concentrations as a function of temperature for the shift reaction using the reformed gas from the BCL gasifier	162
Figure 4-15: Single pass equilibrium concentrations as a function of temperature for methanol synthesis using the BCL makeup gas	163
Figure 4-16: Schematic representation of a methanol synthesis loop based on the ICI low-pressure methanol synthesis technology.	164
Figure 4-17: Schematic representation of the Imperial Chemical Industries (ICI) methanol synthesis reactor	165
Figure 4-18: Schematic representation of the Lurgi methanol synthesis reactor	166
Figure 4-19: Schematic representation of the pressure swing adsorption loop used for hydrogen purification	167
Figure 5-1: Data for three <i>hot</i> streams and the construction of the corresponding hot Composite Curve	196
Figure 5-2: Hot and cold composite curves for a hypothetical process	197
Figure 5-3: Illustration of the need to shift source and target temperatures when constructing the Problem Table.	198
Figure 5-4: Composite curves (top) and the Grand Composite Curve (bottom) for the example problem of Table 5-3.	199
Figure 5-5: Efficiency of producing electricity using combined cycles, STIGs and ISTIGs with natural gas, biomass and coal	200
Figure 6-1: Overall exergy balances for methanol and hydrogen production from natural gas.	238
Figure 6-2: Overall exergy balances for methanol and hydrogen production from biomass using the BCL and IGT gasifiers.	239
Figure 6-3: Overall exergy balances for methanol and hydrogen production from coal using the Shell entrained-bed gasifier.	240
Figure 6-4: Overall thermodynamic performance for all methanol production simulations.	241

Figure 6-5: Overall thermodynamic performance for all hydrogen production simulations.	242
Figure 7-1: Levelized costs of production for methanol and hydrogen from natural gas, coal, and biomass.	313
Figure 7-2: Comparison of different cost estimates for methanol production from natural gas, coal and biomass	314
Figure 7-3: Comparison of different cost estimates for hydrogen production from natural gas, coal and biomass	315
Figure 7-4: Effect of feedstock price on the total cost of production for methanol from biomass, coal, and natural gas.	316
Figure 7-5: Effect of feedstock price on the total cost of production for hydrogen from biomass, coal, and natural gas.	317

List of Tables

Table 1-1: Percentage change in emissions from alternative feedstock/fuel/vehicle combinations for light duty vehicles, relative to the gasoline powered ICEV	8
Table 1-2: Estimate of the biomass needed to fuel the entire US light duty vehicle fleet in the years 1990, 2010, and 2030, using hydrogen or methanol powered fuel cell vehicles.	10
Table 2-1: One estimate of the potential land suitable for the establishment of biomass plantations	21
Table 3-1: Compositional data and heating values for selected types of biomass, coal and natural gas	37
Table 3-2: Sample composition of liquids produced by the IGT Renugas™ gasifier	45
Table 3-3: Basic characteristics of the different types of biomass gasifiers evaluated in this thesis.	48
Table 3-4: Comparison of oxygen blown entrained-bed gasification of coal and biomass based on the Shell gasifier	55
Table 3-5: Operating characteristics of the gasifiers evaluated in this thesis	67
Table 4-1: Relative solubilities of different gases in the SELEXOL® solvent	143
Table 5-1: Chemical equilibrium approach temperatures used in this study.	175
Table 5-2: Pressure drops used in the computer simulations.	176
Table 5-3: Sample stream data and Problem Table for a hypothetical process.	185
Table 5-4: Aeroderivative gas turbine data used to estimate the efficiency of producing electricity from natural gas, coal and biomass	195
Table 6-1: Mass and energy balances for methanol production from natural gas.	214
Table 6-2: Mass and energy balances for the modeling of hydrogen production from natural gas	217
Table 6-3: Exergy balances for methanol and hydrogen production from natural gas.	220

Table 6-4: Material and energy balance summary for all methanol production simulations.	222
Table 6-5: Material and energy balance summary for all hydrogen production simulations.	223
Table 6-6: Exergy balances for methanol production from biomass and coal using the BCL, IGT and Shell gasifiers	224
Table 6-7: Exergy balances for hydrogen production from biomass and coal using the BCL, IGT and Shell gasifiers	225
Table 7-1 Levelized costs of production for plantation biomass grown in the United States and Brazil, and current and projected fossil fuel prices . . .	290
Table 7-2: Estimated production costs for methanol from natural gas, coal and biomass	292
Table 7-3: Estimated production costs for hydrogen from natural gas, coal and biomass	293
Table 7-4: Comparison of cost estimates for methanol and hydrogen production by thermochemical processes from natural gas, coal and biomass, and by water electrolysis using electricity from renewable sources	299
Table 7-5: Comparison of cost estimates for methanol and hydrogen production showing the fossil fuels prices and time frame required for biomass to be cost competitive.	304
Table 7-6: Characteristics of alternative light duty vehicles.	305
Table 7-7: Comparison of lifecycle costs (cents per km) for alternative vehicle/feedstock/fuel combinations. Fuel prices exclude taxes.	307
Table 8-1: Summary of thermodynamic and economic results.	328

Glossary

Beneficiation: The preprocessing of biomass (drying and sizing) to make it more suitable for thermochemical conversion.

BIG/GT: Biomass Integrated Gasification/Gas Turbine technology. Advanced power generation technology based on the coupling of biomass gasification to aeroderivative gas turbines.

BPEV: Battery Powered Electric Vehicle.

Cellulose: The main chemical component of most biomass. Cellulose is a high molecular weight carbohydrate polymer. Cellulose has the same chemical structure in all biomass.

Carbon Utilization: For methanol production, the carbon in the methanol divided by the carbon in the feedstock (natural gas, biomass or coal).

Char: The solid carbon produced during gasification.

Chemical Kinetics: The study of the mechanisms of chemical reactions, including the effects of variables such as temperature and pressure.

Cold Gas Efficiency: A measure of the efficiency of a gasifier, defined as the higher (lower) heating value of the product gas divided by the higher (lower) heating value of the feedstock.

Degree of Perfection: The exergy in the product fuel divided by the exergy of all inputs to the system. Also called the **Exergy Efficiency**.

Electrolyzer: A device that uses electricity to split water into molecular hydrogen and oxygen.

Endothermic: A chemical reaction that absorbs heat is said to be endothermic.

Energy Ratio: The heating value of the product fuel divided by the heating value of the gasifier feed or natural gas feed.

Exajoule (EJ): 10^{18} joules. 1 Quad (10^{15} Btu) = 1.055 EJ.

Exergy: A thermodynamic variable that measures the maximum useful work that can be extracted from a substance. Also called **Availability**.

Exothermic: A chemical reaction that releases heat is said to be exothermic.

FCEV: Fuel Cell Electric Vehicle.

Fuel Cell: An electrochemical device used to convert the chemical energy of a fuel (e.g. H₂) directly into electricity. One particular type of fuel cell that is the leading candidate for automotive applications is the **Polymer Electrolyte Membrane (PEM)** fuel cell.

Gasification: The thermochemical conversion of a solid carbonaceous material such as coal or biomass into a gaseous mixture, the primary combustible components of which are carbon monoxide, hydrogen, and methane.

Gigajoule (GJ): 10⁹ joules.

Hemicellulose: Long chain polymers similar to cellulose, but consisting of different monosaccharide building blocks. Hemicelluloses differ from one type of biomass to the next.

Higher Heating Value (HHV): A measure of the energy content of a fuel when the product water from combustion is in the liquid state.

Hot Gas Efficiency: Similar to the cold gas efficiency, except that the sensible heat of the product gas is also included in the energy output of the gasifier.

ICEV: Internal Combustion Engine Vehicle.

IGCC: Integrated Gasification Combined Cycle. The integration of coal gasification with a gas turbine combined cycle to produce electricity.

ISTIG: Intercooled Steam Injected Gas Turbine.

Lignin: A complex amorphous high molecular weight polyaromatic compound found in biomass. Unlike cellulose or hemicellulose, lignin has no unique chemical structure.

Lower Heating Value (LHV): A measure of the energy content of a fuel when the product water from combustion is in the vapor state.

Megajoule (MJ): 10⁶ joules.

Makeup Gas: The fresh feed gas to a methanol synthesis reactor.

Methanation: The exothermic reaction between hydrogen gas and carbon monoxide to form methane and water vapor ($\text{CO} + 3\text{H}_2 \leftrightarrow \text{CH}_4 + \text{H}_2\text{O}$). Methanation is the reverse reaction of methane reforming.

MMBPD: Millions of Barrels Per Day.

Neat Alcohol Fuels: 100% pure alcohol fuels.

Normal Cubic Meter (Nm³): A standard measure of volume evaluated at 273.15 Kelvin and 101,325 Pascals.

Pressure Swing Adsorption (PSA): The process of separating different gases from one another based primarily on molecular size, using porous materials (e.g. hydrogen purification).

Pyrolysis: The thermal decomposition of biomass, coal, or other carbonaceous materials into gases, char (solid carbon) and heavy tars and oils. Also called **devolatilization**.

Reformat: The product gas of a reformer.

Reforming: The endothermic reaction between methane or other light hydrocarbons and water vapor to produce hydrogen gas and carbon monoxide (e.g. $\text{CH}_4 + \text{H}_2\text{O} \leftrightarrow \text{CO} + 3\text{H}_2$).

Standard Cubic Foot (SCF): A standard measure of volume evaluated at 60°F and 14.697 psi.

STIG: Steam Injected Gas Turbine.

Synthesis Gas: A gas consisting mainly of CO and H₂, produced either by the gasification of a solid feedstock or by reforming natural gas or other hydrocarbons.

Thermal Efficiency: The heating value of the product fuel divided by the heating value of all energy inputs to the system.

Volatile Matter: The components of biomass, coal or other carbonaceous materials that are converted to gases and tars and oils during pyrolysis.

Volatile Organic Compounds (VOCs): Organic compounds emitted in automobile exhaust and during automobile refueling that react photochemically in sunlight to produce ozone (smog). VOCs are also called **Non-Methane Organic Compounds (NMOCs)**.

Zero Emission Vehicle (ZEV): An automobile that emits no atmospheric pollutants such as VOCs or CO (e.g. an electric car). A vehicle that would emit carbon dioxide and/or water vapor but nothing else might also qualify as a ZEV.



List of Symbols

- $b_{ch,i}$ the specific chemical exergy of species i in a gaseous mixture
- b_{ch}^o the standard chemical exergy of a substance
- B the flow availability function ($H - T_oS$)
- B_{ch} the chemical exergy of a stream
- B_i the exergy of a stream at state i
- B_{tm} the thermomechanical exergy of a stream
- B_{total} the total exergy of a stream
- C_p the specific heat capacity of a stream (e.g. kJ/kmol-K)
- CP the heat capacity flowrate of a stream (e.g. kW/kmol-K)
- ΔB the change in exergy of a stream from state i to state j
- Δh^o the change in specific enthalpy of a chemical reaction when measured at T_o and P_o
- ΔH the total change in enthalpy of a stream
- ΔT_{app} the approach temperature to chemical equilibrium
- ΔT_{min} the minimum temperature difference between two streams
- E_{elec} the amount of net external electricity required by a process
- E_{feed} the higher heating value of the feedstock (natural gas, coal, or biomass)
- E_{fuel} the higher heating value of the fuel produced (methanol or hydrogen)
- E_{heat} the amount of net external heating required by a process
- ER The Energy Ratio (E_{fuel}/E_{feed})
- h_f^o the standard heat of formation of a chemical compound
- H_c the enthalpy of combustion of a fuel
- H_i the enthalpy of a stream in state i

- H_o the enthalpy of a stream at the standard conditions, T_o and P_o
 H_p, h_p the enthalpy of the products of a chemical reaction
 H_r, h_r the enthalpy of the reactants of a chemical reaction
 \dot{m} the mass flow rate of a stream
 N_i the molar flow rate of species i in a mixture
 P_o the pressure of the standard reference state (101,325 Pascals)
 Q the heat added or removed from a stream
 $Q_{c,min}$ the minimum external cooling required by a process (the *cold utility*)
 $Q_{h,min}$ the minimum external heating required by a process (the *hot utility*)
 \mathbb{R} the Universal gas constant (8,314 J/kmol-K)
 S_i the entropy of a stream in state i
 S_o the entropy of a stream at the standard conditions, T_o and P_o
 T_o the temperature of the standard reference state (273.15 Kelvin)
 T_s the source (initial) temperature of a stream being heated or cooled
 T_t the target (final) temperature of a stream being heated or cooled
 y_k the mole fraction of species k in a gaseous mixture
 y_{ok} the mole fraction of species k in the reference environment

 η_{carbon} the overall carbon conversion in methanol production
 η_{elec} the efficiency of electricity generation
 η_{exergy} the overall exergy efficiency of a process (also called the *Degree of Perfection*)
 η_{heat} the efficiency of producing process heat
 η_{th} the overall thermal efficiency of a process

Chapter 1: Introduction

1.1 Introduction

As the 21st century approaches, there is growing interest in low polluting alternative and renewable energy sources. Although the recent conflict in the Persian Gulf has reminded us that energy security remains an important issue, of even greater concern today are the environmental impacts of fossil fuel use. According to the International Panel on Climate Change, which was assembled as part of the United Nations Environment Program, the worldwide demand for energy is expected to multiply three- to six-fold by the year 2050 (IPCC, 1991). As a result, many people are concerned that our current energy consumption patterns are not sustainable. Urban air pollution, acid rain, oil spills, the threat of global warming, and the other environmental consequences of continued fossil fuel use compel us to reduce our dependence on these non-renewable resources.

Because the US transportation sector relies almost exclusively on crude oil, much of which comes from the politically volatile Middle East, it is particularly vulnerable to energy supply disruptions. Automobiles are also a principal source of air pollution. Therefore, although the automobile has played a major role in the prosperity and quality of life in the United States and elsewhere, the transportation sector may have to undergo significant changes over the next several decades in order to alleviate the problems associated with the gasoline powered internal combustion engine vehicle (ICEV).

One option with great potential would be to use biomass (organic matter) as a clean, renewable feedstock for producing alternative transportation fuels (methanol and hydrogen) which could be used to power the next generation of high-efficiency, low polluting automobiles. These vehicles would use fuel cells to produce electricity, which would power electric drive trains, instead of internal combustion engines, which power

mechanical drive trains. This thesis examines the technology and economics of methanol and hydrogen production from biomass for use in fuel cell electric vehicles (FCEVs).

1.2 The Challenges Facing the US Transportation Sector

There are four major challenges facing the US transportation sector today, all of which stem from the reliance on gasoline and other fuels produced from crude oil.

1.2.1 Urban Air Pollution

Motor vehicles are the leading contributors to urban air pollution. In 1985, motor vehicles in the United States accounted for 45% of nitrogen oxide (NO_x) emissions and 34% of volatile organic compound (VOC)¹ emissions. Some VOC compounds are toxic (e.g. benzene), but more importantly they react photochemically in the presence of sunlight to produce ozone (smog), which has adverse effects on human health and can damage crops and forests (Ogden and Williams, 1989). In 1987, 130 million Americans lived in areas where ozone levels exceeded federal standards (Ogden and Williams, 1989). NO_x also contributes to smog formation and is a precursor to some forms of acid deposition, which has had severe ecological consequences in certain regions. Even though automobile emissions standards have stiffened considerably over the past several decades, the increased number of vehicle miles travelled, and less stringent controls on other types of vehicles, have led to only moderate reductions in the levels of these and other pollutants (see Figure 1-1). According the US Department of Energy's (DOE) 1991 *National Energy Strategy (NES)*, only modest reductions in NO_x and VOCs can be expected between now and the year 2030 (DOE, 1991). This implies that fundamental

¹ VOCs are also called NMOCs for non-methane organic compounds.

changes to the US transportation sector may be necessary to achieve significant improvements in urban air quality.²

1.2.2 Global Warming

The threat of global warming may dictate the use of fuel cycles with low greenhouse gas emissions (mainly carbon dioxide -- CO₂). According to the US Environmental Protection Agency (EPA), CO₂ emissions may need to be reduced by as much as 50-80% worldwide in order to stabilize its concentration in the atmosphere over the long term (Lashof and Tirpak, 1990). Direct fuel use accounts for approximately 75% of all CO₂ emissions worldwide, of which more than 50% comes from oil, almost all of which is used in the transportation sector (Johansson, et al., 1992). This means that oil use alone accounts for roughly 40% of all energy related CO₂ emissions, more than double the emissions from all coal fired power plants worldwide. Therefore, switching to fuel/vehicle cycles with low or zero CO₂ emissions is perhaps the most effective way to combat the buildup of greenhouse gases.

1.2.3 US Reliance on Oil Imports

The United States is becoming increasingly reliant on Middle East oil, a trend that will continue if petroleum continues to be the primary feedstock for transportation fuels, which will almost certainly be the case if gasoline remains the primary automotive fuel. There are two reasons why imported oil will become a larger fraction of total oil consumption with this *business as usual* approach. First, oil consumption in the transportation sector

² In some regions of the United States, air pollution is such a severe problem that legislation is being used to accelerate the introduction of alternative vehicles. In California, the Air Resources Board has mandated that 2% of all cars sold in that state in 1998 to be *zero-emission vehicles* (ZEVs). By 2003, 10% of all cars sold in California (several hundred thousand cars per year) will have to be ZEVs. Several states in the US northeast have also voted to adopt the California standard, and other countries are considering similar measures (Ogden and Nitsch, 1992).

will increase significantly in the future because improvements in fuel economy will not be able to keep pace with the increase in total vehicle miles travelled (DOE, 1991). Second, US crude oil production is expected to decline substantially over the next forty years. In the *Current Policy* scenario of the NES, oil imports are projected to increase from 7.3 million barrels per day (MMBPD) in 1990 to 20.3 MMBPD by the year 2030, 80% of total oil consumption in that year. In this same period, domestic production is projected to fall from 8.8 MMBPD in 1990 to 3.2 MMBPD in 2030. Even under the *Strategy Scenario* of the NES, which assumes greater use of high-efficiency technologies and alternative energy sources, domestic oil production is projected to rise slightly in the near term, but fall to 4.3 MMBPD by 2030. In the same period, imports are predicted to rise to 11.6 MMBPD by 2030, 65% of total consumption in that year.

1.2.4 The High Cost of Alternative Fuels

In light of the three issues described above, one would think that there would be significant interest in clean burning fuels produced from domestic resources. Unfortunately, alternative fuels have never been able to compete with gasoline because such fuels have been, and will almost certainly continue to be, more expensive than gasoline produced from crude oil at today's prices (~\$20/barrel). Furthermore, it is very possible that crude oil will remain in the \$20-25 per barrel range³ for several decades (Johansson, et al., 1992a), so that it will continue to be the most economic feedstock for ICEVs. Given the fact there are no technical barriers to producing synthetic fuels from coal, biomass or natural gas, this is perhaps the single largest obstacle facing alternative fuels today.

³ Unless otherwise noted, costs are given in constant 1991 US dollars throughout this thesis.

1.3 The Motivations for Producing Transportation Fuels from Biomass

It is the goal of this thesis to show that methanol and hydrogen derived from biomass can play significant roles in addressing each of the above challenges, in spite of the constraints inherent in the use of biomass energy. The ability to produce energy from biomass on a large scale is limited by several factors, including the low efficiency of photosynthesis,⁴ large water requirements, and the availability of suitable land. Nevertheless, these constraints are manageable when combined with high-efficiency conversion and end-use strategies, so that biofuels can play a major role in meeting the future energy needs of the US transportation sector. This is in sharp contrast to the way in which biomass energy has traditionally been used: in inefficient, low technology applications. By far, the principle use of biomass energy today is for cooking and heating in rural areas of developing countries (Hall, et al., 1992). Where biomass energy is used commercially to produce electricity (mainly in the United States), it is almost always in low efficiency steam-Rankine cycles, a technology that was commercialized about 100 years ago, and has changed little since the early 1960s (Williams and Larson, 1992). Fuel ethanol is produced in the US from the fermentation of corn, but it requires substantial government subsidies to be cost competitive (Johansson, et al., 1992). There are no commercial facilities producing methanol or hydrogen from biomass.

In spite of the prevailing view that biomass is a low efficiency, expensive feedstock that is only appropriate for use at small scales, recent research and development efforts are showing that biomass can become a highly competitive, large scale energy source for both fuels and electricity. Electricity from biomass has received the most

⁴ Photosynthesis only captures about 1/2-1% of the solar energy that reaches the plant. By comparison, modern, field tested photovoltaic (PV) modules (large arrays of solar cells) have achieved stabilized efficiencies of 10-12%. Prototype modules have achieved efficiencies of up to 18%, and the theoretical limit for individual cells is as high as 33% (Kelly, 1992).

attention because it appears that biomass-based systems using advanced aeroderivative gas turbines will be able to produce electricity at costs comparable to existing coal or natural gas systems (Williams and Larson, 1992). On the other hand, hydrogen and methanol derived from biomass will almost certainly be more expensive than gasoline derived from crude oil costing \$20-25/bbl. Therefore, if biomass is to become an economical energy source for transportation fuels, it will be necessary to employ efficient end-use devices that cannot be used with gasoline but that can be used with fuels derived from biomass. FCEVs are just such a technology. The remainder of this section describes how biomass and biofuels, coupled with fuel cell vehicles, could be used to meet all four challenges facing the US transportation sector.

1.3.1 Urban Air Pollution

Although ICEV emissions could be reduced by replacing gasoline with methanol or hydrogen, a much larger benefit would come from using methanol and hydrogen in FCEVs. Interest in FCEVs is motivated by their very high efficiency and extremely low emissions characteristics, and a number of demonstration vehicles are currently under development (Huff, 1991; Ogden and DeLuchi, 1992). A fuel cell is similar to a battery in that the chemical energy of the fuel is converted directly to electricity, which can then be used to power a vehicle.⁵ Thus, a FCEV is similar to a battery powered electric vehicle (BPEV). An important distinction is that a BPEV requires several hours to recharge whereas a FCEV would be refueled in a few minutes. Although they would consume fuel, FCEVs based on proton exchange membrane (PEM) fuel cells would

⁵ Most low temperature fuel cells use hydrogen directly. In the case of the methanol powered FCEV, methanol would be *reformed* and *shifted* on board the vehicle to produce H₂ and CO₂ via the following overall reaction: CH₃OH + H₂O → CO₂ + 3H₂. The steam would be produced in the fuel cell and some methanol would be burned to drive the endothermic reforming reaction. While this system is more complex and less efficient than using hydrogen directly, methanol can be stored much more easily and cheaply on-board vehicles than hydrogen.

produce no NO_x because of their low temperature operation, and virtually no VOC emissions because of the types of fuels they would use (hydrogen and methanol).⁶ In fact, hydrogen FCEVs would qualify as *zero emission vehicles* (ZEVs) because their only emission would be water. There would be minor pollutant emissions associated with methanol FCEVs, but these would only be a small fraction of gasoline ICEV emissions. Table 1-1 compares estimated exhaust emissions for several types of alternative vehicles, and also shows that if the fuels for FCEVs were to be produced from a renewable resource such as biomass, greenhouse gas emissions would decrease substantially. In the biomass options presented in Table 1-1, greenhouse gases emissions are not zero, in part because it was assumed that the electricity for hydrogen compression prior to refueling would be provided by the projected average mix of power sources in the US in the year 2000, which includes fossil fuel-fired power plants. Also, estimates of greenhouse gas emissions associated with growing, harvesting, and processing the biomass were included.

1.3.2 Global Warming

If biomass is grown and used sustainably to produce methanol and hydrogen, it will contribute little or no net CO_2 to the atmosphere, because on average, any CO_2 released is reabsorbed by the growing plants through photosynthesis. Biomass would help reduce greenhouse gas emissions to the extent that it could replace existing fossil fuel use (Hall, Mynick and Williams, 1991).

⁶ The PEM fuel cell is a promising technology for fuel cell vehicles because of its low operating temperature (25-120°C), high power density, and low volume requirement (1.33 kW/kg and 1.20 kW/liter, compared to 0.12 kW/kg and 0.16 kW/liter for the commercially available phosphoric acid fuel cell) (Johansson, et al., 1992).

Table 1-1: Percentage change in emissions from alternative feedstock/fuel/vehicle combinations for light duty vehicles, relative to the gasoline powered ICEV. Adapted from DeLuchi (1992) and Williams (1993) (NG = natural gas).

Feedstock/Fuel/Vehicle	NMOC ^a	CO	NO _x	SO _x	PM ^b	Greenhouse gases ^c
NG/Methanol/ICEV	-50	0	0	-100 ^d	lower	-3
Solar/Hydrogen/ICEV	-95 ^e	-99 ^e	f	-100 ^d	lower	-88 ^j
NG/Hydrogen/FCEV	-100	-100	-100	-100 ^d	-100	-67
Biomass/Methanol/FCEV	-90 ^g	-99 ^h	-99 ^h	-100 ^d	-100	-93 ⁱ
Biomass/Hydrogen/FCEV	-100	-100	-100	-100 ^d	-100	-89 ^j
Solar/Hydrogen/FCEV	-100	-100	-100	-100 ^d	-100	-95 ^j
All solar/Hydrogen/FCEV	-100	-100	-100	-100	-100	-100
US power mix/BPEV ^k	-95	-99	-56	+321	+153	-44
All Solar/BPEV	-100	-100	-100	-100 ^d	-100	-100
Baseline emissions for a Gasoline ICEV (g/km) ^l	0.48	3.81	0.28	0.03	0.01	305.3

- (a) NMOC = non-methane organic compounds.
- (b) PM = particulate matter.
- (c) Measured in grams of carbon per km. Non-CO₂ gases have been converted to an equivalent amount of CO₂ according to the global warming potential factors of the Intergovernmental Panel on Climate Change (IPCC).
- (d) Assuming no sulphur is present in the fuel, which would be the case for hydrogen and methanol.
- (e) Emissions are not completely reduced since some oil is burned in the engine.
- (f) While lean combustion of hydrogen could greatly reduce the amount of NO_x produced, the precise quantity is not yet known. Nevertheless, it is well established that gaseous fuels that contain hydrogen produce significantly less NO_x when burned than fuels that do not contain hydrogen.
- (g) Some NMOCs would evaporate during distribution and refueling.
- (h) There would be minor emissions associated with the on-board reforming of methanol.
- (i) There would be some greenhouse gas emissions from the energy used for growing, harvesting and transporting biomass.
- (j) The electricity for H₂ compression was assumed to come from the projected national mix of power sources in the year 2000.
- (k) The *US power mix* is the projected mix of power sources in the year 2000.
- (l) Based on a year 2000 Ford Taurus operating on reformulated gasoline and conforming to the standards of the 1990 Clean Air Act in the year 2000. The fuel economy is assumed to be 25.9 miles per gallon (9.08 liters/100 km).

1.3.3 US Reliance on Oil Imports

Clearly, hydrogen and methanol produced from biomass grown in the United States would reduce dependence on Middle East oil. The question is, can enough biomass be grown in the US to displace a significant amount of imported oil? Consider the following numerical example:

Assumptions:

- Higher heating value (HHV) of gasoline = 34.5 MJ/liter.
- HHV of biomass = 20 GJ/dry tonne (see Ch. 3) (GJ = gigajoule = 10^9 joules).
- Energy plantations produce an average of 15 dry tonnes/hectare/year.
- Biomass is converted to hydrogen at an overall HHV efficiency of 68% (see Ch. 6).
- Biomass is converted to methanol at an overall HHV efficiency of 63% (see Ch. 6).
- Hydrogen powered FCEVs using PEM fuel cells achieve the gasoline-equivalent of 3.24 liters/100 km (Williams, 1993).
- Methanol powered FCEVs using PEM fuel cells and on-board reforming achieve the gasoline-equivalent of 3.81 liters/100 km (Williams, 1993).

Based on these assumptions, the hydrogen FCEV would require 111.8 MJ/100 km, and the methanol FCEV would require 131.4 MJ/100 km. Table 1-2 summarizes the biomass requirements for each case, assuming the entire US light duty vehicle (LDV) fleet is converted to FCEVs. Estimates have been made using the NES projections for total LDV miles travelled for the years 1990, 2010, and 2030 (DOE, 1991). Table 1-2 shows that it would be possible to fuel the entire LDV fleet with biofuels using 50-70% of the projected excess cropland in the United States. The oil displaced represents a significant fraction of imports. Under the *Current Policy* scenario, 9.3 MMBPD is equal to 46% of projected imports in the year 2030, and in the *Strategy Scenario*, 6.4 MMBPD is 55% of projected oil imports in 2030. Therefore, although total biomass resources are

somewhat limited, targeting biomass energy specifically for the transportation sector can have a significant impact on oil imports, and hence, the strategic vulnerability of the United States to oil supply disruptions or monopoly pricing. Methanol and hydrogen imported from other regions such as Latin America or sub-Saharan Africa would increase the diversity of the US fuel supply, and therefore help protect the US from future energy supply disruptions or price instability (Johansson, et al., 1992).

Table 1-2: Estimate of the biomass needed to fuel the entire US light duty vehicle fleet in the years 1990, 2010, and 2030, using hydrogen or methanol powered fuel cell vehicles.

Year	VMT ^a (10 ⁹ km)	Hydrogen Powered FCEVs		Methanol Powered FCEVs		Idle Cropland in the US ^c (10 ⁶ Hectares)	Oil Displaced ^d (10 ⁶ bbl/day)	
		EJ ^b Hydrogen	10 ⁶ Hectares	EJ ^b Methanol	10 ⁶ Hectares		Current Policy	Strategy Scenario
1990	2834	3.17	15.5	3.72	19.7	33	6.1	6.1
2010	4508	5.04	24.7	5.92	31.3	---	8.6	7.5
2030	5331	5.96	29.2	7.00	37.0	52	9.3	6.4

(a) VMT = vehicle miles travelled. From DOE (1991).

(b) 1 EJ = 1 exajoule = 10¹⁸ joules.

(c) US Department of Agriculture (1990).

(d) Assuming gasoline is produced from crude oil at 90% overall thermal efficiency, crude oil has a higher heating value of 6.13 GJ/barrel (38.6 MJ/liter), gasoline has a higher heating value of 34.5 MJ/liter, and that the gasoline powered light duty vehicle fleet has the following fuel economies: *Current Policy* -- 12.62 liters/100 km in 1990, 11.09 l/100 km in 2010, and 10.18 l/100 km in 2030; *Strategy Scenario* -- 12.62 liters/100 km in 1990, 9.75 l/100 km in 2010, and 7.04 l/100 km in 2030. Fuel economies are based on NES projections (DOE, 1991).

1.3.4 The High Cost of Alternative Fuels

Due to the uncertainties inherent in medium- to long-term energy price projections, this thesis attempts to be as conservative as possible. Retail prices for methanol and hydrogen derived from biomass are anticipated to be significantly higher than the retail cost of gasoline. As well the purchase price of a FCEV will likely be several thousand dollars higher than the price of a comparable ICEV. Nevertheless, these higher costs will be offset by the fact that FCEVs will be 2.4-2.8 times more efficient than comparable

gasoline ICEVs (DeLuchi, et al., 1991; DeLuchi, 1992). Furthermore, because electric vehicles are mechanically simpler than ICEVs, FCEVs are expected to last longer and have lower maintenance costs than ICEVs. As a result, when measured on a lifecycle cost basis (\$ per km), biofuel powered FCEVs will probably be cost competitive with gasoline powered ICEVs, even if crude oil prices are lower in the future than they are today (Ogden and DeLuchi, 1992; Johansson, et al., 1992a) (see also Chapter 7).

1.4 Additional Benefits of Biomass Energy Use

Biomass appears to have certain advantages over other forms of renewable energy, despite the low efficiency of photosynthesis, the large amounts of water needed for growing biomass, and the careful planning that will be required to produce biomass sustainably for long periods of time. Biomass provides a natural "built-in" means of storing solar energy, unlike wind, solar thermal and solar photovoltaic (PV) energy sources, which are intermittent. Also, since biomass contains carbon, it is perhaps the only renewable feedstock that can be used to produce methanol or other hydrocarbons.⁷ Overall, biomass appears to be the least expensive renewable resource for producing hydrogen and methanol (Takahashi, 1989; Larson and Katofsky, 1992).

In North America and other industrialized regions, tens of millions of hectares of idle cropland could be used to grow biomass energy crops. At present, US farmers are paid tens of billions of dollars each year to keep farmland out of production, in order to

⁷ PV and wind electricity could be used to produce hydrogen via the electrolysis of water, a well established technology. If a ready supply of carbon dioxide were available, it is also conceivable that methanol could be manufactured from PV or wind power alone. Another possibility would be to use PV or wind energy to produce hydrogen to augment the production of methanol from biomass, since biomass systems are typically hydrogen deficient and must therefore reject excess carbon as CO₂.

keep food prices high or to prevent erosion.⁸ Using this land to grow energy crops could save taxpayers billions of dollars each year in farm subsidies by providing farmers with additional income. In developing countries, biomass plantations could help reclaim deforested and otherwise degraded land.⁹ A labor intensive biomass-based energy industry could also play an important role in rural development in developing countries, and thus help curtail poverty and urban migration (Hall, et al., 1992).

Finally, since biomass conversion facilities will be relatively capital intensive, the energy industries that wish to exploit this resource will need a secure supply of biomass throughout the lifetimes of these facilities -- 20 years or more. In principle, this should encourage the use of biomass that can be grown sustainably, rather than increase deforestation (Johansson, et al., 1992).

1.5 Scope of this Study

In this thesis, I assess the technology and economics of producing methanol and hydrogen from biomass via thermochemical gasification, for use in fuel cell vehicles. Over the last 10-15 years there have been numerous feasibility studies on the production of methanol from biomass, but none has focussed on this particular end-use technology, mainly because interest in FCEVs is a recent development. For this reason, there has been almost no interest in hydrogen production from biomass, because previously the goal was

⁸ In the United States in 1990, 33 million hectares of cropland were kept idle, and as a result of continued productivity gains, this number is expected to climb to 52 million hectares by the year 2030, even though the US Department of Agriculture expects exports of maize, wheat and soybeans to double during this period (US Department of Agriculture, 1990).

⁹ It has been estimated that nearly 760 million hectares of degraded lands are suitable for reforestation in developing countries (Hall, et al., 1992). If all this land were used to grow energy crops, it would have been able to supply approximately 70% of the world's primary energy needs in the year 1985, which was approximately 320 EJ. 1 hectare = 2.49 acres = 10,000 m².

to find direct substitutes for gasoline. However, since PEM fuel cell vehicles can be fueled with either methanol or hydrogen, a self-consistent evaluation of both hydrogen and methanol production from biomass is warranted. Moreover, as this thesis will show, hydrogen production from biomass is actually a simpler, less expensive, and more efficient process than methanol production from biomass. Hydrogen powered FCEVs will also be more efficient than methanol powered FCEVs. Because of the need to address the challenges facing the US transportation sector, and because of the advances that have been made in recent years in biomass conversion and fuel cell vehicle technology, it is necessary to reevaluate the potential of biomass derived fuels.

To accomplish this goal, I have constructed a set of self-consistent computer models using ASPEN PLUSTM, a state-of-the-art chemical process simulation software package. This thesis compares the production of methanol and hydrogen using a variety of promising biomass conversion technologies, some of which have not been previously evaluated for this purpose. Methanol and hydrogen production from natural gas, both of which are commercial processes, provide benchmarks for comparing the different biomass gasification technologies evaluated here. The production of methanol and hydrogen from coal was also considered, because in addition to biomass, coal is a practical alternative to natural gas that will likely be a direct competitor with biomass in the future.

Pinch analysis techniques were used to analyze the data from the ASPEN PLUS simulations, resulting in thermally optimized fuel production facilities. Exergy analysis was also used to better understand the differences between the three feedstocks and the limitations inherent in biomass conversion. To the author's knowledge, this thesis is the first application of these techniques for evaluating all of these processes within one consistent analytical framework, and is perhaps the most comprehensive overall assessment of methanol and hydrogen production from biomass for use in fuel cell vehicles.

The comparison with natural gas is important since most methanol and hydrogen produced today is derived from natural gas, and this will be the primary feedstock when these fuels are first introduced into the transportation sector. Also, at today's energy prices, natural gas processes would produce by far the least costly fuels. Coal is an abundant resource that will almost certainly cost less than biomass grown in North America. Given this choice of feedstocks, this thesis will examine the effect of projected future energy prices to determine if biomass-based systems (from raw biomass to FCEVs) will be able to stand on their own technological merits, or if incorporating environmental externalities into energy prices will be required to make biomass the feedstock of choice (for example, by imposing a carbon tax). This thesis also examines whether or not biofuels used in fuel cell vehicles will be able to compete with gasoline derived from crude oil at today's prices.

Chapter 2 reviews why biofuels have not yet been considered as serious alternatives to gasoline. Chapter 3 is a detailed review of the fundamental and practical aspects of biomass gasification. Chapter 4 evaluates the theoretical and practical considerations of methanol and hydrogen production from *synthesis gas*.¹⁰ The results of this investigation form the bases for the thermodynamic computer models, which are described in Chapter 5. Chapter 6 presents the results and evaluation of the simulations for the five biomass gasifiers evaluated in this thesis, a modern "second generation" coal gasifier, and the natural gas processes. Wherever possible, comparisons with other works are made. Chapter 7 is an economic assessment of the production and use of methanol and hydrogen, and explores the issues of scale, feedstock price, and the competition

¹⁰ Synthesis gas (or syngas) is the generic term used to describe a gaseous mixture whose primary combustible components are CO and H₂. Syngas can be produced from biomass or coal gasification, or from the conversion of other feedstocks such as natural gas or residual oils.

between the three different feedstocks and between biofuels and gasoline, assuming that biofuels would be used in fuel cell vehicles. Chapter 8 summarizes the findings of this thesis and makes recommendations for further study.

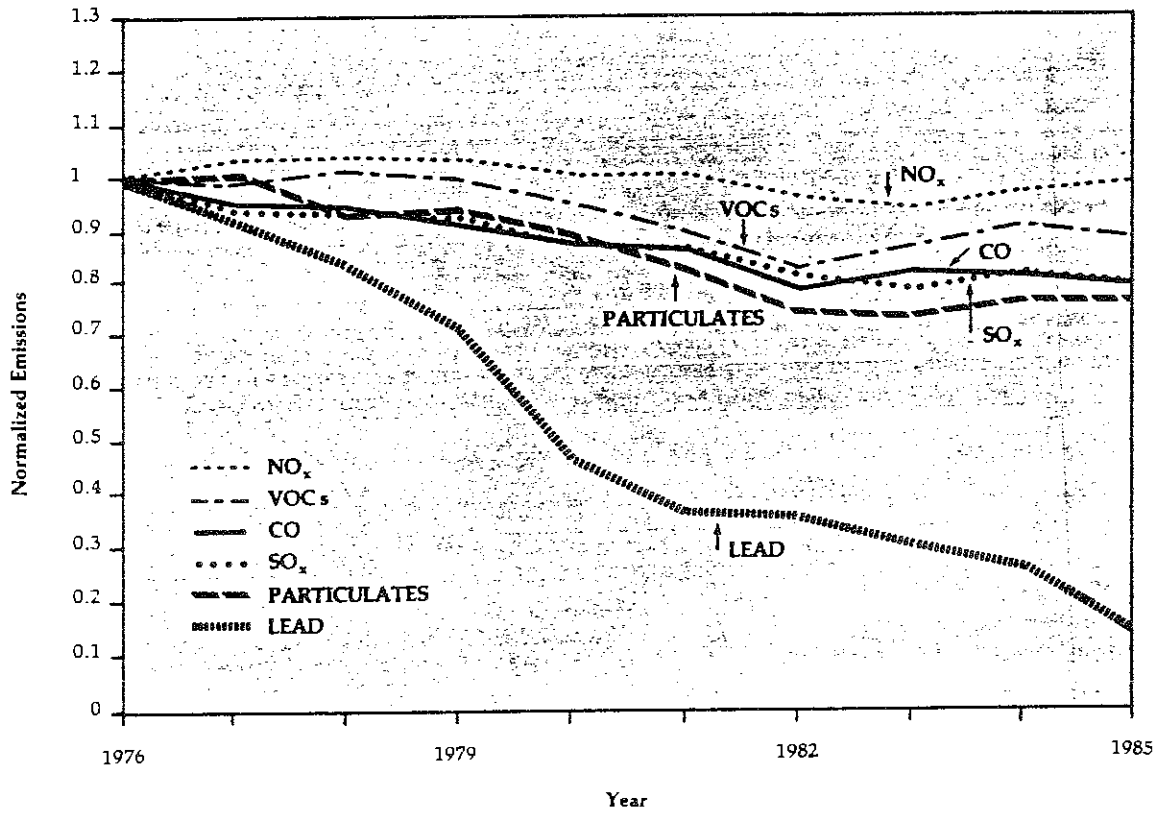


Figure 1-1: Normalized pollutant emissions from all mobile sources in the United States (Walsh, 1988). 1976 = 1.

References

- DeLuchi, Mark A. *Hydrogen Fuel-Cell Vehicles*. Research Report ECD-ITS-RR-92-14, Institute of Transportation Studies, University of California, Davis, September 1992.
- DeLuchi, Mark A., Larson, Eric D., and Williams, Robert H. *Hydrogen and Methanol: Production from Biomass and Use in Fuel Cell and Internal Combustion Engine Vehicles*. PU/CEES Report No. 263, Princeton, New Jersey: Center for Energy and Environmental Studies, Princeton University, 1991.
- DOE (Department of Energy). *National Energy Strategy, Technical Annex 2: Integrated Analysis Supporting the National Energy Strategy: Methodology, Assumptions and Results*. (DOE/S-0086P) Washington DC: US Department of Energy, 1991.
- Hall, D.O., Mynick, H.E., and Williams, R.H. "Alternative Roles for Biomass in Coping with Greenhouse Warming." *Science and Global Security*, Vol. 2, 1991, pp. 1-39.
- Hall, David O., Rosillo-Calle, Frank, Williams, Robert H., and Woods, Jeremy. "Biomass for Energy: Supply Prospects." *Renewable Energy: Sources for Fuel and Electricity*. Ed. T.B. Johansson, H. Kelly, A.K.N. Reddy, and R.H. Williams. Washington DC: Island Press, 1992.
- Huff, James R. Presentation at the Fuels Cells for Transportation TOPTEC Conference, Arlington, VA, November 4-5, 1991.
- IPCC (Intergovernmental Panel on Climate Change - World Meteorological Organization/United Nations Environment Program). *Climate Change: The IPCC Response Strategies*. Washington DC: Island Press, 1991.
- Johansson, Thomas B., Kelly, Henry, Reddy, Amulya K.N., and Williams, Robert H. "Renewable Fuels and Electricity for a Growing World Economy: Defining and Achieving the Potential." *Renewable Energy: Sources for Fuels and Electricity*. Ed. T.B. Johansson, H. Kelly, A.K.N. Reddy, and R.H. Williams. Washington DC: Island Press, 1992.
- Johansson, Thomas B., Kelly, Henry, Reddy, Amulya K.N., and Williams, Robert H. "A Renewables-Intensive Global Energy Scenario (Appendix to Chapter 1)." *Renewable Energy: Sources for Fuels and Electricity*. Ed. T.B. Johansson, H. Kelly, A.K.N. Reddy, and R.H. Williams. Washington DC: Island Press, 1992a.
- Kelly, Henry. "Introduction to Photovoltaic Technology." *Renewable Energy: Sources for Fuels and Electricity*. Ed. T.B. Johansson, H. Kelly, A.K.N. Reddy, and R.H. Williams. Washington DC: Island Press, 1992.

- Larson, Eric D. and Katofsky, Ryan E. *Production of Methanol and Hydrogen from Biomass*. PU/CEES Report No. 271. Princeton, NJ: Center for Energy and Environmental Studies, Princeton University, July 1992.
- Lashof, Daniel A. and Tirpak, Dennis A. *Policy Options for Stabilizing Global Climate*. Report to Congress. Washington DC: United States Environmental Protection Agency, Office of Policy, Planning and Evaluation, December 1990.
- Ogden, Joan M. and DeLuchi, Mark A. *Solar Hydrogen Transportation Fuels*. PU/CEES Report. Princeton, NJ: Center for Energy and Environmental Studies, Princeton University, February 1992.
- Ogden, Joan, M. and Nitsch, Joachim. "Solar Hydrogen." *Renewable Energy: Sources for Fuels and Electricity*. Ed. T.B. Johansson, H. Kelly, A.K.N. Reddy, and R.H. Williams. Washington DC: Island Press, 1992.
- Ogden, Joan M. and Williams, Robert H. *Solar Hydrogen: Moving Beyond Fossil Fuels*. Washington DC: World Resources Institute, 1989.
- Takahashi, P.K. *Hydrogen from Renewable Sources*. Report to the Solar Energy Research Institute by The Hawaii Natural Energy Institute, University of Hawaii, Honolulu, 1989.
- US Department of Agriculture. *The Second RCA Appraisal: Soil, Water, and Related Resources on Nonfederal Land in the United States: Analysis of Conditions and Trends*. Miscellaneous Publication No. 1482, Washington DC, 1990.
- Walsh, Michael P. *Pollution on Wheels*. Report to the American Lung Association, February 11, 1988.
- Williams, Robert H. (Senior Research Scientist). Center for Energy and Environmental Studies, Princeton University. Princeton, NJ. Personal Communication. April 1993.
- Williams, Robert H. and Larson, Eric D. "Advanced Gasification-Based Biomass Power Generation." *Renewable Energy: Sources for Fuels and Electricity*. Ed. T.B. Johansson, H. Kelly, A.K.N. Reddy, and R.H. Williams. Washington DC: Island Press, 1992.

Chapter 2: Literature Review

2.1 Introduction

Given the tremendous potential of biomass/FCEVs to address all of the challenges facing the US transportation sector, it is necessary to understand why biomass has never been considered seriously as a feedstock for transportation fuels. To accomplish this, this chapter expands on some of the concepts presented in Chapter 1 and briefly reviews existing biofuels programs, previous attempts to develop synthetic fuels in the US, as well as previous studies of methanol and hydrogen production from biomass. Within this context, this chapter will outline how this thesis differs from previous assessments of biofuels technology and how it contributes to the current state of understanding of biofuels technology.

2.2 Reasons Why Biomass Energy has not Been Considered Seriously to Date

2.2.1 Biomass Supplies are Limited

Chapter 1 touched upon several reasons why biomass has not been considered seriously as a feedstock for modern energy carriers (both fuels and electricity). One of these was the perception that biomass is a relatively limited, low technology resource. This implies that large scale use of biomass would increase deforestation, and therefore have negative environmental impacts. This conclusion is not without basis. The reliance on wood fuel in developing countries, where nearly 40% of primary energy comes from biomass (Hall, et al., 1992), has had very serious ecological consequences such as deforestation and soil erosion. Nevertheless, biomass is still a widely available resource, and if managed properly can be used sustainably to produce substantial amounts of energy in many parts

of the world.¹ Because of the concerns over species diversity and sustainability, it has been proposed that biomass energy plantations be established on deforested and otherwise degraded lands in developing countries and on excess agricultural land in industrialized countries (Johansson, et al., 1992). This would not only produce energy, but could simultaneously help curtail land degradation, restore previously degraded lands, and improve the lives of the people who live there.

As for the potential magnitude of biomass resources, it was shown in Chapter 1 that there is more than sufficient excess agricultural land in the US to supply all the fuel needs of the US light duty vehicle fleet through the year 2030 and beyond. Although it is difficult to measure precisely the amount of land suitable for energy production worldwide, extensive areas are good candidates for biomass plantations (see Table 2-1). In fact, in some regions of the world, like Latin America and Africa, the potential land suitable for reclamation using energy plantations is so large that these regions could actually become major exporters of fuels in a renewables-intensive energy future (Johansson, et al., 1992).

In order to illustrate the technical feasibility of large scale biomass plantations, consider the case of Brazil. Brazil has perhaps the most extensive experience with biomass plantations, which came into use following the passing of the National Forestry Act of 1965 (Carpentieri, et al., 1992). Today, there are between 4 and 6 million hectares of commercial wood plantations (mostly *Eucalyptus*) supplying feedstocks for the pulp and paper and steel industries (Carpentieri, et al., 1992).² Commercial *Eucalyptus* plantations in Brazil range in size from 1,200 to 100,000 hectares. The experience with

¹ In contrast, transportation fuels are produced almost exclusively from crude oil, of which most of the world's recoverable reserves are concentrated in relatively few regions.

² Wood is converted to charcoal for use in producing steel from iron ore.

Table 2-1: One estimate of the potential land suitable for the establishment of biomass plantations (Hall, et al., 1992).

Region	Land suitable for biomass plantations		
	Area ^a (10 ⁶ hectares)	Energy ^b (EJ/year)	Percent of commercial energy use in 1985
US/Canada	116	34.8	39.6
Europe	38	11.4	14.3
Japan	3	0.9	5.4
Australia + NZ	60	17.9	497.2
Former USSR	155	46.5	81.7
Latin America	171	51.4	295.4
Africa	176	52.9	575.0
China	54	16.3	70.7
Other Asia	111	33.4	120.6
Total	885	265.5	82.4

(a) Assuming that plantations could be established on 10% of the land currently in forests/woodlands + cropland + permanent pasture. This is a relatively conservative measure. Other estimates given in Hall, et al. (1992) are much higher; in Latin America and Africa alone, there may be over 1100 million hectares of excess potential cropland and, including Asia, nearly 760 million hectares of degraded lands suitable for plantations.

(b) Assuming a biomass yield of 15 dry tonnes/hectare/year and a higher heating value of 20 GJ/dry tonne.

commercial plantations in Brazil has shown that yields vary significantly from one bioclimatic region to the next, from over 20 dry tonnes/hectare/year to as little as 7 dry tonnes/hectare/year. More importantly, the Brazilian experience has shown that relatively large plantations can be established on previously deforested and degraded lands, and that soil fertility and high biomass yields can be sustained over relatively long periods of time (decades). There have also been substantial improvements in plantation management and technology over the last two decades. For example, maintaining a certain percentage of a plantation in a natural state using native trees (especially fruit bearing species) helps attract birds and other insectivores, which reduces crop losses from insects and pests. By interplanting nitrogen-fixing species within the *Eucalyptus* stands, it becomes possible to

reduce or eliminate the need for nitrogen fertilizers (Hall, et al., 1992). Given the current level of research in Brazil, the prospects are excellent for future improvements in all aspects of plantation management and technology (Carpentieri, et al., 1992).

Of course, as with the use of other energy sources, there have been some negative impacts associated with large scale biomass energy use in Brazil. Most wood fuel still comes from natural forests, which contributes to deforestation, soil erosion, and other environmental problems. The dumping of stillage (waste water) from commercial fuel ethanol facilities based on sugarcane has also had negative environmental impacts. Nevertheless, these problems can be overcome within a properly managed biomass energy industry.

In addition to energy plantations, it has been estimated that of the approximately 111 exajoules (EJ -- 10^{18} joules) of biomass residues produced worldwide each year, up to 31 EJ may be recoverable on a sustainable basis, roughly 10% of global primary energy use in 1985 (Hall, et al., 1992).³ Municipal waste is also a large potential source of biomass. Energy production from urban waste gasification would help address the landfill space problem and would probably have less environmental impact than incineration. An *urban energy industry* could become an important source of economic activity and employment in urban centers, where the bulk of the waste is generated.

A third source of biomass is existing forests. Although perhaps more controversial than using plantations or residues, a properly managed forest can sustainably yield biomass for energy applications. For example, the US Office of Technology Assessment

³ This includes crop residues, forestry residues and dung. Many residues would not be recoverable because they must be left on the ground to help maintain soil fertility, or because it would be prohibitively expensive to recover them.

(OTA) estimated that in the 1970s, there were 400-800 million dry tonnes per year of net annual growth in US commercial forests, while in the same period, only 180 million dry tonnes were cut per year. Since forest yields of high quality roundwood tend to be lower when harvests are less than growth (Hall, et al., 1992), removing low quality wood for energy applications would increase the yield of high quality roundwood. The OTA reported that it would be possible to collect 12-28 exajoules of biomass per year from US forests for energy purposes (Hall, et al., 1992). This would have been enough energy to satisfy 14-32% of total US primary energy use in 1987, which was approximately 87 exajoules. If we assume that the higher heating value of the wood is 20 GJ/dry tonne, this corresponds to 600-1400 million dry tonnes per year, roughly 3-8 times what was harvested in US commercial forests in the 1970s. Clearly such a program would require good forest management practices to protect natural forests and to preserve biodiversity.

2.2.2 Biomass Conversion is Inefficient and Uneconomical

Electricity production from biomass today is based on the steam-Rankine cycle. Due to the dispersed nature of biomass, it is used at much smaller scales (less than 100 MW_e)⁴ than those typical of modern coal or nuclear powered steam-electric plants (500-1000 MW_e). This places biomass at an economic disadvantage because steam turbine capital cost (\$ per kW) is strongly dependent on scale (smaller being more expensive). In order to help reduce the cost of smaller turbines, lower grade materials are used, which lowers the operating temperatures and pressures of small turbines. As a result, small steam turbines are less efficient than large ones. For example, in California, biomass-fired power plants have efficiencies of 14-18%, compared to approximately 35% for a large, modern coal-fired steam-electric plant (Williams and Larson, 1992).⁵

⁴ MW_e = megawatts of electricity produced.

⁵ Unless otherwise noted, efficiencies are quoted and calculated on a higher heating value basis throughout this thesis.

The historically low efficiency and small scale of biomass-based power generation helps explain why there has never been much interest in large scale biomass energy use: it simply cannot compete with large central station power plants fired with abundant, inexpensive fossil fuels. Furthermore, because existing biomass facilities have such low efficiencies, they are only economic using low-, zero- or even negative-cost feedstocks (usually agricultural or forestry residues). Although the supply of such residues has not been exhausted, it is a limited resource that is best suited for use at the site where it is generated (e.g. a pulp and paper mill). Any effort to use biomass energy on a large scale to produce transportation fuels would require the use of higher cost biomass that would be grown on dedicated energy plantations or collected from commercial forests. Therefore, for biomass to be cost competitive with fossil fuels, the efficiency of using biomass will need to increase significantly, which contradicts the conventional wisdom regarding biomass energy. Nevertheless, conventional wisdom is giving way to new attitudes towards biomass energy systems, and the prospects are good for high-efficiency, cost competitive biomass-based power generation using modern gasification systems and aeroderivative gas turbines. A number of demonstration projects are currently under development (Williams and Larson, 1992). Biomass can also be efficiently and economically converted to fuel grade methanol and hydrogen, as described in detail in this thesis.

Another key challenge facing biofuels is that they have historically been uneconomical when compared to gasoline. Until now, the production of commercial fuels from biomass has focussed on ethanol via fermentation of sugar crops (e.g. sugarcane and corn). In Brazil, where there exists a large, technologically mature fuel-ethanol industry

based on the use of sugarcane,⁶ ethanol is still more expensive than gasoline, and must be subsidized by the government to be cost competitive. To a lesser extent fuel ethanol is produced in the US (mainly from maize), where substantial government subsidies are required to make ethanol profitable (Johansson, et al., 1992).⁷ Because fuel ethanol is not cost competitive with traditional automotive fuels, this has led to the belief that biomass in general is not a cost effective feedstock for transportation fuels.

Although ethanol is not profitable today, the prospects for substantial cost reductions appear quite good (Goldemberg, et al., 1992; Williams and Larson, 1992; Wyman, et al., 1992), and by the year 2000 ethanol could be cost competitive with gasoline when oil is approximately \$25/barrel, provided that certain technical opportunities are exploited.⁸ On the other hand, hydrogen and methanol produced thermochemically from biomass will almost certainly be more expensive than gasoline at today's prices.

2.2.3 Previous Attempts to Develop Synthetic Fuels in the US have been Unsuccessful

Another factor affecting the willingness of government and industry to develop fuels from alternative energy sources is that previous attempts have been remarkably unsuccessful. Although the aborted synfuels program of the 1970s and 1980s clearly showed that the

⁶ Over 12 billion liters of ethanol were produced in Brazil in 1989, enough to fuel 4.2 million neat-ethanol cars and 5 million gasohol cars (which burn an ethanol-gasoline blend containing 22% ethanol) (Goldemberg, et al., 1992).

⁷ The current US ethanol production capacity is approximately 3 billion liters per year, most of which is used to manufacture gasohol, a 10% blend with gasoline.

⁸ Cost reductions could be achieved by using advanced enzymatic hydrolysis processes for ethanol production and by making more efficient use of the byproduct residues of sugarcane or corn production. With regards to the latter, coproduction of ethanol from cane juice and electricity from cane residues would make the Brazilian ethanol industry cost competitive (Williams and Larson, 1992).

production of synthetic fuels from coal and oil shale was technically feasible, the combination of inconsistent government policy and a return to stable crude oil prices resulted in the failure to develop a viable synthetic fuels industry (Yanarella and Green, 1987). As a result of this failure, synthetic fuels are generally viewed as a bad business risk in the US. Furthermore, given the low price for crude oil today, synthetic liquid transportation fuels produced from coal or oil shale would be more expensive than gasoline produced from crude oil. Today, natural gas could be used to produce methanol that is cost competitive with gasoline, although natural gas prices may rise faster than oil prices over the next 40 years (DOE, 1991).

2.3 Previous Assessments of Methanol and Hydrogen Production from Biomass

2.3.1 Methanol Production

Unlike ethanol from biomass, there are no commercial facilities that produce methanol from biomass. Nevertheless, there have been several assessments of methanol production from biomass over the past decade, some of which are summarized below. These studies have all concluded that the only remaining technical barrier is the development of commercial biomass gasifiers suitable for fluid fuels production. Each of these assessments considered similar synthesis gas processing steps to those evaluated here, but typically focussed on only one type of gasification technology, and did not consider the use of fuel cell vehicles to help make methanol from biomass cost competitive. As a result, these studies concluded that methanol from biomass would only be cost competitive if (i) crude oil prices rose considerably, or (ii) government subsidies were used artificially lower the retail price of methanol from biomass.

In 1982, The Solar Energy Research Institute (SERI)⁹ organized a workshop on producing methanol from biomass (Reed and Graboski, 1982). The papers presented at the workshop covered a wide range of topics including an evaluation of relevant coal technologies, the state of the art in methanol synthesis at the time, various biomass gasifier research projects, the utilization of methanol, and several evaluations of the feasibility of methanol production from biomass. The papers clearly indicated that methanol from biomass was technically feasible, and that small scale biomass-to-methanol plants could be cost competitive with large scale coal-based facilities. Several papers presented at the workshop focussed on the economic advantages of small scale shop fabrication over the economies of scale of very large plants based on coal.

Arnason (1983) assessed the prospects for producing methanol from biomass and urban refuse using the Wright-Malta indirectly heated gasifier.¹⁰ His main conclusion was that methanol from biomass and urban wastes could become a major energy carrier provided that significant improvements were made in vehicle fuel economy and that gasification technologies could be demonstrated at the commercial scale.

Kosstrin and Himmelblau (1985), at Stone and Webster, considered the use of the SERI downdraft, oxygen blown, fixed-bed gasifier (a pressurized unit)¹¹ for a small scale facility (<300 wet tonnes per day @50% moisture). The choice of such a small facility was based on three factors: the ability to eliminate most transportation costs by using the methanol locally, avoiding potential biomass supply problems, and the ability

⁹ SERI is now known as the National Renewable Energy Laboratory (NREL).

¹⁰ The Wright-Malta gasifier is not commercially available. This and other gasifiers are described in detail in Chapter 3.

¹¹ The SERI downdraft gasifier was extensively tested at the pilot scale, but there is no longer any active research on this gasifier or plans for larger scale demonstrations.

to use shop fabrication to reduce costs by exploiting the advantages of mass production. This analysis included the use of a fluidized-bed combustor to burn residual char and wood fines to augment energy production. Overall energy efficiency (HHV basis) was estimated to be approximately 58%, and it was concluded that the methanol would only be profitable by taking full advantage of a federal tax credit of \$10.50/GJ (\$0.19/liter).¹²

Larson and Kertamus (1988) also considered the use of the SERI downdraft gasifier as well as the high temperature Winkler (HTW) gasifier, a pressurized, oxygen blown fluidized-bed unit developed for coal. The former was deemed better suited to the scale considered in the study (450 wet tonnes per day @50% moisture). The small size was selected for similar reasons to those mentioned above. They estimated a levelized production cost of \$23/GJ, which included the federal tax credit of \$10.50/GJ. For comparison, the estimated *retail* cost of gasoline today (without taxes) from crude oil that costs \$20-25/barrel is \$8.50-9.50/GJ (\$0.29-0.33/liter).¹³ Larson and Kertamus also considered the use of an experimental once-through, low temperature methanol synthesis process that could utilize the *low Btu gas* produced by air-blown gasification, which would reduce capital costs. No quantitative estimate of cost savings was reported.

Another evaluation of methanol from biomass was conducted by CREUSOT-LOIRE, a French company that developed a pressurized, fluidized-bed oxygen-blown gasifier (Lemasle, 1988). The cost of producing methanol from this gasifier at a feed rate of approximately 1000 dry tonnes per day was estimated to be 60-120% higher than the

¹² All costs in this thesis have been converted to 1991 US dollars, using the GDP deflator (Council of Economic Advisors, 1992).

¹³ The price of gasoline is calculated using the following formula from Johansson, et al. (1992a): $P_{\text{gasoline}} = 0.00699 * P_{\text{crude}} + 0.156$, where P_{crude} is in \$/barrel and P_{gasoline} is in \$/liter. Gasoline is assumed to have a higher heating value of 34.8 MJ/liter.

cost of methanol produced from natural gas in France at the time of the study. It was also noted that for the same gasifier throughput, if oxygen were produced by an electrolyzer instead of by cryogenic separation, methanol output would increase from 500 tonnes per day to 800 tonnes per day, due to the addition of hydrogen (also produced by the electrolyzer) to the hydrogen deficient synthesis gas. However, no cost estimates for this second configuration was given. The CREUSOT-LOIRE gasifier was actually built, but was tested only briefly, and is no longer in operation.

More recent conceptual studies have attempted to estimate the production costs for methanol from biomass at larger scales and using a wider variety of gasification technologies, including several advanced gasification technologies. The results of these studies, which are more encouraging than earlier assessments, are partly what have motivated the present investigation.

In a scoping study of alternative fuel use in the US transportation sector, the US Department of Energy considered the use of biomass to produce methanol (OPPA, 1990). The study evaluated several gasifiers including some of those included in this thesis. Two cases were studied in detail. The *present technology* case made use of the Koppers-Totzec (K-T) atmospheric pressure, oxygen-blown entrained-bed gasifier. This commercially available gasifier was designed for coal but was also considered to be adaptable to biomass. The Institute of Gas Technology (IGT) pressurized, oxygen-blown fluidized-bed gasifier was selected for the *near future* case.¹⁴ A plant size with a feed rate of 1800 dry tonnes per day was selected, which is comparable to the size of a

¹⁴ The IGT gasifier was designed specifically for biomass and has been extensively tested at the pilot scale. A larger demonstration plant is in the planning stages (see Chapter 3).

modern biomass processing facility such as a pulp mill. A much larger plant size of 10000 tonnes per day was also considered to evaluate the effect of scale on production costs.¹⁵ Biomass for this facility would come from a dedicated plantation growing short rotation crops. At the smaller scale, levelized production costs were estimated to be \$22/GJ and \$16/GJ for the present and near future technology cases respectively. Methanol produced from the large near future technology facility was estimated to cost \$10/GJ, which is close to the estimated retail cost of gasoline today. If we assume that neat-methanol ICEVs are 20% more efficient than gasoline ICEVs (Wyman, et al., 1992), and that transportation and refueling adds \$2.80/GJ to the retail price of methanol (Ogden and Nitsch, 1992), then according to this study, even a very large biomass facility could not produce methanol that was less expensive than gasoline.

More recently, Wyman, et al. (1992) evaluated several biomass gasifiers for the production of methanol. Perhaps the most important conclusion of this study was that using an advanced indirectly heated gasifier that has good prospects for commercialization (that of the Battelle Columbus Laboratory, or BCL) is the least expensive method of producing methanol from biomass.¹⁶ Furthermore, methanol produced using indirect gasification was found to cost less than methanol from coal, even though it was assumed that the price of biomass was 65% higher than the price of coal and the coal facility was nearly five times the size of the biomass facility. At a 6% (12%) discount rate and a

¹⁵ There may not be many places where such a large facility could be sited. The only way to supply the biomass for such a large facility would be using a very large dedicated energy plantation. If we assume a biomass yield of 15 dry tonnes per hectare per year, that 75% of the plantation area is devoted to energy crops, and that the conversion facility has a 90% capacity factor, then this plantation would cover about 3000 km².

¹⁶ The BCL gasifier has extensive pilot scale operating experience (500 kg/hour). Unlike most gasifier designs, indirectly heated gasifiers can produce a gas suitable for methanol production without the use of costly oxygen which reduces overall production costs (see Chapter 3 for more details on indirect gasification).

methanol output of 1110 tonnes/day using the BCL gasifier, the cost of production was estimated to be \$9.60/GJ (\$11.60/GJ), which would not be competitive with gasoline. For a plant five times larger (5550 tonnes per day), which would require a plantation similar in size to the large facility described above, the calculated cost was \$6.80/GJ (\$7.90/GJ), which was comparable to the cost estimate of methanol from a natural gas-based facility producing 2500 tonnes/day of methanol. Therefore, if it were feasible to produce methanol from such a large biomass facility, methanol from biomass might be cost competitive with gasoline if crude oil cost roughly \$25/barrel. However, it should be noted that the large biomass facility included the use of an advanced *hot gas conditioning* process that is not yet commercially available.

2.3.2 Hydrogen Production

Because PEM fuel cells consume hydrogen, and because PEM fuel cells have only recently begun attracting substantial attention for automotive applications, there have been no comprehensive studies of hydrogen production from biomass. Nevertheless, Takahashi (1989) recently concluded that biomass gasification was the least expensive method of producing hydrogen from renewable resources.

In a novel approach to the gasification of extremely moist biomass (e.g. marine biomass), Manarungson (1991), at the University of Hawaii, was able to produce a hydrogen rich gas via gasification in supercritical water. Work there continues on the gasification of biomass in supercritical water.

In the only demonstration plant of its kind, VEBA OEL, a German company, is in the process of developing a 1 tonne per hour pilot plant to produce hydrogen from *Miscanthus* (elephant grass), starting with fluidized-bed gasification (Rupp, 1992).

2.4 Conclusions

This chapter has illustrated several important points regarding biofuels. First, although biomass could probably not be used to meet all future energy requirements, the worldwide potential for sustainable bioenergy production is substantial. Applied specifically to producing transportation fuels, biofuels could probably replace all gasoline use. Two crucial elements to realizing this technical potential are the ability to efficiently convert biomass into modern energy carriers and then use to these fuels in high efficiency fuel cell vehicles. To accomplish this will also require a change in the prevailing view that biomass is a low technology resource. Actual experience with commercial biomass derived fuels (i.e. ethanol) has shown that gasoline is still less expensive at prices prevailing today, although ethanol may become cost competitive in the future. Conceptual studies of methanol production from biomass have shown that it too would be more expensive than gasoline, except perhaps if biomass were converted in very large facilities using advanced technology that is not yet commercially available.

Because of the shortcomings of using biofuels in internal combustion engine vehicles (only marginal reductions in air pollution and unfavorable economics), it will be necessary to use fuel cell vehicles to extract the maximum benefit from biofuels, and at the same time meet the environmental challenges facing the US transportation sector at costs that are competitive with gasoline ICEVs. Since methanol and hydrogen are the fuels that are best suited for fuel cell vehicles using PEM fuel cells, this thesis focusses on evaluating the efficiency and cost of producing methanol and hydrogen from biomass, for use in fuel cell vehicles. In this respect, this thesis differs from previous assessments of biomass derived fuels, which emphasized using methanol or ethanol in internal combustion engine vehicles. In order to evaluate the true potential of biofuels, this work maintains a systems perspective, evaluating the entire fuel cycle, from raw biomass to the use of the fuels in FCEVs. This thesis also assesses a wider variety of gasification

technologies than previous works, including three indirectly heated gasifiers, one of which has not been the subject of earlier independent analyses.

References

- Arnason, Birgir. *Methanol from Biomass and Urban Refuse: Prospects and Opportunities*. M.S.E. Thesis, Mechanical and Aerospace Engineering Department, Princeton University, Princeton, New Jersey, June, 1983.
- Carpentieri, A.E., Larson, E.D., and Woods, J. *Prospects for Sustainable Utility-Scale Biomass-Based Electricity Supply in Northeast Brazil*. PU/CEES Report No. 270. Princeton, NJ: Center for Energy and Environmental Studies, Princeton University, 1992.
- Council of Economic Advisors. *Economic Indicators*. Prepared for the Joint Economic Committee. Washington DC: US Government Printing Office, June 1992.
- DOE (Department of Energy). *National Energy Strategy, Technical Annex 2: Integrated Analysis Supporting the National Energy Strategy: Methodology, Assumptions and Results*. (DOE/S-0086P) Washington DC: US Department of Energy, 1991.
- Goldemberg, José, Monaco, Lourival C., and Macedo, Isaias C. "The Brazilian Fuel-Alcohol Program." *Renewable Energy: Sources for Fuels and Electricity*. Ed. T.B. Johansson, H. Kelly, A.K.N. Reddy, and R.H. Williams. Washington DC: Island Press, 1992.
- Hall, David O., Rosillo-Calle, Frank, Williams, Robert H., and Woods, Jeremy. "Biomass for Energy: Supply Prospects." *Renewable Energy: Sources for Fuels and Electricity*. Ed. T.B. Johansson, H. Kelly, A.K.N. Reddy, and R.H. Williams. Washington DC: Island Press, 1992.
- Johansson, Thomas B., Kelly, Henry, Reddy, Amulya K.N., and Williams, Robert H. "Renewable Fuels and Electricity for a Growing World Economy: Defining and Achieving the Potential." *Renewable Energy: Sources for Fuels and Electricity*. Ed. T.B. Johansson, H. Kelly, A.K.N. Reddy, and R.H. Williams. Washington DC: Island Press, 1992.
- Johansson, Thomas B., Kelly, Henry, Reddy, Amulya K.N., and Williams, Robert H. "A Renewables-Intensive Global Energy Scenario (Appendix to Chapter 1)." *Renewable Energy: Sources for Fuels and Electricity*. Ed. T.B. Johansson, H. Kelly, A.K.N. Reddy, and R.H. Williams. Washington DC: Island Press, 1992a.

- Kosstrin, H.M. and Himmelblau, D.A. "Economic Feasibility of a Small Scale Wood Gasification to Methanol Plant." *Energy from Biomass and Wastes IX*. Chicago: Institute of Gas Technology, 1985, pp. 1305-36.
- Larson, L.E. and Kertamus, N.J. "Production of Methanol from Biomass." *Energy from Biomass and Wastes XI*. Chicago: Institute of Gas Technology, 1988, pp. 1053-70.
- Lemasle, J.M. "Steam-Oxygen Gasification of Wood in a Fluid-bed Reactor at Atmospheric and Elevated Pressures for Methanol Production." *Energy from Biomass and Wastes XI*. Chicago: Institute of Gas Technology, 1988, pp. 1041-52.
- Manarungson, S. *Pyrolytic Gasification of Glucose and Wet Biomass in Supercritical Water to Produce Hydrogen*. M.S.E. Thesis, Mechanical Engineering Department, University of Hawaii, Honolulu, 1991.
- Ogden, Joan M. and Nitsch, Joachim. "Solar Hydrogen." *Renewable Energy: Sources for Fuel and Electricity*. Ed. T.B. Johansson, H. Kelly, A.K.N. Reddy, and R.H. Williams. Washington DC: Island Press, 1992.
- OPPA (Office of Policy, Planning, and Analysis). *Assessment of Costs and Benefits of Flexible and Alternative Fuel Use in the US Transportation Sector, Technical Report Five: Costs of Methanol Production from Biomass*. (DOE/PE-0097P) Washington DC: US Department of Energy, December 1990.
- Reed, T.B. and Graboski, M.S., eds. *Proceedings: Biomass-to-Methanol Specialists Workshop*. Solar Energy Research Institute, Golden, Colorado, March 1982.
- Rupp, M. VEBA OEL, Gelsenkirchen, Germany. Personal communication. Sept. 1992.
- Takahashi, P.K. *Hydrogen from Renewable Sources*. Report to the Solar Energy Research Institute by The Hawaii Natural Energy Institute, University of Hawaii, Honolulu, 1989.
- Williams, Robert H. and Larson, Eric D. "Advanced Gasification-Based biomass Power Generation." *Renewable Energy: Sources for Fuels and Electricity*. Ed. T.B. Johansson, H. Kelly, A.K.N. Reddy, and R.H. Williams. Washington DC: Island Press, 1992.
- Wyman, Charles E., Bain, Richard L., Hinman, Norman D., and Stevens, Don J. "Ethanol and Methanol from Cellulosic Biomass." *Renewable Energy: Sources for Fuels and Electricity*. Ed. T.B. Johansson, H. Kelly, A.K.N. Reddy, and R.H. Williams. Washington DC: Island Press, 1992.
- Yanarella, Ernest J., and Green, William, C. *The Unfulfilled Promise of Synthetic Fuels: Technological Failure, Policy Immobilism, or Commercial Illusion*. New York: Greenwood Press, 1987.

Chapter 3: Biomass Gasification

3.1 Introduction

The first step in producing fluid fuels from biomass is gasification, the conversion of solid biomass into a gaseous mixture that can then be upgraded to liquid methanol or gaseous hydrogen. Apart from gasification, the technologies used to produce methanol and hydrogen are similar for biomass, coal, and natural gas. Therefore, the specific technologies used to gasify biomass are what will distinguish biomass systems from coal and natural gas systems. As a result, a key requirement to achieving the full potential of biomass energy is efficient biomass gasification. The main goal of this chapter is to show that biomass gasification technology has indeed advanced to a level of maturity where this is now possible. In order to understand the key elements of biomass gasification technology, this chapter first reviews the physical and chemical properties of biomass and the fundamentals of biomass gasification chemistry. The different types of biomass gasifiers are also described here, with an emphasis on those evaluated in the subsequent analysis. For more detailed treatments of biomass gasification chemistry and technology, the reader is referred elsewhere (Antal, 1980; Antal, 1981; Reed, 1981; Sofer and Zaborsky, 1981; Antal, 1982; Antal 1983; Probststein and Hicks, 1982; Overend, et al., 1985; Hall and Overend, 1987). This chapter includes a detailed comparison of biomass and coal gasification to illustrate the issues that are unique to biomass-based systems.

3.2 Physical and Chemical Properties of Biomass

Biomass is composed primarily of three compounds: cellulose, hemicellulose, and lignin (Figure 3-1 and Figure 3-2). Cellulose has the same chemical structure in all types of biomass: a linear carbohydrate polymer with a high degree of polymerization (the average molecular weight is 100,000). Cellulose chains aggregate into a crystalline structure that gives wood its mechanical strength. Hemicelluloses are mixtures of polysaccharides

comprised mainly of glucose, mannose, galactose, xylose, arabinose, methylglucuronic acid and galacturonic acid, and have a lower degree of polymerization than cellulose (the molecular weight is <30,000). Unlike cellulose, hemicellulose does not form a crystalline structure, but is amorphous (Deglise and Magne, 1987). Lignin is a complex, amorphous, randomly linked, high molecular weight, ringed structure that helps bind the cellulosic fibers together. Dry wood is typically 45-50% cellulose by weight, 15-25% hemicellulose, and 20-30% lignin (Sudo, et al., 1989). In addition, biomass contains 0.1-2% ash, and even smaller quantities of elements such as chlorine and sulphur (<0.01-0.1%) and alkali metals (mainly potassium and sodium).

Since biomass is a solid feedstock, a logical comparison to make is to coal (Table 3-1). On a dry, ash free basis, biomass has a heating value that is roughly 60-70% that of coal. As well, biomass has a lower mass density, higher initial moisture content (40-60% for fresh woody biomass, compared to 2-12% for most bituminous coals),¹ and is dispersed over a wide area. Because of this high initial moisture content, the *as received* heating value of biomass is only about 30-40% the heating value of coal. Even so, the chemical properties of biomass make it superior to coal in many ways (Hall, et al., 1992). As seen in Table 3-1, compared to coal, biomass contains far less inert material (ash) and significantly less sulfur. Biomass ash is usually free of toxic metals (such as arsenic) and other potentially hazardous materials that can make the disposal of coal ash difficult and complicate syngas processing. Biomass ash can actually be used as fertilizer, to restore nutrients to the land where it was grown (Hall, et al., 1992).

¹ Moisture content is measured on a "wet" basis. Therefore, 1 kg of wood that is 15% moisture is 0.15 kg H₂O and 0.85 kg dry wood. Most other properties (such as heating value) are typically measured on a dry basis (i.e. per kg of dry wood).

The low sulfur content of biomass alleviates a major environmental concern associated with the use of coal. While coal is typically 0.5-5% sulfur, biomass is only 0.01-0.1% sulfur.² Since some of the catalysts used to produce hydrogen and methanol are sensitive to deactivation by sulfur, the low sulfur content of biomass reduces the costs associated with the cleanup of the product gas produced via gasification.

Table 3-1: Compositional data and heating values for selected types of biomass, coal and natural gas.^a

Feedstock Type ^b	Proximate Analysis (weight %)				Ultimate Elemental Analysis (weight %)						
	HHV (MJ/kg)	VM ^c	Fixed Carbon	Ash	C	H	O	N	S	Cl	Ash
Douglas fir	20.37	87.30	12.60	0.10	50.64	6.18	43.00	0.06	0.02	0.00	0.10
Maple	18.86	87.90	11.50	0.60	49.89	6.09	43.27	0.14	0.03	0.00	0.58
Ponderosa pine	20.02	82.54	17.17	0.29	49.25	5.99	44.36	0.06	0.03	0.01	0.30
White oak	19.42	81.28	17.20	1.52	49.48	5.38	43.13	0.35	0.01	0.04	1.61
Poplar	19.38	82.32	16.35	1.33	48.45	5.85	43.69	0.47	0.01	0.10	1.43
Eucalyptus grandis	19.35	82.55	16.93	0.52	48.33	5.89	45.13	0.15	0.01	0.08	0.41
Sugarcane bagasse	17.33	73.78	14.95	11.27	44.80	5.35	39.55	0.38	0.01	0.12	9.79
Wyoming sub-bituminous coal	26.78	44.68	46.12	9.20	68.75	4.89	15.55	0.89	0.69	0.00	9.24
Illinois no.6 bituminous coal	26.67	37.50	43.40	18.18	65.34	4.20	6.59	1.02	4.55	0.00	18.30
Natural gas ^d	52.94	n/a	n/a	n/a	71.99	23.78	0.38	3.84	0.00	0.00	n/a

- (a) All values are given on a dry basis, which excludes all moisture but includes ash. n/a = not applicable.
- (b) Biomass data is from Jenkins (1989), coal data is from Williams and Larson (1992), and natural gas data is from Probststein and Hicks (1982).
- (c) VM = Volatile matter.
- (d) This is high quality Louisiana natural gas having the following composition: 94.7% CH₄, 2.8% C₂H₆, 0.2% CO₂, 2.3% N₂+Ar (Probststein and Hicks, 1982).

² Since biomass and coal have no distinct molecular structures, compositional data is measured on a weight basis (i.e. percent sulfur, carbon, moisture, etc). Conversely, the composition of gaseous mixtures is reported on a molar (volume) basis.

Table 3-1 also shows that natural gas has a significantly higher heating value than either biomass or coal, on both a mass basis and per unit of carbon. Since there is no need for an energy intensive gasification step when using natural gas, the overall energy conversion efficiency of producing methanol and hydrogen from natural gas is higher than for either coal or biomass (as discussed in detail in Chapter 6).

Perhaps the most important difference between biomass and coal is the much higher volatile fraction of biomass. For this reason, biomass is considerably more reactive than coal. Figure 3-3 shows that cellulose, the main component of wood, pyrolyses (decomposes) more completely and at lower temperatures than coal. Furthermore, biomass char (the carbon that remains after pyrolysis) is 10-30 times more reactive than coal char (Graboski, 1982). The effect of temperature on the char gasification rate is shown in Figure 3-4, which shows that biomass chars gasify more rapidly and at lower temperatures than coal chars. This fundamental difference between coal and biomass has important implications for the design of biomass gasifiers: biomass is easier to gasify than coal in the sense that lower operating temperatures are required to achieve the same gasification rates and degree of conversion from solid to gas. This is seen in practice. Commercial oxygen-blown coal gasifiers (the type that would be used to produce hydrogen or methanol from coal) operate at temperatures of 1300-1800°C whereas the biomass gasification technologies included in this study operate between 600-1100°C. The main advantages to lower operating temperatures are economic: less stringent materials requirements, the lack of expensive high temperature gas cooling equipment, and lower oxygen consumption in the case of oxygen-blown gasification. Furthermore, at lower gasification temperatures a smaller fraction of the feedstock energy is converted to heat, meaning that more is converted to chemical energy in the product gas. Biomass gasifiers also operate well below biomass ash fusion temperatures (typically >1300°C), avoiding the need for slag removal. By comparison, most modern

oxygen-blown coal gasifiers are slagging systems. The fact that biomass can be effectively gasified at relatively low temperatures also opens up the possibility for innovative gasification technologies that do not require an expensive oxygen plant but at the same time produce a gas that is undiluted by nitrogen (N_2), an important requirement for hydrogen and methanol production. These technologies are described in detail below.

There are drawbacks to lower operating temperatures, such as the presence of condensable hydrocarbons (tars and oils) in the synthesis gas, which can foul heat exchangers and clog reactors. This and other consequences of lower temperature gasification will also be discussed in more detail later in this chapter.

3.3 Fundamentals of Biomass Conversion

Thermochemical conversion of biomass can be divided into three basic steps: feedstock preparation, pyrolysis, and char gasification and combustion (see Figure 3-5). Feedstock preparation (also known as beneficiation) entails drying and sizing the biomass to suit the particular gasifier. Pyrolysis (also known as devolatilization or thermal decomposition) takes place at temperatures above about 200°C , and produces a mixture of non-condensable gases, condensable hydrocarbons (tars and oils) and char (solid carbon). At temperatures in excess of 600°C , the volatile pyrolysis products undergo secondary gas-phase reactions that most closely resemble the hydrocarbon cracking reactions used in the petrochemical industry for manufacturing ethylene and propylene (Antal, 1981). In the final step, the char reacts endothermically with steam (and to a lesser extent CO_2) to produce mainly CO and H_2 . Char reactions require higher temperatures than pyrolysis, and for biomass only proceed rapidly above approximately 700°C (Antal, 1981). In most gasifiers developed to date, some of the char and/or biomass is burned by adding air or oxygen, which generates the heat needed for the endothermic pyrolysis and char gasification reactions.

Other than feedstock preparation, which precedes gasification, the thermochemical steps described above may take place sequentially or simultaneously, depending on the design of the gasifier. However, on a microscopic scale, an individual biomass particle will sequentially undergo drying (of the remaining moisture in the biomass), pyrolysis, char gasification, and in some cases char combustion.

The kinetics of biomass gasification are complex, and there are several competing reaction pathways in the thermochemical conversion of biomass. The extent to which one pathway is favored over another depends strongly on several parameters, including the heating rate, final temperature, pressure, composition of the ambient atmosphere, the presence of ash or additives (catalysts), and the chemical structure of the feedstock itself (Antal, 1983). The design of a particular gasifier and the choice of operating conditions can be tailored to favor one type of product over another (i.e. gases, liquids, or solids, and the composition of these phases).

3.3.1 Feedstock Preparation

Chipping is generally the first step in biomass preparation, for which the total primary energy requirements for woody biomass are approximately 100 kJ/kg of wet biomass, or 0.5% of the higher heating value (Jenkins, 1989). Biomass is then usually dried to 10-15% moisture in order to reduce the heat required for gasification and to reduce the moisture content of the product gas. Drying is an energy intensive step that consumes roughly 10% of the energy content of the feedstock. Nevertheless, there is usually low grade waste heat available from elsewhere in the process that is suitable for drying.³ Although the heat of vaporization of water is 2250 kJ/kg, in practice approximately 3500 kJ is required to evaporate one kg of water, reflecting both the dryer efficiency and the

³ This is indeed the case with both hydrogen and methanol production.

heat capacity of the solid biomass (roughly 1.4 kJ/kg-K for wood) (Bain, 1981). Drying is usually performed using direct contact with hot air or flue gases. Efforts are made to avoid high temperatures in the drying step so that pyrolysis does not occur. Otherwise, pyrolysis products may be carried away with the gases leaving the dryer. Another possibility that is under development is to dry biomass in superheated steam, and then use this *dirty* steam for gasification or power production. This would return much of the energy used for drying to the system, but would require higher quality waste heat. This concept is being developed for power generation, where the high grade waste heat of a gas turbine would be used to dry moist fuels such as biomass and peat (Hulkkonen, et al., 1991).

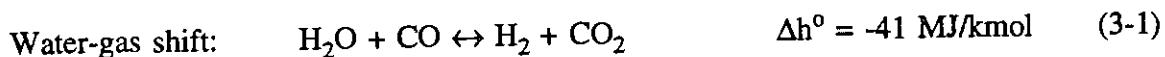
Following chipping and drying, the feedstock may undergo further mechanical processing in order to meet the feed size and density requirements of a particular gasifier. For example, some gasifiers require a feed with a relatively high bulk density, whereas others require a feed with a very fine particle size. Densification into pellets, cubes or briquettes involves mechanically compressing the biomass at temperatures between 50-100°C. At these temperatures the lignin fraction softens but the cellulose remains stable. The lignin acts to bind the densified biomass and gives the final form its mechanical strength. Pellets are approximately 10 mm in diameter whereas cubes are typically 25-50 mm across (Bain, 1981). Pelletizing requires only 1-3% of the energy of the feedstock (Bain, 1981) but can be relatively capital intensive (Probstein and Hicks, 1982).

For some gasifiers grinding would be required. This would be the case if entrained-bed coal gasification were to be adapted to biomass. Entrained-bed gasification requires a very fine particle size (-30 to -100 mesh -- 125-600 µm). While it is relatively easy to crush coal to this specification, grinding biomass would be both energy and capital intensive. In previous studies, it was estimated that grinding would more than

double the cost of feed preparation over that required for gasifiers that can accept a feedstock with a wider range of characteristics, increasing total capital costs by more than 10% (OPPA, 1990; Wyman, et al., 1992). Thus, entrained-flow gasifiers are probably not good candidates for biomass-based systems.

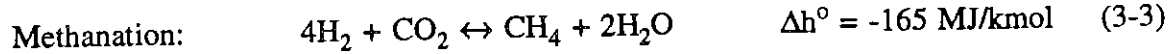
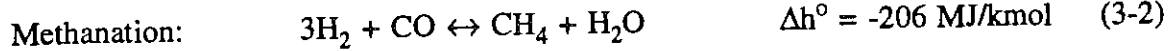
3.3.2 Pyrolysis and Secondary Gas-phase Reactions

Pyrolysis is broadly defined as the incomplete thermal degradation of carbonaceous materials into char, condensable liquids (tars and oils) and non-condensable gases (CO, CO₂, H₂, H₂O, CH₄, and other light hydrocarbons) (Milne, 1981). Since biomass is typically 75-85% volatile matter, pyrolysis is the dominant step in biomass gasification. It is a good example of a chemical process that depends strongly on the operating conditions of the gasifier. For example, the heating rate strongly affects the composition of the pyrolysis products. Slow pyrolysis maximizes the production of char (as in charcoal manufacture), whereas fast pyrolysis is used to produce either liquids or gases.⁴ In fact, cellulosic biomass can be completely volatilized (i.e. no char is produced) if heating rates are sufficiently high (>10,000°C/sec) (Antal, 1981). Flash pyrolysis (very rapid heating) combined with rapid quenching (cooling) would produce high levels of liquid products, called pyrolysis oils, which can be valuable chemicals.⁵ Longer reaction times permit these primary pyrolysis products to further decompose into non-condensable gases and secondary char. The key secondary gas-phase reactions of interest are:



⁴ Slow pyrolysis is characterized by heating rates of a few degrees per second or less, whereas fast pyrolysis (including flash pyrolysis) describes heating rates of several hundred to a thousand or more degrees per second.

⁵ The destructive distillation of wood was once the primary method used to produce methanol. Methanol accounted for approximately 5% of the liquids produced in this manner (Probstein and Hicks, 1982).



Similar cracking (thermal decomposition) and reforming reactions (the opposite of methanation) involving higher hydrocarbons also occur. As with the primary pyrolysis reactions, the rates at which these reactions take place depend on the operating characteristics of the gasifier, which in turn determine to what extent these chemical species approach their equilibrium concentrations. For example, in most biomass gasifiers developed to date, the fractions of methane and other light hydrocarbons (e.g. C_2H_4 and C_2H_6) in the product gas vary widely, from less than 10% to nearly 35% (dry gas basis).

The endothermic pyrolysis step is usually carried out under reducing conditions at temperatures above 200°C . Gas residence times in most gasifiers are too short for chemical equilibrium to be reached at gasifier operating temperatures. The relatively large amount of methane and other light hydrocarbons produced by most biomass gasifiers is evidence of the non-equilibrium nature of pyrolysis. At the operating temperatures and pressures of these gasifiers, chemical equilibrium calculations predict that hydrocarbons should be present in much smaller quantities; typically 2% or less. Also, approximately 1-4% of the feed is converted to tars and oils in most biomass gasifiers, and these compounds are also not expected at chemical equilibrium.

Experimental studies aimed at identifying the various reaction pathways of biomass pyrolysis often focus one of the two main chemical components (i.e. cellulose or lignin). Of the two, cellulose pyrolysis is better understood, not because it has received more attention, but because its solid-phase chemical structure is much simpler than that of lignin (Antal, 1983). Nevertheless, the reaction mechanisms are similar (see Figure 3-6). The first step is the depolymerization of the biomass, producing compounds

such as levoglucosan (in the case of cellulose pyrolysis) and other reactive intermediates, which quickly decompose further into tars and oils, non-condensable gases, and char. The extent to which condensable pyrolysis products decompose further (crack) into non-condensable gases, secondary char and residual tars and oils, is again determined by the specific gasifier design and operating conditions. It is primarily the lignin portion of the biomass, which decomposes more slowly than the cellulosic fraction, that is responsible for the production of most of the char and residual tars and oils. Cellulose decomposes more rapidly and is converted mostly to non-condensable gases. As seen in Table 3-2, condensable gases that exit a gasifier are mostly in the form of polyaromatic hydrocarbons including small amounts of oxygen and nitrogen containing compounds.

The presence of tars and oils has important implications for biomass based systems. First of all, they have a much higher energy content (per kg) than the rest of the product gas and the feedstock, so that if tar production is 1 wt% of the feed, this is equivalent to approximately 2-3% of the energy content of the total product gas.⁶ If the product gas is cooled below the dew point of these compounds, they can foul heat exchangers and clog chemical reactors. Therefore, tars and oils must be converted to permanent gases or removed from the product gas prior to other synthesis gas processing steps (see Chapter 4). Consequently, the energy content of tars and oils may be lost, unless it is possible to recycle them to the gasifier, burn them to produce energy, or crack them outside the gasifier. Ideally, if hydrogen or methanol is the desired end-product, the gasifier would produce no tars or oils, which would simplify downstream processing and make better use of the energy content of the original feedstock.

⁶ Tars and oils have higher heating values of approximately 40 MJ/kg, synthesis gas that contains no N₂ averages approximately 10-15 MJ/kg (wet basis), and dry biomass has a HHV of 19-20 MJ/kg.

Table 3-2: Sample composition of liquids produced by the IGT RENUGAS gasifier (an oxygen-blown fluidized bed) during pilot scale testing with biomass (Evans et al, 1988).^a

Compound	Weight Percent of Condensate
One-ring Hydrocarbons	31.5
Benzene	26.1
Toluene and Xylene	2.0
Others	3.4
Two-ring Hydrocarbons	33.8
Naphthalene	28.5
Methylnaphthalene	0.6
Others	4.7
Three-ring Hydrocarbons	9.2
Fluorene	2.3
Phenanthrene and Anthracene	5.8
Others	1.1
Four-ring Hydrocarbons	8.2
Five-ring Hydrocarbons	3.4
Higher Aromatic Hydrocarbons	2.0
Total Hydrocarbons	88.0
O-containing Compounds	0.6
Phenol and Cresols	0.04
Benzofurans and Dibenzofurans	0.5
Others	0.01
N-containing Compounds	1.3
S-containing Compounds	0.02
Total Heterocyclic Compounds	1.9
Unidentified Compounds	10.1

(a) The total amount of liquids produced during this test run was 1.96 kg/100 kg dry wood. This test was conducted at a temperature of 790°C and a pressure of 2.17 MPa.

3.3.3 Char Gasification and Combustion

Once the volatile components of the biomass have been driven off by the pyrolysis step, the remaining char can react further. In most gasification systems (coal and biomass), the source of heat is the combustion of char:





The main char reaction is with steam, the so-called *gasification* reaction:



Steam can be added to biomass gasifiers to promote this reaction as well as the secondary gas-phase reactions described above (Reactions 3-1, 3-2, 3-3). A second endothermic reaction involving char is the *Boudouard* reaction:



The CO_2 is produced from the combustion of char (Reaction 3-5) and during pyrolysis. A third char reaction is the *hydrogasification* reaction:



Since it is exothermic, this reaction will tend to favor char production under most gasifier operating conditions, and is therefore not a major mechanism of char conversion. Kinetic considerations indicate that reactions (3-6), (3-7) and (3-8) do not occur to any significant extent at temperatures below 500°C , and that temperatures in excess of 800°C are preferable for rapid char conversion (Graboski, 1981).

3.3.4 The Overall Effects of Key Operating Parameters

The preceding discussion has illustrated that a variety of parameters influence the gasification process. In order to provide a general idea of the range of operating parameters for actual biomass gasifiers, Table 3-3 summarizes the basic operating

characteristics for the three main types: fixed-bed, fluidized-bed, and entrained-bed gasifiers. Simplified schematic representations of these three types of gasifiers are given in Figure 3-7. The specific operating principles of these and other gasifiers are given in subsequent sections.

Due to the complexity of biomass gasification chemistry, it is difficult if not impossible to predict the precise composition of the product gas given a set of input specifications (Probstein and Hicks, 1982). This is in contrast to the use of chemical equilibrium computations, for which only one composition is possible given the input and operating conditions.⁷ This is the case since chemical equilibrium is not concerned with reaction mechanisms, but only with the final composition after a sufficiently long time has elapsed. Nevertheless, the qualitative effects of different operating conditions are well understood, and chemical equilibrium calculations can actually be used to illustrate most of them, even if chemical equilibrium is not achieved in practice (Desrosiers, 1981). Therefore, a chemical equilibrium model has been developed to complement this discussion with quantitative examples. The general principles extracted from this model will be used to explain the operating characteristics of actual gasifiers in Section 3.4. This model is also used later to simulate the realistic entrained-bed gasification of biomass, which can be approximated using chemical equilibrium computations.

The model will show that within the range of operating parameters given in Table 3-3, the product gas composition varies considerably. The main variables to consider are: temperature, pressure, feed moisture content, the amount of steam and/or oxygen added, and the residence time. The key assumptions of the model are: 100% carbon conversion to gas, adiabatic operation and the presence of the following chemical

⁷ Of course, it is also necessary to assume which chemical compounds will be present at equilibrium.

Table 3-3: Basic characteristics of the different types of biomass gasifiers evaluated in this thesis.

	Fixed Bed ^a	Fluidized Bed ^b	Entrained Bed ^c
Development status with biomass feedstocks	limited pilot scale testing	atmospheric - commercial pressurized - pilot/demo	conceptual studies
Commercial Mfgs. (coal and biomass)	Lurgi Dry Ash (coal) Bioneer (biomass)	Lurgi, Studsvik, Ahlstrom	Texaco, Koppers-Totzek (coal)
O ₂ (kg/kg dry feed) ^d	0.30-0.36	0.20-0.45	0.45-0.56
Indirectly heated ^e	no	yes	no
Feed characteristics	high bulk density; large particles (e.g. wood chips or densified biomass: 2-5 cm). Low moisture is better.	wide range of sizes, bulk densities and moisture content. Low moisture is better.	very fine particles (<1 mm) with low moisture content (~10% or less).
Exit gas Temperature (°C)	500-600	750-1000	>1000 ^f
Operating Pressure (MPa) ^g	2.1	0.10-3.45	0.10-2.43
Steam requirement (kg/kg dry feed)	0.40-0.47	0.3-1.4	0.03
Solids residence time	minutes	minutes	seconds
Tar production (kg/kg dry feed)	0.04	0.01-0.02	zero

- (a) Based on limited pilot scale tests (approximately 1 tonne/hour) with air as the oxidant (General Electric, 1992). The value for oxygen consumption is based on the O₂ fraction of the air.
- (b) Based on several gasifiers at various stages of development (OPPA, 1990; Evans, et al., 1988; Black, 1991; and Waldheim and Rensfelt, 1982).
- (c) Based on OPPA (1990) and the entrained bed model developed in this thesis.
- (d) For directly heated gasifiers only, assuming pure oxygen as the oxidant.
- (e) All three of these gasifier designs were originally developed as directly heated units. Fluidized-bed gasifiers are also being developed as indirectly heated gasifiers.
- (f) Actual exit temperatures may be lower due to external cooling of the reactor, but operating temperatures are well in excess of 1000°C.
- (g) The pressures shown here are for actual gasifiers, and are not indicative of limitations inherent with any particular design. Any of these gasifier types could be designed to operate over a range of pressures.

species at equilibrium: H₂, CO, CO₂, CH₄, and H₂O. Complete details of this model are available in Appendix 3A at the end of this chapter.

(i) Oxygen Consumption

Figure 3-8 shows the effect of O_2 consumption on temperature and gas composition, keeping all other input parameters constant. Not surprisingly, temperature increases quite rapidly with O_2 addition as more of the feedstock is oxidized. Initially, $CO+H_2$ production also increases since CO_2 and CH_4 are thermodynamically less favored at higher temperatures. CO and H_2 are grouped together since they are the compounds that are ultimately converted into pure hydrogen or methanol. However, as O_2 consumption continues to rise and more of the feed is burned rather than gasified, $CO+H_2$ production starts to fall, the extreme case being biomass combustion (not shown in Figure 3-8) rather than gasification. Even though CO_2 is less favored at higher temperatures, CO_2 production eventually begins to rise as more of the feed is oxidized. Generally, the production of fully oxidized compounds such as CO_2 and H_2O increases as more and more O_2 is consumed. Fewer hydrocarbons are produced with increased O_2 addition, since they are less thermodynamically favored at higher temperatures. In the equilibrium model used here, when oxygen consumption is 0.45 kg/kg dry wood, $CO+H_2$ production is near its maximum value, and essentially no hydrocarbons are produced.

(ii) Steam Rate

Figure 3-9 shows the effect of steam addition on temperature and syngas production when all other variables are held constant. H_2 production increases with steam addition due to the equilibration of the water-gas shift reaction and other gas-phase reactions that involve H_2O (e.g. Reactions 3-2 and 3-3). The effect of steam on the shift reaction also means that less CO and more CO_2 is produced. In the model, CH_4 levels actually rise slightly with increased steam addition, due to the lower temperatures that accompany high steam:biomass ratios. If temperature were held constant (e.g. by adding more oxygen), CH_4 production would actually fall with increasing steam use due the effect of the methanation reactions. This illustrates an important point, namely that temperature

generally has a much stronger effect than other variables such as reactant concentrations and pressure.

In practice, kinetic factors will limit the effect steam has on gasification; the level of steam will reach a point, beyond which, additional steam passes unreacted through the gasifier, and only serves to add to the heat load of the gasifier. For the actual gasifiers evaluated in the thesis, the amount of steam used varies over a wide range, from zero to nearly 1.4 kg/kg dry wood. For most biomass gasifiers developed to date, values of 0.3-0.5 kg/kg dry wood are typical.

(iii) Temperature

As mentioned above, this is perhaps the most important variable of all. In general, if hydrogen or methanol is the desired end-product, higher temperatures produce a better quality synthesis gas since it will contain fewer hydrocarbons and condensable compounds. $\text{CO}+\text{H}_2$ production also increases with temperature whereas the CO_2 concentration falls, all else being equal. Figure 3-10 shows these effects for a fixed overall C:H:O ratio of 1:2:1.6, which is fairly typical of biomass gasification. In this simple model, Figure 3-10 shows that virtually no methane is present above 1400 K, so that at higher temperatures, H_2 production falls and CO production increases due to the equilibration of the water-gas shift reaction, which favors CO at higher temperatures. This is the same reason why H_2O production continues to rise at higher temperatures. Because virtually no methane is present at high temperatures, $\text{CO}+\text{H}_2$ production is essentially constant above 1400 K (the only reaction taking place at these temperatures is the shift reaction, Reaction 3-1).

Because reaction rates increase exponentially with temperature, a biomass gasifier will produce a gas that is close to chemical equilibrium when temperatures are sufficiently

high. The motivation for such a design would be to generate a gas that is basically hydrocarbon free (including tars and oils). It is therefore desirable to determine the minimum temperature required to create these conditions, since in practice, higher temperatures are achieved by expending more energy, usually in the form of more direct combustion of the feed, which eventually reduces the overall efficiency of gasification. Furthermore, if the gasifier is oxygen-blown, minimizing the amount of O_2 required reduces both capital and operating costs. The model used here suggests that there is little reason to gasify biomass at temperatures above approximately 1400 K, provided that chemical equilibrium is actually reached. As will be seen in the subsequent analysis, in actual systems, the benefits of gasifying biomass at lower temperatures outweigh the advantages of generating a hydrocarbon and tar free gas.

(iv) Pressure

LeChatelier's principle can be used to explain the effects of pressure on gasification chemistry. As pressure is increased, the system responds by favoring chemical species that reduce the total volume of gas produced - a direct response to the *stress* placed on the system by increasing the pressure. Therefore, higher pressures favor the production of hydrocarbons and CO_2 . For the same reason, $CO+H_2$ production decreases with pressure. The Boudouard reaction (3-7) is a good example. As pressure increases, the equilibrium shifts towards the formation of one mole of CO_2 rather than two moles of CO (solid carbon has no effect on pressure). Similarly, methanation (Reaction 3-2) converts 3 moles of H_2 and one mole of CO into just one mole of CH_4 and one mole of H_2O . Some of these effects are seen in Figure 3-11. $CO+H_2$ production does indeed decrease with pressure, while methane and H_2O production increase. CO_2 production actually decreases slightly since higher pressures result in slightly higher temperatures (all else being equal), and the effect of temperature on CO_2 production dominates over the effect of pressure in this equilibrium model. This last result is not necessarily indicative of

actual biomass gasifiers. If temperature were held constant (e.g. by reducing the amount of O₂ consumed at higher pressures), increasing the pressure would in fact increase CO₂ formation.

The main motivation for gasifying at elevated pressures is economic. In particular, methanol and hydrogen production processes both require a high pressure synthesis gas. If a gasifier operates at elevated pressure, this reduces or eliminates the need for syngas compression, which in turn reduces both capital and operating costs. For this reason, pressurized gasification is generally considered advantageous for fluid fuels production, even though atmospheric pressure gasifiers are simpler to build because there is no need for a pressure vessel. As will be seen in subsequent chapters, pressurization has other effects on syngas processing that are not necessarily advantageous for the production of fluid fuels. Overall, this is an important design issue that needs more investigation.

(v) Residence Time

The effect of residence time cannot be illustrated with chemical equilibrium calculations, which are independent of time. A longer residence time allows the product gas to more closely approach its equilibrium composition, which generally means that fewer hydrocarbons and tars are produced. Char conversion is also higher for a longer solids residence time. The main drawback to a long residence time is that the specific throughput (tonnes/hr/m² of reactor cross-section) decreases, so that a larger gasifier is needed to process the same amount of feed, which increases its capital cost. Nevertheless, good carbon conversion is important for the gasifier to have a high overall thermal efficiency. As will be seen later in this chapter, biomass gasifiers with lower operating temperatures (and in particular, low peak temperatures) each employ different strategies to achieve high carbon conversion.

Residence time is a more important parameter for gasifiers with lower operating temperatures since reaction rates are lower. Using coal gasification as an example, high temperature gasifiers such as entrained beds are characterized by high throughput rates and very short residence times for both gases and solids (of the order of a few seconds). At the other extreme, lower temperature, dry-ash, fixed-bed coal gasifiers have solids residence times on the order of 1 hour (Synthetic Fuels Associates, 1983). In fact, entrained-bed coal gasification was developed precisely for this reason: gasifiers with short residence times are smaller, and therefore more economically attractive than gasifiers with long residence times, even though they require more oxygen and high temperature materials. The motivation for such a design is that it minimizes the processing required downstream of the gasifier while exploiting the chemical characteristics of coal. Thus for coal, the tendency has been towards higher temperature gasification, resulting in shorter residence times. For biomass gasifiers, reasonably short residence times can be achieved at milder operating conditions because biomass is more reactive than coal. Residence times for gases are typically on the order of a few seconds, and on the order of a few seconds to a few minutes for solids. Of course, the actual values are strongly dependent on the particular gasifier. Because of lower operating temperatures, these residence times are generally too short for chemical equilibrium to be achieved in biomass gasification, but sufficiently long to achieve high carbon conversion rates.

(vi) Feed Moisture Content

A higher feed moisture content means that more energy must be used to achieve a given reaction temperature, which increases the amount of feed combustion and reduces overall gasifier efficiency. The product gas will also contain more moisture, which lowers its heating value. Therefore, most biomass gasifiers use biomass that has been dried to approximately 10-15% moisture. Fortunately, drying can usually be accomplished using

waste heat that would otherwise be rejected to the environment. The effect of moisture content can be seen in Table 3-4, which shows two biomass gasification cases with identical operating conditions, except that one is for biomass with a 5% moisture content and the other is for a moisture content of 11% (using the same equilibrium model as above). In the former, the exit temperature is higher, as is CO+H₂ production. Also, CO₂, H₂O, and CH₄ production is lower when the moisture content is lower. Therefore, with a lower moisture content, it is possible to achieve a given temperature with less oxygen, which would increase the efficiency of the gasification process and reduce overall costs. Notice that on a higher heating value basis, the *cold gas efficiencies*⁸ are approximately equal, but on a lower heating value basis, the case with the lower moisture content is more efficient, because less energy is expended vaporizing H₂O.

3.3.5 A Comparison to Coal Gasification

Since biomass is typically 75-85% volatile material by weight, pyrolysis is the dominant step in gasification. By comparison, coal is only 20-50% volatile matter, so that most of the energy in coal is contained in the char. This is the main reason why higher temperatures (and hence larger amounts of oxygen) are needed to achieve high reaction rates with coal, and why coal gasification takes place at much higher temperatures than biomass gasification: biomass pyrolysis is a low temperature process whereas coal char gasification requires temperatures in excess of 1000°C to proceed rapidly (see Figure 3-3 and Figure 3-4). In fact, modern coal gasifiers produce such high peak temperatures (up to 1800°C) that the reactor vessels must be cooled to avoid damage to the refractory

⁸ The *cold gas efficiency* is a standard measure for gasifier efficiency. It is defined as the ratio of the higher (lower) heating value of the product gas divided by the higher (lower) heating value of the feedstock. Here the cold gas efficiency does not include the heat needed to dry the biomass or to raise steam for gasification, since it is assumed that this energy is available from elsewhere in the process. When the sensible heat of the product gas is also included in the energy produced by the gasifier, this is known as the *hot gas efficiency*.

Table 3-4: Comparison of oxygen blown entrained-bed gasification of coal and biomass based on the Shell gasifier. The two biomass cases correspond to two feed moisture contents: 5% and 11%.

	Coal ^a	Biomass-5% ^b	Biomass-11% ^b
Feed HHV (MJ/kg, dry basis)	29.69	19.28	19.28
Feed moisture after drying (%)	5.00	5.00	10.89
Steam (kg/kg dry feed)	0.03	0.03	0.03
Oxygen (kg/kg dry feed)	0.80	0.45	0.45
Oxygen (kg/GJ feed)	28.36	23.34	23.34
Overall O:C ratio	1.06	1.49	1.59
Pressure (MPa)	2.43	2.43	2.43
Exit Temperature (°C)	1371	1167	1084
Gas Composition ^c (mole %)			
H ₂	31.8	30.2	30.7
CO	64.3	43.3	39.0
CO ₂	1.7	10.1	11.8
CH ₄	0.0	0.0	0.1
H ₂ O	2.1	16.3	18.4
Higher heating value (MJ/kg, wet gas)	12.62	10.74	10.33
Lower heating value (KJ/kg, wet gas)	11.93	9.73	9.25
Gas yield (dry kmol/tonne dry feed)	90.47	63.82	64.73
Cold Gas efficiency (HHV) ^d (%)	80.4	85.4	85.3
Cold Gas efficiency (LHV) ^e (%)	78.8	82.3	81.2
Hot Gas efficiency (HHV) ^d (%)	94.0	>97.0	>97.0

(a) Based on actual operating data (Synthetic Fuels Associates, 1983).

(b) Based on chemical equilibrium calculations (see Appendix 3A for more details). "Biomass-5%" refers to a feed moisture content of 5%, and "Biomass-11%" refers to a feed moisture content of 11%.

(c) Small quantities of sulfur and nitrogen compounds are not shown.

(d) The cold gas efficiency is defined as the higher (lower) heating value of the product gas divided by the higher (lower) heating value of the feed. The hot gas efficiency includes the sensible heat of the product gas in the numerator.

(e) For Illinois #6 bituminous coal, the ratio of the lower to higher heating value was taken to be 0.965 (Johansson, et al., 1992a). The biomass used here was a mixture composed primarily of oak (Evans, et al., 1988). The ratio of the lower to higher heating value was assumed to be 0.94 (Jenkins, 1989).

lining. This is accomplished in one of two ways; a water jacket surrounding the gasifier cools the vessel and produces steam, or the coal is fed in a water slurry, which moderates the temperature of the reaction. Furthermore, expensive gas cooling equipment is required to cool the product gas from coal gasifiers, which can exit the reactor at temperatures of 1400°C or higher. By comparison, neither of these steps are required for biomass gasifiers.

Two disadvantages of lower gasification temperatures that are not problems for modern coal gasifiers are the higher hydrocarbon content of the gas and the presence of some tars and oils in the product gas. For methanol or hydrogen production, hydrocarbons must be converted to CO and H₂, which increases the processing requirements of the syngas when compared to the syngas produced from most coal gasifiers, which contain negligible amounts of hydrocarbons (1% or less). Tars can foul heat exchangers and clog reactors, and must be removed from the synthesis gas before it can be processed into methanol or hydrogen. This may lead one to believe that biomass should therefore be gasified at higher temperatures (>1000°C exit temperatures) to reduce the hydrocarbon content of the product gas to low enough levels to eliminate the need for some downstream processing, and to eliminate the production of tars and oils. To do so would require additional oxygen and possibly the use of high temperature materials and gas coolers similar to those used for coal gasification. Unlike for coal gasification, in actual biomass systems the benefits of low temperature operation dominate are more important.

Comparing the overall relative atom populations in coal and biomass gasification reveals another key difference between the two processes. Even though coal gasification requires significantly more oxygen per kg of feed than biomass gasification, the resulting coal synthesis gas typically has a molar O:C ratio near 1:1, so that when combined with

the high operating temperatures of coal gasification, nearly all the carbon is converted to CO, the preferred form for producing fuels and other chemicals from syngas. Because dry biomass is approximately 40% oxygen by weight, the overall feed for a biomass based system has a higher O:C ratio (on the order of 1.5-2:1). As a result, there will be higher levels of CO₂ and H₂O in the product gas, which lowers its heating value. To illustrate this point, consider the Shell entrained-bed gasification technology (a pressurized gasifier) applied to both biomass and coal as summarized in Table 3-4. Biomass has not actually been gasified in the Shell reactor, but because its operation can be approximated using chemical equilibrium calculations (unlike most other biomass gasifiers), the use of both feedstocks can be easily compared under similar operating conditions. The main difference is that for the biomass case, it is assumed that no external cooling of the reactor is required because of the lower operating temperatures. Two biomass cases are shown, corresponding to two different moisture contents: 5% and 11%. The former was chosen in order to make a direct comparison to the coal case, which also has a feedstock moisture content of 5%. 11% corresponds to the moisture content used in the subsequent analysis in this thesis. The gasification of coal is taken from actual operating data (Synthetic Fuels Associates, 1983).⁹ For the biomass cases, the choice of 0.45 kg O₂/kg dry wood was based on the previous analysis of the effect of O₂ consumption on synthesis gas production. Figure 3-8 showed that at this level of oxygen consumption, CO+H₂ production was near optimum and virtually no methane was present in the product gas. Therefore, assuming that the temperature of 1085°C is sufficiently high to ensure chemical equilibrium, this is the preferred operating point.¹⁰

⁹ Because of the high ash content of coal, the presence of significant quantities of sulfur, and the need to cool the gasifier, it was not possible to model coal gasification using the simple equilibrium model developed here. Rather, actual operating data was deemed to be more appropriate.

¹⁰ Temperature is not the only criterion for assuming chemical equilibrium for entrained-flow gasification of biomass. Since entrained-flow gasification requires a very

The *Shell-biomass* cases produce synthesis gases that are 26-30% $\text{CO}_2+\text{H}_2\text{O}$, as compared to just 3.8% for coal, even though they require only slightly more than half the amount of oxygen, use the same quantity of steam and operate at the same pressure as the coal case. As a result, the higher heating values of the biomass product gases are approximately 20% lower than the coal product gas. Nevertheless, because raw biomass has a significantly lower heating value than coal, the cold gas efficiencies of the biomass cases are actually higher than that for coal. This is also the case if the cold gas efficiencies are calculated on a lower heating value basis. So, although more carbon must be "thrown away" in the biomass cases (as CO_2), less of the feedstock energy is required to generate the synthesis gas. However, in the coal case much of the sensible heat of the product gas is recovered as steam, so that the *hot gas efficiency* of the Shell gasifier operating on coal was reported to be 94% (Synthetic Fuels Associates, 1983). The hot gas efficiencies of the biomass cases are estimated to be >97%, but it is important to note that the equilibrium model neglects heat losses and assumes 100% carbon conversion. The lower oxygen consumption (both per kg and per GJ of feed) and lower temperature also mean that the biomass processes will probably be less expensive.

A third biomass case (not shown), conducted for atmospheric pressure gasification with all else being equal (@ 11% moisture), yielded virtually the same results as the pressurized case; the temperature was within 1°C and the gas composition was almost identical. The reason why pressure has such a small effect here is that at these temperatures, there is virtually no methane produced at either 2.43 MPa or 0.1 MPa. Therefore, the product gas is essentially a mixture of H_2 , CO , CO_2 , and H_2O , which is independent of pressure.

fine particle size, the surface area is larger, which also increases reaction rates. Thus, entrained-bed biomass gasifiers would be characterized by much higher reaction rates than others type of biomass gasifiers.

3.4 Gasifier Types

Biomass gasifiers can be divided into two broad categories.

Directly heated gasifiers were originally adapted from coal gasifiers, and use air or oxygen to partially oxidize the feedstock, thereby providing the heat for pyrolysis and other endothermic reactions. The direct combustion of char produces relatively high peak operating temperatures. For the production of hydrogen or methanol from biomass, oxygen is used instead of air in directly heated gasifiers to reduce the volume of inert gas (N_2) that must be carried through the downstream reactors, which improves the economics of syngas processing.¹¹ Significant quantities of nitrogen also reduce the efficiency of the final hydrogen separation step in hydrogen production, and some N-containing compounds can poison catalysts.¹² The main drawback to requiring pure oxygen is that cryogenic oxygen separation is sensitive to scale, so that it is relatively expensive to produce oxygen at the smaller scales that would be typical of biomass-based facilities when compared to coal or natural gas-based facilities. For example, for the two directly heated biomass cases analyzed in this thesis, the capital costs for the oxygen plants were estimated to be \$84,200 and \$74,500 per daily tonne of O_2 , producing 495 and 743 tonnes/day respectively. A coal-based plant with the same throughput rate as the biomass cases (1650 dry tonnes/day of feedstock) would require 1320 tonnes O_2 /day, which would only cost \$62,700/daily tonne O_2 to install, assuming a scaling power factor of 0.7. Elsewhere, it has been estimated that a 4340 tonnes/day oxygen plant would have capital

¹¹ There is growing interest in methanol synthesis technologies that could utilize the *low-Btu gas* produced by air-blown gasification, and these are discussed in Chapter 4.

¹² Although oxygen separation is usually thought of as an added cost, it is interesting to note that if gasification takes place at pressures above approximately 2 MPa and at a sufficiently large scale, the cost of compressing the nitrogen in the air for air blown units would be greater than the cost of oxygen separation (even for 99.5% O_2 purity) (Klosek, et al., 1986).

costs of approximately \$24,000/daily tonne (Wyman, et al., 1992), significantly lower than the above costs. Cryogenic oxygen separation is also an energy intensive activity, requiring roughly 400 kWh/tonne O₂.

It is also possible to use non-cryogenic oxygen separation, but it is more difficult to achieve high oxygen purity. For methanol and hydrogen production, high purity is important because of the economic effects of inert compounds on downstream processing steps. Pressure swing adsorption (PSA) can be used to produce 90-95% pure oxygen, and membrane separation can achieve oxygen purity as high as 99%, but it is not yet economical to do so (Shelley, 1991). On the other hand, non-cryogenic air separation is rapidly becoming an attractive alternative to cryogenic separation in applications where very high oxygen purity is not essential (e.g. oxygen enriched air for coal combustion), and for purifying nitrogen, which is technically simpler with these systems. In addition to the purity issue, non-cryogenic separation does not benefit from the economies of scale as does cryogenic separation. Commercially available PSA systems are economical up to about 180 kmoles of purified gas per hour (140 tonnes per day) (Shelley, 1991), and commercial membranes separation systems have been designed to produce up to 50 kmol/hour (40 tonnes per day) (*Chemical Engineering*, 1990). At larger scales, cryogenic separation is still the technology of choice.

Indirectly heated gasifiers are designed to take advantage of the high reactivity of biomass. They provide heat indirectly using heat exchangers or an inert heat carrying material such as sand. Although they operate at considerably lower temperatures than directly heated gasifiers, temperatures are high enough to effectively gasify biomass. The main advantage of indirect gasification is that it produces a gas undiluted by nitrogen without the use of costly oxygen. Nevertheless, the lower temperatures of indirectly heated gasifiers do tend to result in higher levels of methane and other light hydrocarbons

in the synthesis gas (8-35 vol%), which increases the cost of downstream processing. Another disadvantage is the potential for higher levels of tars and oils. Lower temperatures also effect the rate of the char gasification reactions, and as will be shown below, each indirectly heated gasifier uses a different strategy for achieving high carbon conversion.

Another key distinction between gasifiers is whether they operate at atmospheric pressure or at elevated pressures. Atmospheric pressure units are easier to operate because there is no need for a pressure vessel or a pressurized feeding system. Nevertheless, using a pressurized gasifier significantly reduces compression costs downstream of the gasifier, so that pressurized gasification is generally considered advantageous. There are several commercially available pressurized coal gasifiers, but all commercial biomass gasifiers in operation today are atmospheric pressure units (Larson, et al., 1989; Williams and Larson, 1992). This is mainly a consequence of the applications for which these biomass gasifiers have been developed; for supplying fuel to boilers and furnaces. As a result, these gasifiers are air-blown units. Conversely, most coal gasifiers have been developed specifically for large scale electricity and fuel production, so that most designs on the market today are pressurized units. There are several pressurized biomass gasifiers now being developed for BIG/GT applications.

Clearly, the application for which a gasifier is being designed determines the ideal characteristics of the product gas, and hence the operating conditions of the gasifier. To illustrate this point, compare the requirements for a gasifier that would be used for methanol and hydrogen production to one designed for BIG/GT applications. In both cases operating the gasifier at elevated pressure reduces or eliminates the need for synthesis gas compression, which in turn reduces both capital and operating costs. A high throughput rate decreases the size of the gasifier, which also results in capital cost

savings. High carbon conversion and low CO₂ production maximizes the production of combustible gaseous products, and results in a high cold gas efficiency. Another desirable characteristic is the ability to gasify feedstocks with minimal pretreatment.

If methanol or hydrogen is the desired end-product, the synthesis gas should consist mainly of CO and H₂, be low in hydrocarbons, and have little or no tars and oils. Furthermore, as discussed above, the syngas should be free of inert compounds such as N₂, implying that oxygen rather than air should be used if the gasifier is directly heated. For such a gasifier, minimum oxygen consumption is preferable since oxygen separation is expensive.

If electricity is the desired end-product, it is possible to use air-blown gasification as long as the product gas has a high enough heating value to be burned in a gas turbine. Because of the dilution effect of nitrogen, it is also important to consider the moisture content of the biomass. If the feed moisture content is too high, the combined dilution effects of N₂ and water vapor in the product gas could lower the heating value of the gas to unacceptable levels. Hydrocarbons in the syngas increase its heating value and are therefore desirable. Also, if particulates and alkali metals, which can damage turbine blades, can be removed from the gas without a low temperature cleanup step (quenching with water), the syngas can be kept above the dew point of the tars and oils, which can then be burned in the gas turbine. In such a configuration, tars and oils may even be desirable, since they increase the heating value of the fuel, and there is no energy penalty associated with a low temperature water quench (Williams and Larson, 1992).

This comparison illustrates that the performance of the gasifier does indeed depend on the application. It is fair to say that there is yet to be a biomass gasifier that meets all of the above requirements for either application. For example, low tar and

hydrocarbon content can only be achieved by using high temperatures and would also require extensive feed pretreatment (milling to <1 mm). As with many engineering systems, actual biomass gasifier designs make compromises between what is ideal and what is practical. Described below are the basic types of biomass gasifier designs.

3.4.1 Directly Heated Gasifiers

There are three basic types of directly heated gasifiers: fixed, fluidized, and entrained beds. Although each operates on a different principle, they all share certain features. All directly heated gasifiers burn some char and/or biomass, and so are characterized by relatively high peak operating temperatures (>1000°C), which occur at the point where the oxidant enters the vessel.

(i) Fixed-bed Gasifiers

This is the simplest type of directly heated gasifier. In a fixed-bed gasifier (an updraft design is shown in Figure 3-7), the feedstock enters at the top of the reactor and sequentially undergoes drying, pyrolysis, char gasification and char combustion. Due to the nature of the fixed-bed design, these steps occur in relatively distinct zones. Peak reactor temperatures of about 1200°C are reached near the grate where char combustion takes place. Dry ash is rejected below the grate that supports the fuel bed. The hot gases produced by char combustion travel countercurrent to the solid feed and provide the heat for the char-steam reactions and for pyrolysis. Because of this countercurrent design, the gases exit the reactor at a relatively low temperature (600°C or less). Low pyrolysis temperatures result in a gas with a large fraction of condensable hydrocarbons. Fixed-bed gasifiers also require a feed with a relatively high bulk density, such as densified biomass or wood chips (2-5 cm in size), to ensure good feed flow down the reactor.

An example of a fixed-bed gasifier is the Lurgi dry-ash design for coal (Figure 3-12). This commercial pressurized unit has extensive operating experience with coal (Williams and Larson, 1992). Recent limited pilot scale tests with biomass conducted by the General Electric Company indicate that the Lurgi technology may be best suited for "close-coupled" processes where the hot product gas is burned directly (e.g. in a BIG/GT) without the need to cool the gas below the dew point of the condensable components of the gas (Kimura, 1992).¹³ In such a configuration, the energy content of the tars and oils could be utilized in the gas turbine. This would require an advanced hot-gas cleanup system that could remove nearly all entrained particles and alkali metals, since these compounds would otherwise damage the turbine blades.¹⁴ Although this technology appears to be well suited to electricity production (Williams and Larson, 1992), due to the high fraction of condensable gases produced by fixed-bed gasifiers, much of the energy content would not be recoverable if used for methanol or hydrogen production. Therefore, such a design is not well suited to fluid fuels production and was not modeled in this thesis.

(ii) Fluidized-bed Gasifiers

In fluidized-bed gasifiers (Figure 3-7) the feedstock usually enters through the sidewall of the reactor. The feed mixes into a bed containing an inert material such as sand or a catalytic material such as dolomite ($\text{CaMg}(\text{CO}_3)_2$), which is used to help crack tars.¹⁵

¹³ In those tests, which used pelletized sugarcane bagasse and wood chips, approximately 4 wt% of the dry feed was converted to tars and oils, corresponding to roughly 8-10% of the heating value of the feed (General Electric, 1992).

¹⁴ Such hot-gas cleanup systems are under development. See Chapters 4 for more details.

¹⁵ Ahlstrom, a Finnish company, is developing a fluidized-bed gasifier that uses calcined dolomite as the bed material. Studsvik, a Swedish company, has developed a two stage system that also uses dolomite. The gas exiting the gasifier is sent to a fluidized-bed *catalytic cracker* that uses oxygen to partially oxidize some of the feed to

A fluidized state is maintained by the injection of steam and oxygen (or air) from below. The high degree of mixing in a fluidized bed eliminates the distinct reaction zones characteristic of fixed beds, except perhaps for the combustion zone, which would be located near the entry point of the oxidant. Due to the vigorous mixing in a fluidized-bed gasifier, it is characterized by relatively uniform temperatures throughout the bed (800-1000°C) and the gas exits the reactor essentially at the bed temperature. Since average bed temperatures are higher in a fluidized bed than a fixed bed, the product gas contains fewer tars and oils. Particulate emissions are higher than with a fixed bed, again as a result of the active mixing within the bed. Ash, unreacted char and particulates are entrained within the product gas and are largely removed using a cyclone (see Chapter 4). In a bubbling fluidized bed (BFB) they are removed for disposal, but in a circulating fluidized bed (CFB) they are recycled to the bed, thereby increasing the carbon conversion (to gases and liquids) to near 100%.

Because of the higher average bed temperatures, fluidized-bed gasifiers have higher specific throughput rates than fixed beds. They are also capable of utilizing feedstocks with a wide range of sizes and bulk densities, although very fine particles tend to get blown out of the reactor. In fact, it is because of this fuel flexibility that fluidized-bed gasifiers may become the technology of choice for biomass applications, given the wide variety of biomass feedstocks that could be used to produce fuels and electricity (Williams and Larson, 1992). Most biomass gasification research and development today is focussed on fluidized bed technology.

provide heat for the tar cracking reactions. The Battelle Columbus Laboratory is also developing a similar two stage system that is adiabatic (i.e. it uses the sensible heat of the product gas rather than adding oxygen).

An example of an oxygen-blown, pressurized bubbling fluidized-bed gasifier that has been designed specifically for biomass is the Institute of Gas Technology (IGT) RENUGAS[®] gasifier (Figure 3-13). It has been under development since 1980 and has perhaps the most extensive pilot-scale experience of any BFB unit (Evans et al., 1988). A 50 tonnes per day demonstration plant is under construction in Hawaii, where it will operate on sugarcane bagasse (Trenka, et al., 1991). Because the IGT gasifier has had so much operating experience, and because it has been the focus of other studies of methanol production from biomass (OPPA, 1990; Stevens, 1991; Wyman, et al., 1992), it is one of the five gasifiers that has been chosen for further analysis in this thesis.

The IGT test reactor, with a capacity of 455 kg of biomass per hour, has been operated at pressures of 0.58-2.23 MPa and at temperatures up to 980°C, but no data exists for operation on pure oxygen. Gasifier performance using pure O₂ was estimated in a study of methanol production from biomass by the Office of Policy, Planning and Analysis of the US Department of Energy (OPPA, 1990). Table 3-5 includes the product gas composition for the IGT gasifier under the operating conditions assumed in that study (3.45 MPa and 980°C). Two important characteristics of the syngas are the relatively large CO₂ and CH₄ fractions. The high methane content is a result of the non-equilibrium nature of biomass gasification and of pressurized operation. Relatively large amounts of CO₂ are produced by the direct heating, high pressure, and the high overall O:C ratio (2:1). With conventional gas processing technology, a large CO₂ content means that overall yields of fluid fuels will be relatively low.

In addition to the IGT RENUGAS gasifier, a number of other bubbling fluidized-bed biomass gasifiers have reached various stages of development (Larson and Katofsky, 1992). They include Creusot-Loire (France), MINO (Sweden), BIOSYN (Canada), Rheinbraun/Uhde HTW (Germany) and Tampella (Finland) (see Figure 3-14). Of these,

Table 3-5: Operating characteristics of the gasifiers evaluated in this thesis. n/a = not available.

	Directly heated gasifiers			Indirectly heated gasifiers		
	IGT ^d	Shell-coal ^f	Shell-bio ^e	WM ^a	MTCI ^c	BCL ^b
Bed type	Bubbling-fluidized	Entrained	Entrained	Rotor kiln	Bubbling-fluidized	Fast-fluidized
Feedstock characteristics						
Type	wood	coal	wood	wood	wood	wood
Dry, ash free composition	CH _{1.52} O _{0.68}	CH _{0.91} O _{0.11}	CH _{1.52} O _{0.68}	CH _{1.5} O _{0.67}	CH _{1.63} O _{0.66}	CH _{1.46} O _{0.60}
HHV (GJ/dry tonne)	19.28	28.21	19.28	20.93	19.40	20.12
Moisture % (after drying)	15	5	11	45	20	10
Additional inputs						
Steam (kg/kg dry feed)	0.3	0.028	0.03	0	1.37	0.314
Oxygen (kg/kg dry feed)	0.3	0.8	0.45	0	0	0
Air (kg/kg/dry feed)	0	0	0	0	2.10	1.46
Reactor characteristics						
Exit temperature (°C)	982	1371	1085	600	697	927
Pressure (MPa)	3.45	2.43	2.43	1.5	0.101	0.101
Throughput (dry kg/m ² -s)	1.9	n/a	n/a	0.18	0.07	2.7
Solids residence time	minutes	~1 second	~1 second	~1 hour	minutes	~1 second
Product gas characteristics						
Yield (kmol/dry tonne)	82.0	92.4	79.3	90.3	138.6	58.3
Molecular weight (kg/kmol)	22.52	20.53	20.08	21.82	17.65	21.22
HHV (MJ/kg wet)	8.67	12.62	10.33	11.11	9.35	14.22
Composition ^g (mole % wet [dry])						
H ₂ O	31.8 [0]	2.1 [0]	18.4 [0]	42.0 [0]	49.5 [0]	30.8 [0]
H ₂	20.8 [30.5]	31.8 [32.5]	30.7 [37.6]	12.0 [20.7]	25.3 [50.0]	14.6 [21.1]
CO	15.0 [22.0]	64.3 [65.7]	39.0 [47.8]	4.0 [6.9]	11.2 [22.1]	32.4 [46.8]
CO ₂	23.9 [35.0]	1.7 [1.7]	11.8 [14.4]	22.0 [37.9]	9.9 [19.4]	7.8 [11.3]
CH ₄	8.2 [12.0]	0 [0]	0.1 [0.1]	20.0 [34.5]	4.0 [8.0]	10.3 [14.9]
C ₂ +	0.3 [0.5]	---	---	---	0.2 [0.4]	4.2 [6.1]
Net carbon conversion ^h (%)	96.2	>99	100	98.5	83.5	80.3
Cold gas efficiency ⁱ (%)	83.0	80.4	85.3	85.9	87.8	87.4

- (a) WM is the Wright-Malta gasifier. Based on Hooverman (1979), Coffman (1981), and Coffman (1991).
- (b) BCL is the Battelle-Columbus Laboratory gasifier. Based on Paisley (1991). In all cases, "kg dry feed" refers to the total biomass feed for the combustor and gasifier beds.
- (c) MTCI is the Manufacturing and Technology Conversion International gasifier. Data are based on Durai-Swamy, et al. (1991a).
- (d) IGT is the Institute of Gas Technology. Data is based on OPPA (1990).
- (e) Shell-bio is the Shell entrained-bed gasifier operating on biomass. For a complete description of the assumptions used to estimate the performance of this system see Appendix 3A.
- (f) From Synthetic Fuels Associates (1983).
- (g) Small quantities of N and S containing compounds and Argon are not shown.
- (h) This is the net carbon conversion to synthesis gas. For the BCL and MTCI gasifiers, carbon converted to gas in the combustors is counted as part of the feed carbon but not as carbon converted to gas.
- (i) Defined as the higher heating value of the product gas divided by the higher heating value of all energy inputs to the gasifier, including the combustors in the BCL and MTCI cases and the external heating in the WM case. The energy for raising steam or drying biomass is not included.

only the HTW (High Temperature Winkler) technology has been commercially applied to producing chemicals; since 1988, an HTW unit has operated successfully on peat at a Finnish ammonia plant (Larson and Katofsky, 1992).¹⁶

A number of circulating fluidized-bed biomass gasifiers have also been developed (Figure 3-14). Lurgi (Germany), Ahlstrom (Finland), Studsvik (now TPS) and Gotaverken (Sweden) have several atmospheric pressure units operating commercially (Larson et al., 1989). Lurgi (with Rheinbraun/Uhde) and Ahlstrom are also developing pressurized CFB gasifiers, of which there are no commercial units. These gasifiers are being developed primarily for heat and power generation, but if they are proven commercially, there is no reason why they cannot be adapted to fluid fuels production, provided they are oxygen-blown units.

(iii) Entrained-bed Gasifiers

The third basic type of directly heated gasifier is the entrained-bed gasifier (Figure 3-7). This design was originally developed for coal, and unlike fluidized- or fixed-bed gasifiers, there is no operating experience with biomass. In entrained-bed coal gasification, pulverized coal is fed into the reactor dry or in a water slurry, where it reacts with a large amount of oxygen (approximately 0.8-1.0 kg/kg dry coal). The resulting high operating temperatures (1300-1800°C) completely gasify the coal and produce a tar-free gas that is close to chemical equilibrium with virtually no CH₄ and no higher hydrocarbons. At the high temperatures characteristic of entrained-bed oxygen-blown coal gasification, the ash melts and is removed as slag.

¹⁶ Air blown gasification can be used for ammonia synthesis since it requires nitrogen in the feed.

Several entrained-bed coal gasifiers have operated commercially. Table 3-5 includes the operating characteristics for the Shell entrained-bed gasifier, which has been extensively tested at feed rates up to 400 tonnes per day (Synthetic Fuels Associates, 1983; Trognus, et al., 1989).¹⁷ Because high temperatures can be achieved with coal when the O:C ratio is close to 1:1, CO₂ comprises less than 2% by volume of the gas on a dry gas basis and the CH₄ content is essentially zero. Three commercial entrained-bed coal gasifiers worth mentioning are the Texaco, Dow, and Koppers-Totzek (K-T) units. Like the Shell gasifier, the Texaco and Dow designs are pressurized, while the K-T gasifier is an atmospheric pressure unit. The Shell and K-T gasifiers use a dry, pulverized feed and the Texaco and Dow designs use a coal-water slurry.¹⁸ A coal-water slurry is used to moderate the reactor temperature, whereas the K-T and Shell gasifiers require external cooling in the form of a water jacket that produces steam. Considerably more steam is produced by the K-T gasifier than the Shell unit, since more oxygen is used. Because it uses a dry feed and requires less oxygen, the Shell gasifier has a higher cold gas efficiency and generates a higher quality synthesis gas (for producing fluid fuels) than either the Texaco, Dow, or K-T gasifiers.

There are two main reasons why there has been little interest in entrained-bed gasification of biomass. First, entrained-bed gasification requires a very fine particle size (~125-600 microns), and while it is relatively easy to crush coal, grinding biomass is

¹⁷ A 250 MW_e integrated coal gasification combined cycle power plant (IGCC) using a single Shell gasifier is currently under construction in the Netherlands, and is scheduled to come into service in late 1993 (Jensen, et al., 1990).

¹⁸ Both the Dow and Texaco concepts have been proven commercially. Since April 1987 a Dow gasifier has been supplying fuel gas to an existing 161 MW_e combined cycle power plant in Plaquemine, Louisiana (Webb and Moser, 1989). The Texaco gasifier was part of the Cool Water Coal Gasification Program in California, the first commercial scale demonstration project of an IGCC power plant. It successfully supplied fuel gas for a 100 MW_e combined cycle from June 1984-January 1989 (Cool Water Coal Gasification Program, 1990).

energy and capital intensive. Second, as has been discussed earlier in this chapter, biomass gasification does not require the high peak temperatures characteristic of entrained-bed gasification to achieve high carbon conversion and high throughput rates, the two main motivations for the development of entrained-bed coal gasification. However, neither reason is compelling. In fact, if biomass were gasified in an entrained-bed gasifier, the equilibrium model used earlier showed that the operating temperatures would be considerably lower than those for coal, and that much less oxygen per kg of feed would be required.¹⁹ Under such conditions, the dry ash would be carried out by the gas as it is in fluidized-bed designs, eliminating the need for slag removal.

Although entrained-bed biomass gasification is not practical, largely because of the high feedstock preparation costs and large O₂ requirements, it is nevertheless modeled in this thesis to provide an example of what might be considered the ideal directly heated biomass gasifier for fluid fuels production: it produces no tars or oils, converts 100% of the carbon to gas, and since the product gas reaches chemical equilibrium at high temperatures, it is virtually free of hydrocarbons. The Shell gasifier was selected for modeling purposes since it operates using a dry feed, and of the three entrained-bed gasifiers mentioned above, it requires the least amount of oxygen per kilogram of feed (Synthetic Fuels Associates, 1983). Because of the differences between coal and biomass gasification, it is unlikely that the entrained-bed biomass gasifier would require external cooling, either using a water jacket or a slurry feed. Also, a water slurry is probably not practical with biomass and would require relatively more oxygen to achieve the same

¹⁹ OPPA (1990) estimated that if the K-T gasifier were to operate using biomass, it would require 0.56 kg O₂/kg dry wood, roughly 60% the amount required for coal (Synthetic Fuels Associates, 1983). For comparison, I estimate that a Shell type gasifier operating on biomass would require 0.45 kg O₂/kg dry wood, which is 56% the amount required for coal (Synthetic Fuels Associates, 1983).

temperature as a dry feed system.²⁰ The pressurized operation of the Shell gasifier is also a desirable characteristic.

The operating conditions for the Shell-biomass gasifier shown in Table 3-5 have been selected based on the parametric analysis carried out earlier in this chapter, where it was shown that for a moisture content on 11%, the optimum syngas composition corresponded to an oxygen consumption rate of 0.45 kg/kg dry feed (see Figure 3-8). At lower temperatures, there is more methane in the synthesis gas, CO+H₂ production is less than the maximum, and some tars may be produced. At higher temperatures, there is virtually no methane in the product gas so that additional oxygen consumption would only oxidize some of the CO and H₂ to CO₂ and H₂O.

3.4.2 Indirectly Heated Gasifiers

Although there are no commercial facilities using indirect biomass gasification, pilot scale units have successfully operated using a variety of heat transfer methods (Figure 3-15). Operating conditions vary from atmospheric pressure to 1.5 MPa and exit temperatures of 600-930°C (see Table 3-5). Because of their low operating temperatures, indirectly heated units typically produce gases that contain significant quantities of hydrocarbons (mostly methane) and some tars. Low temperature operation also means that low carbon conversion is a potential problem, and each gasifier described here uses a different method for ensuring high carbon conversion rates. For fluidized-bed units, steam is the fluidizing medium, although recycled product gas can also be used.

²⁰ A slurry feed is practical for coal gasification because the high temperatures must be moderated in some manner. With biomass, gasification temperatures would not be high enough to warrant the use of a slurry to moderate the temperature. Rather, you want to minimize the energy required to achieve a certain temperature. Thus a slurry would achieve the opposite effect with biomass.

(i) The Battelle-Columbus Laboratory (BCL) Gasifier

The Battelle-Columbus Laboratory (BCL) gasifier is an atmospheric pressure, twin bed, fast-fluidized-bed unit (Feldmann et al., 1988; Paisley, 1991; Wyman et al., 1992) (Figure 3-16) that resembles fluid catalytic crackers commonly used in the petrochemical industry (Refining Handbook, 1990). The term fast-fluidized-bed has been used to describe the BCL system since the specific throughput rate of the BCL gasifier is significantly higher than a conventional fluidized-bed like the IGT gasifier (see Table 3-5). To date, the BCL gasifier has operated at a dry feed rate of up to 500 kg/hr, and has over 10,000 hours of operating experience on a variety of biomass feedstocks (Paisley, 1993).

In one bed, biomass (dried to 10% moisture) is pyrolyzed in steam at temperatures up to 930°C. Ash, char and sand (the bed material) are entrained in the product gas, separated using a cyclone, and sent to a second bed where the char is burned in air to re-heat the sand. The heat is transferred between the two beds by circulating the hot sand back to the gasification bed. This is similar to char recirculation systems used with commercial fluidized-bed coal combustors (Paisley, 1993). This system allows one to provide heat by burning some of the feed, but without the need to use oxygen because combustion and gasification occur in separate vessels, and is possible with biomass because of its high volatile content. As a way of producing higher temperatures in the gasification bed, some additional biomass can be burned directly in the combustor to augment the heat provided by the combustion of char alone. Ash is rejected from the combustor, and no char is produced. Tars and oils (approximately 1% of the feed) are collected from the quench water and recycled to the combustor. Therefore, the BCL system is characterized by nearly 100% overall carbon conversion. An advantage of this system is the inherently high heat transfer rates of the direct mixing of hot sand and

biomass. Therefore, although the system as a whole is indirectly heated, biomass heating rates are high.

If the BCL gasifier were to operate in *balanced mode*, where the heat available for gasification is that produced by burning char alone in the combustor, gasification temperatures would be low (approx. 800°C) with correspondingly low carbon conversion in the gasifier (<70%). Using a heat and material balance model developed at BCL, it was found that by increasing the gasification temperature, the overall production of synthesis gas increases, even though some additional biomass must be burned in the combustor (Paisley, 1991). Table 3-5 presents operating data for this type of configuration. A gasification temperature of 927°C results in good carbon conversion in the gasifier (88%) while limiting the amount of biomass which must be burned in the combustor to less than 10% of the total feed. Thus, overall carbon conversion to synthesis gas is 80.3%, and because of the rapid indirect heating, CO₂ accounts for only 11.3% by volume of the synthesis gas on a dry basis. Higher temperatures are possible, but would result in more heat leaving the combustor as waste heat in the flue gases²¹ rather than being transferred to the gasifier by the circulating sand.

The BCL gasifier illustrates one way in which high overall carbon conversion can be achieved with indirect heating; design a reactor that actually relies on poor carbon conversion for its operation. To accomplish this requires two basic conditions, which can be explained in terms of the earlier discussion of gasification fundamentals: avoid high peak temperatures and keep solids residence times very short compared to the characteristic reaction time of the char-steam reaction. The first condition is satisfied by the use of indirect heating, and the second is by design: the BCL gasifier is designed to

²¹ The combustor bed was assumed to have an exit temperature 167°C higher than the gasifier operating temperature (Paisley, 1991).

have residence times on the order of 1 second (Paisley, 1993). As a result, the char produced during pyrolysis is not gasified, but is entrained within the product gas. Pyrolysis is the only step that occurs to any significant extent in the gasifier. Since temperature and heating rate are the most important variables affecting pyrolysis, it is not surprising that during the testing of the BCL gasifier, changing the fluidizing medium from steam to nitrogen had a negligible effect on both carbon conversion and the inert free gas composition (Feldmann, et al., 1988). Furthermore, since less char is produced at higher temperatures and heating rates, it is also not surprising that carbon conversion in the gasification bed was found to be directly proportional to the bed temperature. Since char gasification need not occur in the gasification bed, the specific throughput rate is very high, which helps reduce the capital cost of the BCL gasifier.

In summary, the heat and carbon balance of the BCL system is quite different from all other gasifiers discussed here. Not only is the endothermic char-gasification step bypassed, but essentially all the char that is produced is burned, as is some of the feed. One would therefore expect there to be a significant amount of waste heat produced in the BCL process, a result that is evident in the analysis of Chapter 6. When coupled with the high cold gas efficiency of the BCL gasifier, this high grade waste heat, which can be used to generate a fair amount of electricity, makes it the most efficient gasifier included in this thesis.

(ii) The Manufacturing and Technology Conversion International (MTCI) Gasifier

A second indirectly heated gasifier is being developed by Manufacturing and Technology Conversion International (MTCI), a small US company (Figure 3-17). The MTCI gasifier combines an atmospheric pressure bubbling fluidized-bed with pulse-combustion-enhanced in-bed heat exchange tubes that provide the heat for gasification (MTCI, 1990; Durai-

Swamy, et al., 1991a).²² Some of the gas produced during gasification is burned in the pulse combustor to provide the heat for gasification. The oscillatory behavior of the pulse combustor is a result of natural combustion-induced instability, and the combustion chamber and heat exchange tubes are designed specifically to amplify these effects at a particular resonant frequency (Turdera and Zahradnik, 1992). Pulsed combustion produces large velocity fluctuations within the fire tubes, enhancing heat transfer rates by a factor of five over conventional heat exchangers.²³ Even so, because indirect heat transfer is used, reactor temperatures are low (650-800°C), but are more than sufficient to gasify biomass. In the MTCI system, large quantities of steam are added to promote char conversion, which would otherwise be unacceptably low at these low temperatures. It is also possible to recycle residual char and tars and oils to the pulse combustor or the gasifier (Durai-Swamy, 1992; Turdera and Zahradnik, 1992). The overall carbon conversion to synthesis gas in the gasification of wood has been estimated to be approximately 83.5%.²⁴

²² Although it has not been tested at elevated pressures, MTCI does not anticipate any major difficulties in designing their gasifier to operate at pressures up to approximately 1.5 MPa. The pulse combustor would also need to be operated at pressure, which would increase the heat flux and hence the throughput rate of the MTCI gasifier. A detailed feasibility study of pressurized operation using coal is given in Turdera and Zahradnik (1992), where they assessed the use of the MTCI gasifier in an integrated gasification/combined cycle (IGCC).

²³ A similar design, but one that does not use pulse combustion, was developed at the University of Missouri in the early 1980s (Flanigan, et al., 1988).

²⁴ I have estimated the overall carbon conversion by using actual test data for the gasification of wood chips, for which carbon conversion in the gasifier was 93%. I then used a heat and material balance model provided by MTCI and the ASPEN PLUS simulations to estimate the amount of carbon (as CH₄, CO, char, etc...) consumed in the pulse combustor. Accounting for this carbon, I estimate the net carbon conversion to be approximately 83.5%.

Until now, most work with the MTCI gasifier has focussed on the gasification of "unusual" biomass fuels such as black liquor (the lignin rich by-product of cellulose extraction during chemical pulp production) (Black, 1991) and pulp mill sludge (Durai-Swamy, et al., 1991b). Limited tests have also been successfully conducted on dried municipal sewage sludge, refuse derived fuel (RDF) and wood chips (Durai-Swamy, et al., 1991a). The MTCI gasifier is at a fairly advanced stage of development. A 22 tonnes per day gasifier operating on pulp mill sludge has operated extensively at an Inland Container Corporation cardboard recycling mill in Ontario, California, and a 44 tonnes per day black liquor²⁵ gasifier is currently being installed at a pulp mill in New Burn, North Carolina (Durai-Swamy, 1993). The MTCI gasifier was also selected for a cost shared demonstration project as part of the US Department of Energy's Clean Coal IV Program. A commercial scale (430 tonnes per day) MTCI gasifier operating on sub-bituminous coal will be built and operated at a Weyerhaeuser paper mill in Gillette, Wyoming (Durai-Swamy, 1992).²⁶

Based on limited data from gasification trials with wood chips, on discussions with the developers of the MTCI gasifier, and using a heat and material balance program developed at MTCI, I have developed a model for the scaled up operation of the MTCI gasifier with wood (see Table 3-5). A large amount of steam (1.37 kg per kg dry wood)

²⁵ This is the amount of black liquor solids being gasified, which corresponds to approximately 67 tonnes per day of black liquor.

²⁶ Although coal would seem like an unlikely feedstock for this low temperature gasifier, pilot scale testing of coal gasification has yielded good results. At moderately high temperatures (>800°C) it is possible to gasify the relatively more reactive sub-bituminous coals. The use of large amounts of steam and the catalytic effects of calcium in the bed result in carbon conversion efficiencies in excess of 90% (Durai-Swamy, 1992). Of course, this does not account for the combustion of a portion of the gas in the pulse combustor. Experiments with high rank coals have included a pretreatment section where hot air is bubbled through the coal in an effort to add oxygen to make it more reactive before being fed to the gasifier.

is added to the partially dried biomass (20% moisture by weight) to produce a hydrogen rich gas with a relatively low hydrocarbon content (8.4% on a dry basis), which includes small amounts of ethylene, propylene, propane, butane, and pentane. The low hydrocarbon content is a result of the effect of excess steam, which promotes secondary gas phase reactions such as methane steam reforming. The high H₂ content (nearly 50% on a dry basis) is also consistent with this explanation. In addition to its effect on reforming reactions, the excess steam also promotes the water-gas shift reaction which further increases the H₂ content, and is responsible for the low CO content, and relatively large CO₂ content. Because of the low temperatures, 4% of the carbon exits as char and 3% as tars and oils (corresponding to approximately 1.5 wt% of the dry feed). Furthermore, because char gasification takes place in the gasifier, residence times are longer than for the BCL gasifier, which lowers the throughput rate (see Table 3-5). The use of in-bed heat exchange tubes also increases the overall size of the gasifier for a given throughput rate.

(iii) The Wright Malta (WM) Gasifier

The WM gasifier is a pressurized (1.5 MPa) rotor kiln (Figure 3-18) that utilizes wet biomass directly, without the need for drying (Coffman, 1981; Coffman and Hooverman, 1978). Biomass enters one end of the cylindrical kiln and is continuously mixed by slowly rotating vanes within the kiln. The unit is tilted slightly so that solids transport is accomplished using gravity. Ash and unreacted char exit from the other end, as does the product gas. In addition to utilizing a wet feed, the WM gasifier differs in other ways from most gasifiers. It is characterized by unusually low temperatures (up to 600°C), a long solids residence time (approximately 1 hour), and does not require any steam, air or oxygen. The long residence time and the catalytic effects of ash recirculation produce a tar free gas that is near its equilibrium composition (Wright-Malta, 1981) (Table 3-5). As a result, methane accounts for 34% of the gas on a dry basis, by far the highest of all

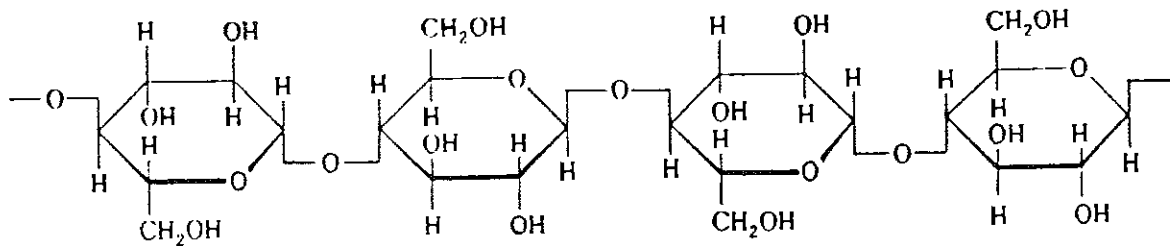
the gasifiers considered in this thesis. The heat for gasification is supplied through a heat exchanger system within the rotating vanes of the kiln (Figure 3-18). According to experimental results, some heat is also supplied by pyrolysis, which is reported to be mildly exothermic under the operating conditions of the WM gasifier (Hooverman, 1979).

Experience with the WM gasifier has been limited to a process demonstration unit (PDU) rated at up to six tonnes of wet biomass per day. Due to the pressurized rotor kiln design, some difficulties were encountered with the sealing of the rotating parts. Mechanical considerations and the low specific throughput rate resulting from the long residence time suggest that the size of a full-scale unit would be limited to about 300 green tonnes per day (Coffman, 1991). In order to achieve higher throughput rates with the WM gasifier it would be necessary to use multiple units in parallel, which would limit the economies of scale. A pilot scale demonstration plant of the WM design is in the planning stages (Coffman, 1991).

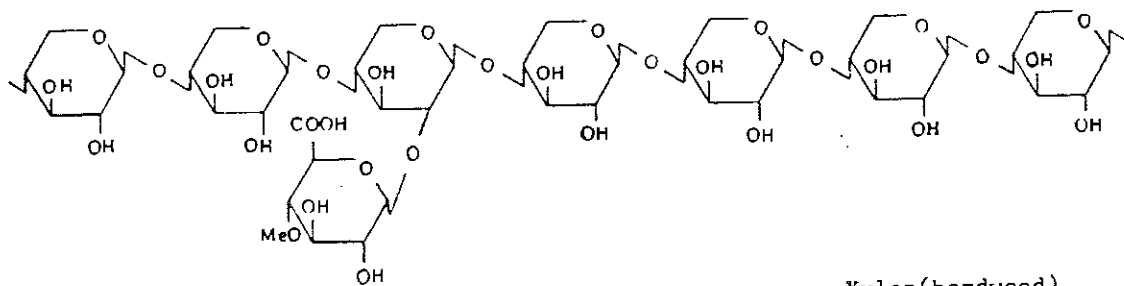
3.5 Summary

The relatively high reactivity of biomass opens up the possibility for innovative gasification processes that are not possible with coal. In particular, by using indirect gasification, it is possible to generate a nitrogen free synthesis gas without the need for a costly oxygen separation facility. Biomass gasification is also characterized by lower operating temperatures, lower levels of sulfur compounds in the product gas, less ash production, and ash that does not contain hazardous compounds. This chapter has also shown, that because of its chemical properties, biomass can be gasified more efficiently than coal in properly designed gasifiers. Nevertheless, coal gasification is at a more advanced stage of development, and in addition to the need for more commercial demonstration projects of biomass gasification technologies, there are two important issues that need to be addressed with biomass gasification systems that are generally not

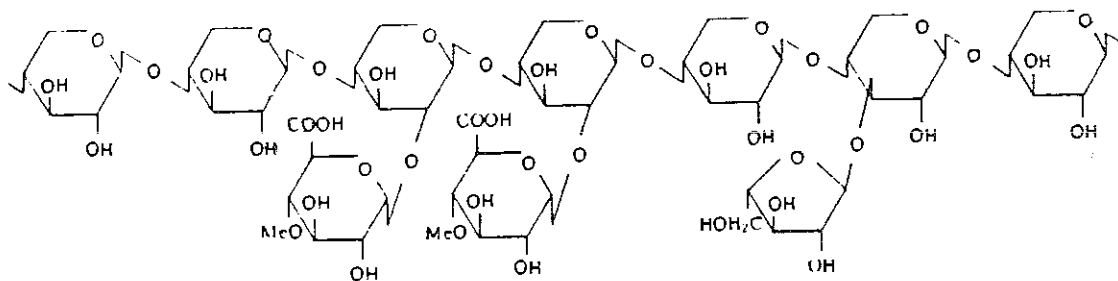
problems with coal gasification systems, for fluid fuels production. They are the presence of tars and oils in the product gas, and the relatively high levels of methane and other hydrocarbons in the product gas. Strategies for dealing with these compounds will be addressed in the upcoming chapters.



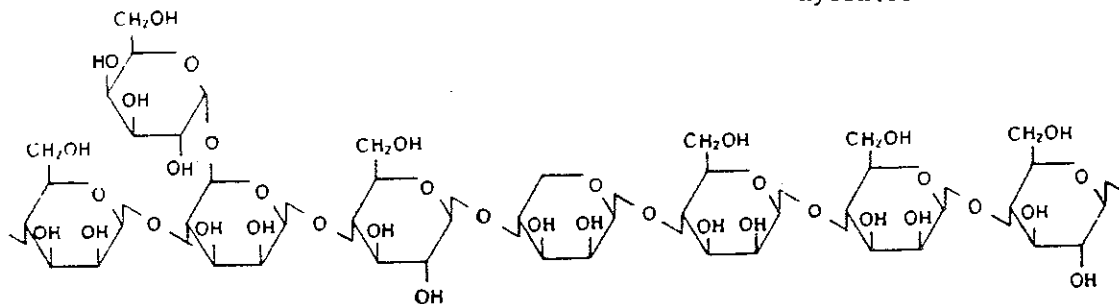
Cellulose



Xylan(hardwood)



Xylan(softwood)



Glucomannan(softwood)

Figure 3-1: The chemical structures of cellulose (top) and three different types of hemicellulose, two of the main components of biomass (Sudo, et al., 1989).

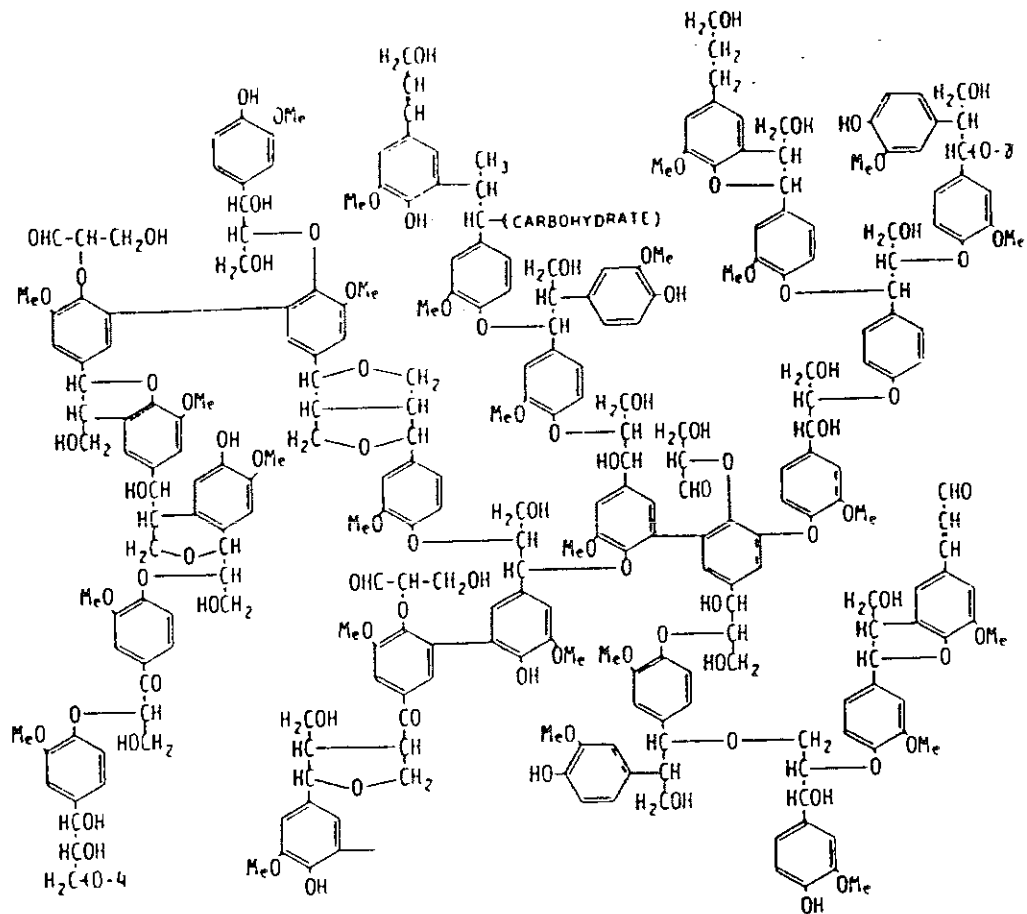


Figure 3-2: The chemical structure of lignin, a main component of wood (Sudo, et al., 1989).

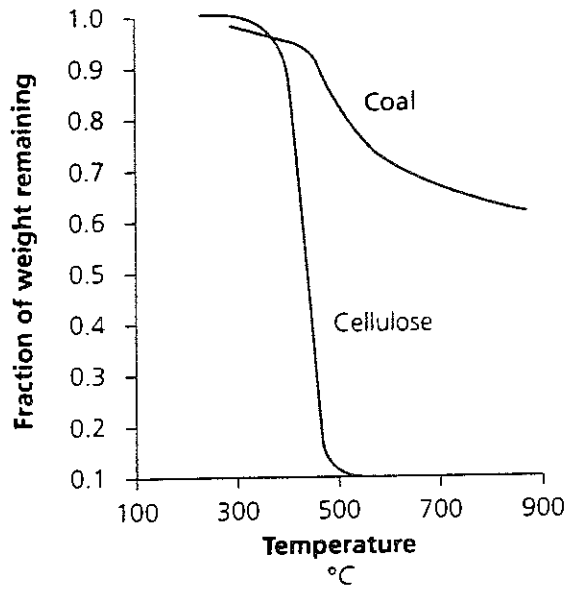


Figure 3-3: Comparison of coal and cellulose pyrolysis (the main component of biomass). Due to the higher volatile content of wood, wood pyrolysis is more complete than coal pyrolysis and takes place at lower temperatures (Antal, 1980).

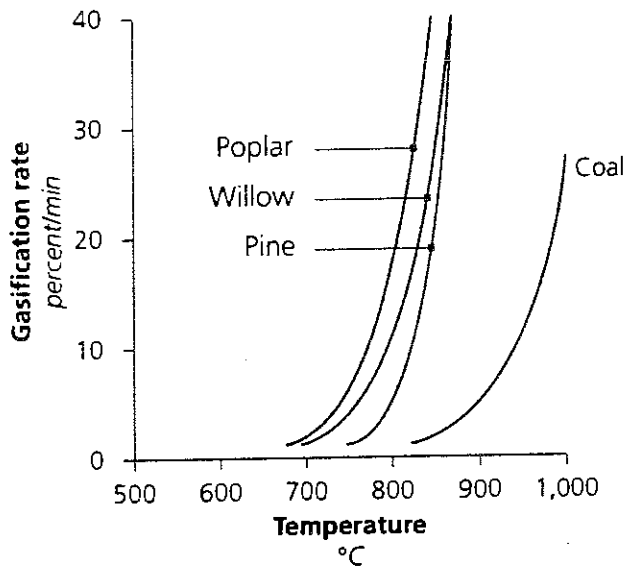


Figure 3-4: Comparison of the reactivity of coal and biomass chars. Biomass chars are much more reactive than coal chars and so gasify more rapidly and at lower temperatures than coal chars (Waldheim and Rensfelt, 1982).

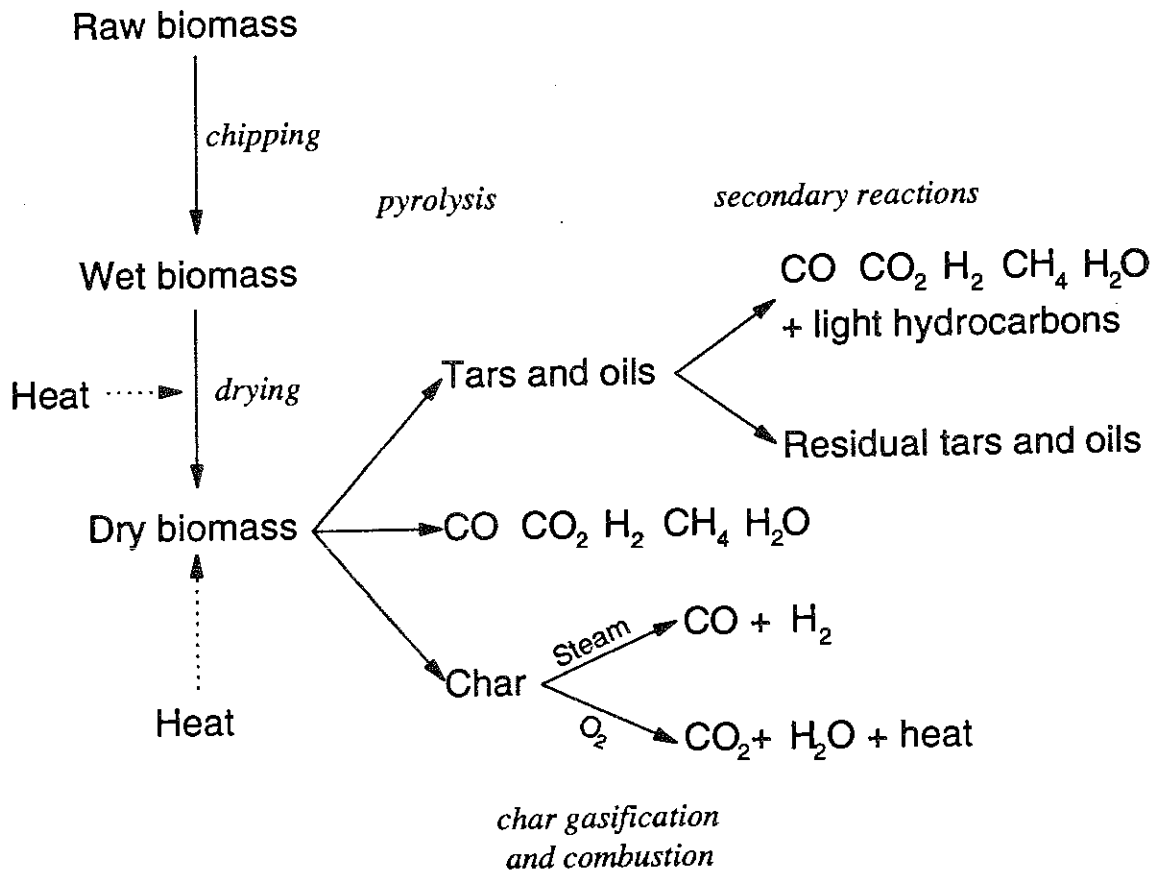


Figure 3-5: Simplified schematic representation of biomass gasification.

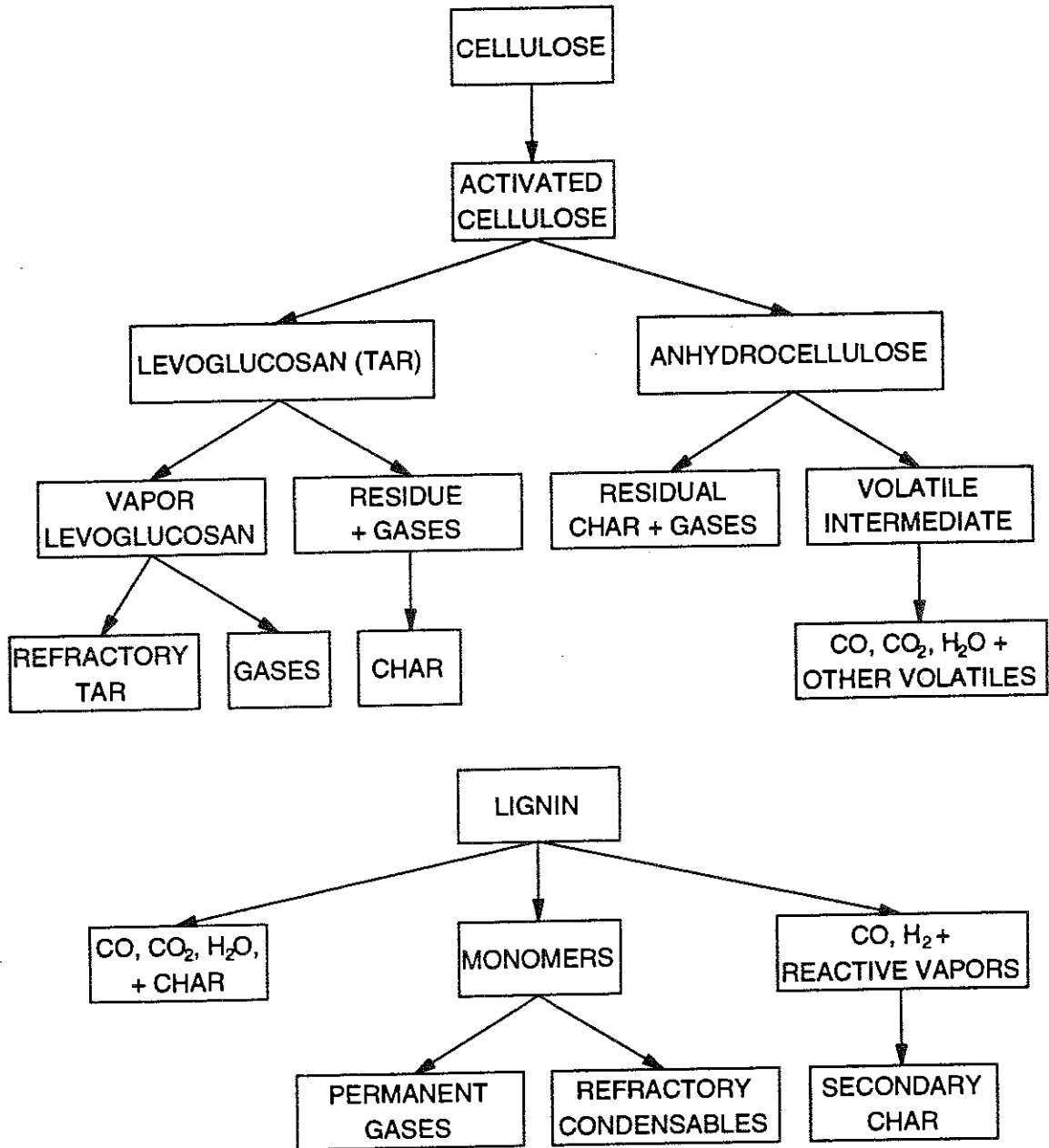


Figure 3-6: Schematic representations of cellulose and lignin pyrolysis (based on Antal, 1983).

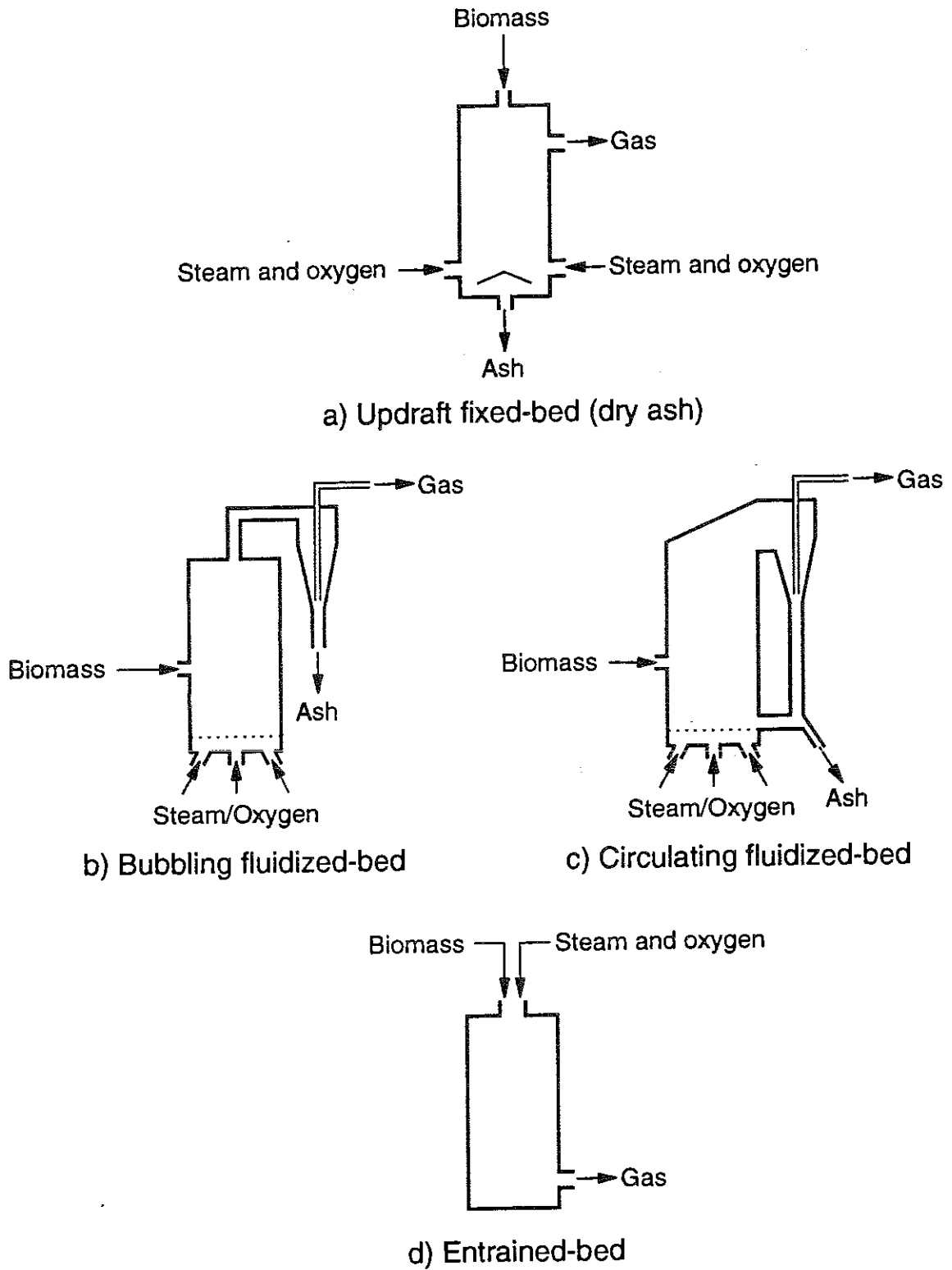
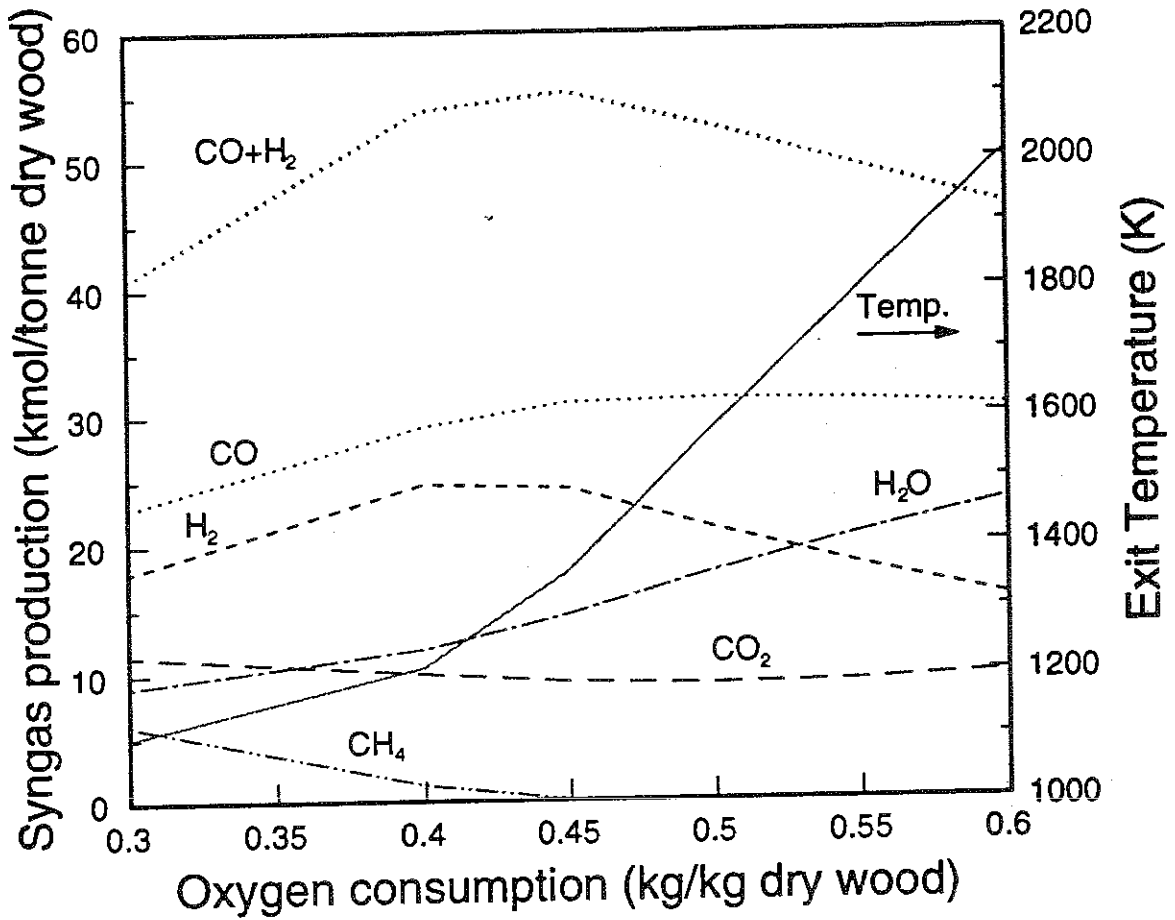
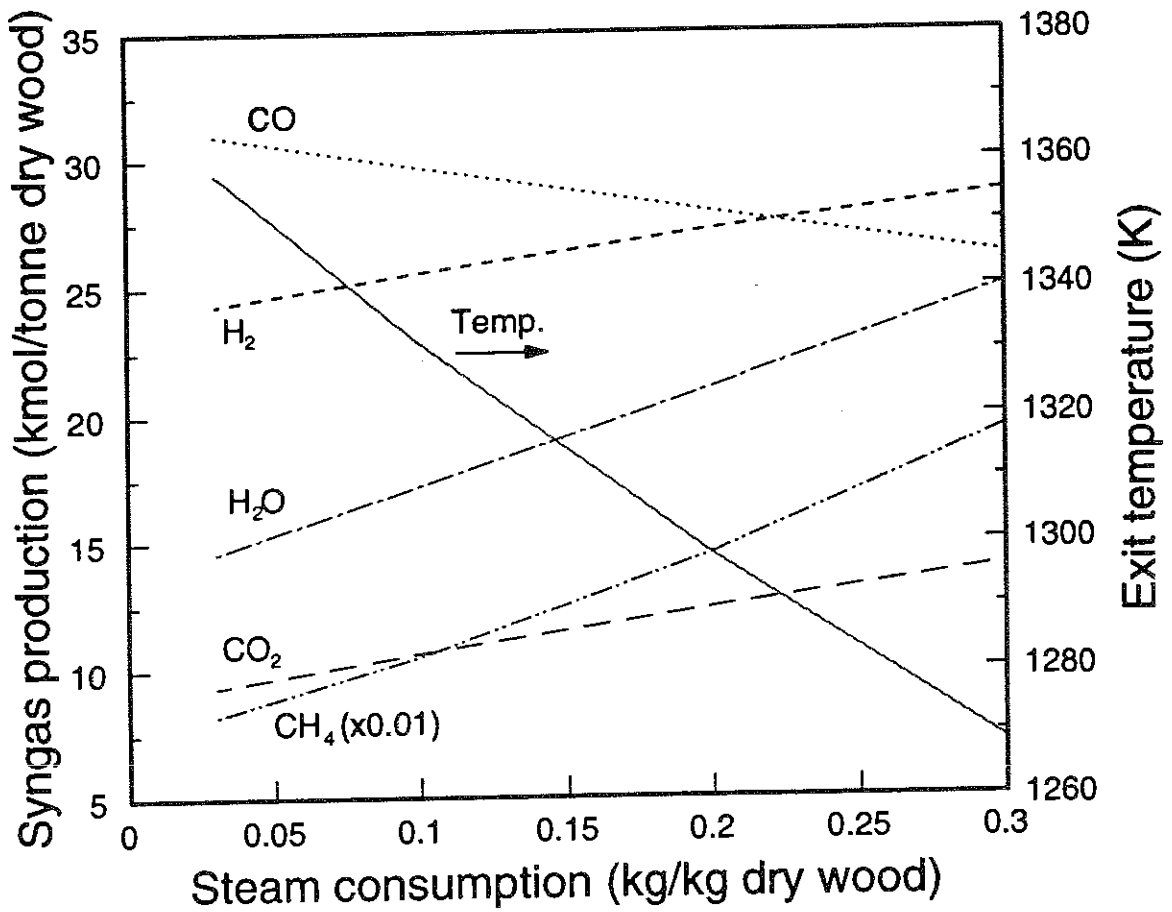


Figure 3-7: Schematic representations of directly heated gasifiers.



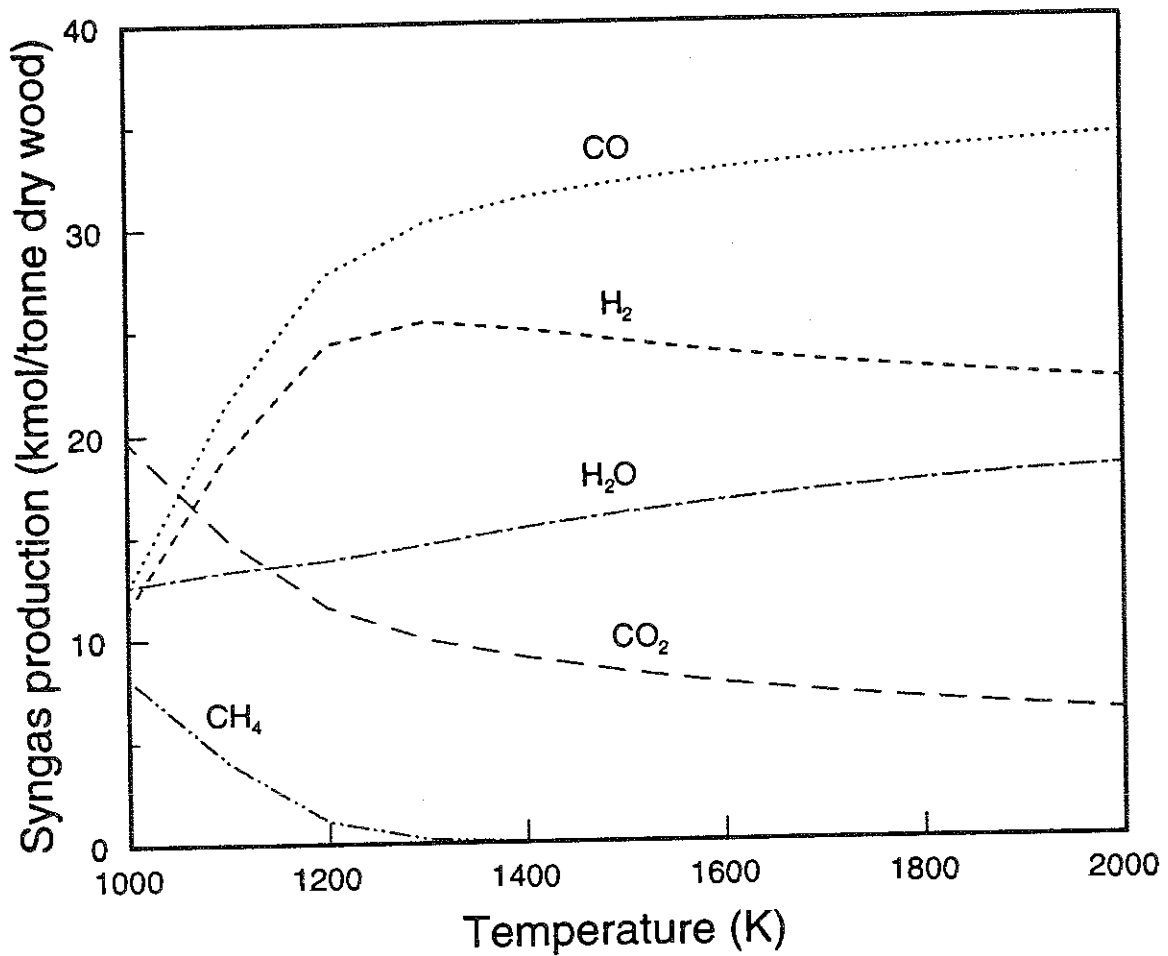
- Pressure = 24 atmospheres (2.43 MPa)
- Steam consumption = 0.03 kg/kg dry wood
- feed moisture content = 11 wt%

Figure 3-8: Effect of oxygen consumption on synthesis gas production and temperature for oxygen blown biomass gasification, assuming chemical equilibrium.



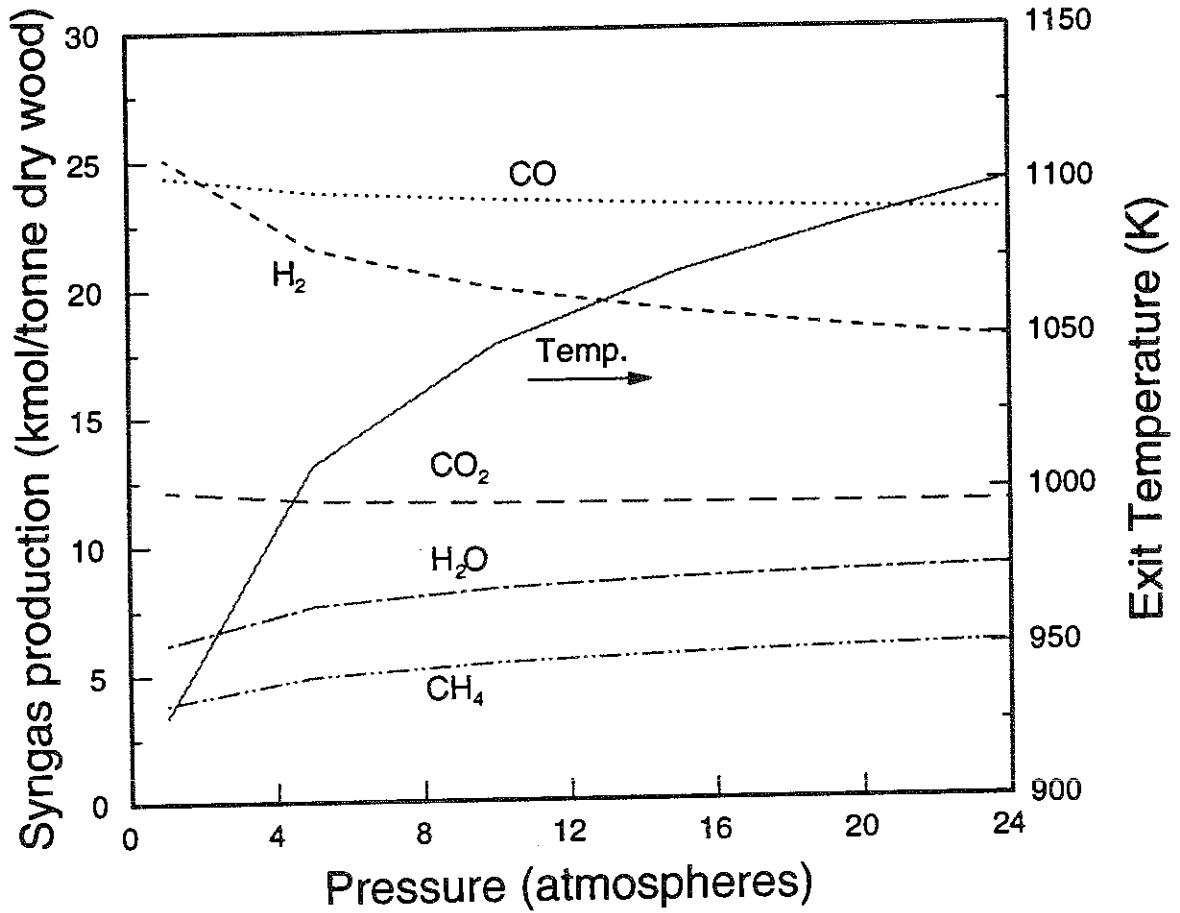
- Pressure = 24 atmospheres (2.43 MPa)
- Oxygen consumption = 0.45 kg/kg dry wood
- feed moisture content = 11 wt%

Figure 3-9: Effect of steam rate on synthesis gas production and temperature for oxygen blown biomass gasification, assuming chemical equilibrium.



- Pressure = 24 atmospheres (2.43 MPa)
- C:H:O = 1:2:1.6

Figure 3-10: Effect of temperature on synthesis gas production for biomass gasification, assuming chemical equilibrium and a fixed C:H:O ratio.



- Oxygen consumption = 0.30 kg/kg dry wood
- Steam consumption = 0.03 kg/kg dry wood
- Feed moisture content = 11 wt%

Figure 3-11: Effect of pressure on synthesis gas production and temperature for oxygen blown biomass gasification, assuming chemical equilibrium and a fixed level of oxygen consumption.

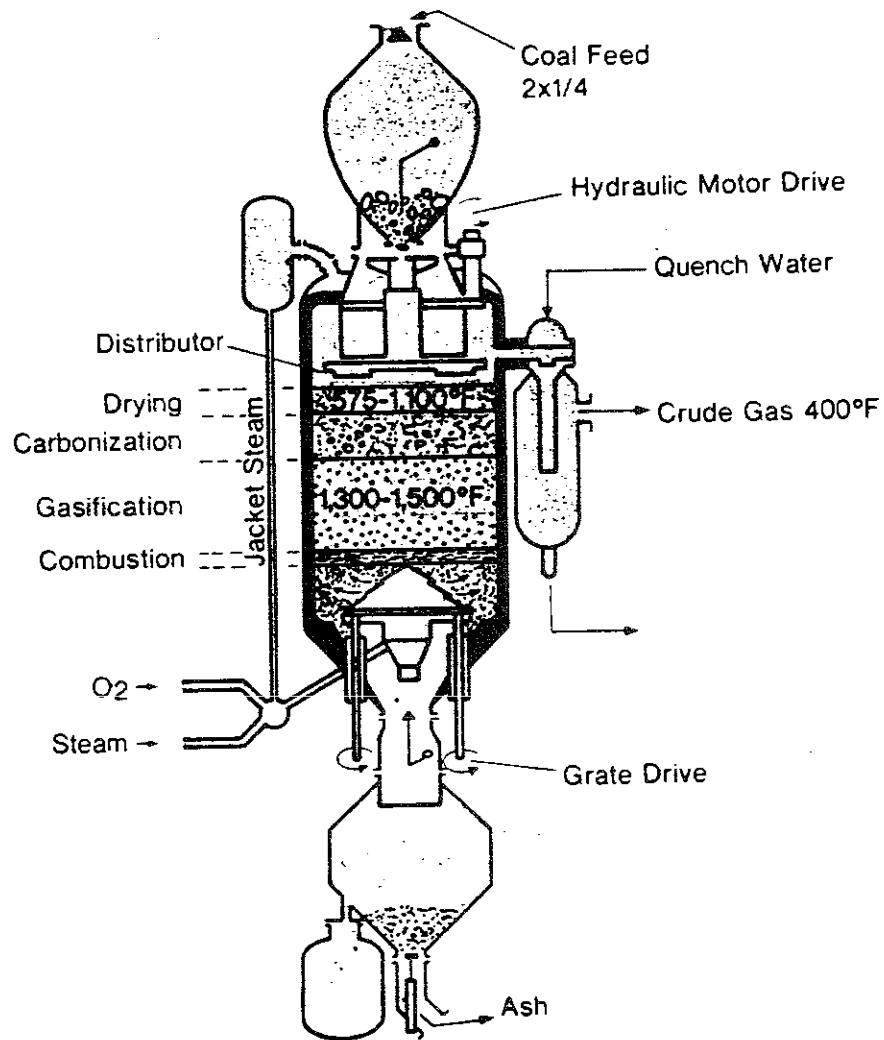


Figure 3-12: The Lurgi fixed-bed coal gasifier (Synthetic Fuels Associates, 1893).

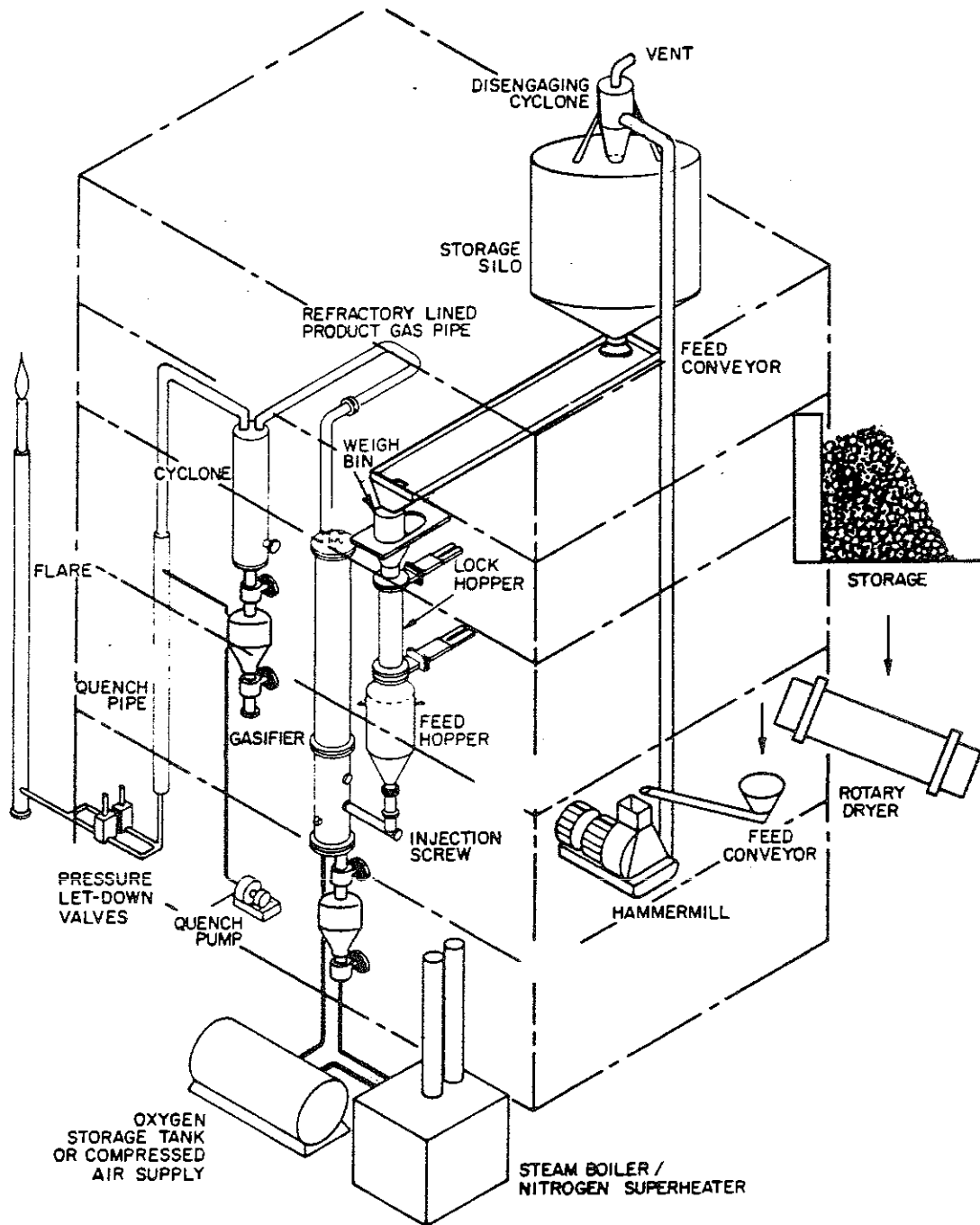


Figure 3-13: The Institute of Gas Technology RENU GAS fluidized-bed oxygen-blown biomass gasifier (Evans, et al, 1988).

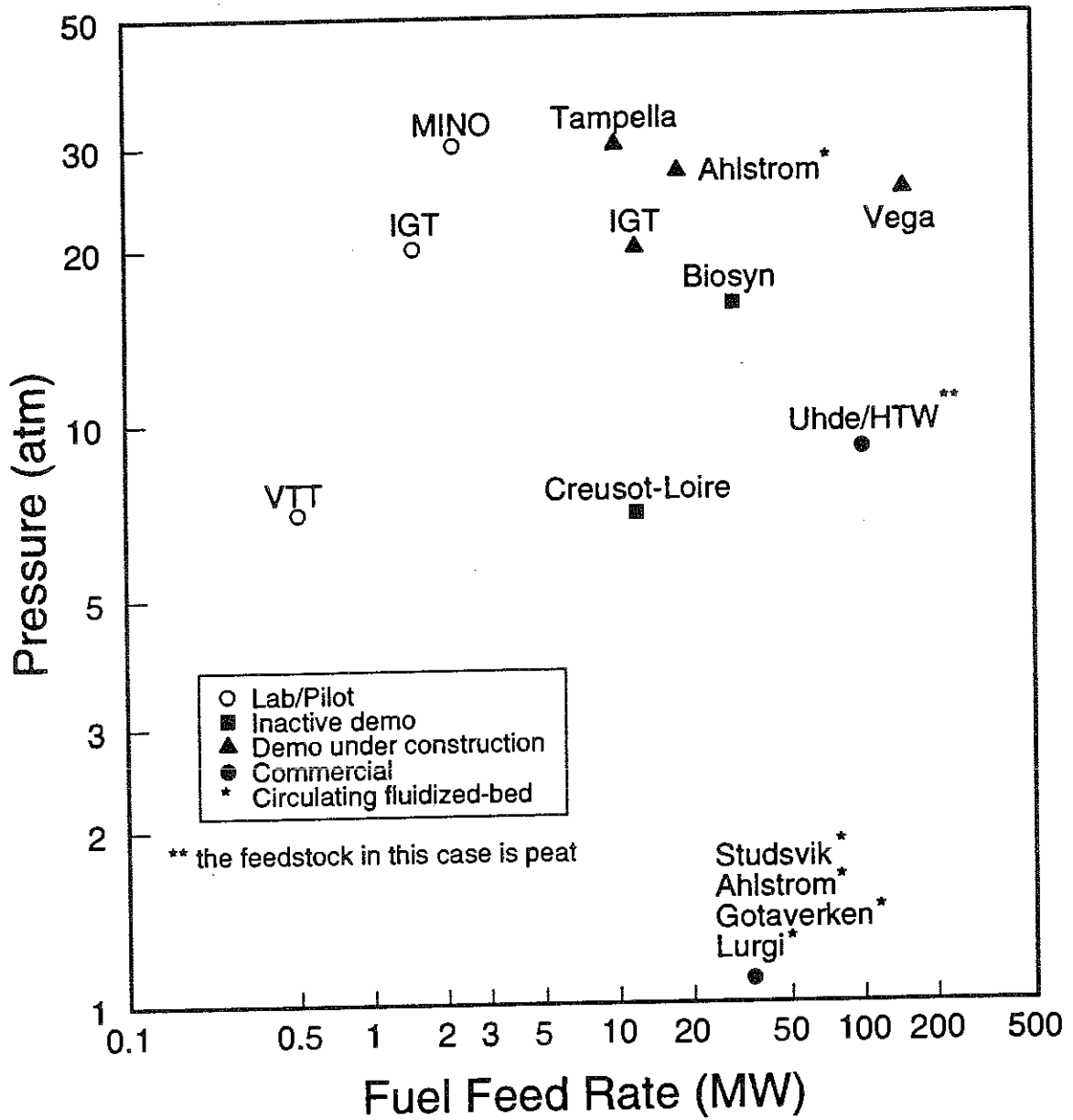
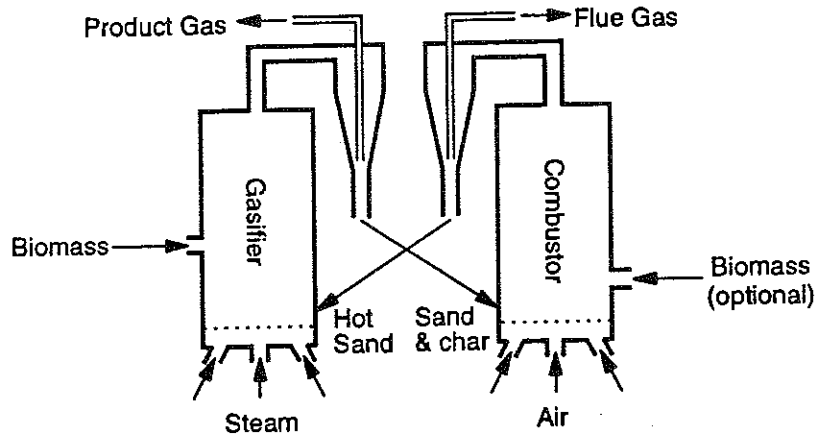
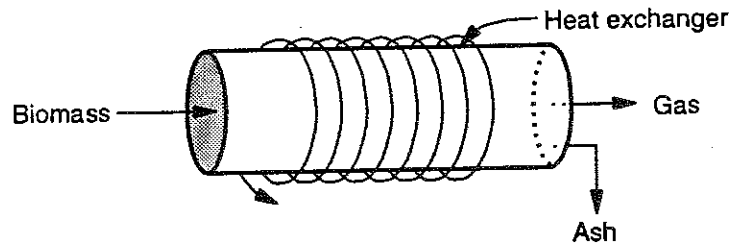


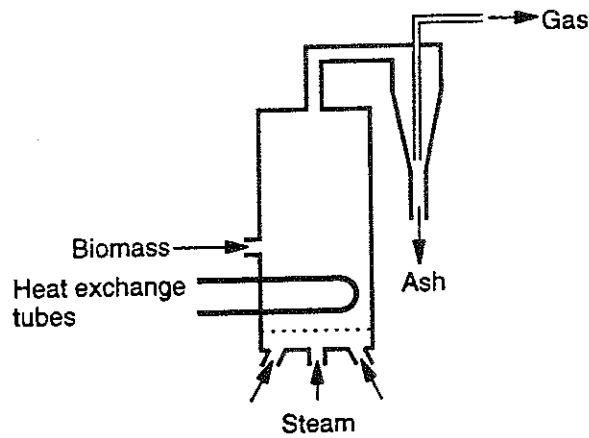
Figure 3-14: Current status of directly heated fluidized-bed biomass gasifiers. Those marked with an asterisk are circulating fluidized beds. All others are bubbling fluidized beds.



(a) indirect heating via direct contact with hot circulating sand.



(b) indirect heating via external heat exchangers.



(c) indirect heating via in-bed heat exchange tubes.

Figure 3-15: Schematic representations of the various heat transfer methods of indirectly heated gasifiers.

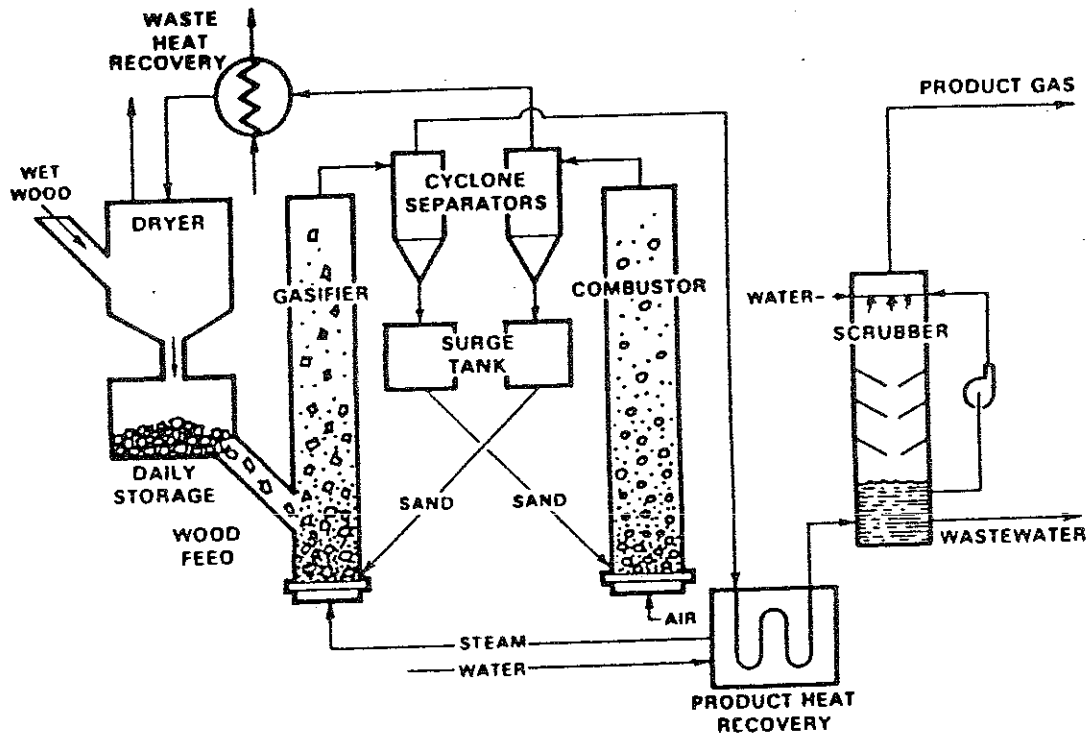


Figure 3-16: Schematic representation of the Battelle-Columbus Laboratory (BCL) indirectly heated gasifier (Feldmann, et al., 1986).

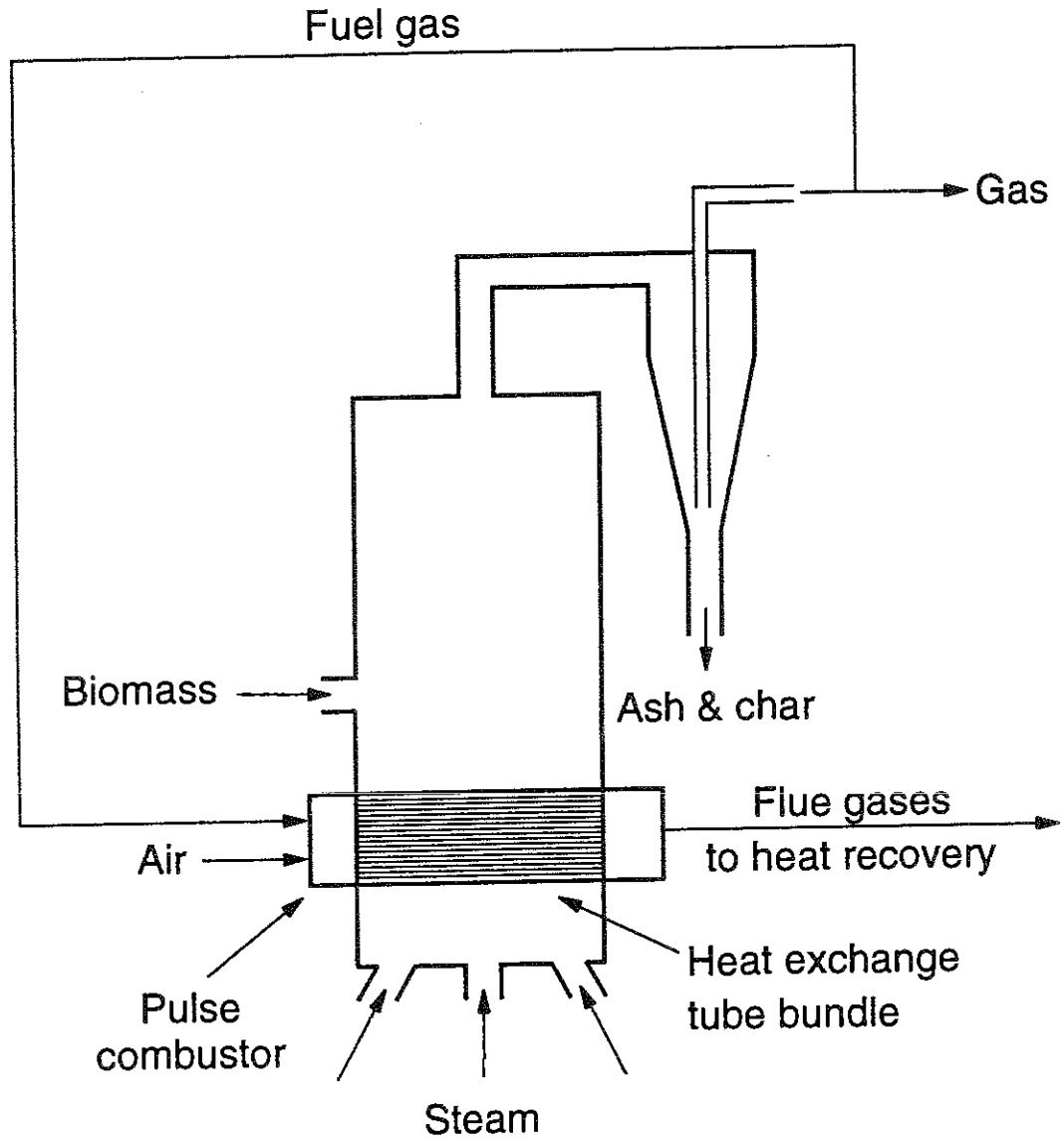
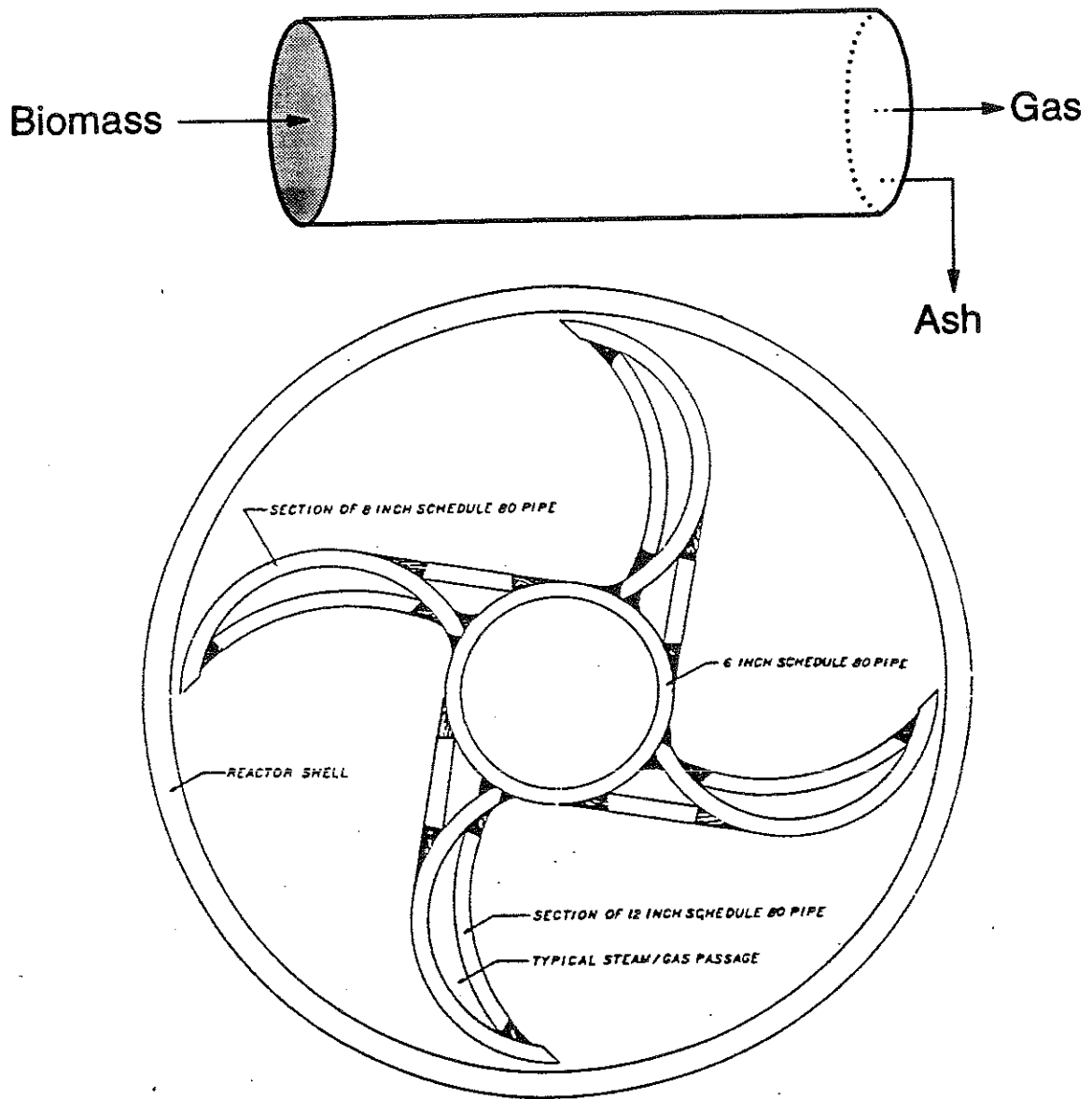


Figure 3-17: Schematic representation of the Manufacturing and Technology Conversion International (MTCI) pulse-enhanced indirectly heated gasifier (based on MTCI 1990).



CURVED VANE ROTOR FOR PDU REACTOR

Figure 3-18: Schematic representation of the Wright-Malta (WM) indirectly heated gasifier. The lower diagram is the cross section.

References

- Antal, M.J. "Thermochemical Conversion of Biomass: The Scientific Aspects." *Energy from Biological Processes*. Vol. IIC. Washington DC: Office of Technology Assessment, 1980.
- Antal, M.J. "The Effects of Residence Time, Temperature, and Pressure on the Steam Gasification of Biomass." *Biomass as a Nonfossil Fuel Source*. Ed. Donald L. Klass. Washington DC: American Chemical Society, 1981.
- Antal, M.J. "Biomass Pyrolysis: A Review of the Literature Part I -- Carbohydrate Pyrolysis." *Advances in Solar Energy*, Vol. 1. Ed. K.W. Boer and J.A. Duffie. New York: American Solar Energy Society, 1982.
- Antal, M.J. "Biomass Pyrolysis: A Review of the Literature Part II -- Lignocellulosic Pyrolysis." *Advances in Solar Energy*, Vol. 2. Ed. K.W. Boer and J.A. Duffie. New York: American Solar Energy Society, 1983.
- Bain, R. "Beneficiation of Biomass." *Biomass Gasification: Principles and Technology*. Ed. T.B. Reed. Park Ridge New Jersey: Noyes Data Corporation, 1981.
- Black, N. "Biomass Gasification Project Gets Funding to Solve Black Liquor Safety and Landfill Problems." *Tappi Journal*. February 1991, pp.65-68.
- "Membranes Shoot for the Big Time." *Chemical Engineering*. April 1990, pp.37-43.
- Coffman, J.A. "Steam Gasification of Biomass." *Proceedings: 13th Biomass Thermochemical Contractors' Meeting*. (PNL-SA-10093) Richland, WA: Pacific Northwest Laboratory, 1981.
- Coffman, J.A. Wright-Malta Corporation, Ballston Spa, New York. Personal Communication, June 1991.
- Coffman, J.A. and Hooverman, R.H. "Power from Wastes via Steam Gasification." *ACS Symposium Series No. 76*. Washington DC: American Chemical Society, 1978.
- Cool Water Coal Gasification Program: Final Report*. (EPRI GS-6806) Prepared by the Cool Water Coal Gasification Program and Radian Corporation for the Electric Power Research Institute. Palo Alto, CA: The Electric Power Research Institute, December 1990.
- Deglise, X. and Magne, P. "Pyrolysis and Industrial Charcoal." *Biomass: Regenerable Energy*. Ed. D.O. Hall and R.P. Overend. Chichester: John Wiley & Sons, 1987.

- Desrosiers "Thermodynamics of Char Gasification." *Biomass Gasification: Principles and Technology*. Ed. T.B. Reed. Park Ridge New Jersey: Noyes Data Corporation, 1981.
- Durai-Swamy, K. (Senior Vice President). Manufacturing and Technology Conversion International, Santa Fe Springs, CA. Personal communication. September 1992.
- Durai-Swamy, K. (Senior Vice President). Manufacturing and Technology Conversion International, Santa Fe Springs, CA. Personal communication. February 1993.
- Durai-Swamy, K. Warren, D.W., and Mansour, M.N. Indirect Steam Gasification of Paper Mill Sludge Waste." *Tappi Journal*. 74(10), October 1991a. pp.137-143.
- Durai-Swamy, K. Mansour, M.N., and Warren, D. *Pulsed Combustion Process for Black Liquor Gasification*. (DOE/CE/40893-T1) Washington DC: US Department of Energy, February 1991b.
- Evans, R.J., Knight, R.A., Onischak, M., and Babu, S.P. *Development of Biomass Gasification to Produce Substitute Fuels*. (PNL-6518) Richland, WA: Pacific Northwest Laboratory, March 1988.
- Feldmann, H.F., Paisley, M.A., Appelbaum, H.R., and Taylor, D.R. "Conversion of Forest Residues to a Methane-Rich Gas in a High-Throughput Gasifier." *Proceedings of the 1985 Biomass Thermochemical Conversion Contractors' Meeting*. (PNL-SA-13571) February 1986.
- Feldmann, H.F., Paisley, M.A., Appelbaum, H.R., and Taylor, D.R. *Conversion of Forest Residues to a Methane-Rich Gas in a High-Throughput Gasifier*. (PNL Report No. PNL-6570) Prepared by the Battelle Columbus Division for Pacific Northwest Laboratory, Richland, WA, 1988.
- Flanigan, V.J., Sitton, O.C., and Huang, W.E. *The Development of a 20-Inch Indirect Fired Fluidized Bed Gasifier*. (PNL-6520) Richland, WA: Pacific Northwest Laboratory, 1988.
- General Electric Company. *Biomass Feedstock Evaluations: Vermont Program*. Schenectady, New York: Corporate Research and Development, 1992.
- Graboski, M.S. "Comparison of Coal and Wood as Feedstocks for Methanol Manufacture." *Proceedings: Biomass-to-Methanol Specialists Workshop*. Ed. T.B. Reed and M.S. Graboski. Solar Energy Research Institute, Golden, Colorado, March, 1982.
- Graboski, M.S. "Kinetics of Char Gasification." *Biomass Gasification: Principles and Technology*. Ed. T.B. Reed. Park Ridge New Jersey: Noyes Data Corporation, 1981.

- Hall, D.O. and Overend, R.P., ed. *Biomass: Regenerable Energy*. Chichester: John Wiley & Sons, 1987.
- Hall, David, O., Rosillo-Calle, Frank, Williams, Robert H., and Woods, Jeremy. "Biomass for Energy, Supply Prospects." *Renewable Energy: Sources for Fuels and Electricity*. Ed. T.B. Johansson, H. Kelly, A.K.N. Reddy, and R.H. Williams. Washington DC: Island Press, 1992.
- Hooverman, Roger H. *Catalyzed Steam Gasification of Biomass, Phase II*. Final Research Report prepared for the US Department of Energy (contract ET-78-C-02-4736). Ballston Spa, New York: Wright-Malta Corporation, May 1979.
- Hulkkonen, S. Raiko, M. and Äijälä, M. *New Power Plant Concept for Moist Fuels, IVOSDIG*. Paper presented at the International Gas Turbine And Aeroengine Congress and Exposition. Orlando, FL, June 3-6, 1991.
- Jenkins, B.M. "Physical Properties of Biomass." *Biomass Handbook*. Ed. Osamu Kitani and Carl W. Hall. New York: Gordon and Breach Science Publishers, 1989.
- Jensen, R.P., Mahagaokar, U., and Krewinghaus, A.B. *SCGP - Progress in a Proven, Versatile, and Robust Technology*. Presented at the Ninth EPRI Conference on Coal Gasification Power Plants. September 1990.
- Johansson, Thomas B., Kelly, Henry, Reddy, Amulya K.N., and Williams, Robert H. "Renewable Fuels and Electricity for a Growing World Economy: Defining and Achieving the Potential." *Renewable Energy: Sources for Fuels and Electricity*. Ed. T.B. Johansson, H. Kelly, A.K.N. Reddy, and R.H. Williams. Washington DC: Island Press, 1992a.
- Kimura, G. General Electric Company, Schenectady, NY. Personal communication to Dr. Eric Larson. March 1992.
- Klosek, Joseph, Smith, Arthur, Solomon, James, and Brown, William R. *Oxygen Production Technologies for Coal Gasification*. Allentown, PA: Air Products and Chemicals, Inc., 1986.
- Larson, E.D., Svenningsson, P., and Bjerle, Ingemar. "Biomass Gasification for Gas Turbine Power Generation." *Electricity: Efficiency End-Use and New Generation Technologies, and Their Planning Implications*. Ed. T.B. Johansson. B. Bodlund, and R.H. Williams. Lund, Sweden: Lund University Press, 1989, pp.697-739.
- Larson, Eric D. and Katofsky, Ryan E. *Production of Methanol and Hydrogen from Biomass*. PU/CEES Report No. 271. Princeton, New Jersey: Center for Energy and Environmental Studies, Princeton University, 1992.

- Larson, L.E. and Kertamus, N.J. "Production of Methanol from Biomass." *Energy from Biomass and Wastes XI*. Chicago: Institute of Gas Technology, 1988, pp.1053-70.
- Milne, L. "Kinetics of Biomass Pyrolysis." *Biomass Gasification: Principles and Technology*. Ed. T.B. Reed. Park Ridge, NJ: Noyes Data Corporation, 1981.
- MTCI (Manufacturing and Technology Conversion International). *Testing of an Advanced Thermochemical Conversion Reactor System*. (PNL-7245) Richland, WA: Pacific Northwest Laboratory, 1990.
- OPPA (Office of Policy, Planning, and Analysis). *Assessment of Costs and Benefits of Flexible and Alternative Fuel Use in the US Transportation Sector, Technical Report Five: Costs of Methanol Production from Biomass*. DOE/PE-0097P. Washington DC: US Dept. of Energy, December 1990.
- Overend, R.P., Milne, T.A., and Mudge, L.K., ed. *Fundamentals of Thermochemical Biomass Conversion*. London: Elsevier Applied Science, 1985.
- Paisley, Mark. Battelle Columbus Laboratory, Columbus, Ohio. Personal communication. December 1991.
- Paisley, Mark. Battelle Columbus Laboratory, Columbus, Ohio. Personal communication. February 1993.
- Probstein, Ronald F. and Hicks, R. Edwin. *Synthetic Fuels*. New York: McGraw-Hill Book Company, 1982.
- Reed, T.B. ed. *Biomass Gasification: Principles and Technology*. Park Ridge, NJ: Noyes Data Corporation, 1981.
- "Refining Handbook 1990: Fluid Catalytic Cracking." *Hydrocarbon Processing*. November 1990, pp.94-98.
- Shelley, Suzanne. "Out of Thin Air." *Chemical Engineering*. June 1991, pp.30-39.
- Sofer, Samir, S. and Zaborsky, Oskar, R., ed. *Biomass Conversion Processes for Energy and Fuels*. New York: Plenum Press, 1981.
- Stevens, D.J. "Methanol From Biomass: A Technoeconomic Analysis." *Energy for Biomass and Wastes XIV*. Ed. D.L. Klass. Chicago: Institute of Gas Technology, 1991, pp.1245-63.
- Sudo, S., Takahashi, F., and Tekeuchi, M. "Chemical Properties of Biomass." *Biomass Handbook*. Ed. Osamu Kitani and Carl W. Hall. New York: Gordon and Breach Science Publishers, 1989.

- Synthetic Fuels Associates. *Coal Gasification Systems: A Guide to Status, Applications and Economics*. (EPRI AP-3109) Palo Alto, CA: Electric Power Research Institute, June 1983.
- Trenka, A.R., Kinoshita, P.K., Takahashi, C., Caldwell, R., Kwok, R., Onischak, M., and Babu, S.P. "Demonstration Plant for Pressurized Gasification of Biomass Feedstocks." *Energy From Biomass and Wastes XV*. Ed. D.L. Klass. Chicago: Institute of Gas Technology, 1991.
- Trogus, F.J., Krewinghaus, A.B., and Perry, R.T. "Status of the Shell Coal Gasification Demonstration Plant." *Eighth Annual EPRI Conference on Coal Gasification*. (EPRI GS-6485) Palo Alto, CA: Electric Power Research Institute, August 1989.
- Turdera and Zahradnik, *Feasibility Evaluation and Conceptual Design of a Pulse Tube Combustion System for a Commercial Scale Integrated Coal Gasification (IGCC) Power Plant*. Draft report prepared for the US Department of Energy (contract DE-AC21-90MC27346) Washington DC: K&M Engineering and Consulting Corporation, April 1992.
- Waldheim, L. and Rensfelt, E. "Methanol from Wood and Peat." *Proceedings: Biomass-to-Methanol Specialists Workshop*. Ed. T.B. Reed and M.S. Graboski. Solar Energy Research Institute, Golden, Colorado, March, 1982.
- Webb, Rodney M. and Moser, Kenneth W. "The Dow Syngas Project: Recent operating Experience." *Eighth Annual EPRI Conference on Coal Gasification*. (EPRI GS-6485) Palo Alto, CA: Electric Power Research Institute, August 1989.
- Williams, Robert H. and Larson, Eric D. "Advanced Gasification-Based biomass Power Generation." *Renewable Energy: Sources for Fuels and Electricity*. Ed. T.B. Johansson, H. Kelly, A.K.N. Reddy, and R.H. Williams. Washington DC: Island Press, 1992.
- Wright-Malta. *Methanol from Biomass Phase MI: Advance Engineering Process Development Unit*. Prepared for the US Department of Energy (contract No. DE-AC02-78ET-23025). Wright-Malta Corporation with Foster Wheeler Synfuels Corporation, February 1981.
- Wyman, Charles E., Bain, Richard L., Hinman, Norman D., and Stevens, Don J. "Ethanol and Methanol from Cellulosic Biomass." *Renewable Energy: Sources for Fuels and Electricity*. Ed. T.B. Johansson, H. Kelly, A.K.N. Reddy, and R.H. Williams. Washington DC: Island Press, 1992.

Appendix 3A: Equilibrium Modeling of Entrained-Bed Biomass Gasification

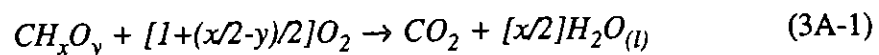
3A.1 Introduction

This appendix outlines the method used to calculate the product gas composition, flow rate, and temperature for entrained-bed biomass gasification, assuming chemical equilibrium. The reasons why chemical equilibrium can be assumed for entrained-bed gasification are (i) the high operating temperatures characteristic of this process, and (ii) the very fine particle size of the feed. Both of these features would produce reaction rates that would be significantly higher than for other types of biomass gasification systems. The technology that has been selected for modeling purposes is the Shell gasifier, a near-commercial, "second-generation", dry feed, entrained-bed gasifier developed for coal that could probably be adapted for biomass.

The gasification step was modeled as an adiabatic, constant pressure process (constant enthalpy). Therefore, the exit temperature is one of the variables determined by the equilibrium calculations, and depends on parameters such as the amount of oxygen or steam added, and the moisture content of the feed. The inputs that are required for the equilibrium model are (i) the relative atom populations, (ii) the enthalpy of the combined feed (J/kg) (iii) the gasification pressure, and (iv) the compounds present at equilibrium.

3A.2 Wood Enthalpy Calculations

The first step is to estimate the enthalpy of the wood based on its dry elemental composition (CH_xO_y) and its heating value. Consider the complete combustion of wood with a stoichiometric quantity of oxygen:



By definition, the enthalpy of combustion (H_c) of a fuel is the difference between the enthalpy of the products (H_p) and the enthalpy of the reactants (H_r) at a given reaction temperature (T_r) and pressure:

$$H_c = H_p(T_r) - H_r(T_r) \quad (3A-2)$$

The higher heating value (*HHV*) is a positive number equal to the magnitude of H_c when the product water is assumed to be in the liquid state.¹ If we set the reaction temperature equal to the reference temperature ($T_o = 298.15$ K) then the enthalpy values in equation (3A-2) correspond to the *enthalpies of formation*, which simplifies calculations.² Therefore, we have:

$$HHV = -H_c = H_r(T_o) - H_p(T_o) \quad (3A-3)$$

Since the heating values of wood are tabulated, and $H_p(T_o)$ is easily calculated using standard heats of formation for CO_2 and H_2O , we can determine the heat of formation of wood by rearranging equation (3A-3):

¹ The lower heating value assumes that the product water is in the vapor phase.

² The enthalpy of a substance is the sum of the *enthalpy of formation* (h_f^o) and the *sensible* enthalpy (which are both functions of temperature and pressure). Since enthalpy is not an absolute quantity, it is always measured relative to some reference state, usually $T_o = 298.15$ K and $P_o = 1$ atmosphere. Pure substances ($\text{C}_{(s)}$, O_2 , N_2 , H_2 , etc.) are defined to have enthalpies of formation of zero, and the enthalpies of formation of all other compounds are measured relative to these compounds (i.e. how much enthalpy must be added or removed at a given T and p when a compound is formed from these pure substances). For example, when 1 kmole of carbon is combined with 2 kmoles hydrogen to form 1 kmole of methane at T_o and P_o , 74.85 MJ must be removed (i.e. $h_{f,\text{methane}}^o = -74.85$ MJ/kmol). For simplicity, the sensible enthalpy of any substance is often defined to be zero at T_o and P_o (as is done here), and increases with temperature. For example, the sensible enthalpy of methane at 1000 K is approximately 38.2 MJ/kmol. For ideal gases, enthalpy is a function of temperature only.

$$H_{f,wood}^o = H_r(T_o) = HHV_{wood} + H_p(T_o) \quad (3A-4)$$

Since higher heating values are usually given per unit weight of fuel, a *molecular weight*³ for the empirical formula of dry wood given in Equation (3A-1) can be computed and used to normalize the enthalpy of the combustion products per unit mass of wood fuel:

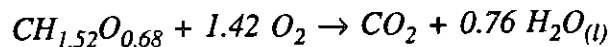
$$MW = 12.011(1) + 1.0079(x) + 16(y) \quad (3A-5)$$

then:
$$h_p(T_o) = H_p(T_o)/MW \quad (3A-6)$$

Now, the enthalpy of formation of wood on a unit mass basis is:

$$h_{f,wood}^o = h_{wood}(T_o) = HHV_{wood} + h_p(T_o) \quad (3A-7)$$

To illustrate, consider the following example. The relevant properties for dry wood are given in Table 3A-1. Equation (3A-1) becomes:



The enthalpy of the products at the reference temperature is:

$$\begin{aligned} H_p(298) &= (1)(-393,520) + (0.76)(-285,830) \\ &= -610,138 \text{ kJ/kmole } CH_{1.52}O_{0.68} \end{aligned}$$

³ This is not a true molecular weight since biomass has no simple chemical structure. Rather this is the empirical molecular weight based on 1 kmole of carbon.

Table 3A-1: Wood properties needed for enthalpy calculations

Element	Ultimate Analysis (weight %)	Relative atom population
C	48.51	1.0
H	6.17	1.5157
O	44.22	0.6843
N	0.12	0.0021
S	0.04	0.0003
Ash	0.94	---
Moisture content (%)	10.49	
HHV (MJ/kg dry wood)	19.28	
Molecular weight (kg/kmole)	24.53	

Dividing by the *molecular weight*, we get:

$$h_p(298) = -24,876 \text{ kJ/kg dry wood}$$

Finally, according to equation (3A-7), the enthalpy of formation of wood is:

$$h_{f,wood}^o = 19,280 + -24,876 = -5,596 \text{ kJ/kg}^4$$

3A.3 Combined Feed Enthalpy Calculations

Now that the enthalpy of formation of the wood is known, it is possible to add the enthalpy contributions of the other inputs to the gasifier and compute an overall enthalpy for the gasifier feed. The overall C:H:O ratio must also be calculated. It is important to make certain that the enthalpy values used for all feeds are based on the same reference temperature. For the purposes of this model, the following assumptions about the remaining inputs were made:

⁴ For comparison, the standard heat of formation of cellulose is -3,959 kJ/kg (Walsh, 1991).

- Steam added to the gasifier has the ideal gas enthalpy of water vapor at 500 K.
- Oxygen added to the gasifier is an ideal gas at 298 K.
- The biomass is fed at 398 K (the assumed exit temperature of the drier).

Because the biomass is fed at 398 K it is necessary to estimate the sensible enthalpy of the wood. The specific heat of dry wood was taken to be 1.4 kJ/kg-K (Jenkins, 1989). Therefore, the enthalpy of the dry wood feed (in kJ/kg) is:

$$h_{wood} = h_{f,wood}^o + (1.4)(100)$$

Any moisture that remains in the feed must also be included in the overall enthalpy balance. The enthalpy used was for saturated liquid water at 398 K. Therefore, for one kilogram of dry wood, the total enthalpy of the combined feed is:

$$h_{feed} = \frac{1 * h_{wood} + m_{moisture} h_{moisture} + m_{steam} h_{steam} + m_{ox} h_{ox}}{1 + m_{moisture} + m_{steam} + m_{ox}} \quad (3A-8)$$

where:

- $m_{moisture}$ = amount of moisture per kg dry wood
- m_{steam} = amount of steam per kg dry wood
- m_{ox} = amount of oxygen per kg dry wood
- $h_{moisture}$ = enthalpy of liquid water @ 398 K = -15,509.3 kJ/kg
- h_{steam} = enthalpy of ideal gas water vapor @ 500 K = -13,038.2 kJ/kg
- h_{ox} = enthalpy of oxygen @ 298 K = 0 kJ/kg

As mentioned above, the model assumes that gasification takes place adiabatically and at constant pressure. Under these conditions, the enthalpy of an open system is conserved,

and since mass is also conserved, the specific enthalpy of the products equals the specific enthalpy of the reactants, that is:

$$h_p(T_f) = h_{feed} \quad (3A-9)$$

where: h_p = the specific enthalpy of the products present at equilibrium.
 T_f = the equilibrium temperature.

For example, if the wood in Table 3A-1 is combined with 0.45 kg O₂/kg dry wood and 0.03 kg steam/kg dry wood, then the enthalpy of the feed is -4,832.49 kJ/kg and the relative C:H:O:N:S populations are 1 : 1.93 : 1.59 : 0.002 : 0.0003.

3A.4 Equilibrium Calculations

The final step is to use this information to calculate the equilibrium composition. This was carried out using STANJAN[®], a PC-based chemical equilibrium solver developed at Stanford University (Stanford University, 1987). In addition to the assumption of adiabatic operation, it was also assumed that carbon conversion to gas was 100% and that the following species would be present at equilibrium: H₂, CO, CO₂, CH₄, H₂O, and N₂ (sulfur is neglected), both of which are consistent with operating experience with entrained-flow gasifiers (Synthetic Fuels Associates, 1983; OPPA, 1990). The pressure was 2.43 MPa (24 atmospheres), the operating pressure of the Shell gasifier (Synthetic Fuels Associates, 1983).

Table 3A-2 gives both the STANJAN output and the overall energy balances for the gasifier under the above operating conditions. Using the STANJAN output it is then possible to calculate the overall gas yield since it provides information on the total number of kmols of gas produced for the atom populations given (in the column titled

"mols*" in the STANJAN output). In this particular case we know the kmoles of gas produced per kmole of carbon (1.964), and we can convert this to the volume of gas produced per kg of dry wood by multiplying by the number of kmoles of carbon per kg of dry wood (0.0408). Therefore, the total gas yield is 80.13 kmol/dry tonne, and on a dry gas basis, it is 65.45 kmol/dry tonne.

References

- Jenkins, B.M. "Physical Properties of Biomass." *Biomass Handbook*. Ed. Osamu Kitani and Carl W. Hall. New York: Gordon and Breach Science Publishers, 1989.
- OPPA (Office of Policy, Planning, and Analysis). *Assessment of Costs and Benefits of Flexible and Alternative Fuel Use in the US Transportation Sector, Technical Report Five: Costs of Methanol Production from Biomass*. (DOE/PE-0097P) Washington DC: US Department of Energy, December 1990.
- Stanford University. *STANJAN[®] Chemical Equilibrium Solver, version 3.52*. Computer Software. Stanford University, 1987.
- Synthetic Fuels Associates. *Coal Gasification Systems: A Guide to Status, Applications and Economics*. (EPRI AP-3109) Palo Alto, CA: Electric Power Research Institute, June 1983.
- Walsh, John H. *Reiterative Procedure for the Calculation of Heat Balances in the Entrained-Flow Gasification of Biomass*. Unpublished manuscript, Ottawa, Ontario, August 1991.

Table 3A-2: Sample STANJAN[®] output and calculated gasifier operating characteristics for entrained-bed gasification of biomass.

STANJAN[®] Output

Independent atom	relative population	element potential		
C	1.00000000E+00	-4.4785		
H	1.93411800E+00	-8.1534		
O	1.58985500E+00	-29.5218		
N	2.12200000E-03	-15.0218		

Composition at T = 1357.83 K P = 2.400E+01 atmospheres

species	mol fraction in the phase	mol fraction in mixture	mass fraction in mixture	mols*
Phase 1: molal mass = 20.075 kg/kmol				
H2	.30667E+00	.30667E+00	.30798E-01	6.02321E-01
CO	.39039E+00	.39039E+00	.54472E+00	7.66744E-01
CO2	.11773E+00	.11773E+00	.25810E+00	2.31221E-01
CH4	.10360E-02	.10360E-02	.82791E-03	2.03469E-03
H2O	.18364E+00	.18364E+00	.16480E+00	3.60669E-01
N2	.54021E-03	.54021E-03	.75385E-03	1.06100E-03

* Species mols for the atom populations in mols.

Mixture properties: molal mass = 20.075 kg/kmol
 T = 1357.83 K P = 2.4318E+06 Pa V = 2.3126E-01 m³/kg
 U = -5.3949E+06 J/kg H = -4.8325E+06 J/kg S = 1.0615E+04 J/kg-K

Made 6 (T,P) iterations; 36 equilibrium iterations; v 3.52 IBM-PC

Overall Gasifier Performance

Overall C:H:O ratio	1:1.93:1.59
Exit Temperature (°C)	1085
Gas Composition (mole %)	
H ₂	30.67
CO	39.04
CO ₂	11.77
CH ₄	0.10
H ₂ O	18.36
N ₂	0.05
Wet gas HHV (MJ/kg)	10.33
Gas yield (dry kmole/tonne dry feed)	65.45
Cold Gas efficiency ^a (%)	85.3

(a) Defined as the higher heating value of the gas divided by the higher heating value of the feed.

Chapter 4: Gas Processing Technology: Fundamental and Practical Considerations

4.1 Introduction

This chapter focusses on analyzing the steps involved in processing the gas produced by biomass gasification, to determine the most suitable operating conditions for the various unit operations. Many of the processes are readily adaptable from natural gas- or coal-based systems or other commercial processes. Advanced technologies that are being developed primarily for natural gas-based processes are also considered, in order to determine if they may be suitable for biomass. The findings of this chapter form the basis for the computer models described in Chapter 5, and the subsequent analysis in Chapter 6.

4.2 Basic Process Configurations for Producing Fluid Fuels from Biomass

Hydrogen and methanol can be produced from biomass using similar processing steps, all of which are commercially available except for the gasifier (Figure 4-1). In both cases, fuel production begins with thermochemical conversion (gasification) of the feedstock. Before the product gas can be processed into hydrogen or methanol it must be cleaned of impurities (particulates, tars and oils, sulfur compounds, and alkali metals) to prevent the fouling or blocking of downstream processing units and the poisoning of certain catalysts (mainly by sulfur). This is accomplished in three steps. First, a cyclone separator removes most of the entrained particulate matter. Second, a direct contact water quench is used to remove smaller particulates, condensable hydrocarbons, alkali compounds, and if present, ammonia (which dissolves readily in water).¹ If necessary, fabric filters can be used for a high degree of removal of very fine (sub-micron)

¹ Waste water treatment is an important issue, but will not be discussed in this thesis.

particulates. Finally, any sulfur in the gas is removed via chemical adsorption on a zinc-oxide guard bed.

Since most biomass gasifiers produce significant quantities of methane and small amounts of other light hydrocarbons, the next step is to *reform* these compounds, so that most of the chemical energy is in the form of CO and H₂.² The methane-steam reforming reaction is:



This step is highly endothermic, and acceptable methane conversion is achieved only at relatively high temperatures (>800°C). Therefore, some energy must be consumed in the form of a fuel gas that is used to supply heat to the reformer. The resulting synthesis gas is then sent to a *shift* reactor that converts CO to H₂ via the water-gas shift reaction:

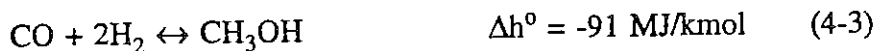


Since it is exothermic, the shift reaction proceeds nearly to completion at low temperatures, and modern catalysts are active as low as 200°C. Following the shift reaction the processing steps differ for hydrogen and methanol production, and each will be described separately.

² On a molar basis, methane and other light hydrocarbons typically account for 10-25% of the combustible components of the gases produced by most biomass gasifiers (the balance is CO and H₂). While this may not seem to be very significant, the heating value of methane on a molar basis is roughly 3 times that of either H₂ or CO, so that methane and light hydrocarbons actually account for approximately 25-50% of the energy content of the product gases.

4.2.1 Methanol Production

In methanol production, if necessary, a shift reactor is used to adjust the H₂:CO ratio to slightly greater than 2:1, the ratio required for methanol synthesis. After the shift reactor, most of the carbon dioxide and all the remaining moisture are removed in a physical separation step and the *makeup* gas is sent to the methanol synthesis loop. The main methanol synthesis reactions are:



Like the shift reaction, methanol synthesis is exothermic, and modern catalysts allow the reactions to proceed at temperatures in the 250-270°C range. A crude methanol product is condensed out by cooling the product gas of the methanol synthesis reactor, and is then sent to a distillation column for purification to fuel grade methanol.³

4.2.2 Hydrogen Production

To produce hydrogen, the shift reactor is used to convert as much of the CO as possible. The gas mixture is then cooled, condensing out most of the remaining moisture. The gas, now approximately 60% hydrogen by volume (the rest being mainly CO₂), is sent to a pressure swing adsorption (PSA) unit that physically separates the hydrogen using molecular sieves. PSA technology exploits the ability of porous materials to trap certain molecules and allow others to pass though unadsorbed. Nearly all the hydrogen is recovered at a purity as high as 99.999%. The hydrogen is then compressed to 7.5 MPa for storage or pipeline transmission. It is also possible to recover hydrogen using several other technologies, but PSA systems produce by far the highest purity H₂, and at the same

³ At this stage the methanol contains water and other impurities such as dissolved gases and higher alcohols formed in the synthesis reactor.

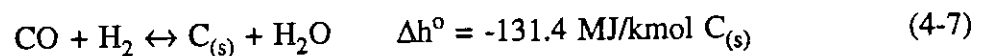
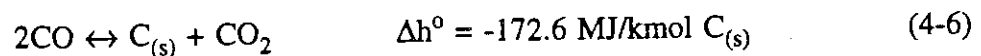
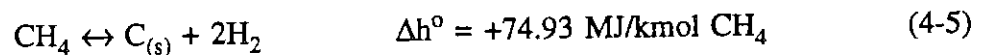
time are cost competitive (van Weenen and Tielrooy, 1983). Moreover, the polymer electrolyte membrane (PEM) fuel cell, the leading candidate for automotive applications, is sensitive to impurities (mainly CO), so that the high purity hydrogen from PSA systems is a definite advantage.

4.3 Some General Considerations for Chemical Reactors

Two important factors must always be considered when designing or modeling chemical reactors: carbon deposition and catalyst activity. Along with temperature and pressure constraints they play large parts in determining the practical limits of a reactor's operating conditions. Therefore, in modeling methanol and hydrogen production from biomass, it is essential to remain within the boundaries set by these two factors, even though, in theory, more favorable operating conditions may exist.

4.3.1 Carbon Deposition

Carbon deposition (or coking) must always be considered in processes that involve hydrocarbons. Coking should be avoided because it reduces the effectiveness of catalysts by blocking active sites and can also clog reactors and foul heat exchangers. Coking also contributes to a small loss of carbon, which lowers overall efficiency. There are three main reactions that can cause carbon deposition:



Reaction (4-5) is the thermal cracking of methane, (4-6) is the Boudouard reaction, and (4-7) is the reverse of the char-steam reaction (char gasification). Considering these reactions as a system, they suggest that excess amounts of steam, carbon dioxide and

hydrogen will help prevent coking, which is indeed the case. In fact, coking is rarely a problem in shift reactors due to the abundance of hydrogen and typically large steam:carbon ratios (Probstein and Hicks, 1982). Since Reactions (4-6) and (4-7) are exothermic, carbon formation from these reactions is reduced at higher temperatures, which is partially offset by the tendency of methane to thermally decompose at higher temperatures. Equilibrium modeling of the six compounds in Reactions (4-5)-(4-7) is given in Figure 4-2 for a pressure of 10 atmospheres and several different C:H:O ratios, some of which correspond to typical values at various stages of hydrogen production. As expected, the figure shows that carbon deposition decreases with increasing temperature as well as with decreasing C:H and C:O ratios.

Although equilibrium calculations are useful for determining the qualitative effects of different parameters on carbon deposition, practical experience has shown that kinetic factors are more important. For example, steam has been found to be more effective than CO_2 at preventing coking. This is due to the fact that the Boudouard reaction (4-6) proceeds much more slowly than the char-steam reaction (4-7). For this reason, and since steam is often a reactant in the system and is more readily available than CO_2 , in practice steam addition is the preferred method of preventing carbon deposition. Overall, carbon deposition has been found to be considerably less likely than what is predicted by equilibrium calculations alone (Probstein and Hicks, 1982). Instead, equilibrium might be used as a good conservative guideline for selecting steam:carbon ratios, although using too much steam would be wasteful.

The steam:carbon ratio will vary from one reactor type to another, and will depend on factors such as the operating conditions, the feed gas composition⁴ and the

⁴ For example, the feed may contain significant quantities of CO_2 and/or H_2 , as is the case with the product gases from some biomass gasifiers.

predisposition of a particular catalyst to promote carbon deposition. With regards to the latter, certain types of coking can be caused by catalyzed reactions that form "polyaromatic coke" by polymerization and dehydrogenation of the feed (Probstein and Hicks, 1982). For example, Short (1989) reported that good temperature control allowed the use of a copper-based shift catalyst instead of an iron-based catalyst at an ammonia synthesis plant. The new catalyst was able to operate at lower a steam:carbon ratio, which reduced overall energy consumption. As another example, Haldor Topsoe, a Danish company, used sulfur to partially poison a nickel-based reforming catalyst, thereby blocking its ability to catalyze carbon formation. In so doing they were able to operate the reformer in a thermodynamic regime in which carbon formation would normally be expected. This method required a highly active catalyst, since partial poisoning also reduced the ability of the catalyst to promote the methane-steam reforming reaction (Dibbern, et al., 1986).

4.3.2 Catalyst Activity

Except for the gasification step, all chemical reactions in the production of hydrogen and methanol rely on catalysts. For exothermic reactions, which are favored at lower temperatures, it is the catalyst that will determine the lowest practical operating temperature. Consider, for example, the water-gas shift reaction (4-2) (see Section 4.6 for more details) that is used to produce hydrogen gas from carbon monoxide. Chemical equilibrium calculations show that lower reaction temperatures more completely shift CO to H₂ (see Figure 4-3). Nevertheless, in the absence of a catalyst, the reaction rate would be so low at these low temperatures that the mixture would be essentially non-reactive. Thermodynamics only determines what the equilibrium composition would be given the temperature, pressure and relative atom population of the mixture, but does not provide any information about the reaction rates and their dependence on variables such as

temperature, pressure and reactant concentrations. The role of the catalyst is to enhance the reaction rate(s) of the desired reaction(s) under favorable thermodynamic conditions.⁵

The limitation imposed by low temperature catalysts is that their activity is also a function of temperature. Therefore, in the case of the low temperature water-gas shift reaction, if the reactor temperature drops below about 200°C, the catalyst itself becomes inactive and the reaction stops, even though hydrogen formation is thermodynamically favored. At higher temperatures the catalyst may be very active but thermodynamics will favor CO formation so that the rate of the desired reaction is again low. This illustrates the trade-off between high reaction rates and favorable thermodynamic conditions characteristic of low temperature reactors. A reactor should be designed to operate in a regime where the desired reaction is thermodynamically favored *and* catalyst activity is high. In such a situation, the driving force of thermodynamics is exploited to the fullest possible extent given the limitations of the catalyst. Figure 4-4 illustrates this principle for the Imperial Chemical Industries (ICI) methanol synthesis catalyst. It shows that the reaction rate of the methanol synthesis reaction peaks at 260°C, but decreases if the temperature is either lowered (low catalyst activity) or raised (methanol formation is not thermodynamically favored). Because reactors are designed to be thermodynamically controlled, they can be modeled using chemical equilibrium calculations. However, chemical equilibrium should not be applied outside a reactor's operating regime.

For endothermic reactions such as methane-steam reforming, which are carried out at high temperatures, catalyst stability is an important concern. Sintering can occur, which results in a loss of surface area and hence reduces the effectiveness of the catalyst.

⁵ In many cases, the thermodynamics are most favorable under conditions for which the reaction would proceed slowly or not at all without the aid of a catalyst.

Materials such as aluminum oxides are often used as inactive support materials for the active compounds.

4.4 Gas Cleanup Technologies

4.4.1 Cyclone Separators

A cyclone separator is the first step in cleaning a gas of solid impurities, and is capable of removing solids down to sizes of approximately 5 μm . The dirty gas tangentially enters a cylindrical or conical vessel so that centrifugal forces push particulates toward the wall of the chamber. The particles eventually fall to the bottom of the cyclone where they are removed. The clean gas exits through the top. An advantage of cyclones is that they are capable of operating at temperatures up to about 1000°C and pressures of 50 MPa and can remove large quantities of entrained solids (i.e. they have a high *solids loading* capability) (Probstein and Hicks, 1982).

4.4.2 Quenching with Water

The use of a direct contact water quench (also called a *scrubber*) is a common method of removing the smaller solid particles that pass through the cyclone as well as condensable hydrocarbons. The inlet temperature of the quench should therefore be above the dew point of these compounds ($\sim 400^\circ\text{C}$) so that they do not condense on any heat recovery equipment that is upstream of the quench vessel. As a result, only some of the sensible heat of the gasifier product gas can be recovered. The gases typically exit the quench step at a relatively low temperature (100°C or less) to ensure adequate removal of condensable compounds. If present, water soluble compounds like ammonia are also removed. The quench step can also be used to remove low boiling point metals such

alkali metals, which are present in small quantities in biomass (mainly sodium and potassium).⁶

The operating principle of a quench vessel is simple. Water is sprayed from the top and descends through the countercurrently flowing gas, trapping particulates along the way. The cooling action of the quench causes tars and oils to condense. Water soluble compounds are dissolved and non-water soluble compounds are simply washed out with the water. The cool, clean gas, saturated with moisture, exits near the top and the water is collected at the bottom for recirculation/treatment. A *Venturi Scrubber* is a specific type of quench system that is used to remove very fine particles (down to 0.5-1 μm).

Since gases enter the quench at relatively high temperatures, the use of a quench step precludes the ability to recover all of the waste heat in the gasifier product gas. As well, the gas must be reheated prior to the reformer or the shift reactors. The resulting energy penalty reduces the overall efficiency of the process. The penalty is more severe with pressurized gasification, since at elevated pressures the moisture fraction of the cooled gas is very low (<5%), necessitating the addition of relatively large amounts of steam for reforming or shifting. By comparison, an atmospheric pressure quench produces a gas with a significant moisture fraction (as high as 50%), which significantly reduces or even eliminates the need for adding steam downstream of the quench step. This "free" steam reduces the energy penalty of the quench step, but is in turn partially offset by the need to compress a relatively large volume of synthesis gas. The energy penalty is also less severe when reforming is not required, since it is not necessary to reheat the synthesis gas to high temperatures.

⁶ If municipal waste were to be gasified, low boiling point metals such as mercury would be present in the product gas, and would also be removed using a low temperature quench.

4.4.3 Sub-micron Particulate Removal

If it is necessary to remove even smaller particles, fabric filters or electrostatic precipitators (ESPs) can be used. Fabric filters are constructed from fiberglass and therefore operate at low temperatures and are sensitive to corrosion, but have very high collection efficiencies (nearly 99.9%),⁷ even for particle sizes down to 0.1 μm . Electrostatic precipitators have the advantage that they can be operated at higher temperatures (300–450°C), but have slightly lower collection efficiencies than fabric filters (90–99%) (Probstein and Hicks, 1982). As the name implies, ESPs remove particulates using electrostatic forces. As a result, the collection efficiencies of ESPs are sensitive to the resistivity of the particles to be removed.

4.4.4 Sulfur Removal

Sulfur, which is usually present as H_2S and COS in syngas, poisons many types of catalysts by chemically bonding to active sites. Since biomass contains little sulfur (0.01–0.1 wt%), bulk removal of sulfur-containing compounds is not necessary, and a zinc oxide (ZnO) guard-bed is sufficient to lower the sulfur concentration below that required for downstream catalysts (~ 0.25 ppm).⁸ Zinc oxide is an inexpensive material which chemically adsorbs sulfur, and is usually disposed of when it is no longer effective. It is also possible to use spent reformer catalyst material as a guard bed, since it too readily adsorbs sulfur (Probstein and Hicks, 1982).

⁷ The collection efficiency measures the fraction of particles of a given size that is removed from the gas. Typically, it is lower for smaller particles sizes.

⁸ For comparison, coal can be up to 5 wt% sulfur, so that it must be removed in two steps. First, a bulk removal system (see Section 4.8) is used to remove most of the sulfur compounds, which are then converted to elemental sulfur in a process known as the Claus Process. Following bulk removal, a ZnO guard bed is used to lower the sulfur level to acceptable levels.

4.4.5 Advanced Hot Gas Cleanup Technologies

Two high temperature processes that could be used to clean synthesis gas are under development. The first process is the catalytic cracking of tars and oils. This process uses a material such as dolomite ($\text{CaMg}(\text{CO}_3)_2$ -- a common mineral) to aid in the decomposition of tars and oils. Two examples are the processes being developed by Studsvik in Sweden and by the Battelle Columbus Laboratory (BCL) in the US (Waldheim, et al., 1991; Paisley, 1993). Both processes use fluidized bed reactors in which the bed material is the catalyst. In the Studsvik design, dolomite is the bed material and air is added to the cracker to maintain a temperature of 800-900°C (the Studsvik gasifier is an air-blown biomass gasifier). The resulting tar/oil content is so low that the gas can be cooled to 200°C before being cleaned of particulates using conventional bag filters and a water scrubber. Waldheim, et al. reported that only small amounts of benzene, toluene and naphthalene remained in the product gas following the cracker. The BCL system is at a less advanced stage of development, and the nature of the catalyst has not been disclosed. This system relies entirely on the sensible heat of the product gas and the exit temperature of the cracker is approximately 800°C. Tar cracking efficiency has been reported to be as high as 90% (Paisley, 1993).

Another promising technology that is close to commercialization is the use of high temperature filters to remove particulates and alkali compounds without the need to cool the gas below the dew point of the tars and oils (Kurkela, et al., 1991; Williams and Larson, 1992). This would be particularly advantageous for BIG/GT applications, which would then be able to burn the tars and oils in the gas turbine combustor. Such filters are similar to the fabric filters described above, but use ceramic fibers or sintered-metal barriers instead of fiberglass, and operate at temperatures up to 720°C. Kurkela, et al. studied the use of SiC-based ceramic filters and reported collection efficiencies greater than 99.8% for a feed with dust particles in the range of 2-7 μm . The concentration of

alkali metals was reduced to less than 0.1 ppm when the filters were operated below 600°C. At these temperatures, alkali metals condense onto particulates, and so can be removed with filters.

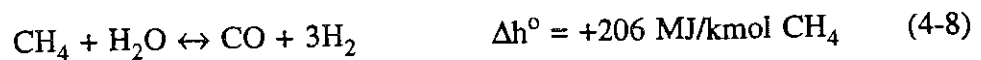
4.5 Methane Reforming

In the presence of a suitable catalyst (usually nickel-based), methane and other light hydrocarbons are reformed into CO and H₂ at high temperatures. Methane reforming is widely carried out by the chemical process industry. It is the first stage in the production of ammonia, methanol, hydrogen chloride and other chemicals, for which natural gas is the primary feedstock.

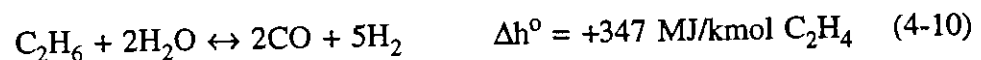
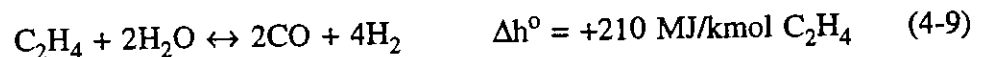
4.5.1 Steam-Methane Reforming

(i) Chemistry

Steam reforming is the most common method of producing a synthesis gas from natural gas. The widespread use of steam reforming in the chemical process industry has produced a mature and efficient technology. Methane is reformed by the following highly endothermic reaction:



Other light hydrocarbons that may also be present in the synthesis gas, such as ethylene and ethane, are reformed similarly:



Since reactions (4-8) to (4-10) are all endothermic, they proceed readily only at relatively high temperatures. As well, since the total number of moles of gas increases significantly, reforming is also favored at lower pressures. Nevertheless, economic and metallurgical considerations place limits on practical operating conditions (see below). The water-gas shift reaction (4-2) also takes place in reformers, so that CO_2 is present in the reformed gas, even if the feed gas is free of CO_2 .

The product gas from the BCL gasifier is used to illustrate the effects of different operating conditions on the reformer product gas (*reformat*) composition. Figure 4-5 shows the effect of temperature for a fixed pressure and steam:hydrocarbon ratio. As can be seen, temperature strongly affects the equilibrium composition. The methane concentration falls off fairly quickly until about 1200 K, at which point it constitutes only about 1% of the gas by volume (wet basis). Methane conversion⁹ is approximately 90% for natural gas systems, and varies from 60-90% for biomass systems, depending on the initial methane concentration and the operating pressure. Conversion of other light hydrocarbons is essentially 100% (Figure 4-6). This should be expected since these larger molecules are much less chemically stable than methane, and are prone to decomposition at elevated temperatures. At temperatures above 1200 K, the reverse of the water-gas shift reaction continues to convert H_2 to CO , whereas little additional hydrogen is being produced by the reforming reaction. As a result, the CO concentration continues to rise with temperature while the CO_2 and H_2 concentrations fall.

Pressure has a much less pronounced effect on equilibrium concentrations than temperature (Figure 4-7). In practice, the economic benefit of operating at elevated

⁹ Defined as the moles of methane converted divided by the moles of methane in the feed, not counting the fuel burned to provide the heat for the endothermic reforming reaction.

pressures (lower volumetric flows rates and hence a smaller reformer) outweighs the thermodynamic advantage of lower pressures (Wyman, et al., 1992). For this reason, reformers typically operate at pressures from 1-3.5 MPa. As well, most other gas processing steps require high pressures (e.g. pressure swing adsorption, methanol synthesis and bulk acid gas removal), so that pressurizing the reformer feed is more economical than pressurizing the reformer product, which has a much higher volumetric flow rate. Furthermore, there is no energy penalty associated with raising high pressure steam because the pressurization takes place in the liquid state, and requires almost no additional work.

Steam is required not only to promote the reforming reactions but also to prevent carbon formation. Molar steam:carbon ratios of 3-5:1 are typical for commercial steam reformers operating on natural gas. This steam requirement adds significantly to the overall heat duty of reforming since not only must a large quantity of steam be raised, but it must also be heated to the reaction temperature. The modeling of carbon deposition in Section 4.3 showed that with the synthesis gas from biomass gasification, no carbon formation occurred at typical reforming temperatures (>1100 K) even though the steam:carbon ratio was less than 3:1 (and recall that equilibrium estimates of carbon formation are conservative). The presence of H_2 and CO_2 in most gasifier product gases helps prevent coking so that additional steam is not required. Figure 4-8 shows the effect of the steam:carbon ratio on reforming of the BCL gasifier product gas for a temperature of 1140 K and a pressure of 1.5 MPa. As expected, adding more steam increases the amount of methane that is reformed, and increases the yield of H_2 through the equilibration of the water-gas shift reaction.

(ii) *Reactor Design and Operating Conditions*

A typical reformer consists of two main sections (Figure 4-9); a convective heating section for preheating the feed, and a furnace with an internal tube bundle which contains the catalyst. The feed is mixed with steam and preheated to approximately 550°C in the convection section. The mixture then enters the reaction section; an array of tubes packed with a nickel based catalyst. In this section, the mixture is simultaneously heated to the reaction temperature and reformed. The heat is provided by the furnace that surrounds the tube bundle. Due to high peak temperatures in the furnace, heat is transferred primarily via radiation rather than convection. These severe operating conditions place stringent materials constraints on the reformer tubes, which are made from high strength nickel alloys. The tubes have a typical operating life of 3 to 7 years, depending on reactor conditions (Minet and Olesen, 1980). To increase the energy efficiency of the reforming step, the flue gases leaving the furnace and the hot reformed gases are used to preheat the feed in the convection section, to raise steam needed for the reformer feed, and to preheat air for the furnace section.

Although conventional steam reformers operate at temperatures of up to 1000°C, a more conservative maximum temperature of 870°C was chosen for the analysis presented in this thesis, which would increase the tube life. Furthermore, higher temperatures are not necessarily required. Because shift and methanol synthesis catalysts are highly selective (i.e. they only catalyze a specific reaction or set of reactions), any methane leaving the reformer (also known as *methane slip* or *methane breakthrough*) is inert and is recovered in a purge stream from the final processing steps in both hydrogen and methanol production. This methane constitutes an important component of the fuel burned in the reformer furnace.¹⁰ Therefore, relatively less severe operating conditions

¹⁰ In the model developed here, the residual methane in the purge gas contains roughly 10% of the energy in the biomass feed on a higher heating value basis.

can be selected since methane slip is not a major concern. In fact, as will be shown in Chapter 6, in most cases the heating value of the purge gas is a good match for the heat duty of the reformer. Nevertheless, too much methane slip results in a high level of inert compounds in the synthesis gas which has negative effects on the economics of downstream equipment.

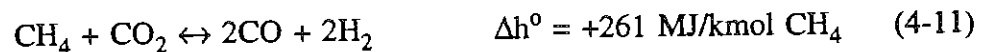
A final practical consideration is that the nickel based reforming catalyst is easily poisoned by sulfur, so that the reformer feed must have a sulfur content as low as 0.25 ppm. The removal of sulfur down to these low levels was discussed in Section 4.4.4. An alternative would be to use catalysts that are resistant to sulfur such as sulfided cobalt/molybdate (Wyman, et al., 1992). However, since other catalysts downstream of the reformer are also sensitive to sulfur, it makes the most sense to remove any sulfur before processing the syngas.

4.5.2 Steam Reforming with CO₂ Recycling/Addition

A fairly common practice with steam reforming of natural gas is to add CO₂ to the reformer feed. The source is usually recycled CO₂ which has been removed from the reformat. CO₂ can also be imported to augment the recycled CO₂.¹¹ The motivation for CO₂ addition is to lower the H₂:CO ratio of the reformat since steam reforming of natural gas produces a synthesis gas with hydrogen in excess of that which is needed for

¹¹ An interesting application might be to use natural gas from fields that are contaminated with CO₂, because this gas is not considered suitable for pipeline transmission (CO₂ reduces the heating value of the gas). For example, Gas Unie, a utility in The Netherlands, will not accept natural gas containing more than 3% CO₂ (Shell, 1990). However, CO₂ contaminated natural gas may be ideally suited for methanol production and could also be used for hydrogen production, even if it contained much higher levels of CO₂.

processes like methanol synthesis or *Fischer-Tropsch* synthesis.¹² H₂:CO ratios produced via steam reforming of natural gas are in excess of 3:1, whereas methanol synthesis and Fischer-Tropsch chemistry require a ratio closer to 2:1. The alternative to CO₂ recycling/addition is usually to purge excess hydrogen and use it as a fuel gas, but this is not the most economical use of hydrogen, since it could otherwise be used to manufacture the final product. The mechanism by which CO₂ affects the H₂:CO ratio is through the equilibration of the water-gas shift reaction (4-2). The CO₂ reforming reaction must also be considered, and becomes a more important route for methane conversion as the concentration of CO₂ increases relative to that of steam. The reaction is:



Although CO₂ recycling is intended for applications where there is excess hydrogen in the synthesis gas, it may also be beneficial for hydrogen production if, as a result, less steam was required for reforming (provided that carbon deposition was not a problem).¹³ This could have a positive effect on the overall energy balance of the system, although the need to raise additional steam for the shift reactors and recompress the CO₂ must also be considered, since pressure swing adsorption produces CO₂ at near ambient pressure. Overall, a 2-3% increase in thermal efficiency can be expected by using CO₂ recycling/addition for natural gas based methanol production (Kuo, 1991) (see also Chapter 6).

¹² Fischer-Tropsch synthesis is the name for a group of processes that are used to produce liquid hydrocarbon fuels (such as gasoline) from syngas.

¹³ Since CO₂ does help inhibit carbon formation, it is possible to reduce the steam:carbon ratio to approximately 2:1 with sufficient CO₂ recycling (Goff and Wang, 1987; Riensche and Fedders, 1991).

Unlike steam reforming of natural gas, biomass gasification often produces a synthesis gas that is hydrogen deficient,¹⁴ requiring that some CO be converted in a shift reactor to raise the H₂:CO ratio prior to methanol synthesis (see Section 4.2). Under hydrogen deficient conditions, CO₂ recycling would produce the opposite effect and simply increase the amount of synthesis gas that must be sent to the shift reactor. Therefore, for biomass systems CO₂ recycling should only be considered if there is excess hydrogen in the makeup gas entering the methanol synthesis loop or if it is possible to improve the energy balances of the overall processes.

4.5.3 Alternatives to Steam Reforming

Although steam reforming is the most common method of producing a synthesis gas from natural gas or other feedstocks, there are other processes that may be well suited to biomass-based synthesis gas processing. Some are commercially available while others are still under development.

(i) Partial Oxidation

Partial oxidation takes place at higher temperatures than steam reforming. As the name suggests, the feed is burned in an oxygen deficient environment, but at sufficiently high temperatures to convert the feed into a synthesis gas. For methane, the stoichiometric partial oxidation reaction is:



¹⁴ For example, the reformed synthesis gas from the IGT gasifier has a H₂:CO ratio of 1.59, whereas that of the BCL gasifier is approximately 1.78. For the entrained-bed gasifier using biomass, the gasifier produces a gas with H₂:CO = 0.78. The exceptions are the WM and MTCI gasifiers which produce gases with some excess hydrogen.

Non-catalytic partial oxidation of natural gas takes place at temperatures in excess of 1000°C, and industry experience has shown that peak temperatures of 1400-1600°C are generally required (Cheng and Saini, 1993). Under these conditions, temperature alone is sufficient to convert methane to a synthesis gas. Although in theory only 0.5 moles of O₂ are required per mole of CH₄, in practice, 40-50% more is required to maintain sufficiently high temperatures, which increases costs considerably if pure oxygen is used instead of air (Solbakken, 1991). The need for excess O₂ is largely due to the stability of the methane molecule.

This process is interesting and potentially advantageous for methanol production because it can operate at high pressures and produces a syngas with a H₂:CO ratio close to 2:1. The reactor is simpler and less expensive than a steam reformer, since neither a catalyst nor high temperature reformer tubes are required. Carbon formation from the thermal cracking of methane does occur, but it is not a major problem since there is no catalyst to become deactivated. The carbon is removed by periodically cleaning the reactor.

Partial oxidation also proceeds at lower temperatures with the aid of a catalyst, which reduces the amount of oxygen required. Traditional catalysts are nickel based, but more recently, researchers at Oxford University have found that high conversion rates are possible over mixed metal oxides of ruthenium at temperatures as low as 775°C (Vernon, et al., 1990; Haggin, 1990). The one drawback to this lower temperature catalyst is that methane conversion decreases substantially at elevated pressures so that good conversion at high pressures requires temperatures characteristic of commercial processes (Vernon, et al., 1990). For these processes, the mechanism of syngas generation is assumed to be, (i) the complete oxidation of part of the feed to CO₂ and H₂O, and then (ii) the non-catalytic reforming of the remaining feedstock via Reactions (4-8) and (4-11).

More recently the use of platinum and rhodium as partial oxidation catalysts was reported by Hickman and Schmidt (1993). Using air, they were able to achieve near complete conversion of methane with very high selectivities for CO and H₂ (>90%)¹⁵ at temperatures of 850-1150°C. An interesting characteristic of their process is that gas-catalyst contact times are on the order of 10 milliseconds, much shorter than most reactors, which have residence times on the order of 1 second. If commercialized, this would enable the use of a much smaller reactor for the same throughput as conventional units. However, the kinetics of this system differ from those described above. The reaction between methane and oxygen in this system is such that if there were any hydrogen in the feed, the oxygen would react preferentially with this hydrogen since this H₂-O₂ reaction is much faster than the CH₄-O₂ reaction (Hickman, 1993). As a result the partial oxidation of methane would be suppressed or stopped altogether. Therefore, this particular process, although promising for natural gas, is not suitable for use with the product gas of biomass gasification.

(ii) Catalytic Autothermal Reforming

Catalytic autothermal reforming (CAR) is a commercially available technology that combines steam reforming with partial oxidation. As with partial oxidation, CAR of natural gas is of interest because it produces a synthesis gas with a lower H₂:CO ratio than conventional steam-methane reforming. In CAR, only part of the feed is oxidized; enough to supply the necessary heat to reform the remaining feedstock. Partial oxidation of the feed gas directly supplies the heat that drives the endothermic reforming reactions, eliminating the need for a separate fuel gas stream and furnace. A catalytic autothermal reformer consists of two sections (Figure 4-10). In the burner section, some of the

¹⁵ Selectivity refers to the ability of a catalyst to favor one product over another, whereas conversion refers to the fraction of the feed that is consumed. For generating a syngas, high selectivity to CO and H₂ is desirable. A low selectivity would mean that compounds such as CO₂ or H₂O were also formed.

preheated feed/steam mixture is burned with air or oxygen to produce CO_2 and H_2O .¹⁶ The balance of the feed is then fed to the reactor and the entire mixture passes through the reforming section that contains the nickel-based catalyst. The elimination of the reformer tubes allows operation at higher temperatures and pressures than conventional steam reforming. Temperatures 900-1000°C are typical for commercial catalytic autothermal reformers. (*Hydrocarbon Processing*, 1984). The pressure is determined by downstream processing pressure requirements.

The higher temperature of CAR compared to conventional steam reforming means that less steam is required.¹⁷ With no CO_2 recycling, steam:carbon ratios of 2-2.5:1 are typical for 100% natural gas feedstocks. With full CO_2 recycling, this ratio can be lowered to 1.5:1 (Goff and Wang, 1987). Since all biomass gasifiers produce a gas that contains some CO_2 , steam:hydrocarbon ratios approaching 1.5:1 will likely be sufficient to prevent coking. Figure 4-11 shows the equilibrium composition as a function of steam:hydrocarbon ratio for the IGT gasifier. The temperature is fixed at 1000°C by adjusting the amount of oxygen in the feed. Although the concentrations of H_2 and CO fall as more and more steam is added (the product gas becomes more diluted with H_2O), the net production of $\text{CO}+\text{H}_2$ per mole of methane, is essentially constant for the range of steam:hydrocarbon ratios shown in Figure 4-11. For a steam:hydrocarbon ratio of 2:1, the composition as a function of temperature is given in Figure 4-12. Note that most of the methane is converted with the need to raise considerably less steam when compared to conventional steam reforming. While this may have a positive impact on the overall

¹⁶ Air would be used if nitrogen containing compounds (such as ammonia) were the desired end-products. Oxygen would be used in cases where nitrogen dilution is not desirable.

¹⁷ Higher temperatures reduce the tendency of carbon formation and some H_2O is produced during partial oxidation.

energy balance of the system, a consequence will be that more steam will have to be raised for the shift reactors. Net synthesis gas production ($\text{CO}+\text{H}_2$) is plotted as a function of temperature and compared to conventional reforming in Figure 4-13. At typical operating conditions, steam reforming of the gasifier product gas does produce considerably more synthesis gas, but requires roughly 2.5 times the quantity of steam. Therefore, in order to determine which reforming process is most appropriate, it is necessary to evaluate the entire fuel production process.

In addition to thermodynamics, a key consideration when selecting the syngas generation technology is economic. Since autothermal reforming does not require expensive reformer tubes or a separate furnace, capital costs are typically 50-60% less than conventional steam reforming, excluding the cost of oxygen separation (Goff and Wang, 1987). This option could therefore be attractive for facilities that already require oxygen for biomass gasification. Indirectly heated gasifiers are therefore not likely candidates for this option.

(iii) Carbon Dioxide Reforming

In this process, CO_2 completely replaces steam as the oxidizing agent, resulting in a syngas with a very low $\text{H}_2:\text{CO}$ ratio.¹⁸ Experiments using natural gas or methane feedstocks have examined a variety of catalysts and operating conditions. Research has shown that carbon formation can be avoided with a $\text{CO}_2:\text{CH}_4$ ratio of at least 1.1:1 in the

¹⁸ Interest in this option is motivated in part by closed-loop chemical heatpipe technology, where a thermal energy source such as solar or nuclear energy is used to drive the endothermic carbon dioxide reforming reaction (4-11). The reformed gases are then transported to the end-use site where the exothermic reverse reaction (methanation) provides heat (Fish and Hawn, 1987; Ashcroft et al, 1990; Dostrovsky, 1991). Several laboratory scale experiments have yielded promising results and a 400 kW solar powered pilot plant is being constructed at the Weizmann Institute of Science in Rehovot, Israel (Dostrovsky, 1991).

feed and an $H_2:CO$ ratio approaching 1:1 in the product gas (Fish and Hawn, 1987). These tests were conducted at pressures of 2-3 MPa and temperatures up to 1050 K. Researchers at Oxford University have also successfully used CO_2 as the oxidizing agent for natural gas reforming (Ashcroft et al., 1990). Under stoichiometric conditions, they achieved H_2 and CO yields of 90%¹⁹ at 1050 K and atmospheric pressure.

Another option combines CO_2 reforming with partial oxidation in a process similar to CAR (Ashcroft et al., 1990). As in CAR, some of the feed is burned to provide the heat directly for the catalyzed CO_2 reforming reaction. In such a system, CO_2 actually becomes the primary feedstock. As with steam reforming with CO_2 recycling, this option may be well suited to CO_2 contaminated natural gas. Using methane as the feed, Ashcroft, et al. were able to achieve CH_4 and CO_2 conversion of approximately 90% at 1050 K and 1 atm over an iridium catalyst with a $CH_4:O_2:CO_2$ ratio of 4:1:9. These experiments were carried out in silica tubes, which the authors suggested was vital to carbon free operation. An alternative would be to use additional CO_2 , which was also found to effectively inhibit carbon formation in conventional reformer tubing.

Since CO_2 reforming of the product gas from biomass gasification would produce a gas with a very low $H_2:CO$ ratio, it is doubtful that much benefit could be derived from using this technology for hydrogen production. However, an interesting application might be to combine different types of CO_2 reforming options with hydrogen augmentation for methanol synthesis. In such a scheme, the shift reactor is eliminated and the $H_2:CO$ ratio is adjusted by adding hydrogen that has been produced in an electrolyzer. The result is a suitable makeup gas with considerably more CO than before, resulting in a substantial

¹⁹ Hydrogen yield was defined as the moles of hydrogen in the products divided by twice the moles of methane in the feed. Similarly, CO yield was defined as the moles of CO in the products divided by the moles of (CH_4+CO_2) in the feed.

increase in the yield of methanol for the same gasifier throughput. Using an electrolyzer also has the added benefit of producing a separate stream of pure oxygen that can be used in gasification and/or autothermal reforming. This would help offset the added capital cost of installing the electrolyzer by reducing or eliminating the need for cryogenic oxygen separation. One source of electricity could be excess production from wind or PV power that would otherwise be wasted. This option would improve the utilization of biomass and reduce *spillage* from intermittent renewable energy sources.

4.6 The Water-Gas Shift Reaction

As mentioned earlier, the water-gas shift reaction (4-2) is used to convert CO into H₂. Due to high catalyst selectivity, all gases except those involved in the water-gas shift reaction are inert. The degree to which the shift reaction is used to convert CO to H₂ depends on the desired end-product. If hydrogen is the final product then as much CO as possible is shifted. For methanol synthesis, the shift reactor is used to increase the H₂:CO ratio, if necessary. Since the shift reaction is exothermic, higher conversion levels are achieved at lower temperatures. The reaction is independent of pressure, but most shift reactors operate at elevated pressures to accommodate both upstream and downstream pressure requirements.

Shift reactors have a much simpler design than reformers because they operate at lower temperatures and do not require external heating. Typically, the catalyst is contained in multiple fixed-beds. Shift reactors can be either adiabatic or isothermal. In adiabatic reactors, the temperature rises as the reaction proceeds towards equilibrium. Isothermal reactors are externally cooled to maintain an even temperature throughout the unit. The choice of which type to use depends primarily on the application. To prevent coking problems and to ensure good conversion, steam is usually added to the feed gas to maintain a steam:carbon ratio of at least 3:1.

In the case of hydrogen production, where essentially complete conversion of CO to H₂ is desired, two shift reactors are used. The first, high temperature, reactor operates in the 350-475°C range, which is based on the catalyst's temperature requirements. This reactor gives relatively low conversion rates but high reaction rates due to the kinetic effect of high temperature operation on catalyst activity. Since precise temperature control is not a major concern in the first stage, the high temperature reactor is usually an adiabatic unit. The second reactor is a low temperature unit operating in the 200-250°C range. Most of the remaining CO is converted, but at a slower rate than the first stage. Since precise temperature control is needed to maintain catalyst activity, the second reactor is typically isothermal. For methanol synthesis, a single, high temperature reactor is sufficient to tune the H₂:CO ratio to the desired level.

The BCL product gas is again used to illustrate the thermodynamic behavior of shift reactors. As can be seen from Figure 4-14, CO conversion is nearly complete at 227°C (500 K), the operating temperature of the low temperature shift reactor used in the simulations in Chapter 6. At this temperature, the CO concentration is approximately 0.5% on a dry basis.

Catalysts for the high temperature reactors are iron oxide-chromium oxide catalysts. The low temperature reactor uses a zinc oxide-copper oxide catalyst, which is prone to deactivation by sulfur. At a reaction pressure of 3 MPa, shift catalysts can be expected to last 1-3 years (Probstein and Hicks, 1982). Due to their simple design, shift reactors are low capital cost items, especially when compared to reformers or methanol synthesis units.

4.7 Methanol Synthesis

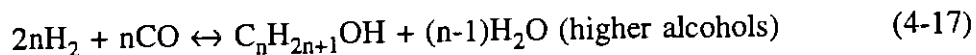
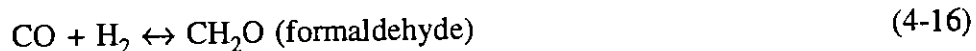
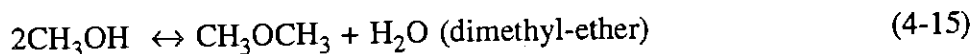
4.7.1 General Process Description

As with many of the technologies discussed in this chapter, methanol synthesis is a well established commercial process. Several different types of reactors are available, with the two most widely used discussed below. Methanol is produced from syngas via the following two reactions:



By far, (4-13) is the primary methanol synthesis reaction. Since (4-14) results in the loss of some of the hydrogen as water, under ideal circumstances there would be no CO_2 in the feed. However, it is well established that a small amount of CO_2 in the feed (1-2%) acts as a promoter of the primary methanol synthesis reaction and helps maintain catalyst activity (Klier, 1982).

Although modern methanol synthesis catalysts are highly selective, some side reactions are possible, primarily:



The formation of these species is limited by the selectivity of the catalyst as well as the by the kinetic factors that predominate at typical methanol synthesis temperatures (240-270°C) (Rogerson, 1984). In practice, to produce fuel grade methanol, water, hydrocarbon impurities and dissolved gases must be removed in a final distillation step.

Since methanol synthesis is exothermic, it is favored at lower temperatures, and as with shift reactors, a balance must be struck between thermodynamic and kinetic factors. Catalyst activity drops off sharply below about 230°C (see Figure 4-4), placing a lower limit on practical operating temperatures. Typically, one would exploit the thermodynamic advantages of lower temperatures when the catalyst is fresh, and gradually raise the temperature as catalyst activity declines with age (Mansfield, 1991).

The temperature constraints of methanol synthesis catalysts results in a thermodynamically limited process, and only a portion of the CO in the feed gas is converted to methanol in one pass through the reactor. Figure 4-15 shows the one pass (no recycling) equilibrium concentrations for the major components of the makeup gas of the BCL gasifier (CH₄ has been omitted for clarity). In practice, the synthesis product gas is cooled to condense most of the methanol and the bulk of the remaining gas is recycled back to the synthesis unit to increase overall carbon conversion (Figure 4-16). A purge stream is used to remove inert compounds from the recycle loop that would otherwise build up to excessive levels. This purge stream is used elsewhere in the process as a fuel gas to provide process heat (i.e. in the reformer) or to produce power, if no high temperature process heat is required. Typically, the molar recycle ratio (recycle feed/makeup feed) is between 4-6, which gives an overall carbon conversion rate in excess of 98%. The main drawback of requiring a recycle loop is that it substantially increases the size (and hence cost) of methanol synthesis reactors. There is also the need for auxilliary equipment such as a recycle compressor, which further increases costs.

Reactions (4-13) and (4-14) also indicate that methanol synthesis is favored by higher pressures. In fact, commercial processes do use relatively high pressures to help offset the temperature constraints imposed by catalysts. Before the introduction of low temperature catalysts (230-270°C) in the 1960s, methanol synthesis was carried out at

pressures between 30-40 MPa and temperatures of 350-450°C. Today, pressures of 5-10 MPa are typical of the so-called *low-pressure* methanol synthesis processes. At pressures above 5 MPa the conversion of CO to methanol is nearly complete (with recycle), however large plants (>1000 tonnes of methanol per day) benefit from the economics of higher pressures, which reduces the size of the reactor and ancillary equipment, even when factoring in the higher compression costs (Mansfield, 1991).

A final practical consideration is the H₂:CO ratio of the synthesis gas. Since the quantity of hydrogen must satisfy the stoichiometry of both methanol synthesis reactions (4-13 and 4-14), the ideal gas composition (known as the R value), is given by (Goff, and Wang, 1987; Kuo, 1991):

$$R = \frac{H_2 - CO_2}{CO + CO_2} = 2 \quad (4-18)$$

In practice, the makeup gas is slightly hydrogen rich because some hydrogen is purged or lost (as H₂O via reaction 4-14), and a hydrogen deficient gas can result in carbon deposition (Probstein and Hicks, 1982). The relative dearth of carbon oxides is also important because it inhibits the oxidation of the active component of the catalyst (copper) (Mansfield, 1992). However, it has been reported that methanol synthesis units have operated with a makeup gas having an R value as low as 2.03 (Kuo, 1991), which was the value used as the control parameter in this thesis. Since H₂ is in slight excess, it too builds up in the recycle loop, and the actual R value of the combined synthesis feed (makeup plus recycle feeds) is typically between 3 and 4.

4.7.2 Commercial Processes

The two most widely used methanol synthesis processes today are the ICI (Figure 4-17) and Lurgi (Figure 4-18) low-pressure methanol synthesis processes. Since the ICI process is the more common of the two it was used in the computer models developed for this thesis. Typical reactor conditions for the ICI unit are 5-10 MPa and 250-270°C. In this system the fresh feed is first mixed with cool recycled gas. Some of the gas is then heated to slightly below the reaction temperature and enters through the top of the reactor, passing through multiple catalyst beds. The bulk of the gas is injected at several locations along the sidewall of the reactor. This *cold shot* is used to control the temperature of the reactor and permits the ICI unit to operate adiabatically, eliminating the need for external cooling. The ICI catalyst is a combination of copper, zinc, and zinc-aluminum oxides. The copper is the active component, while the $ZnAl_2O_4$ is used as a stabilizing support material (Rogerson, 1984). This catalyst is poisoned by both sulfur and chlorine but the presence of free zinc-oxides does help prevent poisoning.

The Lurgi low-pressure process differs considerably from the ICI process. The Lurgi unit operates isothermally and most closely resembles a vertical shell-and-tube heat exchanger. Typical reactor conditions are 6-15 MPa and 230-265°C (Supp and Quinkler, 1984). The catalyst material is packed in the tubes, while the shell is filled with pressurized boiling water. The use of boiling water ensures a very even temperature throughout the catalyst beds. Furthermore, the operating temperature is easily controlled by varying the shell pressure. Steam is produced in the 4-5 MPa range for use elsewhere in the process.

4.7.3 Advanced Methanol Production Processes

Since current methanol synthesis technologies can achieve carbon conversion rates in excess of 98%, current R&D of advanced methanol synthesis processes focusses on ways

to improve economic performance. A major improvement would be the elimination of the recycle loop. This would have several advantages: (i) less need for auxiliary equipment such as a recycle compressor and heat exchangers, (ii) correspondingly less energy input requirements, and (iii) a significantly smaller synthesis reactor since the volumetric flow rate would be reduced by a factor of at least 5. Since methanol synthesis is one of the most capital intensive steps in producing methanol from biomass, a one pass methanol synthesis reactor could significantly reduce the cost of methanol from biomass.

There are several interesting technologies at different stages of development that may achieve once-through methanol synthesis. Researchers at the Brookhaven National Laboratory have developed a low-temperature (active as low as 100°C) liquid-phase catalyst that can convert over 90% of the CO in one pass (Haggin, 1986; Supp, 1990). A liquid catalyst has the added benefit of being a very effective medium for removing heat from the reactor.

Two near term possibilities are the so-called Gas-Solid-Solid Trickle Flow Reactor (GSSTFR) and the Reactor System with Interstage Product Removal (RSIPR) (Westerterp et al., 1988). Both of these concepts operate on a similar principle; the removal of the methanol product as it is formed. In such systems, the methanol concentration remains below its equilibrium value and the synthesis reactions proceed essentially to completion in one pass. The two methods differ in the way methanol is removed. In the GSSTFR system, a solid adsorbent moves countercurrent to the gas flow, removing the methanol almost immediately as it is formed at the catalyst surface. It is estimated that compared to the Lurgi low-pressure process, GSSTFR will save up to 50% on cooling water, 70% on recycling energy and 70% on the amount of catalyst required. In a more conventional approach, the RSIPR process uses several Lurgi type reactors in series with methanol removal between each reactor. Methanol is removed using the liquid absorbent

tetraethylene glycol dimethyl ether. Although multiple reactors are required, each successive reactor is considerably smaller than the previous one. In this case, the estimated savings over the Lurgi process are 60% on cooling water, 70% on recycle energy and 35% on catalyst material.

Another near term option is the co-production of methanol and electricity (e.g. see Chem Systems, 1990). In this configuration, either a conventional low-pressure process or a liquid-phase process (that operates under similar conditions to commercial low-pressure processes) is used to convert as much CO to methanol as possible in one pass. The remaining syngas is used to generate electricity in a combined cycle power plant. Chem Systems is developing a liquid-phase catalyst that can convert CO rich syngas (e.g. like that produced in coal gasification) without the need for a shift converter, which eliminates one step in the process.

A more long term prospect for improved methanol synthesis economics that is being developed specifically for natural gas is the direct partial oxidation of methane to methanol (DPOM) (Gesser and Hunter, 1991; Kuo, 1991; Thomas, et al., 1992; Periana, et al., 1993). DPOM is attracting a great deal of interest because it eliminates the need to generate syngas prior to methanol synthesis. Therefore, a two step process is reduced to a one step process. The principle is straight forward. Methanol is produced via the following partial oxidation reaction:



The most common method uses an iron based catalyst and proceeds at temperatures between 350-500°C. Some formaldehyde, CO, CO₂ and H₂O is also formed, but H₂ is generally not produced. Because of the thermodynamic constraints imposed by

the moderately high operating temperatures, high pressures are required to achieve acceptable single pass conversion rates (50-65 MPa). Therefore, as with conventional methanol synthesis technology, unconverted gas must be recycled to achieve good overall conversion. Because of these high pressures, and because of the need for large recycle ratios, oxygen is preferable to air to reduce compression costs and reactor size. CO₂ is also removed from the synthesis loop. Reactors can be either isothermal or adiabatic, with the latter relying on recycled gas to act as the temperature moderator, as is done with the ICI low-pressure process.

Using iron based catalysts, selectivity to methanol as high as 90% and single pass methane conversion as high as 15% have been reported, although most studies have reported lower values (up to 70% selectivity and approximately 5-10% one-pass methane conversion) (Kuo, 1991). It is generally accepted that selectivities greater than 85% and methane conversion greater than 30% are required for this process to be economical (Periana, et al., 1993). Periana, et al. have recently reported methane conversions as high as 50% at 85% selectivity in a batch reactor, for an overall yield of 43%. Their process differs from previous ones in that it uses sulfuric acid and a mercury catalyst in a multistep reacting system, with the net reaction being Reaction (4-19). An advantage of this system is that it operates at much milder conditions than those described above (180°C).

Although DPOM appears promising for the long term, it is probably not a practical alternative for biomass-based systems, since biomass systems produce a gaseous mixture that is only part CH₄. Therefore, if DPOM were used in conjunction with biomass gasification, there would still be the need for a two step methanol synthesis process; one step to convert the methane (via DPOM), and a second to convert the CO and H₂ in the gas (using a conventional low-pressure process).

4.8 Acid Gas Removal

The two main acid gases that must be removed at some point in both methanol and hydrogen production are hydrogen sulfide (H₂S) and CO₂. H₂S is removed prior to the reformer as described in Section 4.4.4. In hydrogen production, CO₂ is removed using pressure swing adsorption. In methanol production, CO₂ is removed just prior to the methanol synthesis step as described below.

A variety of chemical and physical absorption methods are available for the bulk removal of acid gases (Taylor, 1984; Mohr and Ranke, 1984). In chemical absorption systems an alkaline solution reacts with the acid gases creating a new chemical compound. The solvent is regenerated by reversing the chemical reaction via heating with steam in a *stripper*. Physical absorption systems work on a similar principle except that the acid gases are dissolved in a solvent instead of chemically reacting with it. The CO₂ can then be stripped in a similar manner, or by using a *flash* regeneration.²⁰

The SELEXOL[®] physical separation process from Union Carbide was chosen for CO₂ removal. The solvent is a solution of dimethyl ether of polyethylene glycol in water. A physical absorption process was chosen over a chemical process for several reasons. First, according to Henry's Law, the solubility of a gas in a solvent is proportional to its partial pressure. Thus, physical solvents work well in pressurized applications such as those considered here (Taylor, 1984). Physical processes are also more selective than chemical ones due to the differences in solubility of each gas in the solvent (see Table 4-1). This is particularly important when it is desired to selectively remove certain

²⁰ Depending on the degree of CO₂ removal required, one of these two methods is applied. A flash drum is a vessel used to separate a mixture into different phases, in this case by rapidly reducing the pressure. This causes most of the CO₂ to come out of solution without the need for steam regeneration, and thus reduces the energy requirements of the separation step.

gases from the mixture.²¹ The SELEXOL process is also characterized by moderate operating temperatures (127°C was used in this study) and low solvent losses due to a low vapor pressure, both of which help lower operating costs. As well, since approximately 2% of the CO₂ must remain in the gas a stripper is not required. Rather, a flash regeneration is all that is needed to remove the CO₂ from solution, which eliminates the need to raise steam, which reduces energy consumption. This further reduces the cost of physical separation in this application. The CO₂ would be available at approximately 1.5 atmospheres, but would contain significant quantities of moisture (Union Carbide, 1992).

Table 4-1 Relative solubilities of different gases in the SELEXOL[®] solvent (Epps, 1991).

Gas	Relative Solubility
H ₂	0.2
CH ₄	1.0
CO ₂	15.0
COS	35.0
H ₂ S	134.0
CH ₃ SH	340.0
H ₂ O	11,000.0

4.9 Hydrogen Separation and Purification Technologies

The choice of hydrogen purification process depends on several factors, including the size of the facility, the feed gas properties (e.g. pressure and composition), and of course, the end-use. This section describes the four main types of hydrogen separation technologies available today.

²¹ For example, it is possible to produce separate CO₂ and H₂S streams using the same SELEXOL unit, which simplifies the conversion of H₂S to elemental sulfur. It is then also possible to purge the CO₂ or consider it for use elsewhere in the process, for sale, or for sequestering.

4.9.1 CO₂ Removal and Methanation

In this process the gas leaving the low temperature shift reactor is sent to a CO₂ removal system such as the SELEXOL system described above. The CO₂ free gas is then heated to approximately 300-350°C before being sent to a *methanator*. A methanator uses a nickel based catalyst to convert residual CO to CH₄ and H₂O by reacting it with H₂ in the reverse of the reforming reaction (4-1). Since this reaction is exothermic, the gas exits the methanator 15-20°C higher than the inlet temperature. Depending on the amount of residual methane and CO in the syngas exiting the low temperature shift reactor, the hydrogen produced typically has a purity of 95-98%, but hydrogen recovery is essentially 100% (excluding the hydrogen consumed in the methanator) (Heck and Johansen, 1978; Corr, et al., 1979; van Weenen and Tielrooy, 1983). This process does have the advantage that it produces hydrogen essentially at the feed pressure.

4.9.2 Cryogenic Separation

Cryogenic hydrogen separation relies on the fact that different compounds have different boiling points. In this process, hydrogen is purified by condensing out other impurities, which liquify at higher temperatures than hydrogen. The refrigeration is obtained by the so-called *Joule-Thompson* effect produced by throttling the condensed hydrocarbon liquids that have been removed from the feed stream (Miller and Stoecker, 1989). Therefore, this process is best suited to a feed gas that has a fairly high fraction of hydrocarbons (25% or more) (Wang, et al., 1984). Additional cooling can be obtained from expanding the hydrogen product or by using external refrigeration. Cryogenic separation can produce 95+% purity hydrogen at recovery rates of 92-97% (Miller and Stoecker, 1989).

4.9.3 Pressure Swing Adsorption (PSA)

PSA systems have reached a level of performance such that they can produce hydrogen with extremely high purity (99.999%) at recovery rates of 90% or higher. PSA exploits

the ability of porous materials to selectively adsorb specific molecules at high pressure and desorb them at low pressure. The cyclic pressure *swing* is what gives this process its name. For a continuous process, at least two units must be used in parallel; one is adsorbing while the other is being regenerated (depressurized). PSA systems operate at near ambient temperatures, and the optimal feed pressure range is 1.4 to 2.8 MPa (Miller and Stoecker, 1989).

A variety of natural and man-made substances will work as adsorbents. Two basic categories are carbonaceous and zeolitic adsorbents (White and Barclay, 1989). Zeolites are both naturally occurring and manmade, and are also called molecular sieves. Broadly defined, they are silicates of aluminum with alkali metals.²² The ability of a substance to adsorb a particular gas depends on several factors including pore size, pore size distribution, void fraction and surface activity. Some zeolites contain metal cations which can attract certain gas molecules. There are literally hundreds of different types of zeolites, with pore sizes ranging from 3 to 10 Å. The size of the gas molecule to be adsorbed is therefore important when selecting which zeolite to use. Macroscopic properties are also important. Sufficient *macroporosity* is required to permit rapid diffusion of gases from the surface of the adsorbent into the microscopic structure. Greater macroporosity also reduces pressure losses and allows for rapid desorption during bed regeneration.

Removing hydrogen from a gas mixture that contains CO, CO₂, CH₄ and H₂O is accomplished by using two sets of PSA beds (Figure 4-19).²³ In the first set of beds (the "A" beds), activated carbon selectively adsorbs nearly all CO₂ and all H₂O. The

²² An example is CaO•2Al₂O₃•5SiO₂ (McGraw-Hill, 1978).

²³ The PSA unit described here is the "GEMINI-9" system manufactured by Air Products Ltd. (Solomon, 1991).

remaining gas then passes to the second set of beds (the "B" beds) which contain a zeolite molecular sieve that selectively adsorbs essentially all the remaining compounds and some H₂. One pass through the B-beds leaves 86% of the H₂ unadsorbed (Solomon, 1991).²⁴ The overall recovery of hydrogen can be increased by recycling some of the desorbed gas from the B-beds. For example, recycling 80% of these gases increases the overall hydrogen recovery to 96.5% (Solomon, 1991). Of course, there is a trade off with this option in that the recycled gas must be recompressed and cooled to near ambient temperature, adding to capital and operating costs. A slightly larger PSA unit will also be needed. As with the methanol synthesis loop, some of the recycled gas must be purged to prevent the buildup of methane and other non-hydrogen gases.

The advantage of this PSA unit is that it produces three separate streams: up to 99.999% pure hydrogen, a combustible purge gas undiluted by inert compounds, and high purity CO₂ (that contains some moisture and small quantities of other compounds). The hydrogen is produced essentially at the feed pressure (a 70 kPa pressure drop is nominal) which reduces final hydrogen compression costs. The purge stream is used as a fuel gas elsewhere in the process, and the high purity CO₂ can be sold, used elsewhere in the process, or considered for CO₂ sequestering.²⁵

²⁴ Nitrogen is the most difficult gas to remove, and the one pass recovery rate would be slightly reduced if the mixture contained significant quantities of nitrogen gas (Solomon, 1993). In all cases considered here, it is assumed that nitrogen is not present in large enough quantities to significantly affect the rate of hydrogen recovery. In any event, if some N₂ can be tolerated in the hydrogen, hydrogen with 99.99+% purity can be produced at recovery rates close to those possible when there is no nitrogen in the feed.

²⁵ For example, in depleted natural gas wells (Blok, et al., 1991).

4.9.4 Membrane Separation

Membrane separation is less mature than PSA technology, but has become well established in the last ten years and is well suited for certain applications.²⁶ When small size facilities are considered (e.g. for O₂ separation), membranes can be a cost effective alternative to cryogenic separation, which has poor economics at very small scales.

Membranes are made from a variety of polymers including polyethylene, cellulose acetate, and polyamides. To give them good mechanical strength (they must operate across large pressure differences), membranes are usually constructed using composite materials (Tomlinson and Finn, 1990). The operating principle is simple; different gases permeate through the membranes at different rates. Hydrogen and oxygen are examples of *fast* gases; ones that permeate membranes quickly. Methane and N₂ are examples of *slow* gases. In general, low molecular weight and strongly polar molecules permeate membranes rapidly, whereas high molecular weight and non-polar molecules do not. The driving force that causes a fast gas to diffuse across a membrane is the difference in its partial pressure from one side of the membrane to the other. Therefore, for hydrogen separation, the feed gas must be at a relatively high pressure (7 MPa or more), whereas the purified hydrogen is produced at a substantially lower pressure (<2 MPa). While overall hydrogen recovery is high (90-95%), hydrogen purity is considerably lower than with PSA systems (95-98%) (Tomlinson and Finn, 1990). Methane is the largest impurity.

²⁶ Nitrogen production from air is an example of a process where membranes compete well with the cryogenic separation and PSA technology (Shelley, 1991).

4.9.5 Hydrogen for Use in PEM Fuel Cells

Hydrogen purity is a major issue for polymer electrolyte membrane fuel cells, the leading candidate for automotive applications. Specifically, CO is a strong poison at the anode (the fuel side of the fuel cell). Studies indicate that levels as low as 1-2 ppm will deactivate the platinum catalyst. Since PSA produces by far the highest purity hydrogen, is characterized by recovery rates that are at least as high as the other systems discussed here, and produces hydrogen at elevated pressures, it has been chosen as the system that will be used in the subsequent analysis. PSA systems are also cost competitive with the other options discussed here.

PSA systems produce hydrogen with approximately 2 ppm CO (the remaining impurities in the hydrogen would be N₂ (if present) and approximately 8 ppm methane (Solomon, 1993). Therefore, even PSA purified hydrogen may pose a problem for PEM fuel cell vehicles. Fortunately, there are two simple solutions to the problem of CO poisoning. One is specifically related to hydrogen production, and the other applies to both hydrogen and methanol powered fuel cell vehicles.²⁷ If the fuel is hydrogen, it is possible to use a small *methanator* after PSA separation to catalytically reduce the CO concentration further. The other solution is to add 2-5% oxygen in with the feed to the fuel cell, which oxidizes the CO to CO₂, and thus prevents poisoning (Gottesfeld and Pafford, 1988). Thus, CO in the fuel should not pose a problem for PEM fuel cells.

²⁷ For fuel cells that use methanol, 1-2% CO would be produced by the on-board reforming of methanol.

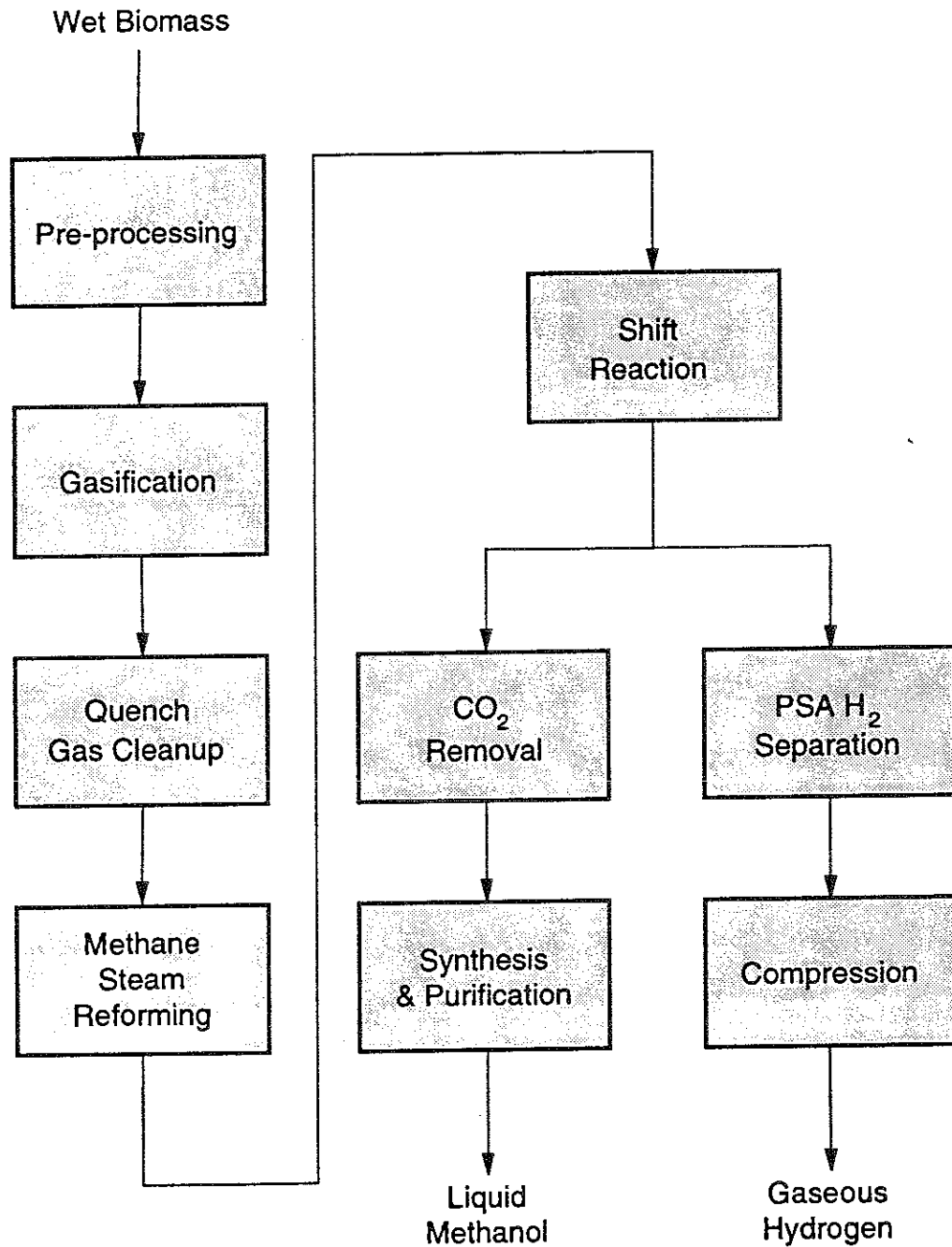


Figure 4-1: Block diagram of the process configurations for the production of methanol or hydrogen from biomass. PSA = pressure swing adsorption.

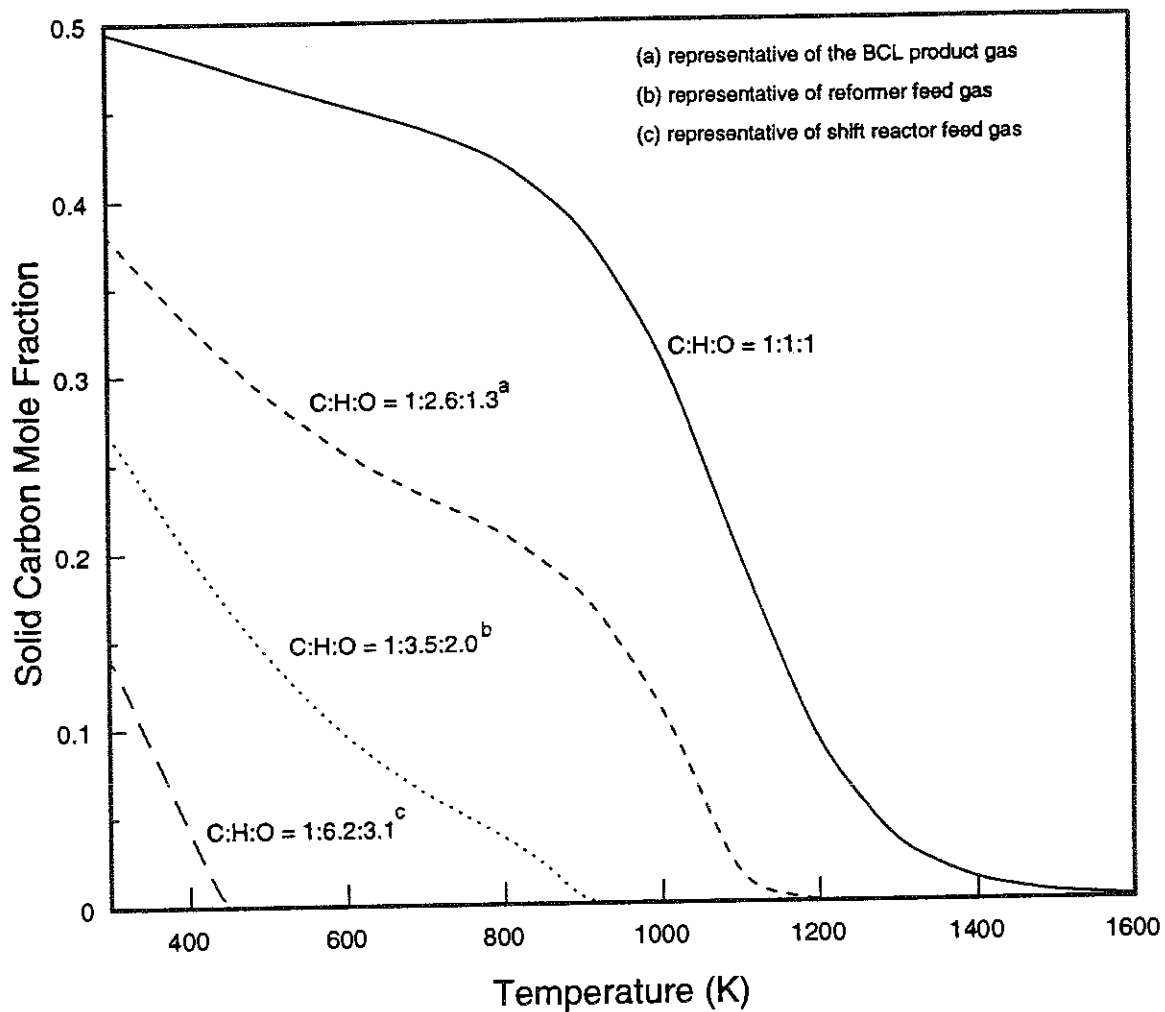


Figure 4-2: Chemical equilibrium modeling showing the conditions necessary for carbon formation at a pressure of 1 MPa, for mixtures containing H₂, CO, CO₂, CH₄, H₂O and C_(s) at different C:H:O ratios.

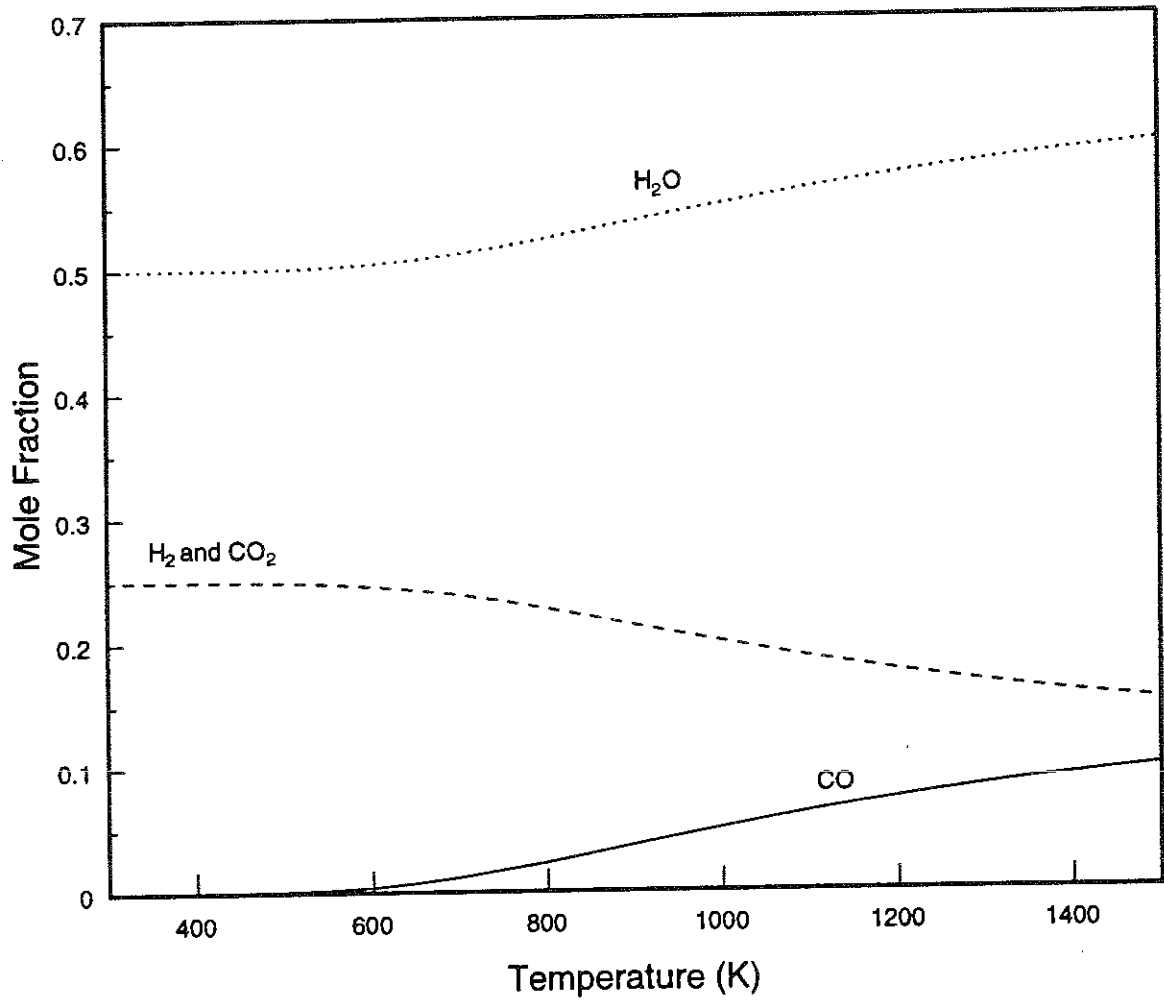


Figure 4-3: Chemical equilibrium composition as a function of temperature for the water-gas shift reaction. The initial composition is a mixture of CO and H₂O with a steam:CO ratio of 3:1.

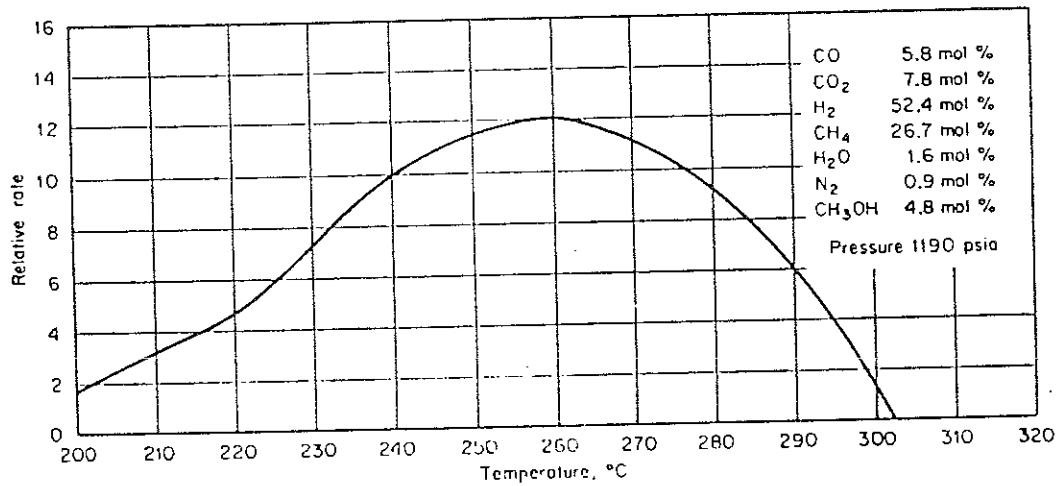
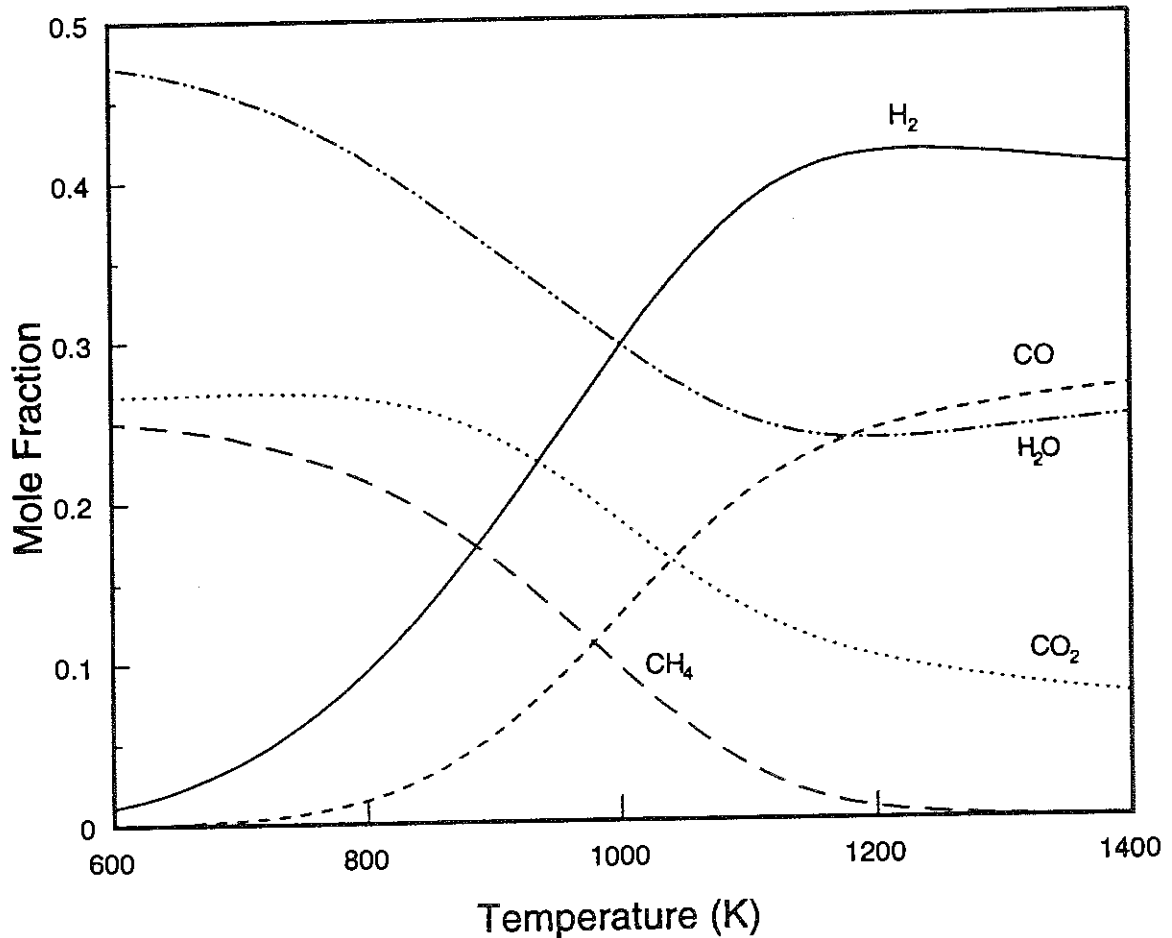


Figure 4-4: Methanol synthesis reaction rate as a function of temperature for the Imperial Chemical Industries (ICI) catalyst (Rogerson, 1984). The reaction is $\text{CO} + 2\text{H}_2 \rightarrow \text{CH}_3\text{OH} + \text{heat}$.



Initial Concentrations (vol %)

	<u>Wet</u>	<u>Dry</u>
H ₂	11.36	20.74
CO	25.26	46.12
CO ₂	6.08	11.10
CH ₄	8.60	15.70
C ₂ H ₄	2.84	5.18
C ₂ H ₆	0.39	0.71
H ₂ O	45.22	---
N ₂	0.24	0.43

Figure 4-5: Chemical equilibrium composition as a function of temperature for steam reforming of the BCL product gas. Steam has been added for a total steam:hydrocarbon ratio of 3:1. The pressure is 1.5 MPa.

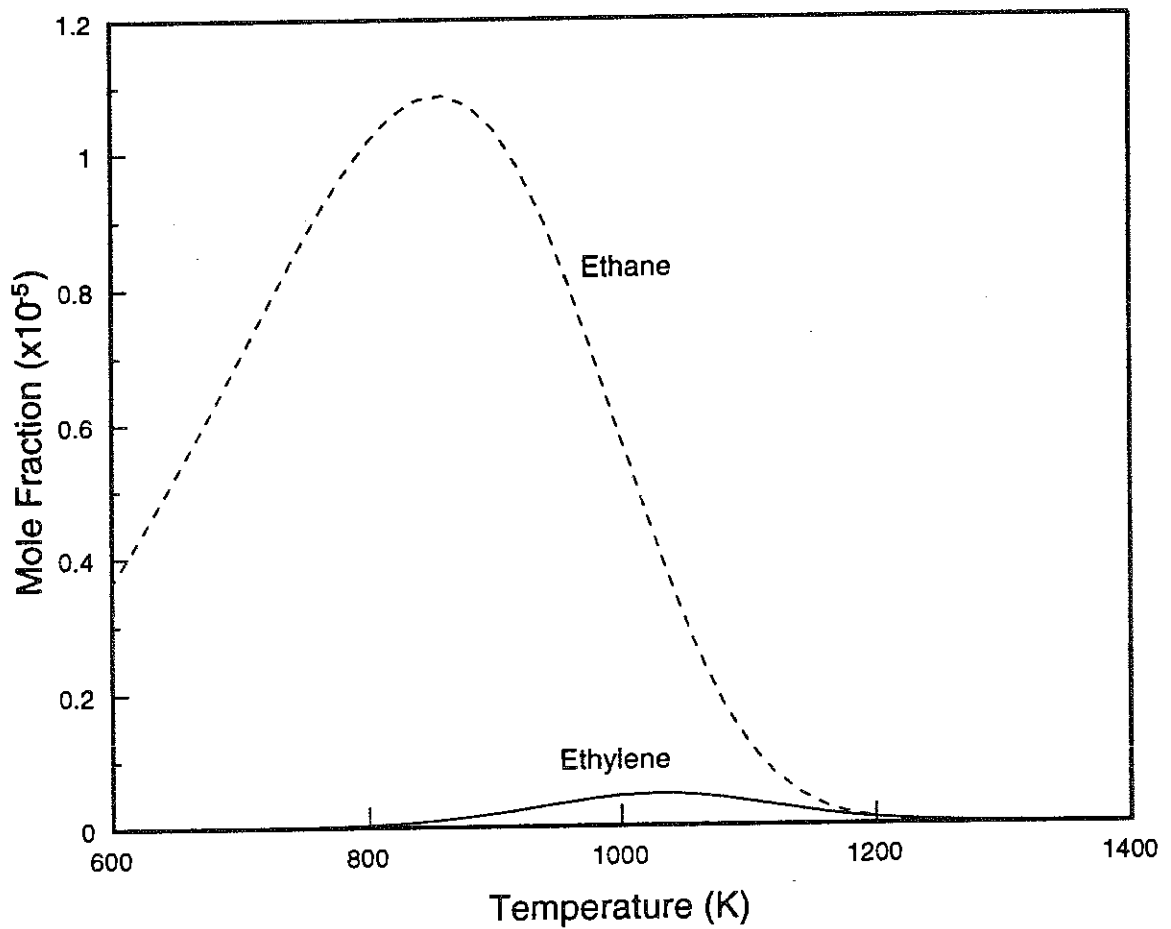
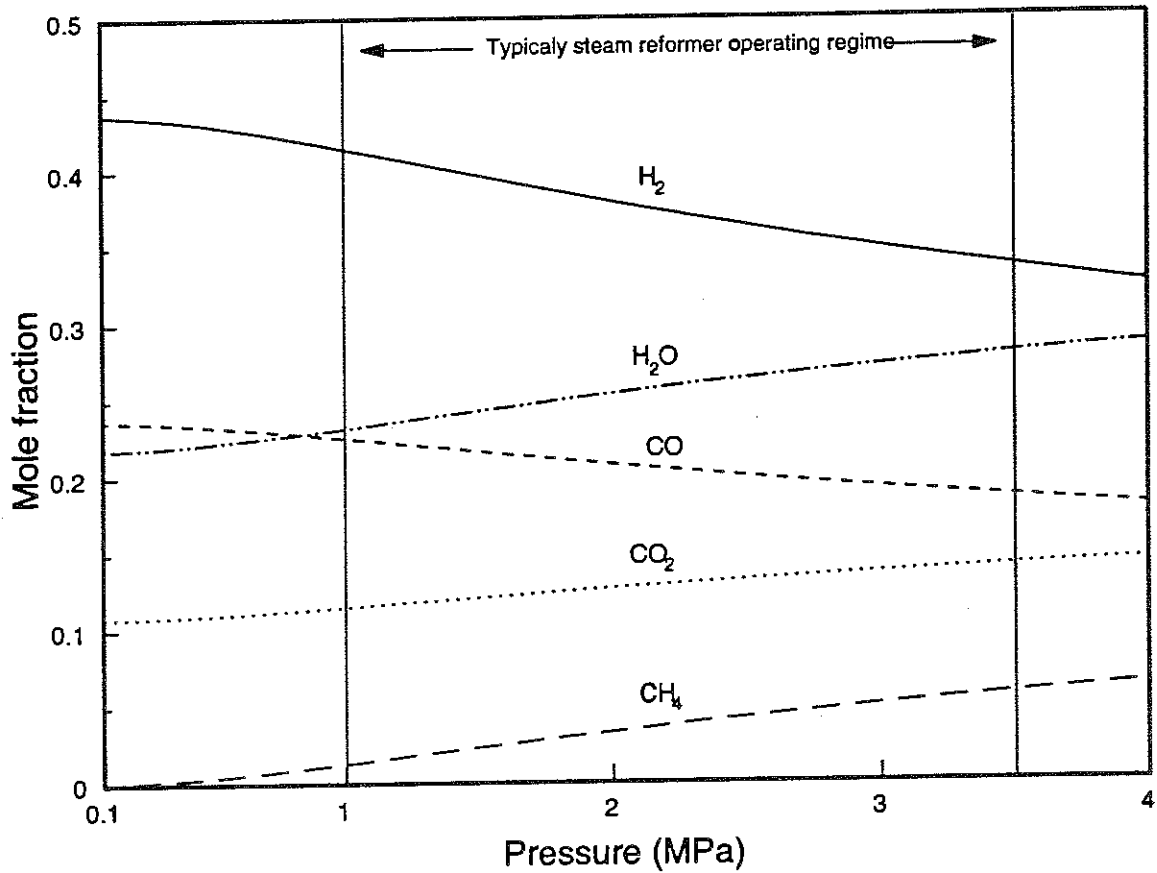


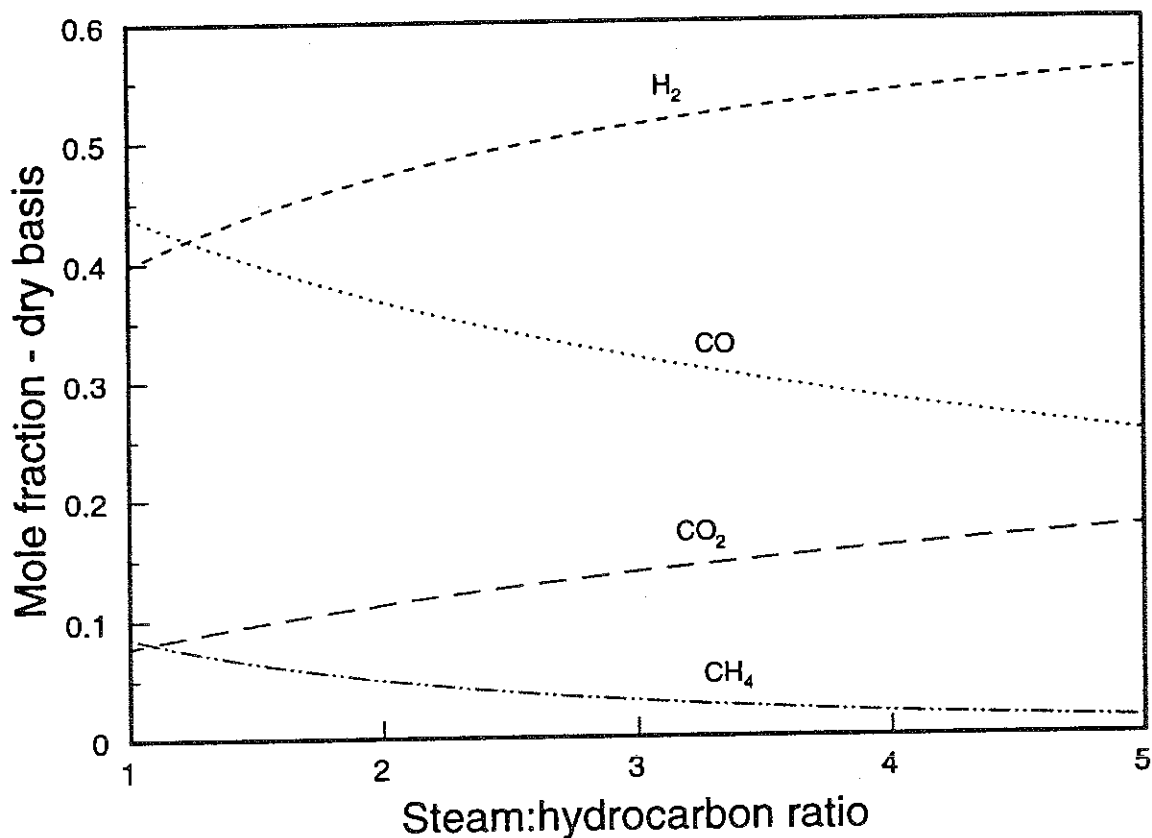
Figure 4-6: Chemical equilibrium concentrations of ethane and ethylene in the reformer product gas using the product gas of the BCL gasifier as the feed. Reformer conditions are the same as those in Figure 4-5.



Initial Concentrations (vol %)

	<u>Wet</u>	<u>Dry</u>
H ₂	11.36	20.74
CO	25.26	46.12
CO ₂	6.08	11.10
CH ₄	8.60	15.70
C ₂ H ₄	2.84	5.18
C ₂ H ₆	0.39	0.71
H ₂ O	45.22	---
N ₂	0.24	0.43

Figure 4-7: Chemical equilibrium composition as a function of pressure for steam reforming of the product gas from the BCL gasifier. Steam has been added for a total steam:hydrocarbon ratio of 3:1. $T = 867^{\circ}\text{C}$.



Initial Concentrations (vol % - dry basis)

H ₂	20.74
CO	46.12
CO ₂	11.10
CH ₄	15.70
C ₂ H ₄	5.18
C ₂ H ₆	0.71
N ₂	0.43

Figure 4-8: Chemical equilibrium composition as a function of steam:hydrocarbon ratio for steam reforming of the BCL synthesis gas. T = 867°C and P = 1.5 MPa.

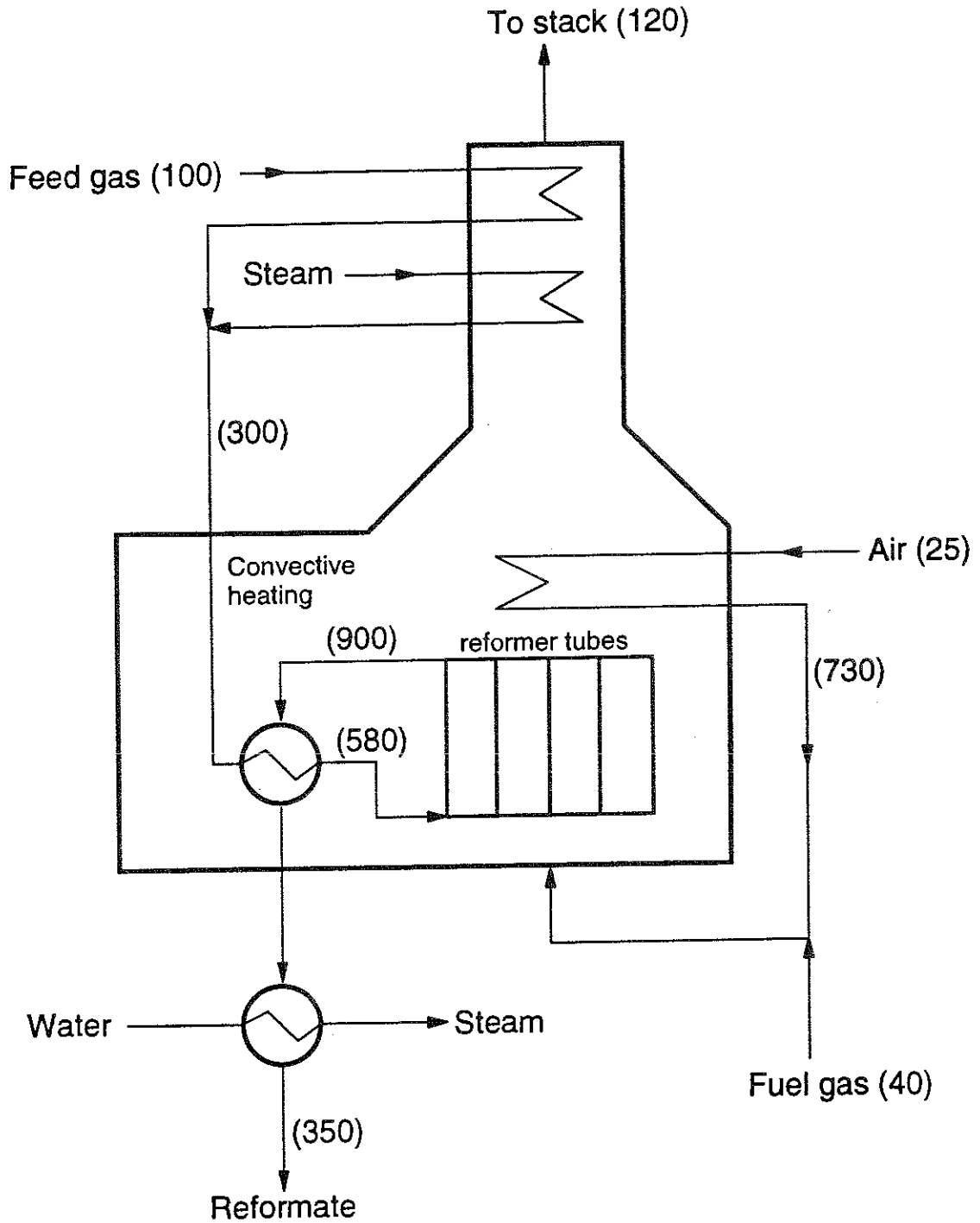


Figure 4-9: Schematic representation of a steam reformer. Typical operating temperatures at various points are given in parenthesis in °C.

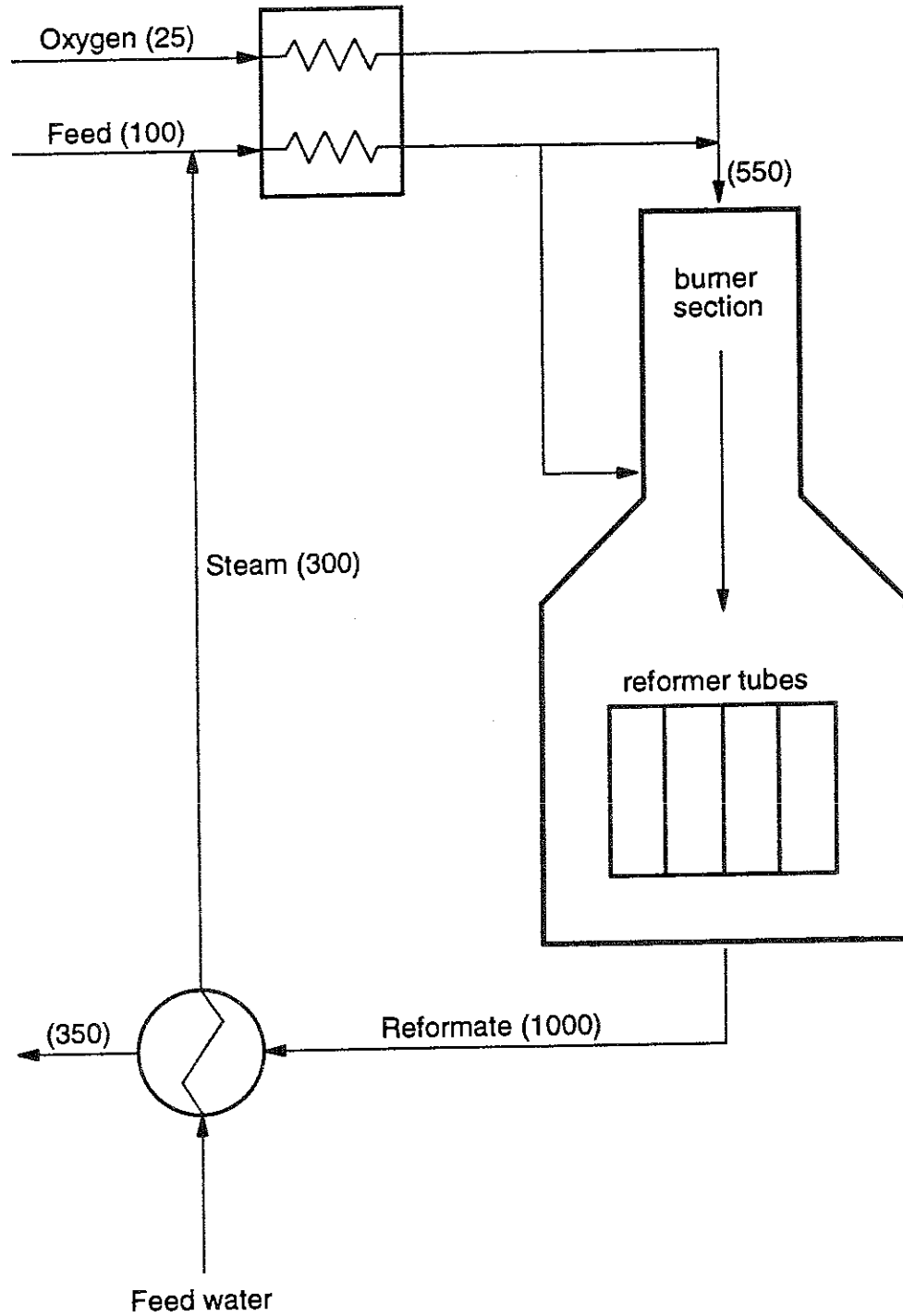
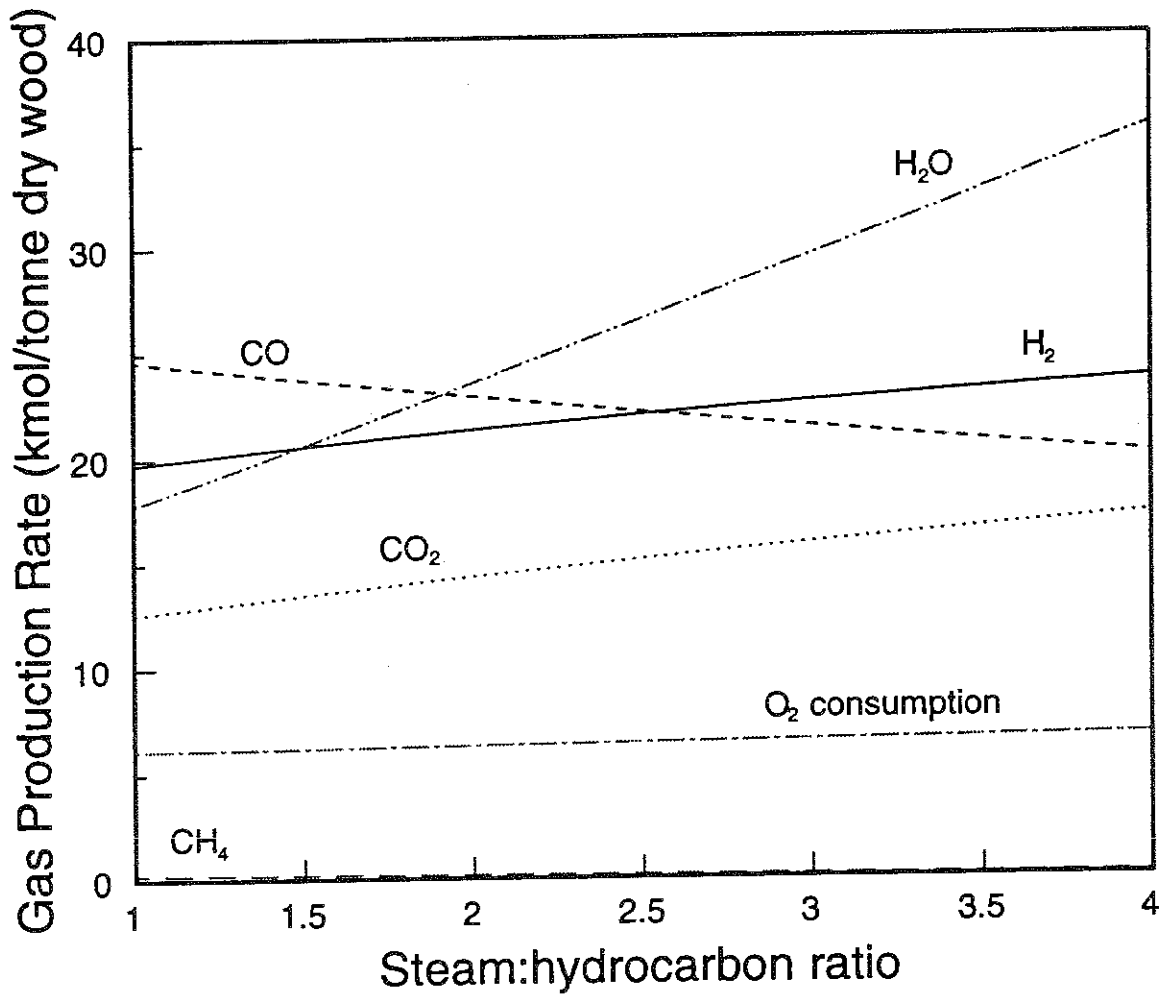


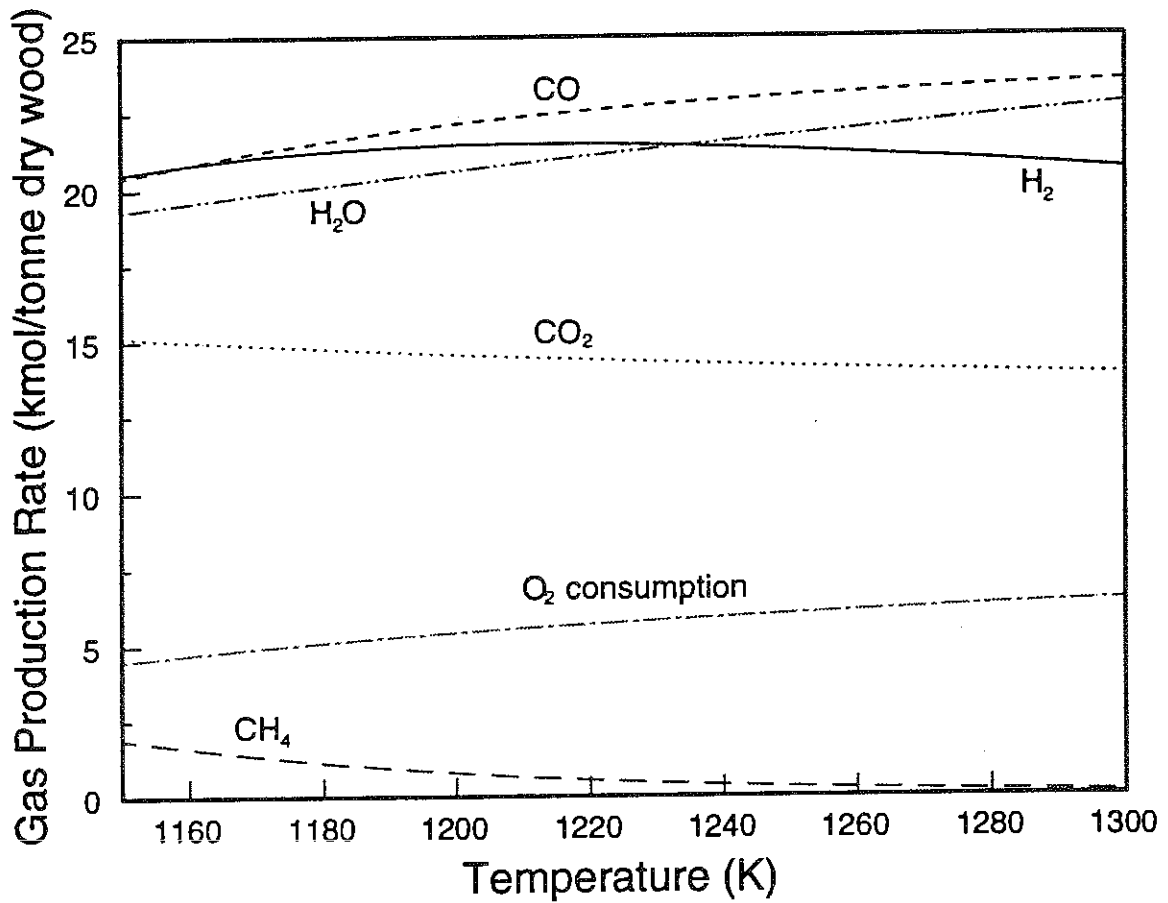
Figure 4-10: Schematic representation of a catalytic autothermal reformer. Typical operating temperatures at various points are given in parenthesis in °C.



Initial Flow Rates (kmol/tdw)

H ₂	16.97
CO	12.30
CO ₂	17.96
CH ₄	6.68
C ₂ H ₄	0.25

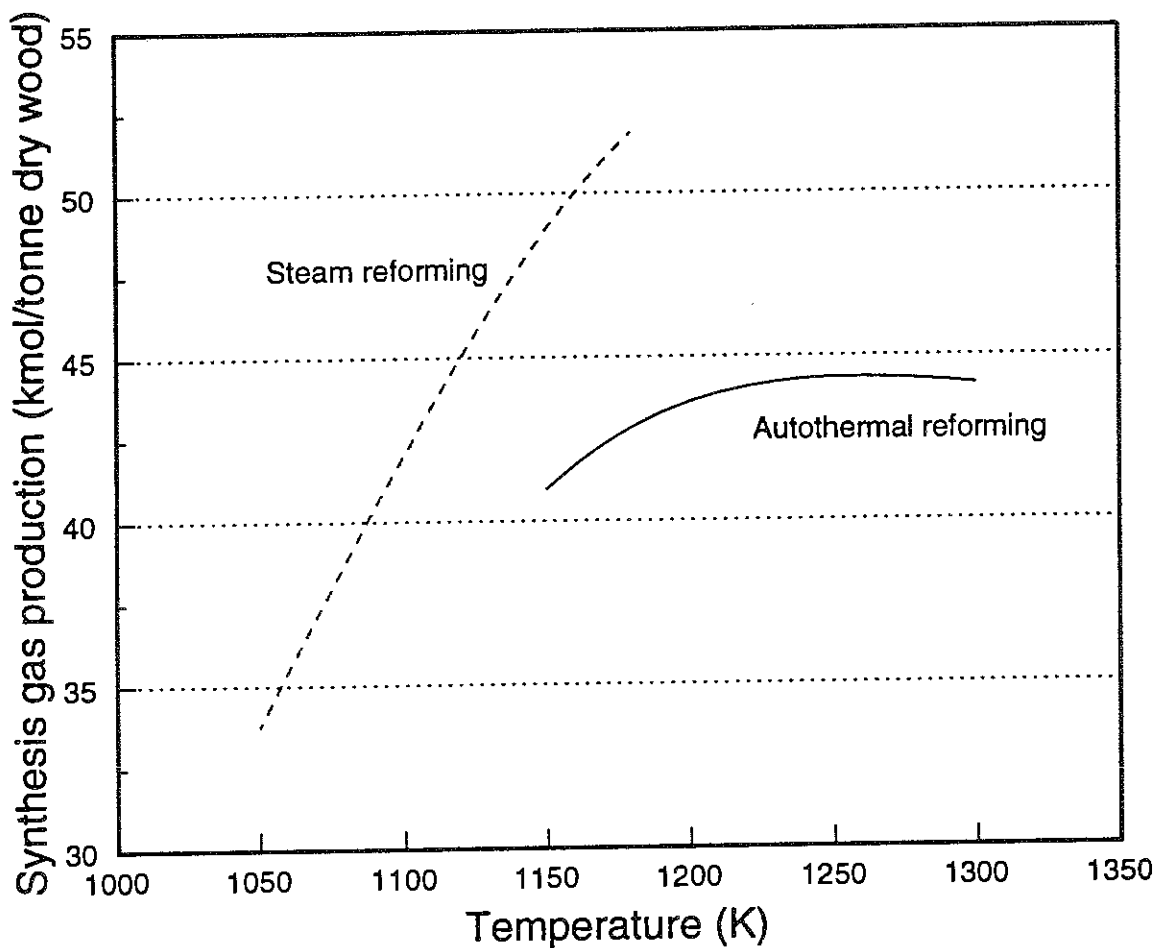
Figure 4-11: The effect of the steam:hydrocarbon ratio on the equilibrium composition of the gas produced via catalytic autothermal reforming using the product gas of the IGT gasifier as the feed. $T = 1000^{\circ}\text{C}$ and $P = 3.3 \text{ MPa}$.



Initial Flow Rates (kmol/tdw)

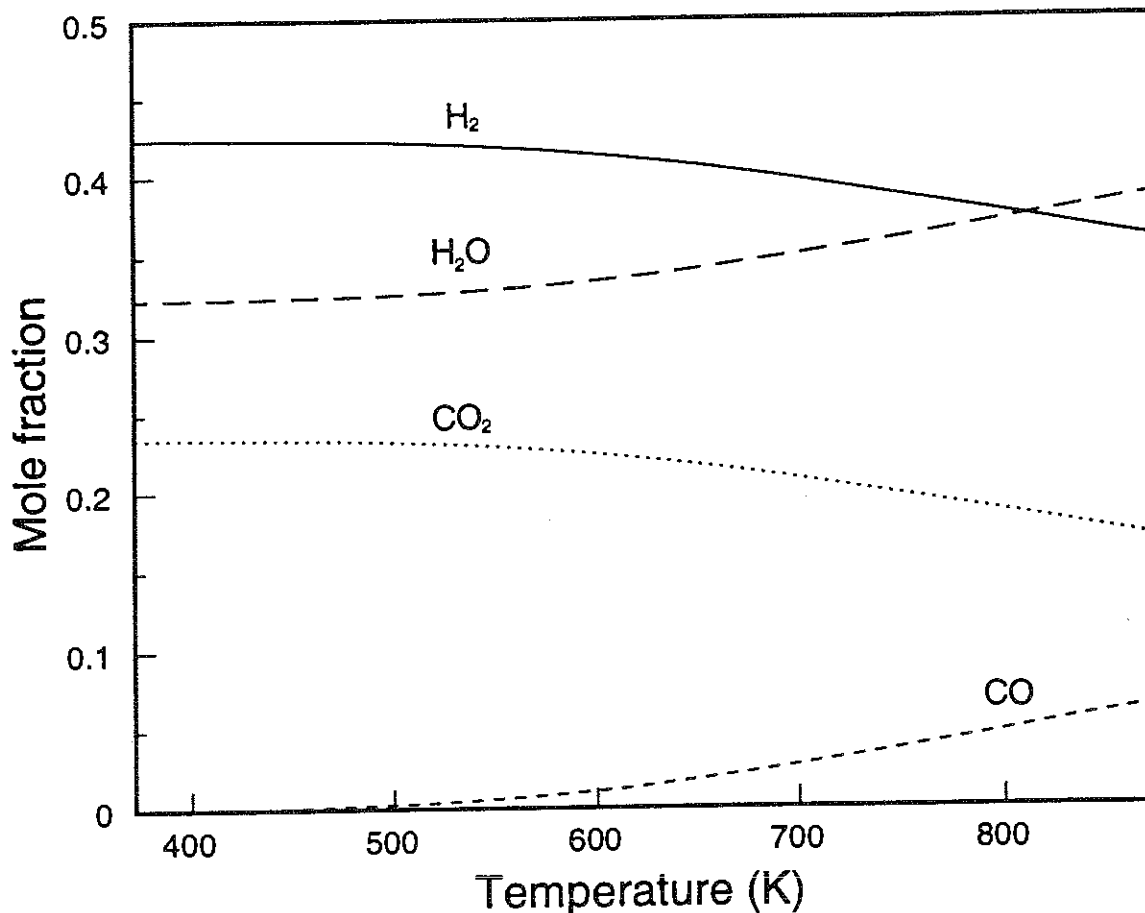
H ₂	16.97
CO	12.30
CO ₂	17.96
CH ₄	6.68
C ₂ H ₄	0.25
H ₂ O	12.77

Figure 4-12: The effect of temperature on the equilibrium composition of the gas produced via catalytic autothermal reforming using the IGT gasifier. The steam:hydrocarbon ratio is 2:1 and the pressure is 3.3 MPa.



Note: Synthesis gas is defined as the moles of $\text{CO} + \text{H}_2$ produced, since all other compounds are inert after the reforming step.

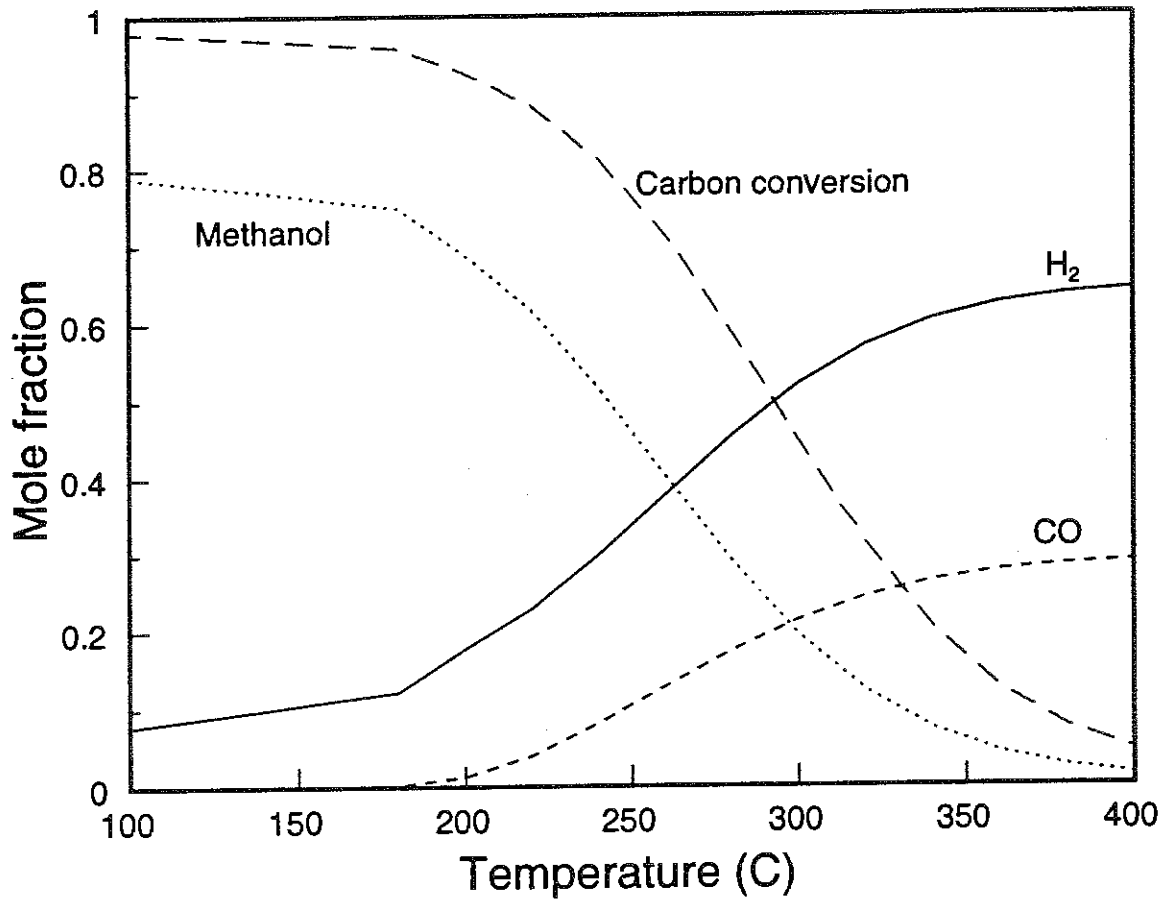
Figure 4-13: A comparison of syngas production for conventional steam reforming and catalytic autothermal reforming using the product gas of the IGT gasifier as the feed.



Initial Concentrations (vol %)

	<u>Wet</u>	<u>Dry</u>
H ₂	26.24	50.88
CO	16.14	31.31
CO ₂	7.32	14.19
CH ₄	1.74	3.36
C ₂ H ₄	0.00	0.00
C ₂ H ₆	0.00	0.00
H ₂ O	48.44	---
N ₂	0.13	0.25

Figure 4-14: Equilibrium concentrations as a function of temperature for the shift reaction using the reformed gas from the BCL gasifier. The steam:CO ratio is set at 3:1. CH₄ is inert and is omitted for clarity.



Initial Concentrations (vol %)

H ₂	65.38
CO	29.18
CO ₂	2.00
CH ₄	3.15
C ₂ H ₄	0.00
C ₂ H ₆	0.00
H ₂ O	0.00
N ₂	0.28

Figure 4-15: Single pass equilibrium concentrations as a function of temperature for methanol synthesis using the BCL makeup gas. The methane is inert and is omitted for clarity. $P = 10.3$ MPa.

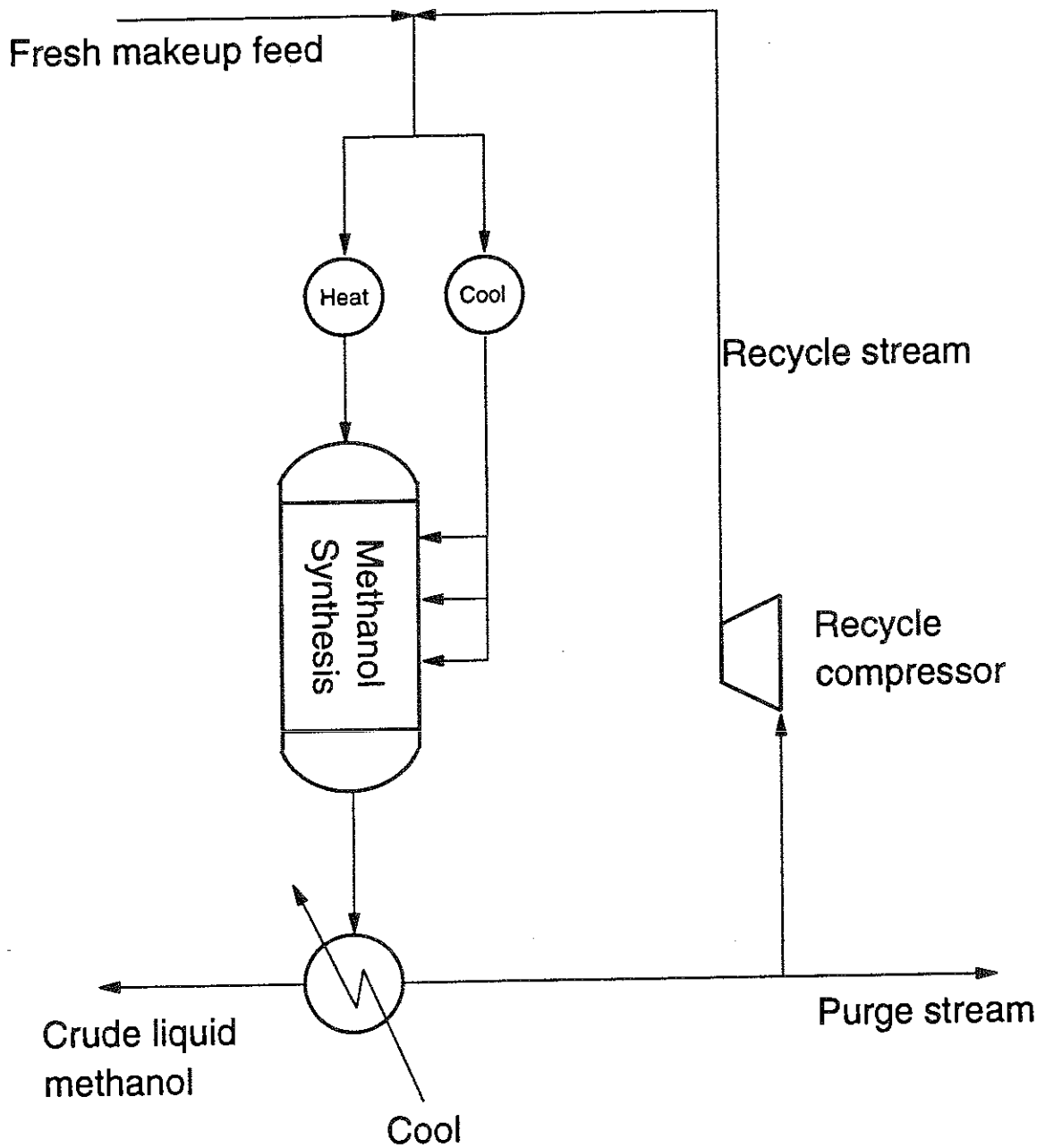


Figure 4-16: Schematic representation of a methanol synthesis loop based on the ICI low-pressure methanol synthesis technology.

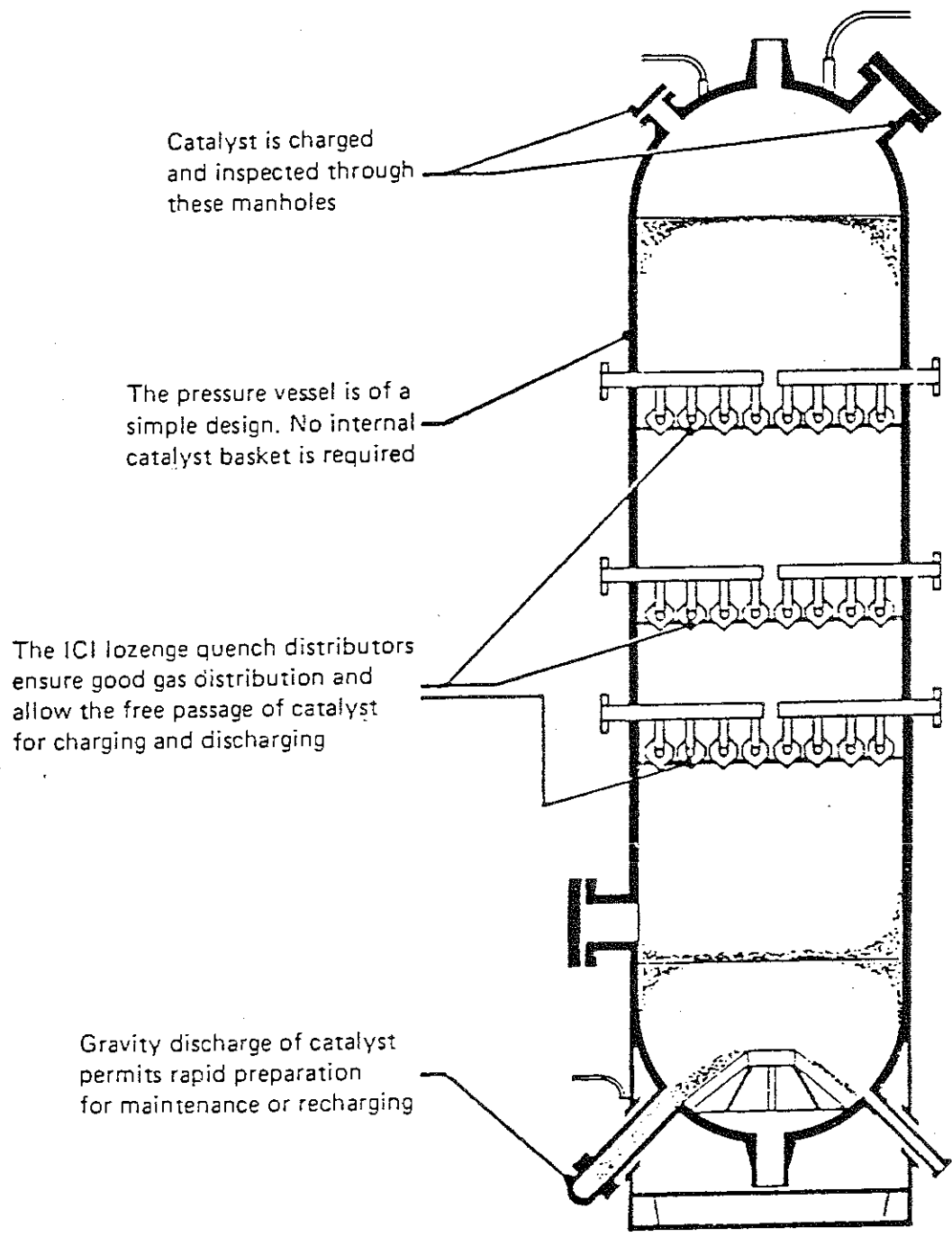


Figure 4-17: Schematic representation of the Imperial Chemical Industries (ICI) methanol synthesis reactor (Rogerson, 1984).

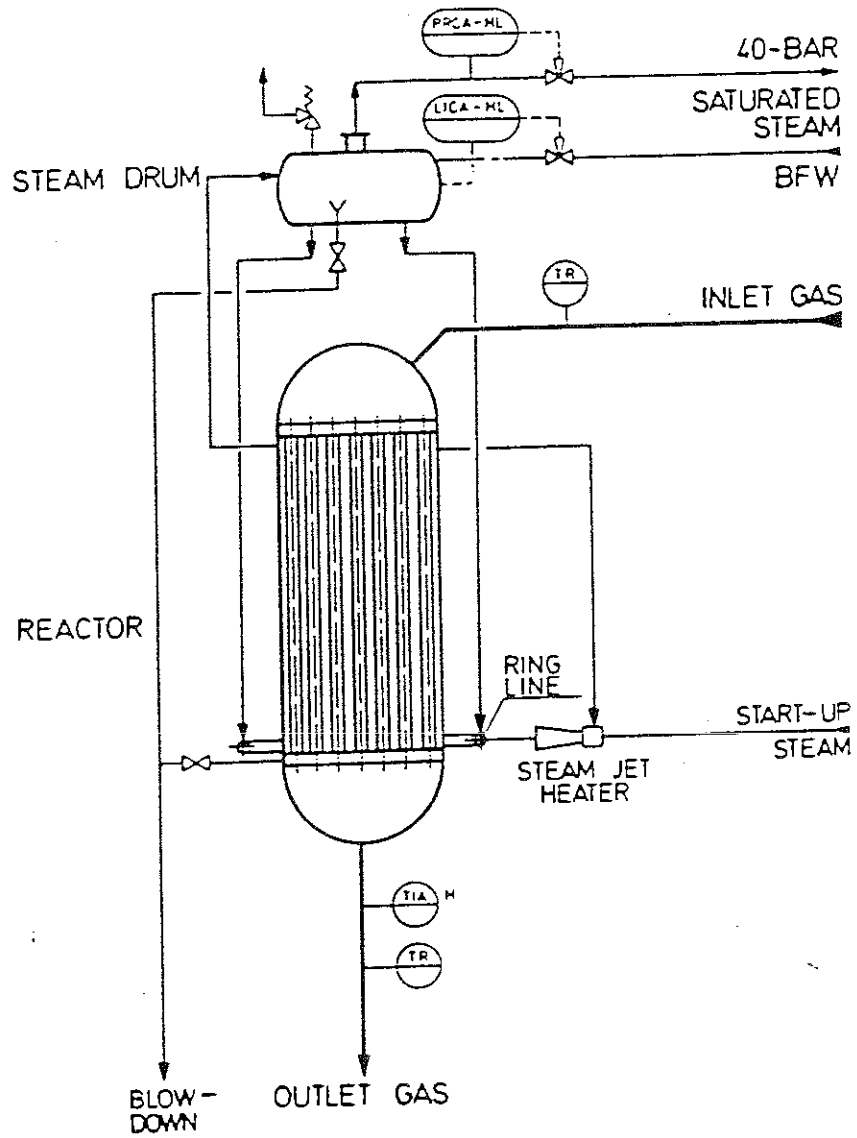


Figure 4-18: Schematic representation of the Lurgi methanol synthesis reactor (Supp and Quinkler, 1984).

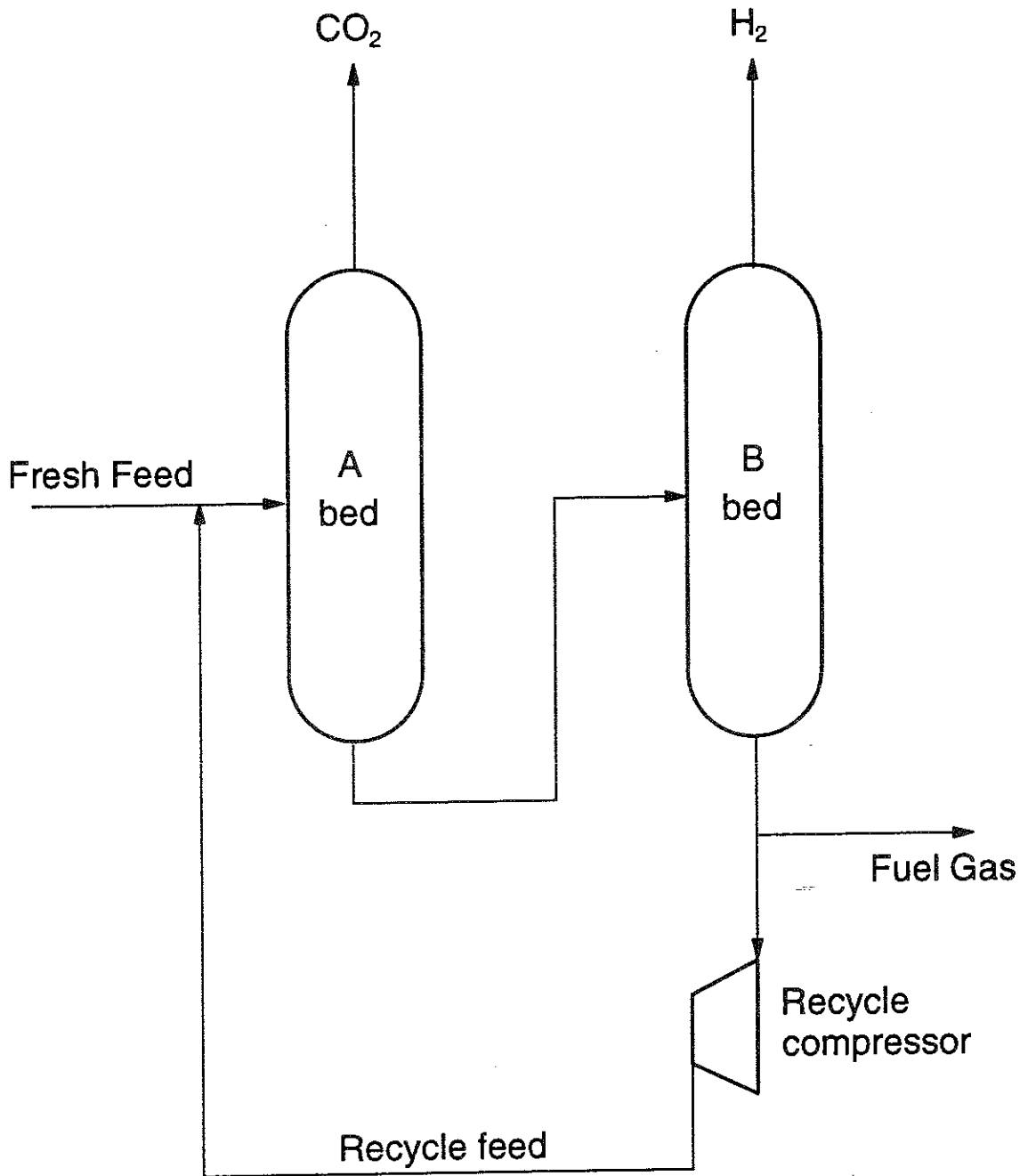


Figure 4-19: Schematic representation of the pressure swing adsorption loop used for hydrogen purification (based on Solomon, 1991).

References

- "Autothermal Reforming." *Hydrocarbon Processing*. Vol. 63, No. 4, April 1984, pp. 103.
- Ashcroft, A.T., Cheetham, A.K., Green, M.L.H., and Vernon, P.D.F. *Carbon Dioxide as an Oxidizing Agent for Natural Gas*. Unpublished manuscript. Oxford University, 1990.
- Blok, K., Hendriks, C.A., Turkenburg, W.C., and Williams, R.H. *Producing Fuel and Electricity from Coal with Low Carbon Dioxide Emissions*. Draft manuscript, University of Utrecht, June 1991.
- Chem Systems. *Optimization of Electricity-Methanol Coproduction*. (GS-6869) Prepared by Chem Systems for the Electric Power Research Institute. Palo Alto, CA: Electric Power Research Institute, June 1990.
- Cheng, Gordon C. and Saini, Riju. *Fuel Reformer Technologies for Fuel Cell Vehicles*. Presented at the 1993 SAE Fuel Cell for Transportation TOPTEC, Diamond Bar, CA, March 10, 1993.
- Corr, F., Dropp, F., and Rudelstorfer, E. "PSA Produces Low-Cost, High-Purity H₂." *Hydrocarbon Processing*. March 1979, pp. 119-122.
- Dibbern, H.C., Olesen, P. Rostrup-Nielsen, J.R., Tottrup, P.B., and Udengaard, N.R. "Make low H₂/CO Syngas Using Sulfur Passivated Reforming." *Hydrocarbon Processing*. Vol. 65, No. 1, January 1986, pp. 71-74.
- Dostrovsky, Israel. "Chemical Fuels from the Sun." *Scientific American*. Vol. 265, No. 6, December 1991, pp. 102-108.
- Epps, Richard (Technical Service Engineer, Specialty Chemical Division). Union Carbide, Houston, TX. Personal communication. June 1991.
- Fish, J.D. and Hawn, D.C. "Closed Loop Thermochemical Energy Transport Based on CO₂ Reforming of Methane: Balancing the Reaction System." *Journal of Solar Energy Engineering*. Vol. 109, August 1987, pp. 215-220.
- Gesser, H.D. and Hunter, N.R. "The Direct Conversion of Methane to Methanol (DMTM)." *Methane Conversion by Oxidative Processes: Fundamental and Engineering Aspects*. Ed. E.E. Wolf. New York: Van Nostrand Reinhold, 1991.
- Goff, S.P. and Wang, S.I. "Syngas Production by Reforming." *Chemical Engineering Progress*. Vol 83, No. 8, August 1987, pp. 46-53.

- Gottesfeld, Shimshon and Pafford, Judith. "A New Approach to the Problem of Carbon Monoxide Poisoning in Fuel Cells Operating at Low Temperatures." *Journal of the Electrochemical Society*. Vol. 135, No. 10, October 1988.
- Haggin, Joseph. "Liquid-Phase Methanol Process Promises Cost Saving." *Chemical and Engineering News*. Vol. 68, No. 3. August 4, 1986, pp. 21-22.
- Haggin, Joseph. "New, Powerful Catalysts for Methane Conversion." *Chemical and Engineering News*. March 1990, pp. 5-6.
- Heck, J.L. and Johansen, T. "Process Improves Large Scale Hydrogen Production." *Hydrocarbon Processing*. January 1978, pp. 175-177.
- Hickman, D.A. Dow Chemical Company, Midland, MI. Personal communication. January 1993.
- Hickman, D.A. and Schmidt, L.D. "Production of Syngas by Direct Catalytic Oxidation of Methane." *Science*. Vol. 259. 15 January, 1993, pp. 343-346.
- Klier, K. "Methanol Synthesis." *Proceedings: Biomass-to-Methanol Specialists Workshop*. Ed. T.B. Reed and M.S. Graboski. Solar Energy Research Institute, Golden, Colorado, March 1982.
- Kuo, James C.W. "Engineering Evaluation of Direct Methane Conversion Processes." *Methane Conversion by Oxidative Processes: Fundamental and Engineering Aspects*. Ed. E.E. Wolf. New York: Van Nostrand Reinhold, 1991.
- Kurkela, E., Stahlberg, P., Laatikainen, J., and Nieminen, M. "Removal of Particulates and Alkali Metals from Pressurized Fluid-bed Gasification of Peat and Biomass--Gas Cleanup for Gas Turbine Applications." *Energy From Biomass and Wastes XV*. Ed. D.L. Klass. Chicago: Institute of Gas Technology, 1991.
- McGraw-Hill Dictionary of Scientific and Technical Terms*. 2nd edition. Ed. Daniel N. Lapedes. New York: McGraw-Hill, 1978.
- Mansfield, K. (Methanol Licensing Manager). ICI Katalco, Billingham, England. Personal communication. December 1991.
- Mansfield, K. (Methanol Licensing Manager). ICI Katalco, Billingham, England. Personal communication. July 1992.
- Miller, Geoffrey Q. and Stoecker, Joerg. *Selection of a Hydrogen Separation Process*. Paper presented at the 1989 National Petroleum Refiners Association Annual Meeting, San Francisco, CA, March 19-21, 1989.

- Minet, R.G. and Olesen, O. "Technical and Economic Advances in Steam Reforming of Hydrocarbons." *Hydrogen: Production and Marketing*. Ed. W.N. Smith and J.G. Santangelo. Washington DC: American Chemical Society, 1980.
- Mohr, Volker H. and Ranke, Gerhard. "Acid and Sour Gas Treating Processes." *Chemical Engineering Progress*. October 1984, pp. 27-34.
- Paisley, Mark. Battelle Columbus Laboratory, Columbus, Ohio. Personal communication. February 1993.
- Periana, Roy A., Taube, Douglas J., Evitt, Eric R., Löffler, Daniel G., Wentreck, Paul R., Voss, George, and Masuda, Toshihiko. "A Mercury-Catalyzed, High-Yield System for the Oxidation of Methane to Methanol." *Science*. Vol. 259. January 15, 1993, pp. 340-343.
- Probstein, Ronald F. and Hicks, R. Edwin. *Synthetic Fuels*. New York: McGraw-Hill Book Company, 1982.
- Riensch, E. and Fedders, H. "Conversion of Natural Gas to CO Rich Syngases." *Natural Gas Conversion*. Ed. A Holmen, K.J. Jens, and S. Kolboe. Amsterdam: Elsevier Science Publishers, 1991.
- Rogerson, P.L. "The ICI Low-Pressure Methanol Process." *Handbook of Synfuels Technology*. Ed. R.A. Meyers. New York: McGraw-Hill, 1984.
- Shell. *Carbon Dioxide Disposal from Coal Based Combined Cycle Power Stations in Depleted Gas Fields in the Netherlands*. (Lucht 91) Prepared by Shell International Petroleum Maatschappij and Koninklijke/Shell Exploratie en Productie Laboratorium for the Ministry of Housing, Physical Planning and Environment, Air Directorate. Leidschendam, the Netherlands, December 1990.
- Shelley, Suzanne. "Out of Thin Air." *Chemical Engineering*. June 1991, pp. 30-39.
- Short, Herb. "NH₃ Break Thru: Small Plants." *Chemical Engineering*. July 1989, pp. 41-45.
- Solbakken, Åge. "Synthesis Gas Production." *Natural Gas Conversion*. Ed. A. Holmen, K.J. Jens, and S. Kolboe. Amsterdam: Elsevier Science Publishers, 1991.
- Solomon, James (Business Manager - Gas Separation). Air Products and Chemicals, Inc., Allentown, PA. Personal communication. July 1991.
- Solomon, James (Business Manager - Gas Separation). Air Products and Chemicals, Inc., Allentown, PA. Personal communication. February 1993.
- Supp, Emil. *How to Produce Methanol from Coal*. Berlin: Springer-Verlag, 1990.

- Supp, E. and Quinkler, R.F. "The Lurgi Low-Pressure Methanol Process." *Handbook of Synfuels Technology*. Ed. R.A. Meyers. New York: McGraw-Hill, 1984.
- Taylor, C.H. "The Purification of Gases Derived from Coal." *Handbook of Synfuels Technology*. Ed. R.A. Meyers. New York: McGraw-Hill, 1984.
- Thomas, Daniel J., Willi, René, and Baiker, Alfons. "Partial Oxidation of Methane: The Role of Surface Reactions." *Ind. Eng. Chem. Res.* Vol 31, No. 10 (1992), pp. 2272-2278.
- Tomlinson, T.R. and Finn, A.J. "H₂ Recovery Processes Compared." *Oil & Gas Journal*. January 15, 1990, pp. 35-39.
- Union Carbide, Personal communication. July 1992.
- van Weenen, Willem F. and Tielrooy, Jack. "Hydrogen Plant Design Economics." *Chemical Engineering Progress*. February, 1983.
- Vernon, Patrick, D.F., Green, Malcolm, L.H., Cheetham, Anthony K., and Ashcroft, Alexander, T. "Partial Oxidation of Methane to Synthesis Gas." *Catalyst Letters*. Vol. 6 (1990), pp. 181-186.
- Waldheim, L., Lundberg, H, and Rensfelt, E, *Project Proposal for the World Bank/Global Environmental Facility Brazilian BIG-AGT (Biomass Integrated Gasification-Advanced Gas Turbine) Program Based on the Studsvik AGT-BG Process*. December 1991.
- Wang, S.I., Nicholas, D.M., and DiMartino, S.P. "Analysis Dictates H₂ Purification Process." *Oil & Gas Journal*. February 6, 1984, pp. 111-117.
- Westerterp, K.R., Bodewes, T.N., Vrijland, M.S.A., and Kuczunski. M. "Two New Methanol Converters." *Hydrocarbon Processing*. Vol. 67, No. 11, November 1988, pp. 69-73.
- White, Donald H. Jr. and Barkley, Glenn P. "The Design of Pressure Swing Adsorption Systems." *Chemical Engineering Progress*. January 1989, pp. 25-33.
- Williams, Robert H. and Larson, Eric D. "Advanced Gasification-Based Biomass Power Generation." *Renewable Energy: Sources for Fuels and Electricity*. Ed. T.B. Johansson, H. Kelly, A.K.N. Reddy, and R.H. Williams. Washington DC: Island Press, 1992.

Chapter 5: Modeling Methanol and Hydrogen Production

5.1 Introduction

This chapter describes the thermodynamic computer models that were developed to simulate methanol and hydrogen production from natural gas, coal and biomass. As with all computer models, the first step was to obtain good input data. For existing gasifiers, performance data was obtained from published literature and through discussions with developers. For the Shell entrained-bed gasifier operating on biomass, for which there is no operating experience, a separate thermodynamic model was constructed (see Chapter 3 and Appendix 3A). Detailed process flowsheets were then developed using ASPEN PLUS, a state-of-the-art, commercially available, chemical process simulation software package. The information derived from these simulations was used to perform a *pinch analysis* to determine the quantities of external power (electricity), heating, and cooling required in each case. Pinch analysis was used to provide a consistent framework for heat integration, and results in a thermally optimized facility. This enables more meaningful thermodynamic comparisons between different process configurations and different gasifiers.

5.2 General Thermodynamic Considerations

5.2.1 Chemical Equilibrium Approximation

As discussed in Chapter 4, chemical reactors that use catalysts must be designed with consideration for both thermodynamic and kinetic factors. Thermodynamics is what drives a mixture towards chemical equilibrium, whereas chemical kinetics describes the mechanisms and rates at which the reactions take place. Specifically, catalysts are designed to enhance the kinetics of a particular reaction or set of reactions. The aim in designing catalysts and chemical reactors is to establish the most favorable thermodynamic regime that can still support high reaction rates. Under such

circumstances a reactor is thermodynamically controlled as opposed to kinetically limited. Since reactors are designed to be equilibrium controlled, the temptation might be to simply use chemical equilibrium calculations to model such reactors, this is not entirely correct, for it is not possible to completely ignore the kinetic aspects of the reactions. Nevertheless, since chemical equilibrium dominates over kinetic factors, most systems can be modeled as approaching chemical equilibrium.

The physical reason why chemical reactors cannot simply be modeled using chemical equilibrium is that residence times in most steady flow chemical reactors are short (~1 second). Since the desired reaction or set of reactions proceeds predominantly on the catalyst surface, the gas-catalyst contact time is often insufficient for all the feed to react, even if kinetics are fast. In fact, the underlying principle behind chemical equilibrium calculations is the assumption that equilibrium concentrations are reached only after an infinite amount of time has elapsed. In reality, many reactions proceed so quickly (e.g. combustion) that for all practical purposes one can assume chemical equilibrium after a very brief period.¹ Strictly speaking however, the effect of finite reaction time is to produce a gas mixture that has come close to but has not fully reached equilibrium. This effect is more pronounced in catalytically enhanced reactions because of the limitations imposed by operating conditions, catalyst activity and reactor design.

¹ An interesting exception in combustion is the formation of NO_x , which cannot be accurately modeled using equilibrium calculations. Therefore, understanding the mechanisms of NO_x formation is only possible with a detailed knowledge of the kinetics of the relevant reactions. This has important implications for the design of new combustors and processes that can reduce the formation of NO_x without the need for expensive treatment of the combustion products.

In spite of the fact that true equilibrium is not achieved in most chemical reactors, the ability to use chemical equilibrium greatly simplifies the computational aspect of modeling hydrogen and methanol production. Equilibrium calculations are straightforward, and numerous algorithms exist for determining equilibrium compositions given temperature, pressure, the chemical species present at equilibrium and the relative atom populations. On the other hand, accurate chemical kinetic calculations require detailed knowledge about how the reaction rate is affected by temperature, activation energy, pressure and even molecular orientation, and this data is subject to considerably more uncertainty than the data used for equilibrium calculations. Furthermore, for complex reacting systems, this information would be required for the many intermediate reactions taking place, which can number literally in the hundreds. Fortunately, the effect of finite time can be successfully modeled using chemical equilibrium and the concept of an *approach temperature*. The degree to which equilibrium is attained is approximated by evaluating chemical equilibrium at a temperature close to the actual reactor temperature, while overall energy balances are evaluated at the actual temperature. For endothermic reactions, which are favored at higher temperatures, the equilibrium composition is evaluated at a temperature slightly below the reactor temperature. For exothermic reactions, which are favored at lower temperatures, equilibrium is computed at a temperature slightly above the reactor temperature. In both cases, the yield of the desired product is slightly lower than if true equilibrium were attained, which accurately reflects the performance of real systems. The precise value of the approach temperature (ΔT_{app}) is based on knowledge about the activity of the catalyst, the residence time in the reactor and the design of the reactor itself. Practical experience shows that the overall effect is small, and values of ΔT_{app} are usually less than 20°C. Table 5-1 gives the values used in the reactor models developed for this thesis.

Table 5-1: Chemical equilibrium approach temperatures used in this study.

Reactor Model	ΔT_{app} (°C)
Reformer	-10 ^a
High temperature shift reactor	+10 ^b
Low temperature shift reactor	+20 ^b
Methanol synthesis unit	+12.5 ^c

- (a) Lloyd (1991) assumed that for pure methane/steam systems, ΔT_{app} was zero above 650°C, but since methane represents a much smaller fraction of the feed in biomass based systems, which leads to slower reaction rates, a more conservative value was chosen for this study. This value is also consistent with other recent studies that modeled methane-steam reforming (Kuo, 1991; Bain, 1991).
- (b) These values were assumed to be similar to those used for the other chemical reactors modeled in this thesis. Since reaction rates are lower at lower temperatures, a larger approach temperature was assumed for the low temperature shift reactor.
- (c) For fresh catalyst material, the approach temperature is essentially zero, whereas after about 3 years, it is approximately 20°C (Mansfield, 1991). For modeling purposes, an intermediate value was chosen that was consistent with a recent study of methanol production from natural gas (Kuo, 1991).

Another consideration that must not be neglected when using chemical equilibrium is the fact that catalysts are selective to specific reactants and reactions. Therefore, chemical equilibrium computations must be restricted to those species that participate in the reaction(s). At the same time, the effect of inert compounds on partial pressures and overall heat balances must be included, since they influence the equilibrium concentrations of the reacting species.

5.2.2 Pressure Losses

Pressure drops across individual components are generally small, but when many units are involved, it is necessary to account for the cumulative effects of pressure losses. The main consequences of pressure losses are increased compression work and minor changes to chemical equilibrium concentrations. In order to include the effects of pressure drops without the need for detailed design calculations for each component, nominal pressure drops were assumed for most blocks, the most important being heat exchangers (because

of their number). For pressurized shell-and-tube heat exchangers, a 0.5 bar pressure drop is fairly typical (Fraas, 1989). Another approach would be to calculate the pressure loss as a percentage of the feed pressure, but using a fixed pressure drop is simpler to model, and was deemed to be adequate to capture the overall effect. The actual values used for the various unit operations are listed in Table 5-2.

Table 5-2: Pressure drops used in the computer simulations.

Unit Operations Block	ΔP (bar)
Mixer ^a	0.0
Splitter ^a	0.0
Heat Exchanger ^b	0.0-0.5
Quench ^c	0.5
Reformer ^c	0.5
Shift Reactor ^c	0.5
Methanol Synthesis ^d	8.1
Methanol Separation ^c	0.5
Boiler ^c	0.5
SELEXOL Unit ^e	0.0
Pressure Swing Absorber ^f	0.7

- (a) These blocks are ASPEN PLUS models and not actual units, so no pressure loss was assumed.
- (b) For heat exchangers operating at atmospheric pressure or involving streams other than the main process streams (e.g. flue gases), zero pressure losses were assumed. Small heat exchangers (e.g. in the recycle loop of the PSA unit) were assumed to have 0.2 bar pressure drops. All other heat exchangers were assumed to have 0.5 bar pressure drops (Fraas, 1989).
- (c) For simplicity, these blocks were assumed to have the same pressure losses as heat exchangers.
- (d) Mansfield, 1991.
- (e) For simplicity, this block was assumed to result in no pressure loss.
- (f) Miller and Stoecker, 1989.

5.2.3 Thermodynamic Properties

Several different thermodynamic property sets were used in the simulations. For pure steam/water streams, ASME steam table correlations were used. Ideal gas behavior was assumed for low pressure gas-phase calculations. High pressure and two-phase

calculations were performed using one of two equation-of-state models that give very similar results: Redlich-Kwong-Soave and BWR-Lee-Starling (Aspen Technology, 1988). Built-in ASPEN PLUS binary interaction parameters that increase the accuracy vapor-liquid equilibrium calculations were also used.

5.3 Heat Integration Using Pinch Analysis

5.3.1 The Motivation for an Integrated Approach to Overall Energy Balances

While it was possible to include process-to-process heat exchange within the ASPEN PLUS models, pinch analysis was used to optimize the integration of process waste heat and ensure a consistent comparison between different process configurations and different gasifier designs. Arbitrarily matching streams in the flowsheets is unlikely to optimize the use of process-to-process heat transfer. Instead, pinch analysis is a systematic method of accounting for all process heating and cooling requirements and then maximizing the use of process waste heat. It is then possible to calculate the minimum amounts of external heating (the hot utility) and external cooling (the cold utility) that must be supplied to a system. Of course, it is ultimately necessary to design a heat exchanger network that can meet these *energy targets* (i.e. the minimum hot and cold utilities), but this is beyond the scope of this thesis.² Rather, the goal here was to determine the values of the minimum hot and cold utilities, which were then used to estimate the amount of electricity (if any) that could be produced from excess waste heat and the amount of additional feed (if any) that had to be burned to provide additional heat and/or electricity. This information was then used in the calculation of the overall energy efficiency of each process (see Chapter 6).

² Process optimization is an active areas of research today, and linear programming methods based on the principles of pinch analysis have been developed to synthesize optimal heat exchanger networks (e.g. see Floudas, et al., 1986).

5.3.2 Pinch Technology Overview and an Illustrative Example

Pinch analysis was first developed about 10 years ago as a tool for analyzing and optimizing the energy performance of industrial processes (Linnhoff, et al., 1982; Karp, 1990). One of the advantages of pinch analysis is that it can be used to identify the minimum external energy requirements (heating and cooling) of a given process *before* detailed design and construction. In determining these energy targets, it is not sufficient to simply sum all heating and cooling requirements of a process, and from that, determine if any excess heat remains. In doing so, one would in all likelihood violate the Second Law of Thermodynamics, which is concerned with the *direction* of heat flow. Simply put, the Second Law states that heat cannot flow from a cold body to a hotter one. This is an important consideration since much of the waste heat in a process may be low temperature heat, making it unavailable for integration into the process. Pinch analysis is used to perform an energy balance for an entire process that satisfies the constraint imposed by the Second Law. The basic procedure is described below.

(i) Data Extraction

Every pinch analysis starts with detailed information for all process heating and cooling requirements, which in this thesis was provided by the ASPEN PLUS computer simulations. In addition, the energy requirements for biomass drying were also estimated for each case. For the BCL cases, the waste heat available from the char combustor flue gases and the air preheat requirements for the char combustor were also included. For the MTCI gasifier, the energy balance around the pulse combustor was integral to the ASPEN PLUS simulations. For the WM cases, the heat required by the gasifier was also estimated and included in the pinch analyses.

To perform a pinch analysis, the following data is required for each stream:

- mass flow rate (\dot{m})
- starting (source) temperature (T_s)
- final (target) temperature (T_t)
- heat capacity (C_p) (e.g. kJ/kg-K)

Although it is necessary to assume that C_p is constant, this is generally a good assumption, even over fairly large temperature changes. In cases where this condition is not satisfied (e.g. streams with phase changes), the stream can be partitioned into several intervals for which it is possible to assume that C_p is constant within each one.

(ii) Composite Curves

Composite curves are used to measure the total amount of heating and cooling required in a process. Two type of streams are defined in pinch analysis: *hot* streams are those that require cooling, and *cold* streams are those that require heating. For each stream, we calculate the *heat capacity flow-rate* (units = kW/degree), which is a measure of the rate of energy flow:

$$CP = \dot{m} * C_p \quad (5-1)$$

Therefore, the total heat transferred to (or from) a stream is:

$$Q = \Delta H = CP *(T_t - T_s) \quad (5-2)$$

where ΔH is the change in enthalpy of the stream.

If a stream is being cooled, Q is negative, and if it is being heated, Q is positive. To calculate the total heat capacity flow-rate for a given temperature interval, one simply sums the heat capacity flow-rates of each stream that passes through that temperature interval. This information is then used to construct what are called the hot and cold *Composite Curves*, as shown in Figure 5-1 for a hot composite curve. Enthalpy flow (ΔH) is plotted along the x-axis (with an arbitrary zero, since we are only interested in changes in enthalpy), and temperature is plotted along the y-axis. Consider for example, the temperature interval T_2 - T_3 in Figure 5-1. All three streams pass through this interval so that:

$$CP_{2-3} = A + B + C \quad (5-3)$$

and

$$\Delta H_{2-3} = (T_3 - T_2)(A + B + C) \quad (5-4)$$

where A , B , and C are the CP s for the three streams in Figure 5-1.

The direction of the arrow indicates that cooling is taking place; as the temperature decreases, so does the enthalpy. Also note that within any interval i , the slope is $1/CP_i$.

This process is then repeated for all the cold streams in a system, and both composite curves can then be placed on a single T-H diagram, as is done for a hypothetical process in Figure 5-2. The resulting plot is somewhat similar to the temperature profiles within a two stream counter-flow heat exchanger. Wherever the two curves overlap, the hot streams can give up their heat to the cold streams, and heat integration is possible. At the hot end (top, right), the horizontal distance between the ends of the two curves is the amount of heating that cannot be supplied by process-to-process heat exchange (the minimum hot utility -- $Q_{h,min}$). Similarly, at the cool end

(bottom, left), the horizontal distance between the ends of the two curves represents the quantity of external cooling required that cannot be supplied by process-to-process heat exchange (the minimum cold utility -- $Q_{c,min}$). At any point, the vertical distance between the two curves is the temperature difference between the hot and cold composite curves. The smallest vertical distance (ΔT_{min}) is the so-called *pinch point*, and is what limits the extent of heat recovery possible. The value of ΔT_{min} can be changed by moving the curves horizontally relative to one another, as shown by the dotted cold composite curve in Figure 5-2. Note that decreasing ΔT_{min} also decreases the size of the minimum hot and cold utilities by increasing process-to-process heat transfer. In order to minimize the need for external heating and cooling, the temptation might be to set ΔT_{min} to zero, but this is not possible in practice because a non-zero temperature difference is required for heat transfer to take place. In practice, typical values for ΔT_{min} are 10-20°C. In general, a larger ΔT means that less heat transfer area is needed, but that less process heat can be recovered.³ Hence there is a trade-off between capital cost (a larger heat transfer area must be purchased for a smaller ΔT) and operating cost (more external heating and cooling is required with a larger ΔT). Nevertheless, ΔT_{min} usually occurs at only one or a few points in a system, so that most heat exchangers operate with larger ΔT s. Therefore a relatively small ΔT_{min} can be chosen (Linnhoff, et al., 1982).

Another interesting element of pinch analysis is that the pinch point divides the process into two distinct regions. Above the pinch, the process is a net heat sink, requiring external heating but not external cooling. The opposite is true below the pinch; the process is a net heat source requiring external cooling but not external heating. If more heat than $Q_{h,min}$ (say $Q_{h,min} + \delta$) is added above the pinch, this increases the amount

³ The rate of heat transfer per unit area (Watts/m²) is directly proportional to the temperature difference between the hot and cold sides of a heat exchanger.

of heat that must be removed below the pinch by the amount δ .⁴ Therefore, δ can also be thought of as external heat supplied to the process below the pinch. However, since the area below the pinch is already a net heat source, it is wasteful to add more heat, which must then be removed by increasing the value of the cold utility. Therefore, one of the basic rules of pinch analysis is that when designing heat exchanger networks, heat should not be transferred across the pinch. Following this rule guarantees that the utilities are minimized.

(iii) The Problem Table and the Grand Composite Curve

Although composite curves are useful for illustrating the concept of pinch analysis, they are not very practical for solving actual problems. Instead, a simple algebraic algorithm known as the *Problem Table Method* has been developed that enables one to quickly and accurately determine the minimum hot and cold utilities and the location of the pinch, even for relatively complex processes (Linnhoff, et al., 1982). The problem table divides the entire system into temperature intervals based on the source and target temperatures of all hot and cold streams. Then, the total heat capacity flow-rate is calculated for each interval by summing the CPs of all the cold streams and subtracting the sum of the CPs of all the hot streams:

$$CP_{net} = \sum CP_{cold} - \sum CP_{hot} \quad (5-5)$$

A positive result means that the interval is a net heat sink, and a negative result means that the interval is a net heat source.

⁴ The heat must go somewhere, and since the region above the pinch is already a net heat source, δ must be removed below the pinch.

Since hot and cold streams are now included in the same interval, it becomes necessary to ensure that within each interval, the hot streams are at least ΔT_{min} hotter than the cold streams. This is necessary because by calculating CP_{net} we are implicitly assuming that the hot streams in an interval can supply heat to the cold streams in that same interval, and must therefore be at least ΔT_{min} hotter than the cold streams. To guarantee this condition, the source and target temperatures of all hot streams are lowered out by $\Delta T_{min}/2$ and those of the cold streams are raised by $\Delta T_{min}/2$. For example, consider a simple two stream system in which a hot stream is to be cooled from 300°C to 100°C, and a cold stream must be heated from 30°C to 150°C. As shown in Figure 5-3, the pinch occurs at the outlet of the cold stream. If ΔT_{min} is 10°C, then the hot stream must be 160°C or more at that point so that ΔT_{min} is maintained. Shifting the hot stream down by $\Delta T_{min}/2$ and the cold stream up by $\Delta T_{min}/2$ allows one to represent the pinch point with a single temperature (155°C), the *corrected* cold stream target temperature.

To illustrate the use of the Problem Table Method, consider the stream data for a hypothetical process given in Table 5-3. There are three hot streams and four cold streams. The corresponding problem table is also given in Table 5-3, and shows the value of CP_{net} for each interval. The column immediately to the right of CP_{net} (labeled " ΔH ") is the net amount of surplus heat (negative) or heat deficit (positive) for each interval. Because the source and target temperatures have all been shifted by $\Delta T_{min}/2$, the hot streams in any interval i are at least ΔT_{min} hotter than the cold streams in interval $i+1$ and subsequent intervals. Therefore, any surplus heat in interval i can be added (*cascaded*) to cooler intervals that are net heat sinks. If two or more subsequent intervals are net heat sources (e.g. intervals 8-10), their combined surplus heat is cascaded, until it is required by an interval that is a net heat sink (interval 11). Physically this represents process-to-process heat transfer. The ability to cascade heat from one interval to the next

is illustrated in the column marked "Cascade". Beginning with zero heat in the cascade, each interval adds its heat to the cascade. The value of the cascade at each interval is a running total of the availability of process waste heat in the system. At some point in the cascade, the heat available is negative (at interval 5 in the example), a physically impossible situation. This means that there was insufficient waste heat in the hotter intervals to meet all the process heating of subsequent intervals (i.e. external heating is needed). This situation is remedied by adding heat to the top of the cascade equal to the largest negative value in the cascade (as shown in the column "Corrected Cascade"). This heat is equal in magnitude to $Q_{h,min}$. By adding $Q_{h,min}$ to the top of the cascade, there is just enough heat in the cascade to supply heat to intervals that are net heat sinks. At the bottom of the cascade there is heat left over, which is equal to $Q_{c,min}$. The point at which the cascade is zero is the pinch point. Therefore, as required, no heat is transferred across the pinch.

The next step is to construct the *Grand Composite Curve*, which provides information regarding the temperatures at which the hot and cold utilities must be supplied. The grand composite curve is a plot of temperature as a function of the corrected cascade. The grand composite curve for the example problem in Table 5-3 is plotted in Figure 5-4. The horizontal distances from the ends of the curve to the y-axis represent the hot and cold utilities. Segments with positive slopes indicate that net heating is required (which is why the value of the cascade is decreasing). Segments with negative slopes indicate that there is excess waste heat at those temperatures. Therefore, where a negatively sloped segment lies above a positively sloped one, heat integration is possible (as indicated by the shaded regions in Figure 5-4). The pinch point occurs where the curve touches the y-axis.

Table 5-3: Sample stream data and Problem Table for a hypothetical process.

Stream Data							
Stream	Type	T_{source} (°C)	T_{target} (°C)	CP (kW/°C)	ΔH (kW)	T_s corrected (°C)	T_t corrected (°C)
1	hot	1100.0	390.0	35.0	-24850	1095.0	385.0
2	hot	500.0	200.0	55.0	-16500	495.0	195.0
3	hot	380.0	100.0	40.0	-11200	375.0	95.0
5	cold	300.0	700.0	45.0	18000	305.0	705.0
6 ^a	cold	450.1	600.0	20.0	2998	455.1	605.0
7 ^a	cold	450.0	450.1	140000.0	14000	455.0	455.1
8 ^a	cold	30.0	450.0	30.0	12600	35.0	455.0

- (a) Streams 6, 7, and 8 represent respectively the superheating of steam, boiling of water and feedwater preheating. Phase changes are assumed to occur across a 0.1°C ΔT to avoid calculating a CP of infinity.

Problem Table									
Interval	T_i (°C)	T_{i+1} (°C)	$T_i - T_{i+1}$ (°C)	ΣCP_{hot} (kW/°C)	ΣCP_{cold} (kW/°C)	CP_{net} (kW/°C)	ΔH (kW)	Cascade (kW)	Corrected Cascade (kW)
								0	3648.0
1	1095	705	390.0	35.0	0.0	-35.0	-13650.0	13650.0	17298.0
2	705	605	100.0	35.0	45.0	10.0	1000.0	12650.0	16298.0
3	605	495	110.0	35.0	65.0	30.0	3300.0	9350.0	12998.0
4	495	455.1	39.9	90.0	65.0	-25.0	-997.5	10347.5	13995.5
5	455.1	455	0.1	90.0	140045.0	139955.0	13995.5	-3648.0	0.0
6	455	385	70.0	90.0	75.0	-15.0	-1050.0	-2598.0	1050.0
7	385	375	10.0	55.0	75.0	20.0	200.0	-2798.0	850.0
8	375	305	70.0	95.0	75.0	-20.0	-1400.0	-1398.0	2250.0
9	305	195	110.0	95.0	30.0	-65.0	-7150.0	5752.0	9400.0
10	195	95	100.0	40.0	30.0	-10.0	-1000.0	6752.0	10400.0
11	95	35	60.0	0.0	30.0	30.0	1800.0	4952.0	8600.0

An important use of the grand composite curve is that it provides information regarding the *quality* (i.e. the temperature) of the waste heat and the external heating required. In the example used here, the external heat must only be hotter than 460°C (the pinch point temperature plus $\Delta T_{\text{min}}/2$). Higher quality heat could be used, but would be

wasteful. Similarly, the cold utility cannot exceed 440°C (the pinch point temperature minus $\Delta T_{min}/2$). Furthermore, the cold utility must fit under the grand composite curve at all times (i.e. it must be colder than the streams it is cooling). Alternatively, if the waste heat in a system is of high enough quality (as is the case here), it can be used to raise steam, which can then be used to generate electricity. This is illustrated by the "steam raising curve" that fits below the grand composite curve in Figure 5-4.⁵ As will be seen in the next chapter, the ability to do so is important, since it affects the overall efficiency and economics of methanol and hydrogen production; any electricity requirements in excess of the amount that can be produced from process waste heat must either be purchased or be produced on-site by consuming additional feedstock.

5.4 Gasifier Performance Estimation

No computer model can produce reliable results if the input data is inaccurate. Chapter 3 illustrated that modeling biomass gasification from a theoretical perspective is difficult for two basic reasons. First, the kinetics and chemistry of gasification are highly complex, and second, each gasifier design would require a separate model (i.e. a fluidized bed model is not suitable for a fixed-bed gasifier). For these reasons, performance estimates for actual gasifiers were taken from published literature and from information received from manufacturers. This was the case for all gasifiers with the exception of the entrained-bed biomass gasifier, for which there is no operating data. This gasifier was

⁵ The steam raising curve or the cold utility can actually be allowed to touch the grand composite curve (but not cross it). To calculate the actual temperature of the cold utility or the steam raising curve it is then necessary to subtract $\Delta T_{min}/2$. This is done because the temperatures of the hot streams being cooled by the cold utility or the steam raising curve have been lowered by $\Delta T_{min}/2$. Thus, the temperature of the cold utility must be lowered by an additional $\Delta T_{min}/2$ to be ΔT_{min} colder. Alternatively, if the temperature of the cold utility is known, it is necessary to add $\Delta T_{min}/2$ before placing it on the grand composite curve. For the hot utility, the argument is reversed.

modeled using chemical equilibrium calculations, which is a reasonable approximation for this type of gasifier (see Appendix 3A).

5.5 Chemical Process Simulation

ASPEN PLUS Release 8.5 was used to evaluate the production of hydrogen and methanol using a Sun4 computer (a Unix based machine). This software package, marketed by Aspen Technology, is of the type known as sequential modular flowsheet simulators. Once the information for each unit operations block is entered (heat exchangers, pumps, compressors, component separators, chemical reactors, etc...), ASPEN PLUS determines the calculation sequence and executes each unit operations block in that order. This sequential algorithm is what gives this type of simulator its name. This software differs from so-called equation oriented simulators, which set up and solve many equations simultaneously.

An ASPEN PLUS input file is defined in several steps. First, the process flowsheet is built graphically with ModelManager™, the graphical user interface that comes with ASPEN PLUS. This step involves inserting all unit operations blocks into the flowsheet and connecting them with material, heat and work streams. Second, the chemical components of the process (H₂, CO, etc...) are specified from any one of several built-in data banks. So called *non-conventional* components such as coal or wood can also be defined, and ASPEN PLUS has various methods for estimating their physical and chemical properties. Third, a suitable physical properties model is specified for the entire flowsheet. To improve accuracy, this general model can be replaced for specific unit operations blocks in the process (e.g. ASME steam table correlations can be used for blocks involving only pure water/steam). Fourth, the operating conditions for each block are specified. These conditions include pressure losses, operating temperatures, chemical

reaction specifications, etc. Lastly, the feed stream conditions and compositions are defined.

More complex flowsheets, such as those developed here, also require the manipulation of various operating parameters during the course of the simulation. This is accomplished by using built in ASPEN PLUS features called design specifications, which act as feed-back controllers, and FORTRAN blocks, which act as feed-forward controllers. Design-specs are used to vary the parameters of a block or stream until a desired condition is met (e.g. varying the outlet temperature of a reactor until adiabatic operation is achieved), and FORTRAN blocks are used to set downstream conditions once certain values are known upstream (e.g. calculating the amount of steam needed for a reactor once the composition and flow rate of the feed are known). Design specifications and FORTRAN blocks can be nested within one another or appear sequentially within the flowsheet. The flowsheets developed here typically contained 4-5 Design-specs and an similar number of FORTRAN blocks.

If recycle loops are present (e.g. as in methanol synthesis), ASPEN PLUS iterates on the necessary block or group of blocks until convergence is achieved.⁶ ASPEN PLUS also iterates automatically on design specifications. For example, consider how ASPEN PLUS satisfies the heat balance of the reformer. The condition to be satisfied (specified by the user) is that the flue gases leaving the reformer furnace must be 20°C above the peak reformer reaction temperature and that the heat supplied be 2% greater than the reformer heat duty (to account for radiative losses). ASPEN PLUS compares the quantity of heat required by the reformer to the heat supplied by the block representing the reformer furnace and varies user-specified flowsheet parameters (e.g. furnace air preheat

⁶ It takes anywhere from a few to over 100 iterations until the heat and mass balances of a loop are within the tolerances specified for the simulations.

and/or the quantity of fuel gas supplied) until the design specification is met. This process is iterative in nature and can require several sets of iterations since other flowsheet parameters that affect the reformer heat balance may also be changing (e.g. burning more fuel gas in the furnace means that less is reformed).

5.6 Modeling Unit Operations

An accurate thermodynamic model does not necessarily require that all steps be included. Specifically, the cyclone separator and the zinc-oxide guard bed were omitted from the computer models since they have a negligible effect on thermodynamics. All other steps were included in the simulations.

5.6.1 Quenching With Water

Two criteria were used to set the quench inlet temperature. If tars and oils were present in the product gas, the gas was cooled only to 400°C to avoid condensation of these compounds. This was the case for the IGT, BCL and MTCI gasifiers. The WM and the entrained-bed gasifiers were assumed to produce tar free gases, so that the product gases from these gasifiers were cooled to 50°C above their dew points⁷ prior to the quench step. The quench was modeled as an adiabatic process, with the clean gas exiting at a maximum temperature of 100°C and saturated with water.

5.6.2 Reforming

Steam reformers for the biomass cases were assumed to operate between 847-867°C and at pressures of at least 1.5 MPa. When atmospheric pressure gasifiers were modeled, the feed gas was first compressed to 1.6 MPa. In cases with pressurized gasification, the reformer was operated at the feed pressure. The natural gas reformers were modeled at

⁷ Here dew point refers to the moisture in the gas and not the tars and oils.

900°C and 2.5 MPa (the feed pressure assumed for the natural gas). The minimum amount of steam required for reforming was that which gave a molar steam:hydrocarbon ratio of 3:1. A maximum value of 5:1 was used depending on whether or not there was enough fuel gas to supply the added heat load that accompanies higher steam:hydrocarbon ratios. The feed was mixed with steam and heated to 577°C in the convection zone prior to entering the reformer tubes. The hot flue gases were assumed to leave the reaction section 20°C hotter than the temperature specified for the reforming reaction. Flue gases were cooled for heat recovery and exited at a stack temperature of 120°C. Air for the reformer furnace was preheated to a maximum temperature of 727°C and the fuel gas to a maximum of 427°C. Fifteen percent excess air was used, which is fairly typical (Kuo, 1991). Each section of the reformer (furnace, preheating, reforming and steam raising) was modeled separately in order to ensure that sufficient heat of sufficient temperature was supplied to the reaction section by the furnace, and to allow for integration with the pinch analysis. The chemical reactions modeled were the reforming reactions (4-8, 4-9, 4-10) and the water-gas shift reaction (4-2).

5.6.3 Shift Reactors

The hot reformat was cooled to 350°C and mixed with additional steam (if necessary) at the same temperature, to give a total steam:CO ratio of 3:1. In cases where there was no reformer in the flowsheet, the cooled quenched gas was heated to 350°C and mixed with steam at this same temperature. The outlet temperature of the adiabatic high temperature shift reactor varied from case to case, but fell in the 425-525°C range, depending on the amount of CO in the feed. The gases were then cooled to 227°C before entering the low temperature shift reactor, which operated isothermally. The heat removed from this reactor was also incorporated into the pinch analysis. All hydrocarbons were assumed to be inert in the shift reactors.

5.6.4 CO₂ Removal Prior to Methanol Synthesis

CO₂ was removed in a SELEXOL physical separation step that also removed all of the remaining moisture in the feed. The unit operated at the feed pressure and a temperature of 127°C. The CO₂ was removed in a flash drum and was assumed to be produced at 0.15 MPa and 127°C.

5.6.5 Methanol Synthesis

The makeup feed was compressed to the methanol synthesis loop pressure of 10.54 MPa, mixed with recycled gas and converted in an ICI type reactor. The reactor operated at an exit temperature of 260°C. Temperature control was achieved by varying the ratio between the cooled feed (the feed used to moderate the temperature) and the preheated feed (the feed entering the top of the reactor at roughly 260°C). Recycle ratios⁸ were between 4 and 5. Crude liquid methanol was produced by cooling the reactor effluent to 27°C before recycling the remaining gases to the synthesis reactor. The only two reactions modeled in this step were the methanol synthesis reactions (4-13 and 4-14).

5.6.6 Pressure Swing Adsorption

The gas exiting the low temperature shift reactor was cooled to 40°C, condensing out most of the moisture. All CO₂ and remaining moisture were removed in the first set of PSA beds using an activated carbon adsorbent.⁹ The second set of beds used a zeolite molecular sieve assumed to have a one pass hydrogen recovery rate of 86%. Eighty percent of the purge gas from the B-beds was recycled, giving an overall hydrogen recovery rate of nearly 97%. Electricity consumption, which was proportional to the amount of CO₂ removed, was based on Solomon (1991); the CO₂ vacuum pump was

⁸ The molar ratio of the recycle stream to the fresh *makeup* stream.

⁹ In reality, some of the CO₂ passes through the A-beds, and is removed by the B-beds (Solomon, 1991). This amount is small, and was neglected for modeling purposes.

assumed to require approximately 4.46 kWh per kmole of CO₂ removed. The CO₂ and purge gas streams were assumed to be produced at 0.13 MPa and 40°C.

5.6.7 Pumps and Compressors

Compressors operating with small pressure ratios were assumed to have polytropic efficiencies of 85%. Large pressure ratio compressors were assumed to be 3 stage compressors with intercooling, with each stage operating with a polytropic efficiency of 85%. The outlet temperatures for the intercoolers varied from case to case, depending on whether or not it was desirable to cool the gas below its dew point (i.e. whether or not the moisture was needed in downstream reactors). Typically, intercoolers operated at exit temperatures between 60-120°C. Except for one case (methanol production using the MTCI gasifier), the heat removed from intercoolers was generally small, and was not included in the pinch analyses. For pumps, which consumed very little electricity in the flowsheet simulations, the default efficiency values provided by ASPEN PLUS were used.

5.6.8 External Heat and Power Production

In order to better compare the performance of the different systems, any net power or heat that was required was assumed to be produced on-site by using additional biomass, coal or natural gas, depending on the case being studied. In this manner, the overall thermal efficiency calculated for each configuration was representative of a facility isolated from all other energy sources. For external heating, a higher heating value efficiency of 80% was assumed. For electricity, if there was excess process waste heat that was suitable for steam production (based on the pinch analysis), steam was produced at 6.2 MPa and 400°C, expanded through a condensing steam turbine with an exhaust pressure of 0.005 MPa and an isentropic efficiency of 75%. The generator efficiency was assumed to be 95%. If additional electricity was required it was generated using combined cycles (natural gas and biomass) and steam-injected gas turbines (STIGs) (coal). Natural gas

fired STIGs and combined cycles based on aeroderivative gas turbines are commercially available, and are relatively low cost, efficient machines, even at the small scales required here (typically 5-30 MW_e). In a combined cycle, steam is generated from the waste heat of the turbine exhaust gases and expanded through a steam turbine. In a STIG cycle, steam is generated from the waste heat of the turbine exhaust gases and injected at points upstream of the turbine. The added mass flow through the turbine increases overall power output. Although not as efficient as combined cycles, STIGs have lower unit capital costs (\$ per kW), because steam turbines are relatively expensive at the small scales required here.

The intercooled steam injected gas turbine (ISTIG) is a variation on the STIG that uses intercooling to reduce compressor work and increase efficiency. Although not commercially available, it could be commercialized within 3 to 5 years (Williams and Larson, 1992). It is also technically feasible to integrate the gasification of biomass or coal with a combined cycle, STIG, or ISTIG cycle. There are no commercial BIG/CC, BIG/(I)STIG or CIG/(I)STIG¹⁰ units, but a coal-fired combined-cycle power plant (IGCC) using the Texaco entrained-bed gasifier successfully operated from 1984 to 1989 at Cool Water, California, demonstrating the technical feasibility of integrated gasification/gas turbine power generation (*Cool Water Coal Gasification Program*, 1990).

In order to approximate the efficiency of generating electricity for each case, correlations were developed based on actual and projected efficiencies for combined cycles, STIG, and ISTIG cycles using natural gas, biomass and coal (Table 5-4). Because each configuration required a different amount of electricity, linear regressions of the form $y = a + bx$ were used to approximate the efficiency for different size units, and are shown

¹⁰ BIG/CC is a biomass integrated gasification/combined cycle, BIG/(I)STIG is the biomass integrated gasification/(intercooled) steam injected gas turbine, etc...

Ryan E. Katofsky

in Figure 5-5. Although this assumes that turbines of any size can be purchased, it is a fair approximation for the purposes of this thesis.

Table 5-4: Aeroderivative gas turbine data used to estimate the efficiency of producing electricity from natural gas, coal and biomass.^a

	Output (MW _e)	HHV Efficiency (%)
Natural Gas/CC^b		
LM-6000	54.1	48.0
LM-5000	43.6	43.0
LM-2500	30.1	44.8
LM-1600	17.9	43.1
571-K	7.7	39.8
Natural Gas/STIG^c		
LM-5000	51.4	40.0
LM-2500	26.3	36.0
LM-1600	17.8	36.5
LM-38	5.3	37.1
BIG/CC		
RB211 ^d	37	39.0
LM-2500 ^e	30	38.0
LM-1600 ^e	18	38.0
BIG/STIG^f		
LM-5000	51.5	35.6
LM-1600	20	33.0
LM-38	5.4	33.1
CIG/STIG^g		
LM-8000 (ISTIG) ^h	109	42.1
LM-5000	50.5	35.6

- (a) The LM series of aeroderivative gas turbines and the 571-K are manufactured by General Electric. The RB211 is manufactured by Rolls-Royce. CC = combined cycle, STIG = steam injected gas turbine, ISTIG = intercooled steam injected gas turbine.
- (b) Farmer (1991).
- (c) Larson and Williams (1990) and Williams and Larson (1992).
- (d) Elliot and Booth (1992).
- (e) Brazilian Biomass Power Generation (1992).
- (f) Williams and Larson (1992).
- (g) Johansson, et al. (1992).
- (h) The LM-8000 is the LM-5000 modified for intercooled operation.

Stream Data (all streams are <i>hot</i> streams requiring cooling)			
Stream	$\dot{m} \cdot C_p$ (CP)	Source Temp.	Target Temp.
1	A	T_2	T_5
2	B	T_1	T_3
3	C	T_2	T_4

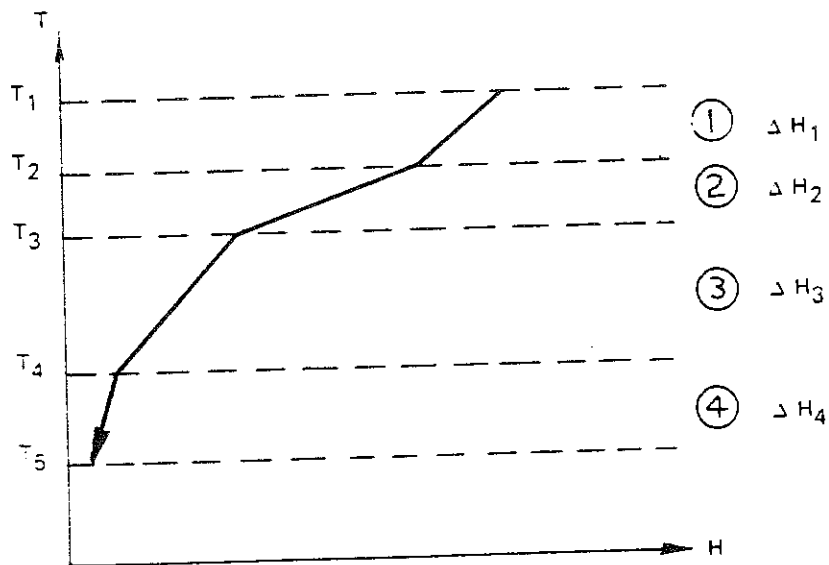
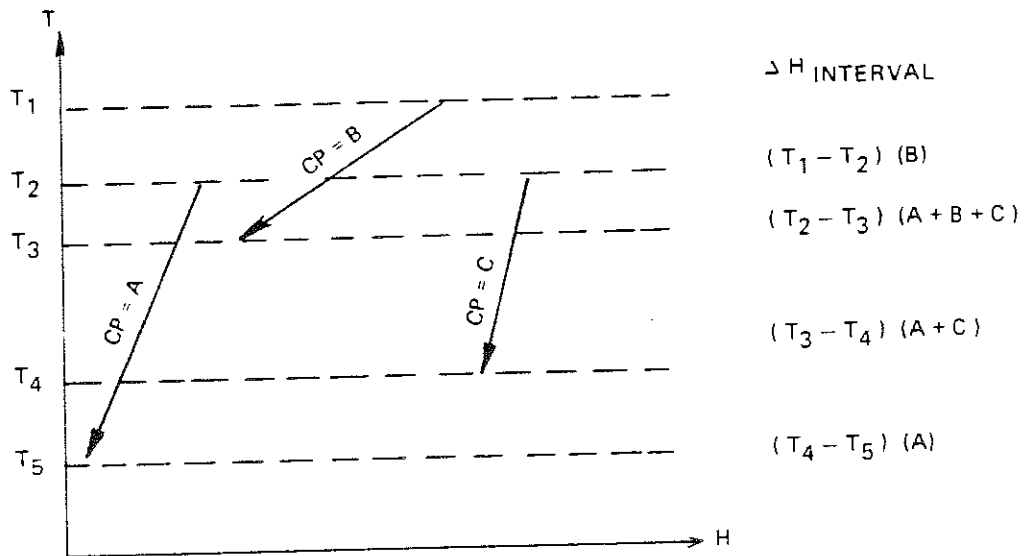


Figure 5-1: Data for three *hot* streams and the construction of the corresponding hot Composite Curve (Linnhoff, et al., 1982).

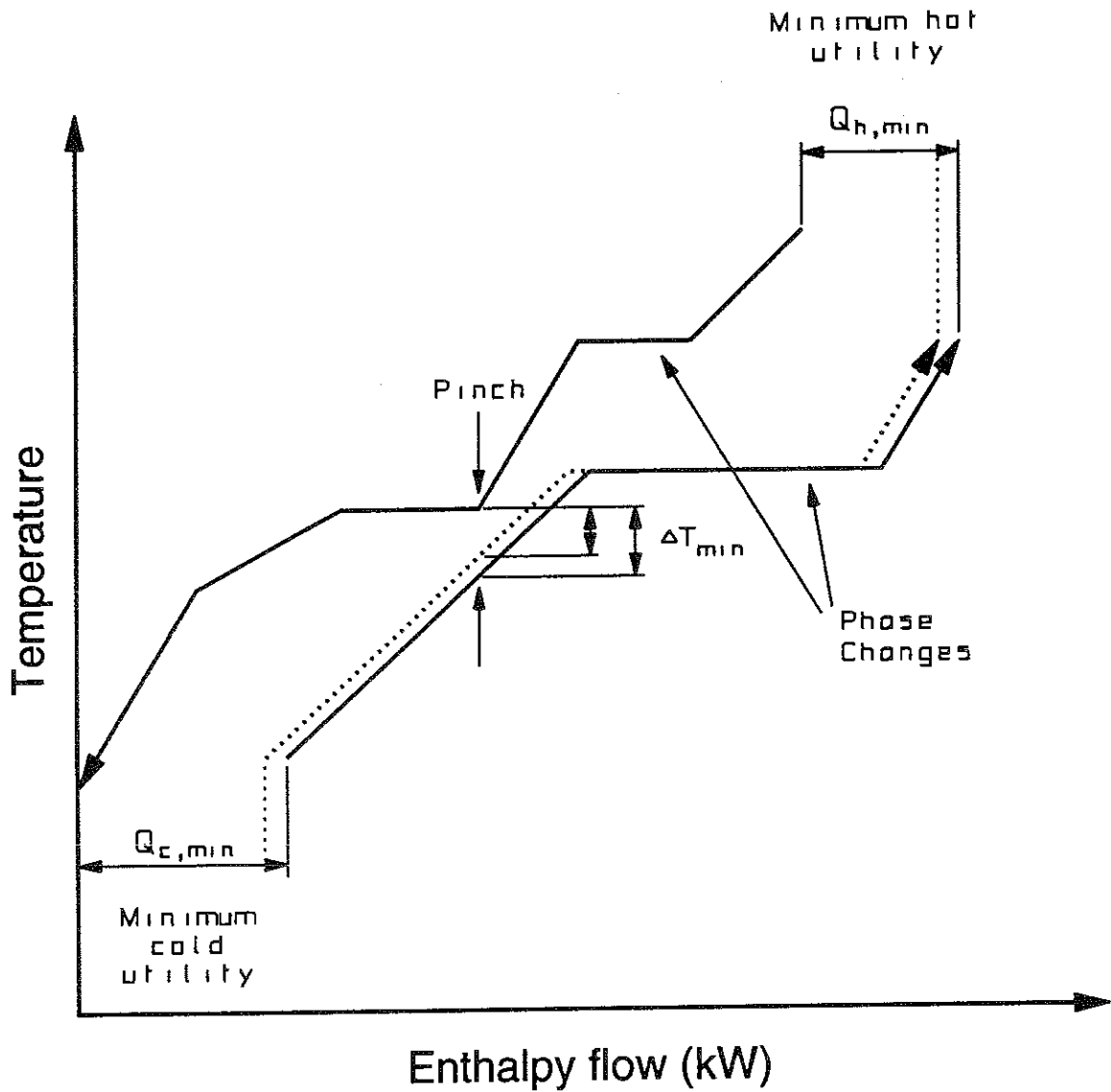


Figure 5-2: Hot and cold composite curves for a hypothetical process. Increasing or decreasing the horizontal distance between the two curves changes the value of ΔT_{min} until it reaches a user specified value.

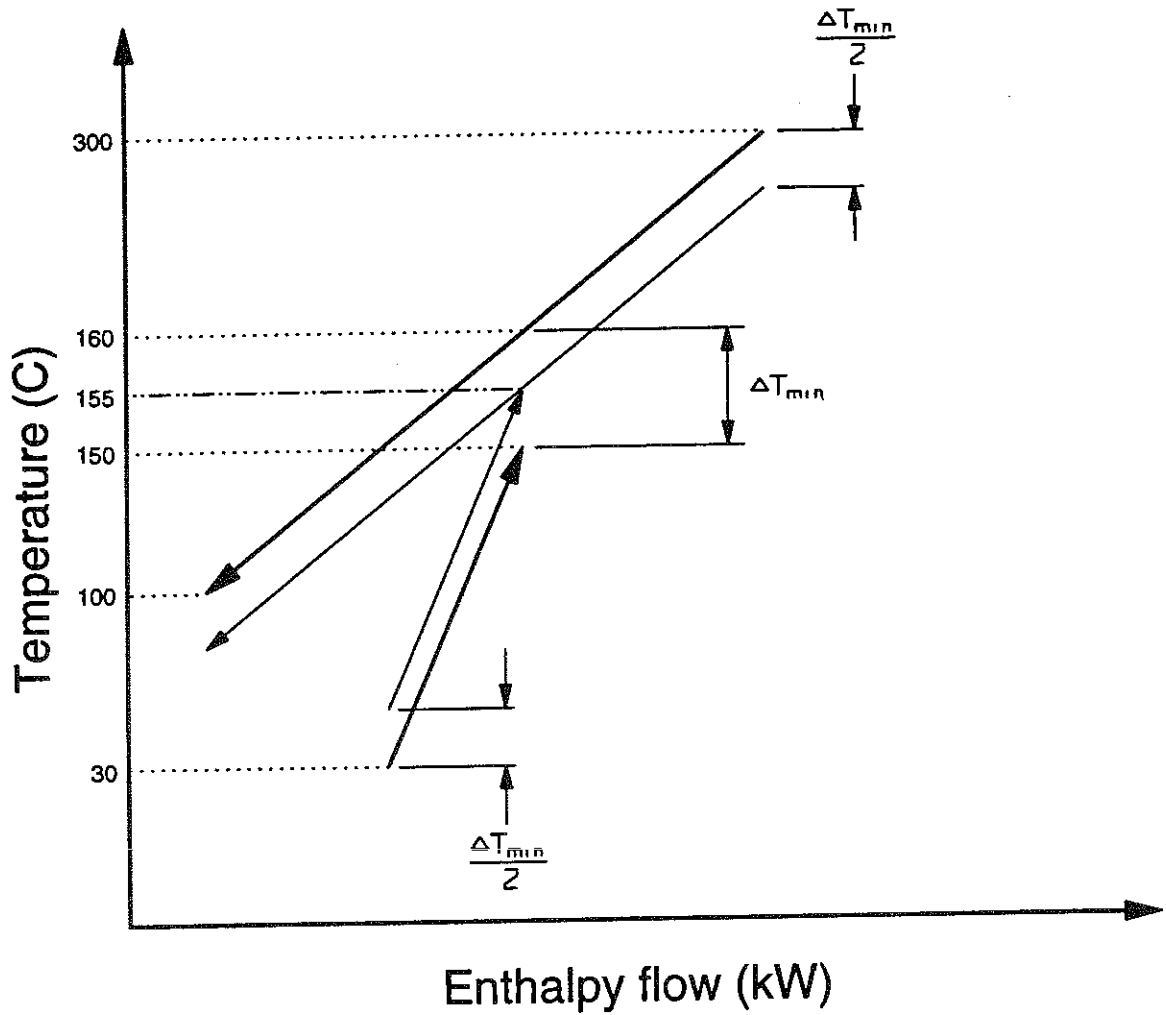


Figure 5-3: Illustration of the need to shift source and target temperatures when constructing the Problem Table.

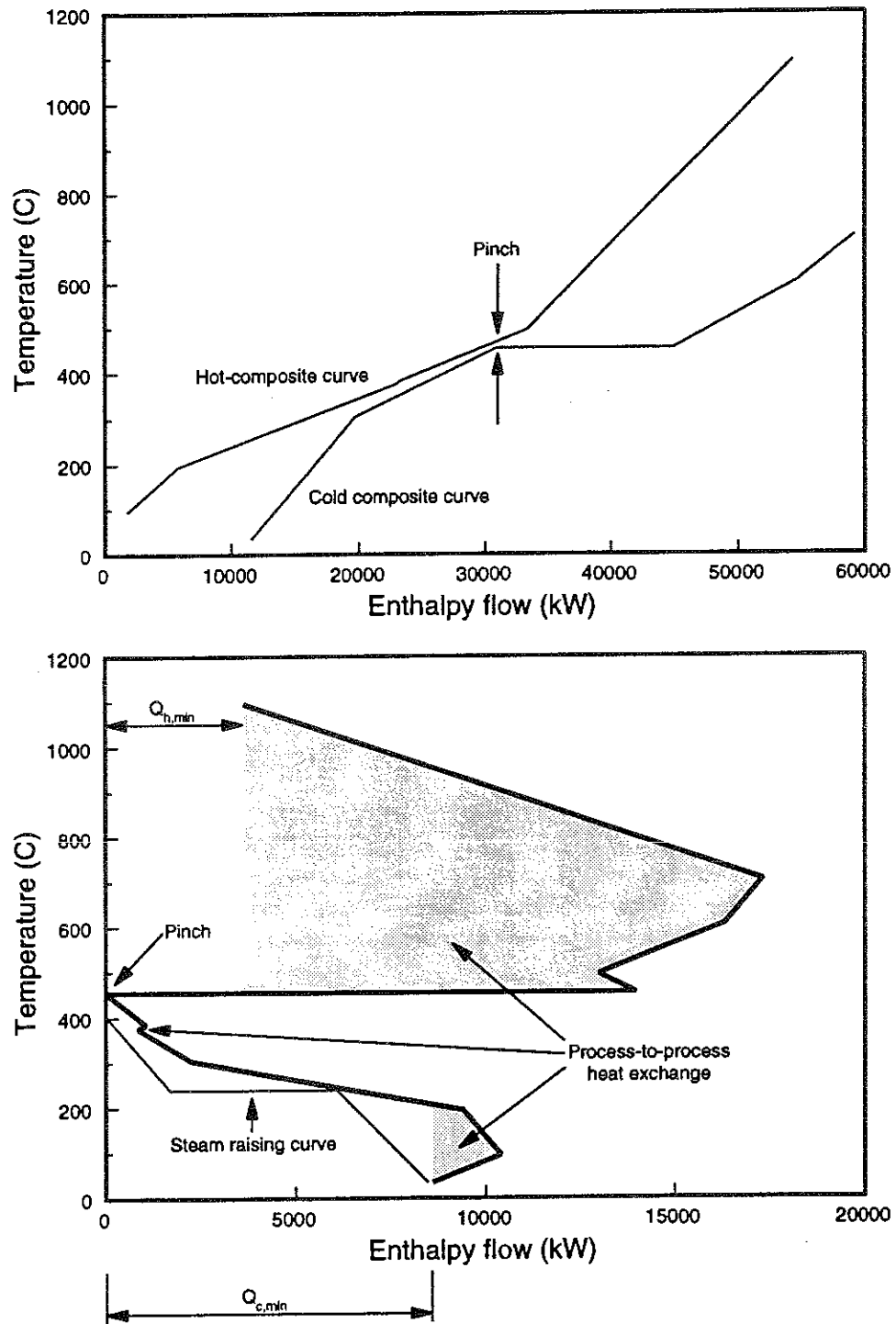
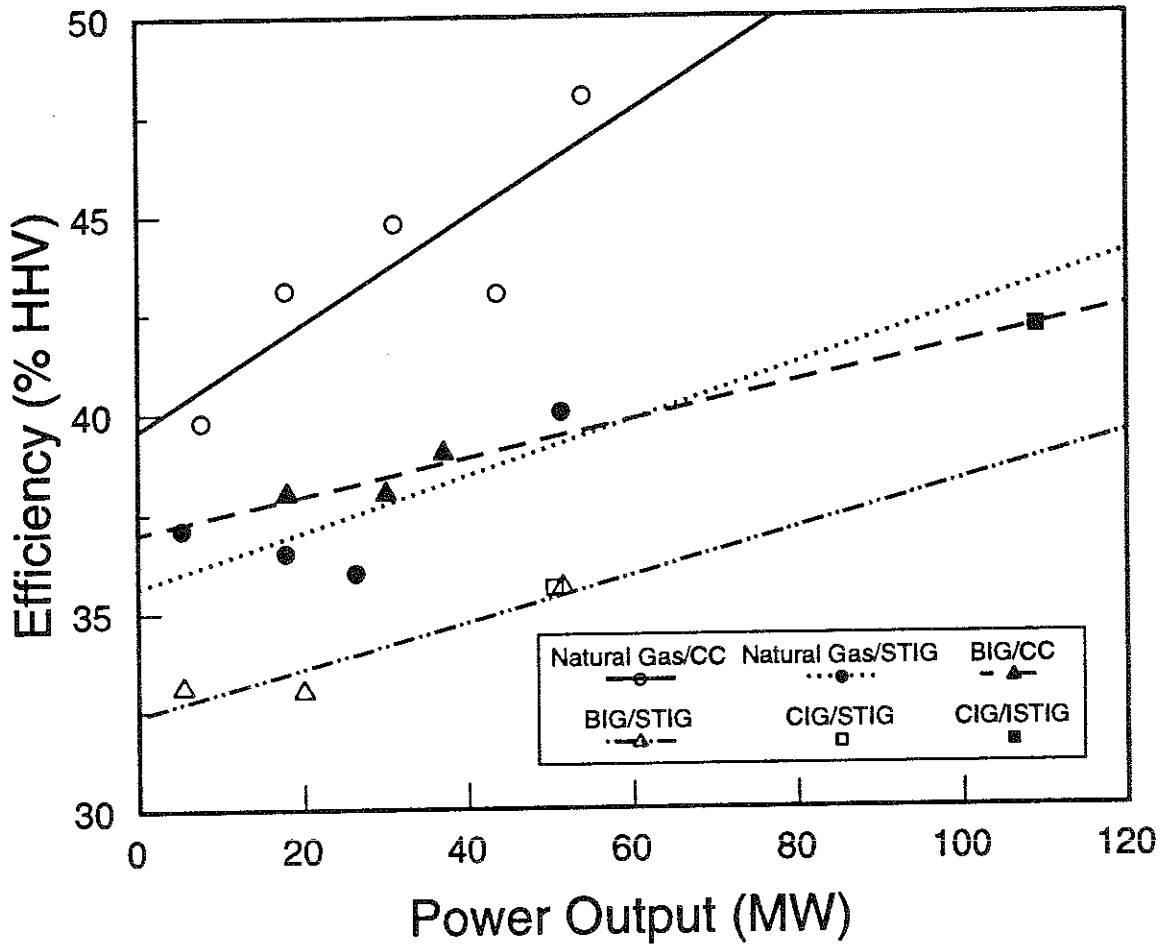


Figure 5-4: Composite curves (top) and the Grand Composite Curve (bottom) for the example problem of Table 5-3.



Regression Data (efficiency = a + b*output)

	<u>a</u>	<u>b</u>
Natural Gas/CC	39.58	0.134
Natural Gas/STIG	35.65	0.070
BIG/CC	37.00	0.047
BIG/STIG	32.39	0.059

Figure 5-5: The Efficiency of producing electricity using combined cycles, STIGs and ISTIGs with natural gas, biomass and coal, based on the data in Table 5-4. Regressions are of the form $y = a + bx$.

References

- ASPEN PLUS User Guide*. Cambridge, MA: Aspen Technology, Inc., August 1988.
- Bain, R. National Renewable Energy Laboratory, Golden, Colorado. Personal communication, November 1991.
- Brazilian Biomass Power Generation*, 1992.
- Cool Water Coal Gasification Program: Final Report*. (EPRI GS-6806) Prepared by the Cool Water Coal Gasification Program and Radian Corporation for the Electric Power Research Institute. Palo Alto, CA: Electric Power Research Institute, December 1990.
- Elliot, Philip and Booth, Roger. *Sustainable Biomass Energy*. London: Public Affairs Department, Shell International Petroleum Company, Ltd., December 1990.
- Farmer, Robert, ed. *The 1991 Gas Turbine World Handbook*. Southport, CT: Pequot Publishing, 1991.
- Floudas, C.A., Cirac, A.R., and Grossman, I.E. "Automatic Synthesis of Optimum Heat Exchanger Network Configurations." *AIChE Journal*, Vol. 32, No. 2, February 1986.
- Fraas, Arthur P. *Heat Exchanger Design*. New York: Wiley, 1989.
- Johansson, Thomas B., Kelly, Henry, Reddy, Amulya K.N., and Williams, Robert H. "Renewable Fuels and Electricity for a Growing World Economy: Defining and Achieving the Potential." *Renewable Energy: Sources for Fuels and Electricity*. Ed. T.B. Johansson, H. Kelly, A.K.N. Reddy, and R.H. Williams. Washington DC: Island Press, 1992.
- Karp, A. *Pinch Technology: A Primer*. (CU-6775) Palo Alto, CA: Electric Power Research Institute, 1990.
- Kuo, James C.W. "Engineering Evaluation of Direct Methane Conversion Processes." *Methane Conversion by Oxidative Processes: Fundamental and Engineering Aspects*. Ed. E.E. Wolf. New York: Van Nostrand Reinhold, 1991.
- Larson, E.D. and Williams, R.H. "Biomass-Gasifier Steam-Injected Gas Turbine Cogeneration." *Journal of Engineering for Gas Turbines and Power*, Vol. 112, April 1990, pp.157-163.
- Linnhoff, B., et al. *User Guide on Process Integration for the Efficient Use of Energy*. London: Institute of Chemical Engineers, 1982.

Lloyd, Ali. *Thermodynamics of Chemically Recuperated Gas Turbines*. M.S.E. Thesis, Mechanical and Aerospace Engineering Department, Princeton University, Princeton, NJ, January 1991.

Mansfield, K. (Methanol Licensing Manager). ICI Katalco, Billingham, England. Personal communication. December 1991.

Miller, Geoffrey Q. and Stoecker, Joerg. *Selection of a Hydrogen Separation Process*. Paper presented at the 1989 National Petroleum Refiners Association Annual Meeting, San Francisco, CA, March 19-21, 1989.

Solomon, James (Business Manager - Gas Separation). Air Products and Chemicals, Inc., Allentown, PA. Personal communication. July 1991.

Williams, Robert H. and Larson, Eric D. "Advanced Gasification-Based Biomass Power Generation." *Renewable Energy: Sources for Fuels and Electricity*. Ed. T.B. Johansson, H. Kelly, A.K.N. Reddy, and R.H. Williams. Washington DC: Island Press, 1992.

Chapter 6: The Technology of Methanol and Hydrogen Production

6.1 Introduction

Based on the analysis of commercially available technology presented in Chapter 4, a total of 15 simulations were conducted (10 biomass, 2 coal and 3 natural gas cases). The results given here are called *base case* scenarios, which could be achieved in the very near term, once the gasifiers are commercialized. In order to permit meaningful comparisons, as much consistency as possible was maintained for all the simulations. Certain parameters do vary from case to case, reflecting the differences in the operating characteristics of each gasifier and the three feedstocks. Detailed mass and energy balances and the pinch analyses for all simulations can be found in Appendix 6A at the end of this chapter.

Natural gas-based processes provide the starting point for the analysis in this chapter, and are used as benchmarks for comparing the coal and biomass systems. Comparing the results of these simulations to previous studies of natural gas processes is also a good method of assessing the accuracy of the thermodynamic models so that they can be applied to coal and biomass with a high degree of confidence.

The analyses themselves were carried out in several steps. The first stage entailed building and running the ASPEN PLUS simulations. Second, detailed mass and energy balances derived from these simulations were used in the pinch analyses and to compute the overall energy and exergy efficiencies for each process configuration. More detailed exergy analyses of several cases were used to pinpoint where the major thermodynamic losses occur, and to better compare gasification based systems to each other and to the natural gas processes.

6.2 Defining the Framework for Evaluating Thermodynamic Performance

The biomass simulations were carried out for a feed rate of 3000 wet tonnes of woody biomass per day having a 45% moisture content (1650 dry tonnes per day).¹ Although size does not have an effect on the thermodynamic models developed here, the economic estimates do depend quite strongly on scale. Larger facilities are feasible, but 3000 green tonnes per day corresponds roughly to the size of a modern pulp and paper facility or a large sugar cane processing facility. As discussed in Chapter 1, it is the need to collect biomass over a wide area that is the main factor that would limit the size of a biomass based facility. To better understand the scale of such a facility, consider the following assumptions about a dedicated energy plantation supplying 1650 dry tonnes per day:

- average yield = 15 dry tonnes per hectare per year.
- the capacity factor of the biomass conversion facility is 90%.
- 75% of the plantation is under cultivation.²

Such a plantation would cover an area slightly greater than 45,000 hectares (approximately 110,000 acres or 450 km²), a relatively large plantation by today's standards (Hall, et al., 1992). To ensure reliability of fuel supply (e.g. against drought, fire or disease) and to provide the fuel for any net external electricity and heating requirements, the plantation would have to be slightly larger (up to 25% larger for some of the cases considered here, which require relatively large amounts of external energy inputs). For the coal cases, the same dry feed rate was used (1650 dry tonnes per day,

¹ 3000 green tonnes per day of biomass corresponds to a fuel input rate of approximately 370-400 MW on a higher heating value basis. For comparison, a large coal fired steam power plant producing 1000 MW of electricity would burn coal at a rate of nearly 3000 MW on a higher heating value basis.

² The remaining 25% would be needed for infrastructure (roads, etc...) and wild vegetation.

including ash), although much larger plants are possible.³ For natural gas, a feed rate of 750 MW (HHV basis -- equivalent to 1.64 million Normal Cubic Meters per day⁴) was used, which corresponds to the size of a large modern natural gas-methanol facility, producing approximately 2000 tonnes of methanol per day (OPPA, 1989).

6.2.1 Overall Energy Balances

Three parameters have been defined to characterize overall thermodynamic performance.

The *Energy Ratio (ER)* is defined as:

$$ER = \frac{E_{fuel}}{E_{feed}} \quad (6-1)$$

where: E_{fuel} = higher heating value (HHV) of the fuel produced.

E_{feed} = HHV of the feed to the gasifier.

This quantity is useful because it provides a direct measure of the ability of a gasifier to convert the solid feed into the fluid fuel. Nevertheless, it does not necessarily give a good indication of the overall energy balance of a system. In order to better account for all energy inputs to the system, the *Thermal Efficiency* (η_{th}) has been defined as follows:

where: E_{elec} = the net quantity of external electricity required.

³ Chapter 7 considers larger coal plants for the economic analysis. However, for the thermodynamic comparisons, it is more useful to compare biomass and coal facilities that have the same throughput rates.

⁴ The Normal Cubic Meter (Nm³) is evaluated at 101.325 kPa and 273.15 Kelvin. There are approximately 37.2 Standard Cubic Feet (SCF) in one Nm³. The SCF is evaluated at 14.696 psi and 60°F (101.352 kPa and 288.56 K).

$$\eta_{th} (\%) = \frac{E_{fuel}}{E_{feed} + \frac{E_{elec}}{\eta_{elec}} + \frac{E_{heat}}{\eta_{heat}}} * 100 \quad (6-2)$$

E_{heat} = the net quantity of external heating required.

η_{elec} = HHV efficiency of producing electricity.

η_{heat} = HHV efficiency of supplying external heat.

The quantities E_{elec} and E_{heat} were computed using data obtained from both the ASPEN PLUS simulations and the pinch analyses. The computer simulations also provided data concerning electricity requirements and, of course, E_{fuel} .⁵ η_{elec} was assumed to be a function of the feedstock and the quantity of electricity required (see Chapter 5). η_{heat} was assumed to be 80% in all cases. Since any external heat or electricity was assumed to be supplied by the feedstock in that simulation, the thermal efficiency represents the overall energy efficiency of producing methanol or hydrogen from a facility that is isolated from all other energy sources.

For methanol production, *Carbon Utilization* is another commonly used measure of the efficiency of a process. It is defined as the ratio of the carbon in the product divided by the carbon in the feed:

⁵ Electricity use was calculated for pumps, compressors, pressure swing adsorption, oxygen purification and pressurized biomass/coal feeding systems. The energy requirements for feedstock preparation were neglected in all cases except the entrained-bed biomass cases, which would require extensive feedstock preparation. It was assumed that 2% of the energy of the feedstock was required for milling and grinding the biomass, which was added to the denominator of the expression for thermal efficiency given in Equation (6-2).

$$\eta_{\text{carbon}} (\%) = \frac{\text{C-atom in product fuel}}{\text{C-atom in feed}} * 100 \quad (6-3)$$

6.2.2 Exergy Analysis

Exergy analysis is another method for evaluating the thermodynamic performance of complex systems. Increasingly, exergy is being used to identify areas where the most significant thermodynamic losses occur in a variety of industrial processes (Rosen and Scott, 1987; Szargut, Morris and Steward, 1988; Rosen, 1991). The *exergy* of a substance (also called *availability*) is a measure of the maximum theoretical work that can be extracted by bringing it into chemical and thermomechanical equilibrium with its environment. Unlike energy, which is always conserved, exergy can be destroyed. Essentially, exergy losses occur due to irreversibilities associated with particular processes.⁶ By defining a standard reference environment (also known as the *dead state*), the availability of different substances and streams can be calculated and compared. The thermodynamic conditions of the dead state were taken to be $T_o = 298.15 \text{ K}$ and $P_o = 101.325 \text{ kPa}$, the standard values used in most exergy analyses (Szargut, Morris and Steward, 1988).

There are two components to availability: chemical and thermomechanical. The latter is a measure of the maximum theoretical work that can be extracted from a substance by bringing it from its current pressure and temperature to the dead state conditions when there is no change in chemical composition (e.g. a gas expanding through a turbine). Chemical exergy is the additional potential for performing work by utilizing the chemical energy of a substance. Clearly, when analyzing biomass gasification

⁶ For example, the transfer of heat across a finite temperature difference results in a loss of exergy. Mixing and throttling are two other examples of processes that involve exergy losses even though energy is conserved.

systems, both components of exergy will need to be considered, which is shown in the following equation:

$$B_{total} = B_{tm} + B_{ch} \quad (6-4)$$

Here B_{total} denotes the total exergy of a given stream (e.g. in MW or kJ/kmol), B_{tm} is the thermomechanical contribution and B_{ch} is the chemical contribution, which is evaluated at T_o and P_o so that it is independent of the thermodynamic conditions of the mixture. Neglecting the exergy associated with velocity or gravitational potential energy, B_{tm} for open systems is defined as follows:

$$B_{tm} = H - H_o - T_o(S - S_o) \quad (6-5)$$

where: H = the enthalpy of the stream.
 H_o = the enthalpy of the stream at T_o and P_o .
 S = the entropy of the stream.
 S_o = the entropy of the stream at T_o and P_o .

The chemical exergy is given by the following relationship:

$$B_{ch} = \sum N_i b_{ch,i} \quad (6-6)$$

where: N_i = molar flow rate of chemical species i .
 $b_{ch,i}$ = specific chemical exergy of species i , evaluated at T_o and P_o .

When evaluating changes in exergy for which no chemical changes occur, the chemical exergy terms cancel so that the change in exergy from state 1 to state 2 is simply:

$$\Delta B = B_2 - B_1 = H_2 - H_1 - T_o(S_2 - S_1) \quad (6-7)$$

Therefore, it is common to define the *flow availability function*, which can be used to compute changes in availability in open system where there are no chemical changes (e.g. heat exchangers).

$$B = H - T_o S \quad (6-8)$$

Evaluating changes in exergy is more complicated when chemical reactions take place, and it becomes necessary to specify the chemical composition of the reference environment. The composition used here corresponds to air at T_o and P_o saturated with water vapor.⁷ Trace elements are commonly grouped together with nitrogen to form what is called *atmospheric nitrogen*, so that the reference environment has the following molar composition: 0.76579 atmospheric N₂, 0.20357 O₂, 0.03030 H₂O, and 0.00034 CO₂.

The methodology used for calculating chemical exergy was based on Szargut, Morris and Steward (1988) and McGovern (1990). In the case of a pure substance, the chemical exergy can be taken directly from tables of standard chemical exergies. However, since we are usually dealing with mixtures of gases, a method must be used which accounts for the fact that some components of these mixtures are found in the reference environment while others are not. If we assume ideal gas behavior for gases

⁷ Defining the reference environment to be saturated with water vapor is somewhat arbitrary. It would be just as valid to choose some other value.

in the dead state, then the chemical exergy of the k^{th} component that is also present in the reference environment is given by:

$$b_{ch,k} = \mathbb{R}T_o y_k \ln\left(\frac{y_k}{y_{ok}}\right) \quad (6-9)$$

where: \mathbb{R} = the Universal Gas Constant = 8.314 kJ/kmol-K.
 y_k = the mole fraction of species k in the mixture.
 y_{ok} = the mole fraction of species k in the reference environment.

For the i^{th} combustible component, the chemical exergy is:

$$b_{ch,i} = y_i(b_{ch}^o + \mathbb{R}T_o \ln(y_i)) \quad (6-10)$$

where: b_{ch}^o = the standard chemical exergy of species i .
 y_i = the mole fraction of species i in the mixture.

Note that in the case of a pure combustible component, $y_i = 1$ so that the logarithmic term in Equation (6-10) is zero and the chemical exergy is simply the standard chemical exergy. Also noteworthy is the fact that non-combustible components such as CO_2 have some chemical exergy, which can be thought of as the reversible work that could be extracted from these compounds by bringing them into chemical equilibrium with the reference environment. Pure water and steam are assumed to have zero chemical exergy, since the reference environment used for these streams was liquid water at T_o and P_o (Szargut, Morris, and Steward, 1988).

For the purposes of this chapter, the detailed exergy analyses considered each major sub-process as a *black box*. Exergy balances were performed for each black box

by calculating the change in exergy between the inlet and outlet streams. In addition, the exergy loss from heat transfer was calculated by summing all exergy changes due to heating and cooling, including the steam raised for on-site power generation. Exergy losses due to mixing and compression were also calculated, as were the exergy losses from generating electricity from waste heat and by burning additional feedstock. Since thermodynamics does not rule out the existence of electric motors and generators that are 100% efficient, the exergy of electricity was assumed to be equal to its electrical energy (McGovern, 1990).

In theory, the sum of all exergy losses plus the exergy of the fuel produced should equal the exergy entering the system. In the analysis that follows there were small differences due to round off error, the effects of physical property estimation, and some of the simplifying assumptions of the models. Nevertheless, as will be seen below, the overall exergy balances were all within 2%, and in most cases were within 1%.

In order to characterize the total exergy losses in a system, the *Exergy Efficiency*, also known as the *Degree of Perfection*, was defined as:

$$\eta_{\text{exergy}} = \frac{\text{exergy of product fuel}}{\text{exergy of all inputs}} \quad (6-11)$$

The standard chemical exergies for gaseous hydrogen and liquid methanol are 236.1 MJ/kmol and 718 MJ/kmol respectively (Morris and Szargut, 1985). The thermomechanical exergy resulting from the fact that the hydrogen was produced at 7.5 MPa was also taken into account (10.79 MJ/kmol). For liquid methanol, the thermomechanical contribution was negligible. The exergies of wood and coal were estimated using correlations based on heating values and relative atom populations found

in Szargut, Morris and Steward (1988), and are considered to be accurate to within $\pm 1\%$ for coal and $\pm 1.5\%$ for wood.

6.3 Natural Gas Processes

Natural gas was assumed to have the following composition: 94.7% CH₄, 2.8% C₂H₆, 0.2% CO₂, 2.3% (N₂+Ar). It was also assumed that sulfur free gas was available at a pressure of 2.5 MPa.

6.3.1 Methanol Production (Figures 6A-1,2,3 and Tables 6A-1,2,3,4)

Two cases were considered for the production of methanol from natural gas; with and without CO₂ recycling.⁸ Since steam-methane reforming (SMR) produces a gas with an R value of approximately 3, the option of complete CO₂ recycling and the addition of CO₂ from an external source was used as a means of producing a balanced synthesis gas (called SMR-CO₂).⁹ A reforming temperature of 900°C, which is slightly higher than that used for the biomass cases, was chosen since higher a reformer temperature favors CO production over H₂ production. CO₂ augmentation also allowed for the use of a lower steam:CH₄ ratio (2:1 instead of 3:1) in the reformer since CO₂ helps inhibit carbon formation, and catalysts have been developed that permit carbon free operation with low steam:CH₄ ratios when there is CO₂ added to the feed (Dibbern, et al, 1986; Goff and Wang, 1987; Riensche and Fedders, 1991).

⁸ The CO₂ recycling/addition case could also correspond to the use of CO₂ contaminated natural gas.

⁹ Recall that the R value is defined as $R = (H_2 - CO_2)/(CO + CO_2)$, for which a value of 2.0 corresponds to a stoichiometric synthesis gas. As described in Chapter 4, R = 2.03 was used as the control parameter.

The process configurations for the two models of methanol production from natural gas are given in Figures 6A-1 and 6A-2. The corresponding stream summaries are given in Tables 6A-1 and 6A-2. The overall mass and energy balances for both cases are presented in Table 6-1. The simulations show that with a steam:CH₄ ratio of 2:1 it is possible to achieve the desired R value when the amount of CO₂ added is 18% of the total fresh feed to the system on a molar basis. CO₂ addition also results in a 5% increase in methanol production and actually requires less natural gas because less external electricity is required; less process steam is required when CO₂ addition is used, so more electricity can be produced from waste heat. This results in an overall increase in the thermal efficiency of the process over the SMR case. The main tradeoffs for the higher efficiency are the use of a CO₂ removal system (for CO₂ recycling), the need to recompress the CO₂, and possibility that additional CO₂ would need to be purchased. These factors tend to offset the cost savings associated with the increased efficiency. However, these costs would be avoided if CO₂ contaminated natural gas were used.

For the conventional reforming case the calculated Energy Ratio is 0.705 and the thermal efficiency is 67.5%. For the CO₂ augmentation case, these numbers increase to 0.740 and 72.1%. These estimates are slightly higher than estimates made previously (OPPA, 1989; Kuo, 1991). The OPPA study of methanol production from natural gas estimated a thermal efficiency for conventional reforming of 56-62%, and 64-68% for combination reforming.¹⁰ Kuo considered steam reforming with and without CO₂ addition, and calculated thermal efficiencies of approximately 66% for conventional reforming and 68% for the CO₂ addition scheme. The slightly higher values here are probably due to the integrated heat balance approach of the pinch analysis and the fact

¹⁰ Combination reforming is steam reforming combined with secondary oxygen reforming, which is an alternative method of producing a synthesis gas with an R value approaching 2.0.

Table 6-1: Mass and energy balances for methanol production from natural gas.

	Conventional Reforming	CO ₂ Augmented Reforming
Natural gas feed (MW) [10^6 Nm ³ /day]	750 [1.64]	750 [1.64]
CO ₂ import (tpd) ^a [kg/kg nat. gas]	---	709.6 [0.58]
Steam use (tpd) [kg/kg nat. gas]	3957 [3.23]	2073 [1.69]
Methanol produced (MW) [tpd]	528 [2012]	555 [2114]
Electricity use (MW)		
Pumps	0.15	0.09
Compressors	24.80	27.34
Total	24.95	27.43
Waste heat suitable for raising steam (MW)	40.00	69.50
Electricity from waste heat (MW)	11.14	19.35
Net external electricity required (MW) ^b	13.81	8.08
Net external cooling (MW) ^c	137.49	83.90
Net external heating (MW)	0.00	0.00
Natural gas utilization ^d (tonnes feed/tonnes methanol)	0.608	0.579
Energy Ratio	0.705	0.740
Carbon utilization ^e (%)	85.6	73.7
Thermal Efficiency (%)	67.5	72.1

(a) tpd = tonnes per day.

(b) Produced in a gas turbine combined cycle at greater than 40% HHV efficiency. The exact value is a function of the size (see Chapter 5).

(c) This is the amount of waste heat that is not used for steam production.

(d) Excluding the natural gas burned to produce electricity.

(e) This includes the CO₂ imported, but excludes the natural gas burned to produce electricity.

that the imported CO₂ was assumed to be available at the system pressure of 25 bar, whereas Kuo assumed it was available at atmospheric pressure. When compared to the OPPA estimate, combination reforming requires energy to purify oxygen, which lowers overall efficiency. The OPPA also study defined a natural gas utilization rate that is

analogous to the Energy Ratio (in MMBtu/tonne methanol).¹¹ Converting the OPPA units to ERs shows that the ER for the SMR case is only slightly higher than the OPPA range for conventional reforming (0.694-0.615). The ER for SMR-CO₂ falls in the middle of the range for combination reforming (0.768-0.717).

The pinch analyses indicate that no external heating is required for either case. This is seen on the grand composite curves (Figure 6A-3), where the *pinch points* occur at 1173 K, the maximum temperature in each system. Therefore, a heat exchanger network can be constructed such that all process heating can be achieved using process-to-process heat transfer. Furthermore, the pinch analyses show that for a natural gas input rate of 750 MW, over 175 MW of net external cooling is required in the conventional reforming case, and over 150 MW of net external cooling is needed in the CO₂ addition case, as measured by the horizontal distance from the y-axis to the lower end of the grand composite curve. In both cases, some of this waste heat is of high enough quality to raise steam, as indicated by the steam raising curves that fit beneath the grand composite curves of Figure 6A-3. More than 11 MW of electricity can be produced using waste heat in the conventional reforming case, and nearly 20 MW can be produced when CO₂ addition is used. In both cases, most of the waste heat is below approximately 150°C, and must be rejected from the systems using cooling water or some other means.

6.3.2 Hydrogen Production (Figures 6A-4,5 and Tables 6A-5,6)

Figure 6A-4 shows the flowsheet configuration used for modeling the production of hydrogen from natural gas. The numbering corresponds to the stream summary in Table 6A-5. The overall mass and energy balances are given in Table 6-2 and the grand composite curve is in Figure 6A-6. As with methanol production, the grand composite

¹¹ 1 MMBtu = 1 million British Thermal Units = 1.055 GJ.

curve shows that there is sufficient waste heat to supply all process heating needs, and that approximately 47 MW of external cooling is required, slightly more than half of which must be rejected from the system. Less than 6 MW of electricity can be produced from waste heat in this case, nearly 75% less than the SMR-CO₂ case. As a result, the thermal efficiency of 84.8% is relatively low when compared to the ER of 0.901, which is unlike the methanol cases, where the ERs and thermal efficiencies differ by only 2-3 percentage points.

This result compares well to similar assessments of hydrogen production from natural gas. Rosen (1991) estimated the energy efficiency of hydrogen production from natural gas to be 86.6%. The difference is probably due to the selection of slightly different operating conditions for the reformer and shift reactors, the fact that Rosen assumed the feedstock was pure methane, and most importantly, that the hydrogen produced in the Rosen study was only 97% pure and at 2.4 MPa. In this study, the hydrogen is purified to 99.999% purity and compressed to 7.5 MPa, which reduces overall efficiency since compression and PSA separation require over 25 MW of electricity at the scale evaluated here. Here, the calculated exergy efficiency is 76.1%, whereas Rosen estimated the exergy efficiency to be 78.5%. For the model developed here, the exergy losses from pressure swing adsorption and compression were estimated to be 2.3% of the input exergy (see Table 6-3 and Figure 6-1), which accounts fairly well for the discrepancy between the two studies. In an earlier study, Heck and Johansen (1978) estimated the energy efficiency of hydrogen production from natural gas using PSA separation to be 84.6%, which is almost identical to the estimate made here.

6.3.3 A Comparison of Methanol and Hydrogen Production

Comparing hydrogen and methanol production (using primarily the CO₂ addition case) reveals some interesting characteristics of the two processes. First of all, both processes

Table 6-2: Mass and energy balances for the modeling of hydrogen production from natural gas (all energy values are on a higher heating value basis).

Natural gas feed (MW) [10^6 Nm ³ /day]	750 [1.64]
Steam use (tpd) [kg/kg nat. gas]	3262 [2.66]
Hydrogen produced (MW) [10^6 Nm ³ /day]	676 [4.56]
Electricity use (MW)	
Pumps	0.12
Compressors	18.61
Pressure swing adsorption	6.66
Total	25.39
Waste heat suitable for raising steam (MW)	20.00
Electricity from waste heat (MW)	5.57
Net external electricity required (MW) ^a	19.83
Net external cooling (MW) ^b	27.18
Net external heating (MW)	0.00
Energy Ratio (ER)	0.901
Thermal efficiency (η_{th}) (%)	84.8

(a) Produced in a gas turbine combine cycle @ 42.2% HHV efficiency.

(b) This is the waste heat not used for raising steam.

require external energy inputs in the form of electricity, so that additional natural gas must be burned or electricity must be purchased. Second, even though CO₂ addition increases the yield of methanol from natural gas by 6.6% over the SMR case (including the natural gas burned to produce electricity), hydrogen production is considerably more energy efficient, as measured by the higher Energy Ratio and thermal efficiency. This is largely due to the fact that the methanol synthesis reaction is more exothermic than the shift reaction. Consider a synthesis gas composed of two moles of H₂ and 1 mole of CO. From this we can produce either 1 mole of methanol or 3 moles of H₂. The ratio of the higher heating values of these two products is:

$$\frac{3*287}{1*727.4} = 1.184 \quad (6-12)$$

This value is close to the actual ratio of hydrogen and methanol produced (using the SMR-CO₂ case since its make-up gas has a more balanced feed than the SMR case), which is 1.22. The reason why they are not identical is due to differences in the actual processes. For example, the methanol synthesis make-up feed is slightly rich in H₂ which lowers the amount of methanol that can be produced. Nevertheless, it is clear from this argument that for a given synthesis gas generation technology that produces a balanced feed for methanol production (i.e. an R value of about 2), hydrogen production will have a higher Energy Ratio than methanol production. The same would be true if measured on a lower heating value basis.¹²

Because methanol synthesis is more exothermic than the shift reaction, one should expect this energy to show up elsewhere in the process, which is indeed the case. According to the pinch analyses, more than 20% of the energy content of the natural gas is converted to excess waste heat during methanol production, more than three times the quantity in hydrogen production. As a result, a higher percentage of the electricity needs can be met by on-site heat recovery in methanol production. In addition, hydrogen production requires more electricity because of the use of pressure swing adsorption. In spite of these two facts, the substantially higher Energy Ratio of hydrogen production results in an overall thermal efficiency that is significantly higher than for methanol production. This will be shown to be the case for the gasification systems as well. Also,

¹² The ratio of the lower and higher heating values of methanol and hydrogen are 0.878 and 0.842 respectively, so the theoretical ratio of hydrogen to methanol produced would be 1.135 on a lower heating value basis.

if efficiency were measured on a lower heating value basis, hydrogen production would still be more efficient, but by a smaller margin.¹³

Table 6-3 gives detailed exergy breakdowns for the three natural gas processes (shown graphically in Figure 6-1). By far, reforming accounts for the largest exergy loss, roughly 40% of all losses, and 9-12% of the input exergy. This is the loss associated with the reforming section only, and is due to the irreversibilities associated with combustion and the transfer of heat across large temperature differences. The losses associated with external electricity production are also significant, again since combustion is involved. Heat transfer also accounts for sizeable losses (some of which are associated with the operation of the reformer), especially in the base methanol case, since most of the waste heat is rejected from the system rather than recovered to produce electricity.

Table 6-3 also shows that the total exergy input is greater in the hydrogen case due to the higher external electricity requirements. Effluent losses are also higher in hydrogen production since CO₂ is purged from the system. As a result, even though the exergy output is also higher, the overall exergy efficiency of hydrogen production is only 6.6 percentage points better than the SMR case, and only 2.3 percentage points higher than SMR-CO₂ case. For biomass and coal gasification, the need for more external electricity in hydrogen production will actually result in the exergy efficiency of hydrogen production being lower than that of methanol production.

¹³ The ratio of the lower and higher heating values for natural gas is approximately 0.9, so that the efficiency of producing hydrogen from natural gas on a lower heating value basis is about 79%, and for methanol production it is about 70% for the SMR-CO₂ case and 66% for the SMR case.

Table 6-3: Exergy balances for methanol and hydrogen production from natural gas (all exergy values are in MW).

	Methanol - SMR			Methanol - SMR-CO ₂			Hydrogen		
Exergy Inputs									
Feed ^a	706.95			706.95			706.95		
CO ₂	---			5.12			---		
Fuel ^b	31.42			18.73			44.25		
Oxidant ^c	0.14			0.13			0.12		
Exergy Output									
	522.80			548.62			581.14		
Exergy Losses									
		<u>% losses</u>	<u>% input</u>		<u>% losses</u>	<u>% input</u>		<u>% losses</u>	<u>% input</u>
Heat transfer	60.60	28.1	8.2	37.65	20.5	5.2	31.55	18.5	4.2
Reforming	89.95	41.7	12.2	78.66	42.9	10.8	67.91	39.9	9.0
Shift reaction	---	---	---	---	---	---	3.84	2.2	0.5
CO ₂ removal	---	---	---	0.95	0.5	0.1	---	---	---
Pumps & compressors	5.53	2.6	0.7	11.31	6.2	1.5	4.21	2.5	0.6
External electricity	17.61	8.2	2.4	10.65	5.8	1.5	24.42	14.3	3.3
Electricity from waste heat	4.17	1.9	0.6	7.26	4.0	1.0	2.09	1.2	0.3
Methanol synthesis	20.70	9.6	2.8	20.96	11.4	2.9	---	---	---
Pressure swing adsorption	---	---	---	---	---	---	13.01	7.6	1.7
Mixing	9.96	4.6	1.3	7.98	4.4	1.1	4.85	2.8	0.6
Effluents ^d	7.32	3.4	1.0	7.88	4.3	1.1	18.33	10.8	2.4
Total losses	215.84	100.0	39.2	183.30	100.0	25.1	170.21	100.0	22.7
Output + Losses									
	738.64			731.92			751.35		
Total Input									
	738.51			730.93			751.32		
Exergy Efficiency (%)									
	70.8			75.1			77.4		
Thermal Efficiency (%)^e									
	67.5			72.1			84.8		

- (a) This is the feed that is processed into methanol or hydrogen.
- (b) This is the fuel burned to provide electricity.
- (c) This is the air burned in the reformer furnace.
- (d) Effluents are all streams leaving the process excluding the fuel produced.
- (e) As calculated previously. Shown here for comparison.

6.4 Summary of Results for Biomass and Coal Gasification

Table 6-4 summarizes the overall mass and energy balances for all methanol production simulations, including the natural gas cases described above. Table 6-5 summarizes the

heat and mass balances for all seven hydrogen simulations. Detailed exergy summaries for three gasifiers (two biomass and one coal) are presented in Table 6-6 (methanol) and Table 6-7 (hydrogen) to elucidate the differences between them and the natural gas processes. Graphical exergy summaries are also presented in Figure 6-2 (biomass) and Figure 6-3 (coal). The Energy Ratios, thermal efficiencies and exergy efficiencies are presented in graphical form in Figure 6-4 (methanol) and Figure 6-5 (hydrogen). As with the natural gas cases, complete stream summaries, process flow diagrams and the pinch analyses are available in Appendix 6A at the end of this chapter.

In all cases the thermal efficiencies are lower than the Energy Ratios, indicating that external energy inputs are required, usually in the form of electricity. In some cases external heat is also needed. Also, as expected, the ERs and thermal efficiencies for hydrogen production are uniformly higher than those for methanol production. Furthermore, less waste heat is available for energy recovery in hydrogen production so that there is a larger spread between the ERs and thermal efficiencies, which is also consistent with the results of the natural gas cases.

As anticipated, methanol and hydrogen cannot be produced more efficiently from coal or biomass than from natural gas. This is because gasification consumes a significant fraction of the feedstock energy (and exergy), and the gas produced is then processed in a similar manner to natural gas. This effect is clearly illustrated in the exergy balances. In the natural gas processes, reforming consumes approximately 9-12% of the feed exergy, whereas gasification plus reforming in the BCL cases consumes 16-18% of the feed exergy. In the IGT cases, which are less efficient than the BCL cases, 23-26% of the feed exergy is destroyed during gasification and reforming. When coal is gasified using the Shell gasifier, 14-16.5% of the feed exergy is destroyed.

Table 6-4: Material and energy balance summary for all methanol production simulations.

	SMR	SMR- CO ₂	Directly Heated Gasifiers			Indirectly Heated Gasifiers		
			Shell Coal	Shell Bio	IGT	WM	MTCI	BCL
Fuel input (MW)	750.0	750.0	567.2	368.2	368.2	399.7	370.5	384.2
Steam use (kg/kg dry feed) ^a	3.23	1.69	1.91	0.92	1.02	0.68	1.37	0.54
Methanol produced (MW)	528.0	555.4	368.7	249.5	208.7	265.9	228.0	248.4
Electricity use (MW)								
Pumps	0.15	0.09	0.13	0.27	0.84	0.21	0.01	0.02
Compressors	24.8	27.34	12.42	7.08	6.33	12.83	29.00	27.42
Lockhopper	0.00	0.00	0.92	0.92	1.15	0.70	0.00	0.00
Oxygen ^b	0.00	0.00	21.10	12.50	8.33	0.00	0.00	0.00
Total	24.95	27.43	34.58	20.76	16.66	13.75	29.01	27.44
Waste heat suitable for raising steam (MW) ^c	40.00	69.50	57.59	25.67	40.25	0.00	72.00	83.66
Electricity from waste heat (MW)	11.14	19.35	16.03	7.14	11.21	0.00	20.04	23.29
Electricity from purge gases ^d	0.00	0.00	8.96	3.57	0.00	0.00	0.00	0.00
Net external electricity required (MW) ^d	13.81	8.08	9.58	10.05	5.45	13.75	8.96	4.15
Net external cooling (MW)	137.49	83.90	79.72	0.00	0.00	31.85	0.00	0.00
Net external heating (MW)	0.00	0.00	0.00	0.00	0.00	13.88	0.00	0.00
Feed utilization (dry tonnes/tonne methanol) ^e	0.608	0.58	1.18	1.64	2.08	1.63	1.90	1.74
Carbon utilization ^e (%)	85.6	73.7	46.1	44.5	37.2	46.7	40.0	42.0
Energy Ratio (ER)	0.705	0.740	0.650	0.678	0.567	0.665	0.615	0.646
Thermal efficiency (η_{th}) (%)	67.5	72.1	61.8	62.0	54.5	58.6	57.8	62.8
Exergy efficiency (%)	70.8	75.1	58.3	57.7	50.8	54.5	54.6	59.3

(a) This is the total amount of steam that is produced for the entire process.

(b) Oxygen production is assumed to require 404 kWh/tonne.

(c) For the coal case, this includes the jacket steam produced by cooling the gasifier vessel.

(d) This electricity is produced using a gas turbine combined cycle for natural gas, purge gas and biomass, and a CIG/STIG for coal. The efficiency is a function of size and feedstock (see Chapter 5).

(e) Excluding the feed that is burned to produce electricity.

In addition to the fact that the exergy losses of syngas generation are larger for gasification systems than for natural gas systems, other components of exergy loss are also proportionally larger (i.e. a larger percentage of the input exergy). For the biomass cases, heat transfer losses are roughly double what they are in the natural gas cases. This is largely a result of the need to dry biomass, which consumes exergy but returns almost none of it to the process. This is in contrast to regular heat transfer, in which most of the

Table 6-5: Material and energy balance summary for all hydrogen production simulations.

	Nat. Gas	Directly Heated Gasifiers			Indirectly Heated Gasifiers		
		Shell Coal	Shell Bio	IGT	WM	MTCI	BCL
Fuel input (MW)	750.0	567.2	368.2	368.2	399.7	370.5	384.2
Steam use (kg/kg dry feed) ^a	2.66	2.99	1.65	1.30	1.11	1.37	1.15
Hydrogen produced (MW)	675.7	440.9	291.3	247.3	313.5	282.5	301.2
Electricity use (MW)							
Pumps	0.12	0.18	0.31	0.88	0.15	0.01	0.04
Compressors	18.61	13.07	6.48	6.88	9.08	26.54	26.69
Lockhopper	0.00	0.92	0.92	1.15	0.70	0.00	0.00
Oxygen ^b	0.00	21.10	12.50	8.33	0.00	0.00	0.00
PSA ^c	6.66	17.43	12.13	10.53	9.41	9.34	9.56
Total	25.40	52.71	32.34	27.77	19.34	35.89	36.28
Waste heat suitable for raising steam (MW) ^d	20.00	17.59	4.00	11.52	0.00	8.00	55.14
Electricity from waste heat (MW)	5.57	4.90	1.11	3.21	0.00	2.23	15.35
Electricity from purge gases ^e	0.00	7.40	5.24	0.00	0.00	0.00	0.00
Net external electricity required (MW) ^e	19.83	40.41	25.99	24.57	19.34	33.66	20.93
Net external cooling (MW)	27.18	83.40	3.97	0.00	15.73	38.68	0.00
Net external heating (MW)	0.00	13.50	0.00	0.00	35.26	0.00	0.00
Energy Ratio (ER)	0.901	0.777	0.791	0.677	0.784	0.762	0.784
Thermal efficiency (η_{th}) (%)	84.8	63.0	65.7	57.2	63.4	61.7	68.6
Exergy efficiency (%)	77.4	51.7	54.0	46.4	51.5	50.8	56.3

(a) This is the total amount of steam produced for the entire process.

(b) Oxygen production is assumed to require 404 kWh/tonne.

(c) Estimated from Solomon (1991). Electricity use is proportional to the amount of CO₂ removed.

(d) For the coal case this includes the jacket steam produced by cooling the gasifier vessel.

(e) This electricity is produced in a gas turbine combined cycle for natural gas, purge gas, and biomass, and a CIG/STIG for coal. The efficiency is a function of size and feedstock (see Chapter 5).

exergy is transferred to the stream being heated, and so remains in the system. Effluent losses are also higher in the biomass and coal cases mainly because larger amounts of CO₂ are purged from these systems than from the natural gas systems. The H₂S removed in the coal cases also contains chemical exergy that is lost. The remaining sources of

Table 6-6: Exergy balances for methanol production from biomass and coal using the BCL, IGT and Shell gasifiers (all exergy values are in MW).

	BCL - biomass			IGT - biomass			Shell - coal		
Exergy Inputs									
Feed ^a	402.22			388.00			589.00		
Fuel ^b	11.68			15.41			30.18		
Oxidant ^c	0.17			2.29			5.79		
Exergy Output	245.36			206.17			364.57		
Exergy Losses		<u>% losses</u>	<u>% input</u>		<u>% losses</u>	<u>% input</u>		<u>% losses</u>	<u>% input</u>
Gasification	62.30	37.0	15.0	90.43	46.7	22.3	103.09	41.5	16.5
Quench + H ₂ S removal	3.39	2.0	0.8	7.23	3.7	1.8	-0.04	0.0	0.0
Heat transfer	38.30	22.8	9.3	29.42	15.2	7.3	42.71	17.2	6.8
Reforming	11.94	7.1	2.9	16.01	8.3	3.9	---	---	---
Shift reaction	0.30	0.2	0.1	0.30	0.2	0.1	4.80	1.9	0.8
CO ₂ removal	-1.01	-0.6	-0.2	-1.46	-0.8	-0.4	-2.35	-0.9	-0.4
Pumps & Compressors	7.06	4.2	1.7	1.88	1.0	0.5	3.82	1.5	0.6
External electricity	7.53	4.5	1.8	9.96	5.2	2.5	20.60	8.3	3.3
Electricity from waste heat	8.74	5.2	2.1	4.20	2.2	1.0	6.02	2.4	1.0
Electricity from purge gas	---	---	---	---	---	---	11.25	4.5	1.8
Methanol synthesis	9.39	5.6	2.3	7.90	4.1	1.9	14.17	5.7	2.3
Mixing	3.20	1.9	0.8	5.28	2.7	1.3	8.13	3.3	1.3
Effluents ^d	17.09	10.2	4.1	22.29	11.5	5.5	35.92	14.5	5.7
Total losses	168.23	100.0	40.6	193.45	100.0	47.7	248.12	100.0	39.7
Output + Losses	413.59			399.62			612.69		
Total Input	414.07			405.70			624.97		
Exergy Efficiency (%)	59.3			50.8			58.3		

- (a) This is the feed that is processed into methanol.
- (b) This is the fuel burned to provide external electricity and heat.
- (c) This is the air burned in the reformer furnace and the air/oxygen used for gasification.
- (d) Effluents are all streams leaving the process excluding the fuel produced.

exergy losses consume roughly the same percentage of the feed exergy as in the natural gas cases. Of the three cases presented in Table 6-7, the coal-hydrogen case has the highest exergy loss associated with external energy requirements, because of the need for large amounts of external electricity as well as external heating.

Table 6-7: Exergy balances for hydrogen production from biomass and coal using the BCL, IGT and Shell gasifiers (all exergy values are in MW).

	BCL - biomass			IGT - biomass			Shell - coal		
Exergy Inputs									
Feed ^a	402.22			388.00			589.00		
Fuel ^b	57.69			67.84			138.21		
Oxidant ^c	0.17			2.29			5.79		
Exergy Output									
	259.07			212.71			379.16		
Exergy Losses									
		<u>% losses</u>	<u>% input</u>		<u>% losses</u>	<u>% input</u>		<u>% losses</u>	<u>% input</u>
Gasification	62.30	30.9	13.5	90.43	37.8	19.7	103.09	30.3	14.1
Quench + H ₂ S removal	3.38	1.7	0.7	7.23	3.0	1.6	0.00	0.0	0.0
Heat transfer	42.57	21.1	9.3	34.21	14.3	7.5	45.56	13.4	6.2
Reforming	12.24	6.1	2.7	15.08	6.3	3.3	---		
Shift reaction	3.98	2.0	0.9	2.93	1.3	0.6	11.10	3.3	1.5
Pumps & Compressors	6.12	3.0	1.3	1.75	0.7	0.4	3.01	0.9	0.4
External electricity	36.76	18.3	8.0	43.28	18.1	9.4	80.28	23.6	11.0
Electricity from waste heat	5.75	2.9	1.3	1.20	0.5	0.3	1.83	0.5	0.3
Electricity from purge gas	---	---	---	---	---	---	8.11	2.4	1.1
External heat	---	---	---	---	---	---	17.52	5.2	2.4
Pressure swing adsorption	12.33	6.1	2.7	15.89	6.6	3.5	23.00	6.8	3.1
Mixing	2.27	1.1	0.5	3.69	1.5	0.8	7.00	2.1	1.0
Effluents ^d	13.70	6.8	3.0	23.34	9.8	5.1	39.41	11.6	5.4
Total losses	201.40	100.0	43.8	239.03	100.0	52.2	339.91	100.0	46.4
Output + Losses									
	460.47			451.74			719.07		
Total Input									
	460.08			458.13			733.00		
Exergy Efficiency (%)									
	56.3			46.4			51.7		

(a) This is the feed that is processed into hydrogen.

(b) This is the fuel burned to provide external electricity and heat.

(c) This is the air burned in the reformer furnace and the air/oxygen used for gasification.

(d) Effluents are all streams leaving the process excluding the fuel produced.

As with natural gas, hydrogen production from coal or biomass requires more external exergy input in the form of fuel. As a result, even though the exergy output is higher for hydrogen production than for methanol production (for a given gasifier and feed rate), the overall effect is that methanol production has a higher exergy efficiency than hydrogen production.

6.4.1 The Shell-coal Gasifier (Figures 6A-6,7,8 and Tables 6A-7,8,9,10)

Performance data for the gasification of Illinois #6 Bituminous coal in the Shell entrained-bed gasifier was taken from Synthetic Fuels Associates (1983). Since coal has a much higher energy density than wood, the coal systems have significantly lower feedstock requirements per tonne of methanol (but higher requirements than the natural gas cases). However, due to the high oxygen requirements and high gasification temperatures, coal gasification requires a large quantity of electricity and produces a large amount of waste heat (21% of the coal HHV in the methanol case), some of which would be used for drying the coal, which is fed to the gasifier at 5% moisture. 72% of the total electricity required can be supplied using excess waste heat, steam generated in the jacket of the gasifier, and the purge gas from methanol synthesis, which is not required elsewhere since a reformer is not part of the process configuration. For methanol production, the Energy Ratio of 0.650 and thermal efficiency of 61.8% fall in the middle of the ranges calculated for the biomass cases. This value for η_{th} is slightly higher than estimates made previously for coal-to-methanol plants (Probstein and Hicks, 1982; Supp, 1990; OPPA, 1989; Wyman et al, 1992). Probstein and Hicks estimated that coal-to-methanol plants would have thermal efficiencies in the 51-59% range and the estimate from Wyman, et al. for a large "second generation"¹⁴ coal-to-methanol plant was approximately 57%. Supp (1990) estimated the efficiency of producing methanol from North Dakota lignite (a low rank coal) using the Lurgi Dry Ash gasifier (a fixed-bed design) to be approximately 52.9%.

¹⁴ Second generation gasification technology refers to pressurized entrained-bed gasification similar to the Shell process (e.g. Texaco or Dow). However, the coal case evaluated in Wyman, et al. (1992) (which is based on OPPA (1989)) was assumed to require significantly more coal per unit of methanol produced than what has been estimated here.

The ER for hydrogen production is higher than for methanol production (0.777 vs. 0.650). In fact, the ratio of the two ERs is 1.195, very close the ratio predicted by Equation (6-12). As with natural gas-based processes, there is less waste heat in hydrogen production compared to methanol production. In fact, as a result, a *pinch* occurs at approximately 230°C, as seen in the grand composite curve (Figure 6A-8). Therefore, no electricity can be generated from waste heat and some additional heat must be supplied externally. The existence of a pinch at such a low temperature has a large impact on the overall energy balances. The thermal efficiency of 63.0% is only slightly better than the thermal efficiency for methanol production despite the much higher ER. The exergy efficiency was calculated to be 51.7%.

In a similar study, Rosen and Scott (1987) analyzed the production of hydrogen from coal using the Koppers-Totzek (K-T) gasifier. They estimated a thermal efficiency of 59% and an exergy efficiency of 49%. These results compare well with the estimates made here, considering that the K-T gasifier has a lower cold gas efficiency than the Shell gasifier (Synthetic Fuels Associates, 1983), and operates at atmospheric pressure. In a previous study of hydrogen production from coal using the Shell gasifier (Blok, et al., 1991), the ER was estimated to be approximately 0.763, which is close to the estimate made here.¹⁵

¹⁵ This represents the energy content of the hydrogen fraction of the hydrogen rich gas produced by cleaning and shifting the product gas, and then removing most of the CO₂. The composition of the hydrogen rich gas was 87.5% H₂, 6.4% CO, 1.2% CO₂, 3.8% N₂, and 1.1% Ar. A more complete shift conversion and PSA recovery of most of the hydrogen (as modeled in this thesis) would yield an ER of approximately 0.78, which is essentially the same as the ER estimated here.

6.4.2 The Shell-biomass Gasifier (Figures 6A-9,10,11 and Tables 6A-11,12,13,14)

The ER of 0.678 is the highest of all the biomass-methanol cases. Nevertheless, the thermal efficiency is only 62.0%, which is high, but not the highest. It is not surprising that these values are higher than the coal case above, since it was shown in Chapter 3 that for a similar gasification technology and operating conditions, entrained-bed biomass gasification was more efficient than entrained-bed coal gasification.

Since no actual data exist for pressurized entrained-bed biomass gasification, it is somewhat difficult to evaluate these results, which are substantially better than estimates made for biomass-to-methanol plants using atmospheric pressure entrained-bed biomass gasification based on the Koppers-Totzek technology (OPPA, 1990; Stevens, 1991; Wyman, et al., 1992). In these studies, the thermal efficiency was estimated to be approximately 49%. The fact that the performance estimates made here are higher is not surprising. In the OPPA study, the K-T gasifier was estimated to require nearly 25% more oxygen than the model developed here for the Shell gasifier (0.56 kg/kg dry wood vs. 0.45 kg/kg dry wood), which is consistent with the relative oxygen requirements for coal gasification (see Chapter 3). Therefore, the model of entrained-bed gasification developed for this thesis indicates that pressurized, adiabatic entrained-bed gasification of biomass could offer significant advantages over atmospheric pressure gasification as represented by the K-T gasifier. It should be pointed out however, that the model for entrained-bed gasification represents what is thermodynamically possible, and may not be fully achievable in practice. For example, heat losses may be non-negligible and 100% carbon conversion might be somewhat optimistic. It may also be necessary to cool the reactor to some degree, as was assumed for the K-T gasifier operating on biomass (OPPA, 1990), and when coal is gasified in the Shell gasifier (Synthetic Fuels Associates, 1983).

When considered for hydrogen production, this gasifier again has the highest ER (0.791), but does not have the highest thermal efficiency. This is due to the fact that virtually no waste heat is suitable for steam production, so that 36 MW of electricity must be supplied externally as compared to 10 MW in the methanol case. The result is a thermal efficiency of 66.4%, which is 12.7 percentage points lower than the ER, a difference that is quite comparable to the coal case.

6.4.3 The IGT RENUGAS Gasifier (Figures 6A-12,13,14 and Tables 6A-15,16,17,18)

The IGT gasifier has both the lowest ERs and thermal efficiencies of all gasification systems considered here, for both methanol and hydrogen production. The ERs and η_{th} s are 0.567 and 54.5% for methanol production, and 0.677 and 57.2% for hydrogen production. The trends of less waste heat and increased electricity consumption characteristic of hydrogen production relative to methanol production are also seen with the IGT gasifier. The high pressure quench also necessitates the addition of relatively large amounts of steam for reforming. There was also sufficient purge gas available to permit steam:hydrocarbon ratios of 5:1 in the reformer, which helped increase the conversion of methane, which was thermodynamically suppressed at the high operating pressures assumed in these simulations. This did reduce the amount of steam available for electricity production, but because of the high pressure operation, relatively little electricity was required.

Although significantly lower than the other gasifiers, the estimates made here are consistent with previous assessments of methanol production from biomass using this technology (OPPA, 1990; Stevens, 1991; Wyman, et al., 1992). These three studies estimated the following performance parameters: ER = 0.580, η_{th} = 55.7%, feed utilization = 1.97 tonnes/tonne methanol, and carbon utilization = 38% (see Table 6-4 for comparison).

The relatively poor performance may be due to several factors. First, the exceptionally high pressure operation considered here favors the production of CO₂ in the gasifier, especially when combined with the high overall O:C ratio (2:1). As a result, much of the carbon exits the gasifier as CO₂ rather than CO. The high O:C ratio is a result of both the direct heating and use of steam as the fluidizing medium to promote char conversion. At these high pressures, other operating parameters should be manipulated to reduce the tendency of CO₂ formation. One option might be to reduce the moisture content of the feed, which would lower the O:C ratio and result in higher temperatures, which would favor carbon conversion and CO production. Also, since approximately 5% of the feed carbon is lost as unconverted char and condensable hydrocarbons, recycling these compounds to the gasifier or burning them to produce electricity would increase overall system efficiency. The advantage of operating at high pressure is the reduced compression costs, especially for methanol production. For hydrogen production, such high pressures may not be necessary. Furthermore, the model of entrained-bed gasification described above suggests that it is possible to achieve thermodynamic performance that is comparable to oxygen-blown coal based systems, which are more efficient than the IGT cases.

6.4.4 The Wright-Malta Gasifier (Figures 6A-15,16,17 and Tables 6A-19,20,21,22)

The WM gasifier has the highest ERs of the indirectly heated gasifiers, but its thermal efficiencies are noticeably lower (0.665 and 58.6% for methanol production, and 0.784 and 63.4% for hydrogen production). This is a consequence of the overall heat balance of the system. The integrated WM system requires external heating as a result of the nature of the gasification process. The WM gasifier is unique in that all the other gasifiers burn some of the feed, either directly or indirectly, to supply heat for gasification, whereas the WM gasifier relies entirely on heat exchange without specifically burning biomass. In both methanol and hydrogen production there is a low temperature

pinch point which eliminates the ability to produce on-site electricity from waste heat and necessitates some external heating. This analysis therefore indicates that if the WM gasifier were to be used for methanol or hydrogen production, some additional feed would need to be burned to augment the heat available from process streams.

It should be pointed out that there is a fair degree of uncertainty regarding the precise amount of external heating that would be required by a full scale WM unit. For the analysis here, it was estimated that approximately 75 MW of external heat is required, equivalent to roughly 20% the higher heating value of the feed.¹⁶ In a previous study of methanol production from biomass and urban refuse using WM technology (Arnason, 1983) it was estimated that the waste heat from the hot reformat was sufficient to run the gasifier. In the simulations here, that corresponds to slightly more than 70 MW, which includes sensible heat from condensing moisture in the gas. Even though there appears to be sufficient on-site waste heat to run the gasifier, when the heat balances of the entire systems are considered, external heating is required, and as expected, the quantity is greater in the hydrogen case.

The WM system is also one of two gasifiers that does not require a shift reactor to tune the R value to 2.03 prior to methanol synthesis. This is a consequence of the fact that the WM product gas contains large amounts of CH₄ (34% by volume on a dry basis), which, when reformed produces a hydrogen rich synthesis gas. Instead of raising the R value using a shift reactor, a CO₂ concentration of 3.2% in the make-up feed gave an R value of 2.03.¹⁷

¹⁶ To vaporize and heat the moisture in the biomass alone requires more than 40 MW at this scale.

¹⁷ The control parameter for cases with a hydrogen deficient synthesis gas was that the makeup gas contain 2% CO₂ by volume.

6.4.5 The MTCI Gasifier (Figures 6A-18,19,20 and Tables 6A-23,24,25,26)

The MTCI gasifier is different from all the other gasifiers studied here since it requires a relatively large flow of gaseous fuel (more than 100 MW on a HHV basis, nearly 30% of the feed HHV). Instead of burning some of the product gas in the pulse combustor (which would be the configuration for power production), it was found that the heat available from the purge gas was a good match for the heat load of the pulse combustor, provided that no reformer was used. This lowers overall capital costs, with no loss in fuel output. As well, due to the low methane content of the product gas (8% by volume on a dry basis), a reformer would have had a relatively small impact on yield. In the MTCI model, it was also assumed that residual char and tars could be burned in the pulse combustor to augment the heat available from the purge gas (Durai-Swamy, 1992; Turdera and Zahradnik, 1992).

The MTCI cases are characterized by moderately high ERs: 0.615 for methanol production and 0.762 for hydrogen production. Nevertheless, thermal efficiencies of 57.8% (methanol) and 61.7% (hydrogen) are relatively low when compared to the other gasifiers. This is due in part to the large amount of compression work required, since the MTCI unit operates at atmospheric pressure and produces a large volume of product gas. Although pressurized operation is likely to be possible with this gasifier (up to 1.5 MPa), it has not yet been demonstrated. To reduce compression costs, intercooled compressors were used to condense out much of the moisture. Since a shift reactor was not required in the methanol case, compression was accomplished in two stages, both prior to and after CO₂ removal. In hydrogen production, compression was carried out downstream of the shift reactors. While this is not a typical configuration, it allowed for the use of the moisture already present in the product gas, eliminating the need to raise additional steam or compress a large volume of gas. At the same time, the compression prior to pressure

swing adsorption made use of intercooling to remove moisture that was no longer needed in the synthesis gas, and hence reduced compression work considerably.

Another possible reason for the lower overall efficiencies is the fact that a large amount of steam is required for the gasification step; more than four times more (per kg of dry feed) than any of the other gasifiers. As a result, even though a reformer was not used, overall steam requirements were relatively high. The large steam requirement is a consequence of needing large steam:biomass ratios in the gasifier to ensure good carbon conversion at relatively low gasification temperatures. Unfortunately, this means that a large amount of heat must be supplied by the in-bed heat exchangers, and thus requires the use of a large amount of fuel gas. Therefore, the MTCI gasifier consumes a large quantity of high quality energy, which is ultimately rejected from the system as low grade waste heat.

As with the WM-methanol case, the MTCI-methanol case produced a make-up gas that was slightly hydrogen rich, eliminating the need for a shift reactor. In this case, the high H₂ content is a result of the high steam:biomass ratio in the gasifier, which causes it to act like a reformer to some degree. The shift reaction equilibrium is also affected by the large amount of steam in the gasifier, which also helps explain the large CO₂ content and low CO content of the product gas. A CO₂ concentration of 2.1% in the make-up gas gave an R value of 2.03.

6.4.6 The BCL Gasifier (Figures 6A-21,22,23 and Tables 6A-27,28,28,30)

The BCL gasifier is characterized by both high ERs and thermal efficiencies: 0.646 and 62.8% for methanol production, and 0.784 and 68.6% for hydrogen production. In fact, the BCL unit has the highest thermal efficiencies of all gasification systems considered here, including the coal cases. One reason is the large amount of high quality waste heat

that can be used to supply virtually all of the electricity requirements, even though gasification is carried out at atmospheric pressure, meaning that more electricity is required. In methanol production, nearly 22% of the feed energy is converted to excess process heat, while in hydrogen production the figure is greater than 14%. Furthermore, according to the pinch analyses, in both the methanol and hydrogen cases, all of this waste heat can be used to generate electricity. As outlined in Chapter 3, this is a direct result of the gasification process, where char and some biomass are burned instead of gasified, producing a large quantity of high grade waste heat. The atmospheric pressure quench also significantly reduces the amount of steam that must be raised for synthesis gas processing, allowing more of this high quality waste heat to be used for electricity production.

Wyman, et al. (1992) conducted an earlier evaluation of the BCL gasifier (methanol production only) using ASPEN-SP, a software package very similar to the one used here. Their results were: $ER \approx 0.690$, $\eta_{th} \approx 63.3\%$, and $\eta_{carbon} = 45.9\%$. Overall, these results are in excellent agreement with those presented here.

6.5 Prospects for Technological Improvements

The economic analysis in Chapter 7 will show that the systems based on the BCL and MTCI gasifiers will be highly cost competitive. Nevertheless, the technologies used in these simulations reflect only what is commercially available (except of course for the gasifiers). In addition, there are a number of advanced technologies that could improve the economics and efficiency of producing fuels from biomass. Some of these options were described in Chapter 4. Some would result in only marginal gains, but others could have significant impacts.

Because the exergy analyses showed that reforming is not a significant source of thermodynamic losses in biomass systems, alternatives to steam reforming would probably only result in marginal efficiency gains, if any. Catalytic tar cracking, while desirable, would also have only marginal benefits since the gasifiers studied here produce only small quantities of condensable hydrocarbons (about 1% or less). The coproduction of electricity, which was shown to reduce costs for coal gasification systems (OPPA, 1989), would probably have a similar impact on biomass systems. The OPPA study estimated that production costs would be approximately two thirds that for an all-methanol facility. However, this option would dramatically reduce the quantity of fuels that could be produced. Since biomass is much less abundant than coal, this is not a realistic option if biomass is to become a major source of transportation fuels. For the coal case considered in OPPA (1989), only 19% of the syngas energy was converted to methanol.

More significant improvements in economics could be achieved by commercializing advanced single-pass methanol synthesis technologies. The effect on overall efficiency would be small, but costs could be substantially reduced. Once-through methanol processes may also permit the use of air-blown gasification instead of oxygen blown gasification, which would make a wider variety of biomass gasifiers cost competitive, by eliminating the need for oxygen separation, which is costly at the scales projected here for biomass conversion facilities. The development of hot gas conditioning could have a similar impact by combining the cracking of tars and the reforming of hydrocarbons, which is relatively capital intensive, although less expensive than methanol synthesis.

Finally, a very interesting option for methanol production would be to use electricity produced from wind or solar-PV energy to produce hydrogen via the electrolysis of water, which would be added to the hydrogen deficient synthesis gas,

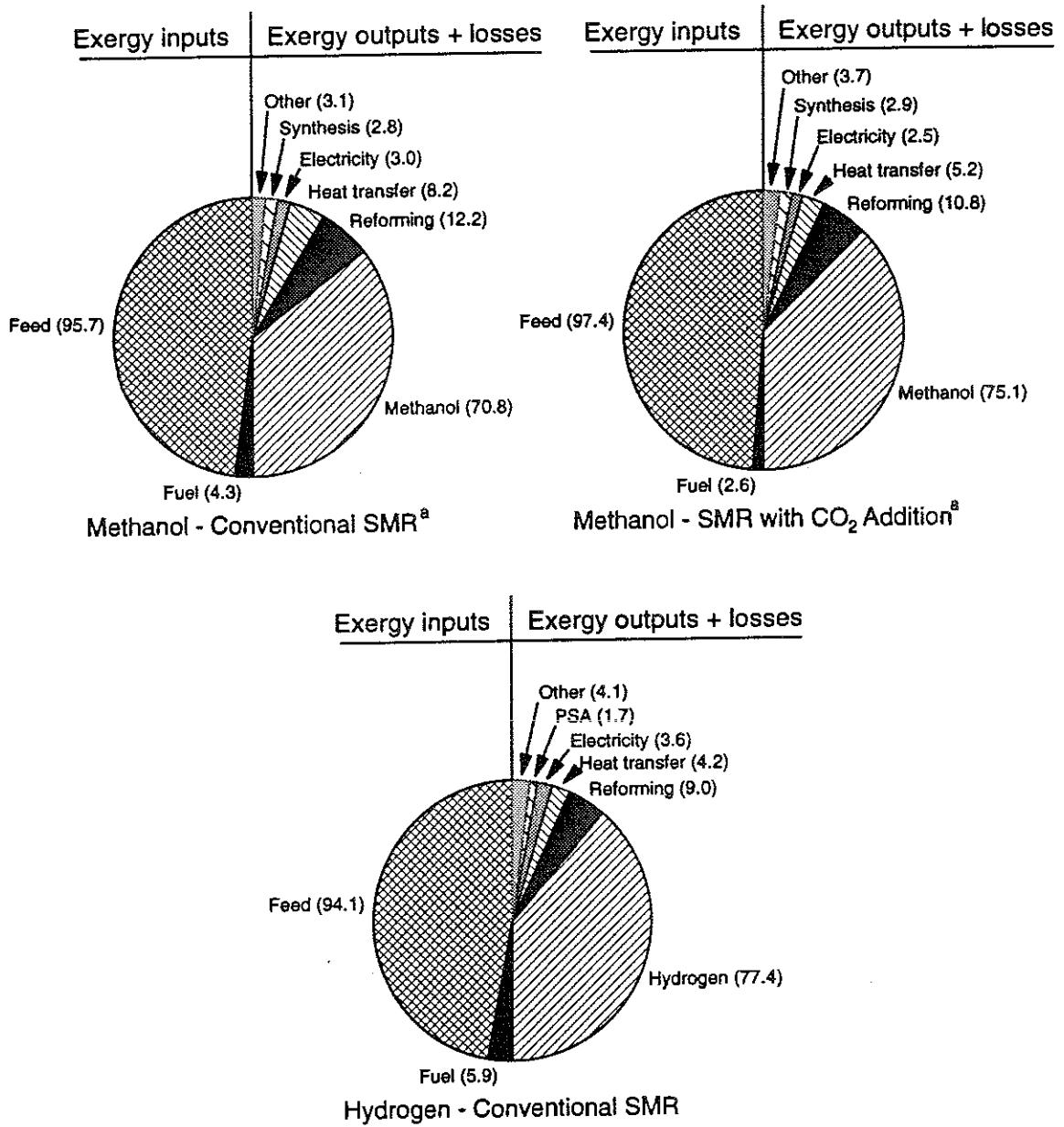
eliminating the need to tune the R value with a shift reactor. This would have multiple benefits. First, more methanol would be produced per unit of biomass. This may become extremely important when resource constraints begin to limit the supply of relatively inexpensive biomass. Thus, this option could make biomass an even more significant resource. Second, in suitable regions, the same land could be used to grow biomass and generate wind power. Third, if these intermittent energy sources are connected to the utility grid, hydrogen augmentation could be used as a means of utilizing excess electricity, when the supply of electricity from renewables exceeds demand. This would improve the economics of intermittent renewables. The by-product oxygen from electrolysis could be used on-site for gasification or reforming, or sold to offset the cost of the electrolyzer. Preliminary modeling indicates that with H₂ augmentation, it would be possible to increase methanol production by 50-100%, depending on the gasifier and the choice of reforming option.

6.6 Conclusions

A systematic comparison of methanol and hydrogen production shows that for a given feedstock hydrogen production would be more efficient. More importantly, this chapter has shown that by exploiting the unique properties of biomass, it is possible to produce fuels more efficiently from biomass than from coal. Similarly, when biomass is gasified using technologies that have been optimized for coal, efficiencies are lower than those achievable in gasifiers designed for biomass. Modern coal gasifiers like the Shell entrained-bed unit are the products of years of development and many millions of dollars in research funding. The result is a gasifier that take full advantage of the properties of coal. Similar gasifiers are needed for biomass. The good thermodynamic performance of indirectly heated gasifiers suggests that further gains can be made by pursuing a more aggressive R&D program to determine the optimal gasification technologies for producing fluid fuels from biomass. The fact that the most efficient biomass gasifier is an

atmospheric pressure unit (the BCL gasifier) demonstrates that technical options deemed advantageous for coal gasification may not be optimal for biomass.

Exergy analysis is a useful tool for gaining insights into the thermodynamics of the production of fluid fuels. The exergy analysis showed that gasification is the single largest source of thermodynamic losses in the overall systems. Reforming accounted for only minor losses relative to gasification. In hydrogen production, the production of electricity was also a major source of exergy losses. This suggests that future research should focus on reducing the losses from gasification and minimizing the need for external electricity in hydrogen production. Future work should also focus on more detailed analyses of the most promising technologies identified here. Specifically, it is important to synthesize heat exchangers networks and assess indirect gasifiers over a range of operating parameters. Because the most efficient biomass gasifier is an atmospheric pressure unit, a better understanding of the effects of pressurized biomass gasification is also needed, because it is generally accepted that pressurization is advantageous. This analysis shows that this may not be the case.



(a) SMR = Steam-methane reforming

Figure 6-1: Overall exergy balances for methanol and hydrogen production from natural gas.

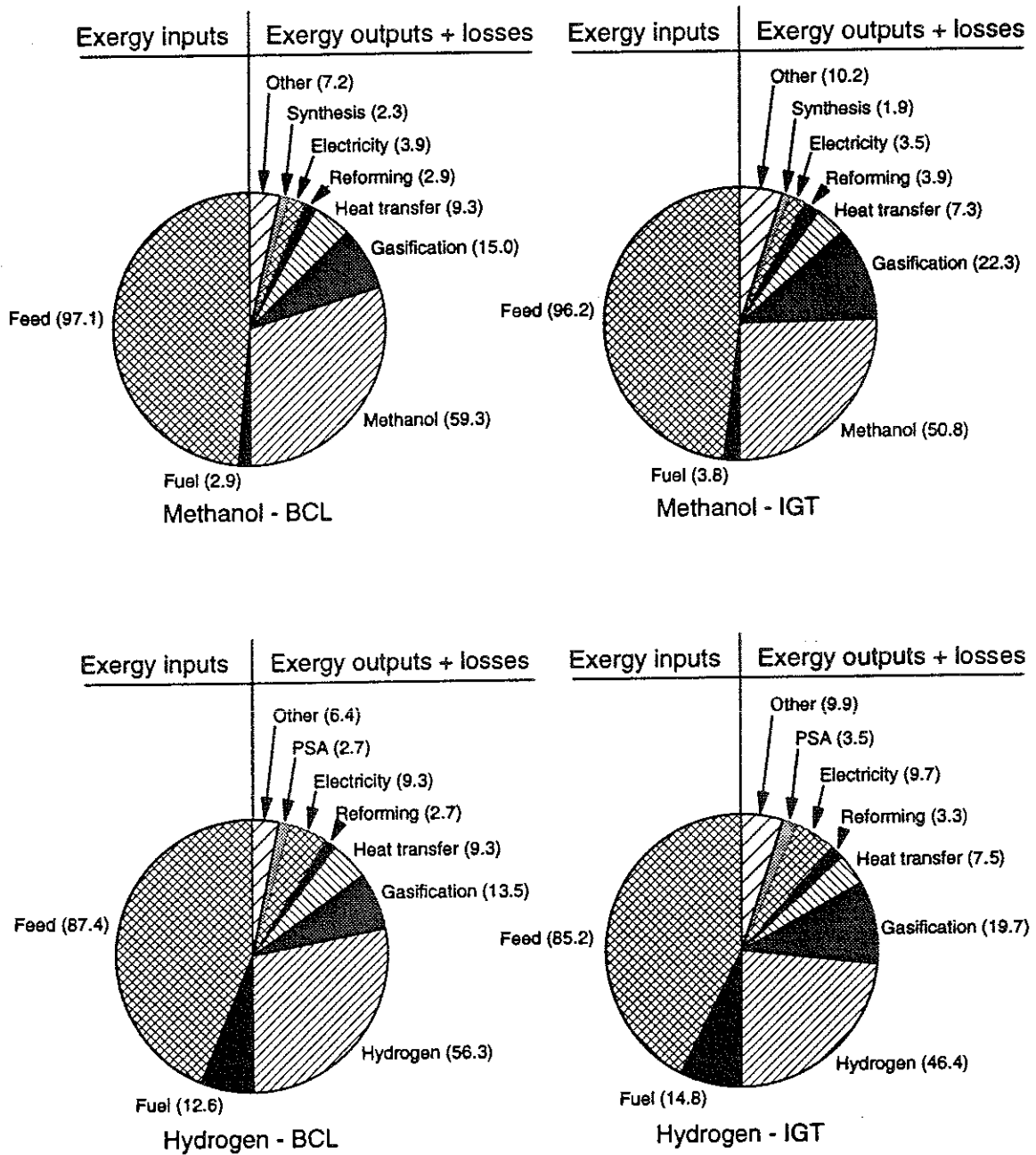


Figure 6-2: Overall exergy balances for methanol and hydrogen production from biomass using the BCL and IGT gasifiers.

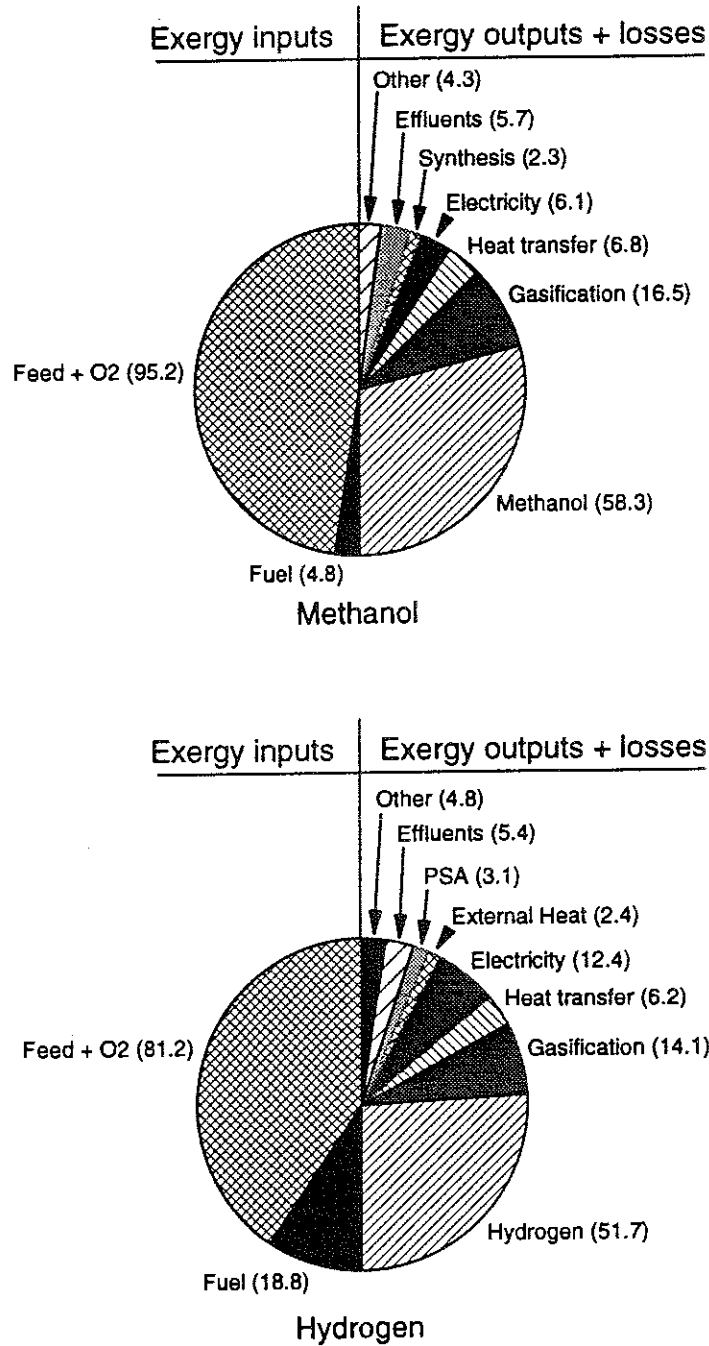


Figure 6-3: Overall exergy balances for methanol and hydrogen production from coal using the Shell entrained-bed gasifier.

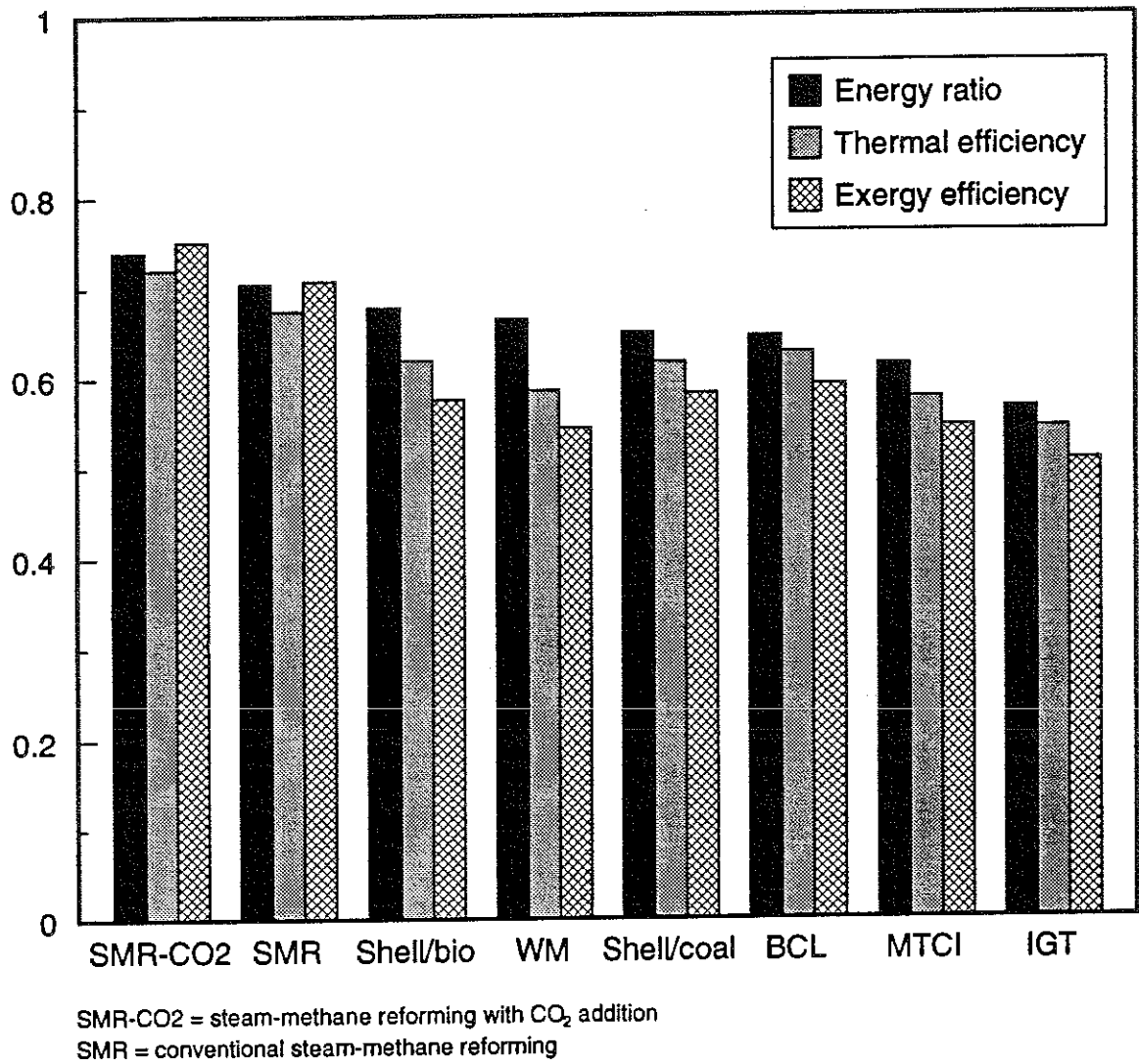


Figure 6-4: Overall thermodynamic performance for all methanol production simulations.

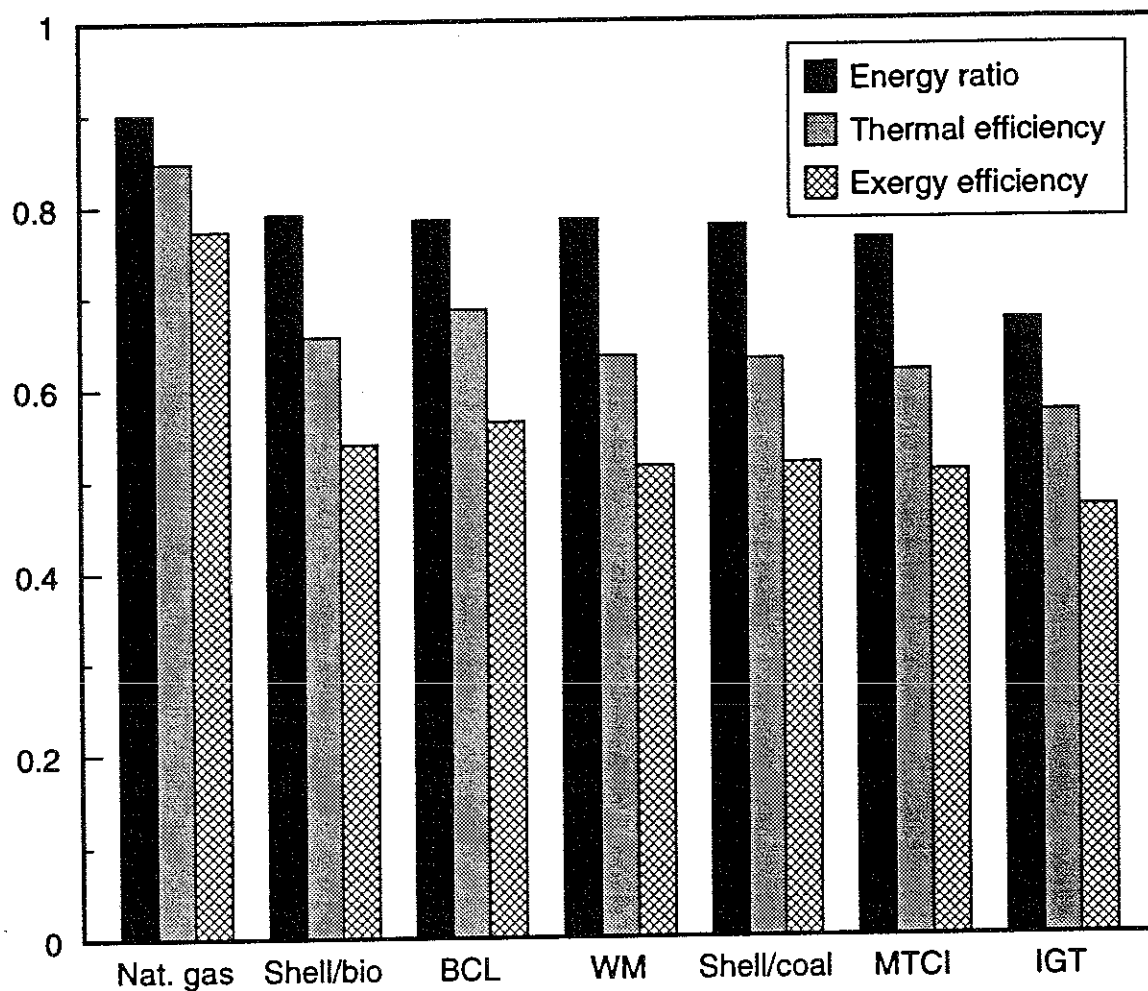


Figure 6-5: Overall thermodynamic performance for all hydrogen production simulations.

References

- Arnason, Birgir. *Methanol from Biomass and Urban Refuse: Prospects and Opportunities*. M.S.E. Thesis, Mechanical and Aerospace Engineering Department, Princeton University, Princeton, NJ, June 1983.
- Blok, K., Hendriks, C.A., Turkenburg, W.C., and Williams, R.H. *Producing Fuel and Electricity from Coal with Low Carbon Dioxide Emissions*. Draft manuscript, University of Utrecht, June 1991.
- Dibbern, H.C., Olesen, P. Rostrup-Nielsen, J.R., Tottrup, P.B., and Udengaard, N.R. "Make low H₂/CO Syngas Using Sulfur Passivated Reforming." *Hydrocarbon Processing*. Vol. 65, No. 1, January 1986, pp. 71-74.
- Durai-Swamy, K. (Senior Vice President). Manufacturing and Technology Conversion International, Santa Fe Springs, CA. Personal communication. September 1992.
- Goff, S.P. and Wang, S.I. "Syngas Production by Reforming." *Chemical Engineering Progress*. Vol 83, No. 8, August 1987, pp. 46-53.
- Hall, David O., Rosillo-Calle, Frank, Williams, Robert H., and Woods, Jeremy. "Biomass for Energy: Supply Prospects." *Renewable Energy: Sources for Fuels and Electricity*. Ed. T.B. Johansson, H. Kelly, A.K.N. Reddy, and R.H. Williams. Washington DC: Island Press, 1992.
- Heck, J.L. and Johansen, T. "Process Improves Large Scale Hydrogen Production." *Hydrocarbon Processing*. January 1978, pp. 175-177.
- Kuo, James C.W. "Engineering Evaluation of Direct Methane Conversion Processes." *Methane Conversion by Oxidative Processes: Fundamental and Engineering Aspects*. Ed. E.E. Wolf. New York: Van Nostrand Reinhold, 1991.
- McGovern, J.A. "Exergy Analysis -- A Different Perspective on Energy, Part I: The Concept of Exergy." *Proc. Instn. Mech. Engrs.*, Vol. 204, 1990, pp. 253-262.
- Morris, David R. and Szargut, Jan. "Standard Chemical Exergy of Some Elements and Compounds on the Planet Earth." *Energy*, Vol. 11, No. 8, 1986, pp. 733-755.
- OPPA (Office of Policy, Planning, and Analysis). *Assessment of Costs and Benefits of Flexible and Alternative Fuel Use in the US Transportation Sector, Technical Report Three: Methanol Production and Transportation Costs*. DOE/PE-0093. Washington DC: US Department of Energy, November 1989.

Ryan E. Katofsky

OPPA (Office of Policy, Planning, and Analysis). *Assessment of Costs and Benefits of Flexible and Alternative Fuel Use in the US Transportation Sector, Technical Report Five: Costs of Methanol Production from Biomass*. (DOE/PE-0097P) Washington DC: US Department of Energy, December 1990.

Probstein, Ronald F. and Hicks, R. Edwin. *Synthetic Fuels*. New York: McGraw-Hill Book Company, 1982.

Riensch, E. and Fedders, H. "Conversion of Natural Gas to CO Rich Syngases." *Natural Gas Conversion*. Ed. A. Holmen, K.J. Jens, and S. Kolboe. Amsterdam: Elsevier Science Publishers, 1991.

Rosen, M.A. "Thermodynamic Investigation of Hydrogen Production by Steam-Methane Reforming." *International Journal of Hydrogen Energy*, Vol. 16, No. 3, 1991, pp. 207-217.

Rosen, M.A. and Scott, D.S. "An Energy-Exergy Analysis of the Koppers-Totzek Process for Producing Hydrogen from Coal." *International Journal of Hydrogen Energy*, Vol. 12, No. 12, 1987, pp. 837-845.

Solomon, James (Business Manager - Gas Separation). Air Products and Chemicals, Inc., Allentown, PA. Personal communication. July 1991.

Stevens, D.J. "Methanol from Biomass: A Technoeconomic Analysis." *Energy from Biomass and Wastes XIV*. Ed. D.L. Klass. Chicago: Institute of Gas Technology, 1991, pp. 1245-1263.

Supp, Emil. *How to Produce Methanol from Coal*. Berlin: Springer-Verlag, 1990.

Synthetic Fuels Associates. *Coal Gasification Systems: A Guide to Status, Applications and Economics*. (EPRI AP-3109) Palo Alto, CA: Electric Power Research Institute, June 1983.

Szargut, Jan, Morris, David R., and Steward, Frank R. *Exergy Analysis of Thermal, Chemical, and Metallurgical Processes*. New York: Hemisphere, 1988.

Turdera, J. and Zahradnik, R.L. *Feasibility Evaluation and Conceptual Design of a Pulse Tube Combustion System for a Commercial Scale Integrated Coal Gasification (IGCC) Power Plant*. Draft report prepared for the US Department of Energy (contract DE-AC21-90MC27346) Washington DC: K & M Engineering and Consulting Corporation, April 1992.

Wyman, Charles E., Bain, Richard L., Hinman, Norman D., and Stevens, Don J. "Ethanol and Methanol from Cellulosic Biomass." *Renewable Energy: Sources for Fuels and Electricity*. Ed. T.B. Johansson, H. Kelly, A.K.N. Reddy, and R.H. Williams. Washington DC: Island Press, 1992.

**Appendix 6A: Process Configurations, Stream Summaries
and Pinch Analyses for Chapter 6**

Table 6A-1: Calculated material flows for methanol production from natural gas using conventional reforming.

Name	Temp [K]	Pres. [bar]	Total Volume Flow [kmol/hr]	Molecular Weight [kg/kmol]	Component Volume Flow Rates [kmol/hr]									
					H ₂ O	H ₂	CO	CO ₂	CH ₄	C ₂ H ₆	O ₂	N ₂	CH ₃ OH	
1 Natural gas feed	293	25.00	3042	16.77	0	0	0	6	2881	85	0	70	0	
2 Reformer feed	475	25.00	12194	17.70	9153	0	0	6	2881	85	0	70	0	
3 Preheated reformer feed	850	24.50	12194	17.70	9153	0	0	6	2881	85	0	70	0	
4 Reformer exit	1173	24.00	17559	12.29	5600	8832	1812	877	369	0	0	70	0	
5 Cooled reformer product	350	23.50	12180	9.76	224	8831	1812	874	369	0	0	70	0	
6 Makeup compressor inlet	350	23.50	11956	9.61	0	8831	1812	874	369	0	0	70	0	
7 Makeup compressor inlet	470	105.88	11956	9.61	0	8831	1812	874	369	0	0	70	0	
8 Hot synthesis feed 1	341	105.88	26570	5.82	3	21873	986	601	2575	0	0	489	42	
9 Hot synthesis feed 2	523	105.38	26570	5.82	3	21873	986	601	2575	0	0	489	42	
10 Synthesis product	533	97.28	54533	6.38	846	43128	434	515	5793	0	0	1100	2716	
11 Crude methanol product	300	96.78	3457	28.65	838	0	0	3	0	0	0	0	2616	
12 Recycle stream	300	96.78	51076	4.87	8	43128	434	512	5793	0	0	1100	100	
13 Recycle compressor feed	300	96.78	47822	4.87	8	40380	406	479	5424	0	0	1030	94	
14 Recycle compressor exit	309	105.88	47822	4.87	8	40380	406	479	5424	0	0	1030	94	
15 Cold synthesis feed 1	341	105.88	33208	5.82	4	27338	1232	752	3218	0	0	611	52	
16 Cold synthesis feed 2	320	105.38	33208	5.82	4	27338	1232	752	3218	0	0	611	52	
17 Purge stream	300	96.78	3254	4.87	1	2747	28	33	369	0	0	70	6	
18 Heated reformer fuel gas	500	96.78	3254	4.87	1	2747	28	33	369	0	0	70	6	
19 Reformer furnace products	1193	1.00	13504	26.03	3499	0	0	436	0	0	308	9262	0	
20 Stack gases	393	1.00	13504	26.03	3499	0	0	436	0	0	308	9262	0	
21 Reformer furnace air	298	1.00	11635	28.85	0	0	0	0	0	0	2443	9192	0	
22 Heated reformer furnace air	855	1.00	11635	28.85	0	0	0	0	0	0	2443	9192	0	
23 Reformer steam	540	25.00	9153	18.02	9153	0	0	0	0	0	0	0	0	
24 Condensate	350	23.50	5379	18.02	5375	1	0	3	0	0	0	0	0	
25 Water removed	350	23.50	224	18.02	224	0	0	0	0	0	0	0	0	

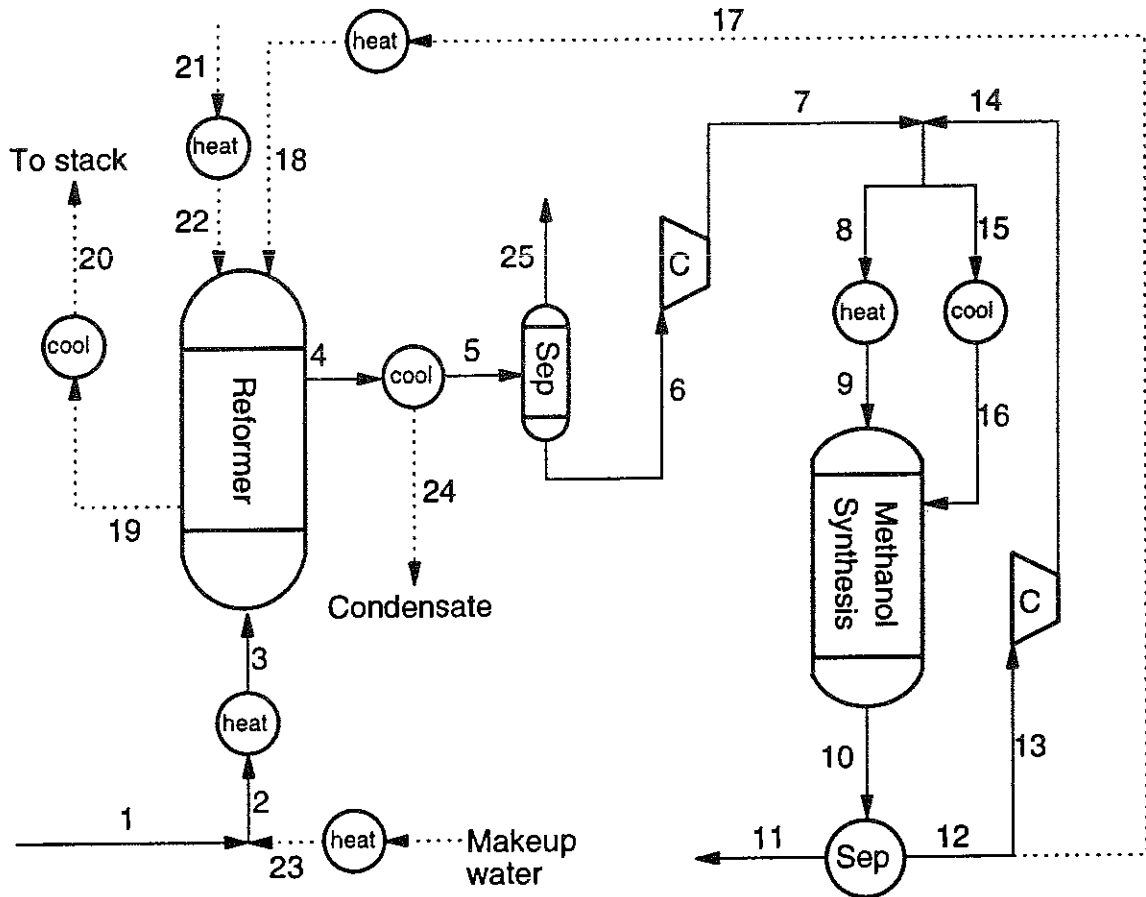


Figure 6A-1: Process configuration for the modeling of methanol production from natural gas using conventional steam reforming.

Table 6A-2: Calculated material flows for methanol production from natural gas using carbon dioxide addition.

Name	Temp [K]	Pres. Flow [bar]	Total Volume Flow [kmol/hr]	Molecular Weight [kg/kmol]	Component Volume Flow Rates [kmol/hr]									
					H ₂ O	H ₂	CO	CO ₂	CH ₄	C ₂ H ₆	O ₂	N ₂	CH ₃ OH	
1 Natural gas feed	293	25.00	3042	16.77	0	0	0	6	2881	85	0	70	0	
2 Natural gas to reformer	293	25.00	2601	16.77	0	0	0	5	2463	73	0	60	0	
3 Carbon dioxide added	298	25.00	672	44.01	0	0	0	672	0	0	0	0	0	
4 Reformer feed	460	25.00	9497	22.27	5217	0	0	1685	2463	73	0	60	0	
5 Preheated reformer feed	850	24.50	9497	22.27	5217	0	0	1685	2463	73	0	60	0	
6 Reformer exit	1173	24.00	13855	15.26	3525	5977	2666	1198	429	0	0	60	0	
7 Selexol feed	400	23.50	11699	14.76	1371	5977	2666	1196	429	0	0	60	0	
8 Selexol exit	400	23.50	9318	11.11	0	5977	2666	186	429	0	0	60	0	
9 Makeup compressor exit	471	105.88	9318	11.11	0	5977	2666	186	429	0	0	60	0	
10 Hot synthesis feed 1	336	105.88	12494	12.99	0	5265	1327	403	4798	0	0	669	31	
11 Hot synthesis feed 2	523	105.38	12494	12.99	0	5265	1327	403	4798	0	0	669	31	
12 Synthesis product	533	97.28	41132	14.73	142	14008	2343	1365	17908	1	0	2498	2868	
13 Crude methanol product	300	96.78	2904	31.42	140	0	0	14	1	0	0	0	2749	
14 Recycle stream	300	96.78	38229	13.46	2	14008	2343	1351	17908	1	0	2498	119	
15 Recycle compressor feed	300	96.78	37273	13.46	1	13658	2284	1317	17460	1	0	2435	116	
16 Recycle compressor exit	308	105.88	37273	13.46	1	13658	2284	1317	17460	1	0	2435	116	
17 Cold synthesis feed 1	336	105.88	34141	12.99	1	14386	3627	1102	13111	1	0	1829	85	
18 Cold synthesis feed 2	320	105.38	34141	12.99	1	14386	3627	1102	13111	1	0	1829	85	
19 Nat. gas to reformer furnace	293	25.00	441	16.77	0	0	0	1	418	12	0	10	0	
20 Purge stream	300	96.78	955	13.46	0	350	59	34	448	0	0	62	3	
21 Heated reformer fuel gas	500	25.00	1396	14.50	0	350	59	35	865	12	0	73	3	
22 Reformer furnace products	1193	1.00	12027	27.66	2124	0	0	986	0	0	291	8626	0	
23 Stack gases	393	1.00	12027	27.66	2124	0	0	986	0	0	291	8626	0	
24 Reformer furnace air	298	1.00	10828	28.85	0	0	0	0	0	0	2274	8554	0	
25 Heated reformer furnace air	1000	1.00	10828	28.85	0	0	0	0	0	0	2274	8554	0	
26 Reformer steam	540	25.00	4796	18.02	4796	0	0	0	0	0	0	0	0	
27 Carbon dioxide recycled 1	400	1.30	2380	29.04	1371	0	0	1010	0	0	0	0	0	
28 Carbon dioxide recycled 2	508	25.00	1429	36.35	421	0	0	1008	0	0	0	0	0	
29 Condensate	400	23.50	2156	18.03	2154	1	0	2	0	0	0	0	0	
30 Stage 2 condensate	400	9.33	952	18.02	950	0	0	2	0	0	0	0	0	

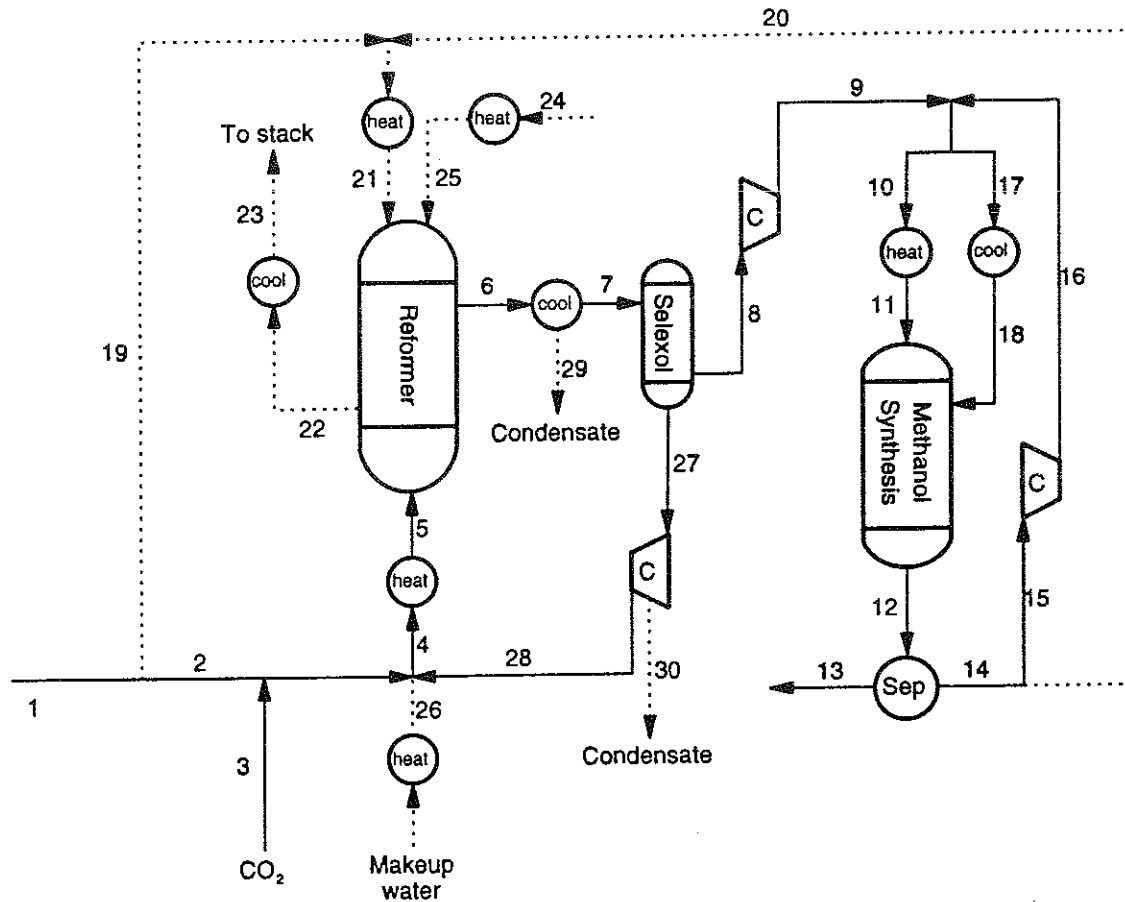


Figure 6A-2: Process configuration for the modeling of methanol production from natural gas using carbon dioxide addition and recycling with steam reforming.

Table 6A-3: Pinch analysis for methanol production from natural gas using conventional steam reforming.

Stream Table (stream names correspond those used in the Aspen Plus[™] simulations)

Streams	T source (K)	T target (K)	H in (GJ/hr)	H out (GJ/hr)	Delta T (K)	Delta H (kW)	CP (kW/K)	T source cor'ctd	T target cor'ctd
COMB1 (h)	1193.0	393.0	-612.21	-978.94	-800.0	-101867	127.33	1188.0	388.0
REFPROD1-a (h)	1173.0	435.9	0.00	-450.54	-737.1	-125151	169.79	1168.0	430.9
SYNPROD-a (h)	533.0	392.4	0.00	-253.43	-140.6	-70399	500.83	528.0	387.4
REFPROD1-b (h)	435.9	410.7	-450.54	-598.06	-25.2	-40977	1623.52	430.9	405.7
REFPROD1-c (h)	410.7	350.0	-598.06	-736.00	-60.7	-38316	631.73	405.7	345.0
SYNPROD-b (h)	392.4	300.0	-253.43	-557.34	-92.4	-84418	913.25	387.4	295.0
COLD1 (h)	341.3	320.0	-641.37	-663.22	-21.3	-6069	284.73	336.3	315.0
AIR1 (c)	298.0	855.1	-0.05	197.75	557.1	54944	98.63	303.0	860.1
REFFEED1 (c)	475.1	850.0	-2375.67	-2173.46	374.9	56169	149.82	480.1	855.0
REFW2-c (c)	496.1	546.0	447.44	471.01	49.9	6548	131.23	501.1	551.0
HOTFEED1 (c)	341.3	523.0	-513.17	-361.58	181.7	42111	231.78	346.3	528.0
PURGE1 (c)	300.0	500.0	-44.88	-24.57	200.0	5643	28.22	305.0	505.0
REFW2-b (c)	496.0	496.1	143.50	447.44	0.1	84428	844281.02	501.0	501.1
REFW2-a (c)	293.0	496.0	0.00	143.50	203.0	39860	196.32	298.0	501.0
						-177493			

Problem Table

Interval	T(i) (K)	T(i+1) (K)	Ti-T(i+1) (K)	Sum CPhot (kW/K)	Sum CPcold (kW/K)	Cpc-Cph (kW/K)	delta H (kW)	Cascade	Corrected Cascade
0		1188.0						0	0
1	1188.0	1168.0	20.0	127.33	0.00	-127.33	-2547	2547	2547
2	1168.0	860.1	307.9	297.12	0.00	-297.12	-91495	94041	94041
3	860.1	855.0	5.1	297.12	98.63	-198.49	-1005	95046	95046
4	855.0	551.0	304.0	297.12	248.45	-48.67	-14794	109840	109840
5	551.0	528.0	23.0	297.12	379.68	82.56	1902	107938	107938
6	528.0	505.0	23.0	797.95	611.46	-186.49	-4289	112227	112227
7	505.0	501.1	3.9	797.95	639.68	-158.27	-611	112838	112838
8	501.1	501.0	0.1	797.95	844789.47	843991.52	84399	28439	28439
9	501.0	480.1	21.0	797.95	704.77	-93.18	-1952	30391	30391
10	480.1	430.9	49.2	797.95	554.95	-243.00	-11955	42346	42346
11	430.9	405.7	25.2	2251.68	554.95	-1696.73	-42825	85170	85170
12	405.7	388.0	17.7	1259.89	554.95	-704.94	-12444	97615	97615
13	388.0	387.4	0.6	1132.56	554.95	-577.61	-326	97941	97941
14	387.4	346.3	41.1	1544.98	554.95	-990.03	-40711	138652	138652
15	346.3	345.0	1.3	1544.98	323.17	-1221.81	-1607	140258	140258
16	345.0	336.3	8.7	913.25	323.17	-590.08	-5125	145383	145383
17	336.3	315.0	21.3	1197.98	323.17	-874.81	-18647	164030	164030
18	315.0	305.0	10.0	913.25	323.17	-590.08	-5901	169931	169931
19	305.0	303.0	2.0	913.25	294.95	-618.30	-1237	171167	171167
20	303.0	298.0	5.0	913.25	196.32	-716.93	-3585	174752	174752
21	298.0	295.0	3.0	913.25	0.00	-913.25	-2740	177492	177492

Table 6A-4: Pinch analysis for methanol production from natural gas using CO₂ addition.

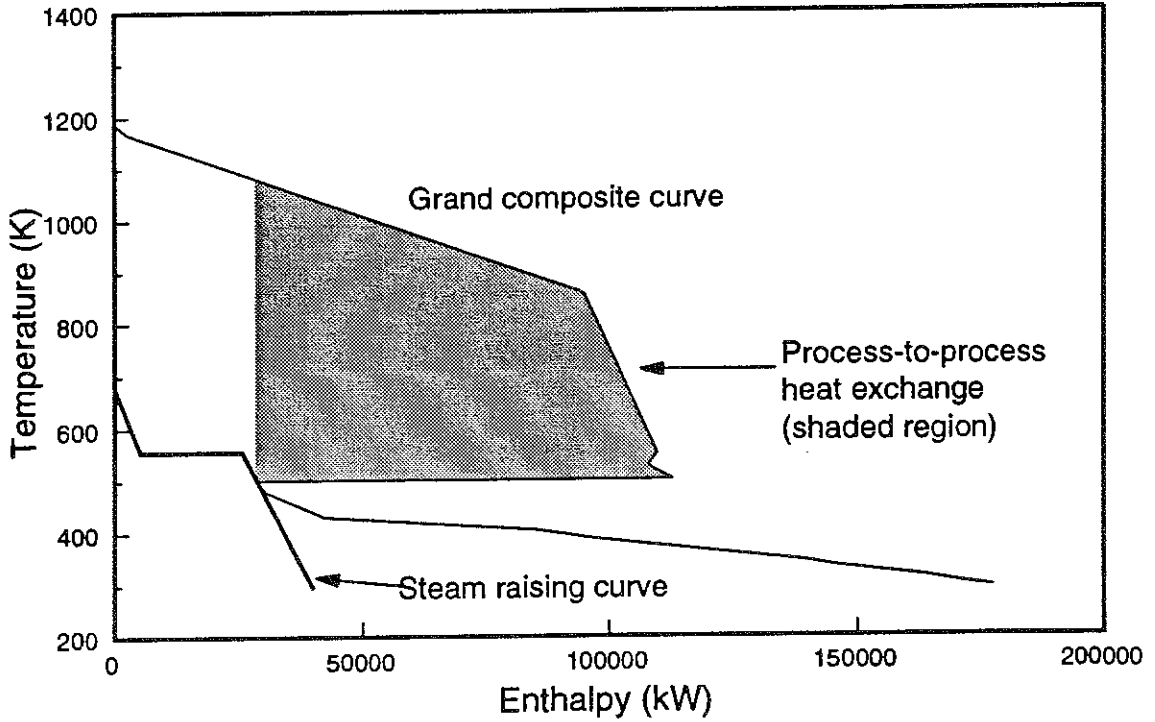
Stream Table

Streams	T source (K)	T target (K)	H in (GJ/hr)	H out (GJ/hr)	Delta T (K)	Delta H (kW)	CP (kW/K)	T source cor'ctd	T target cor'ctd
COMB1 (h)	1193.0	393.0	-537.11	-867.08	-800.0	-91658	114.57	1188.0	388.0
REFPROD1-a (h)	1173.0	418.0	0.00	-408.58	-755.0	-113495	150.33	1168.0	413.0
SYNPROD-a (h)	533.0	384.6	0.00	-245.81	-148.4	-68281	460.23	528.0	379.6
REFPROD1-b (h)	418.0	400.0	-408.58	-466.95	-18.0	-16214	898.49	413.0	395.0
SYNPROD-b (h)	384.6	300.0	-245.81	-490.86	-84.6	-68070	804.27	379.6	295.0
COLD1 (h)	336.0	320.0	-1806.38	-1825.84	-16.0	-5407	337.43	331.0	315.0
AIR1 (cold)	298.0	1000.0	-0.05	235.47	702.0	65420	93.19	303.0	1005.0
REFFEED1 (c)	459.9	850.0	-2072.84	-1897.14	390.1	48808	125.11	464.9	855.0
REFFW2-c (c)	496.1	546.0	234.46	246.81	49.9	3431	68.76	501.1	551.0
HOTFEED1 (c)	336.0	523.0	-661.03	-575.24	187.0	23830	127.45	341.0	528.0
FUEL2 (c)	288.7	500.0	-87.38	-76.19	211.3	3110	14.72	293.7	505.0
REFW2-b (c)	496.0	496.1	75.19	234.46	0.1	44240	442403.26	501.0	501.1
REFW2-a (c)	293.0	496.0	0.00	75.19	203.0	20887	102.87	298.0	501.0
						-153399			

Problem Table

Interval	T(i) (K)	T(i+1) (K)	Ti-T(i+1) (K)	Sum CPhot (kW/K)	Sum CPcold (kW/K)	CPc-CPh (kW/K)	delta H (kW)	Cascade	Corrected Cascade
0		1188.0						0	0
1	1188.0	1168.0	20.0	114.57	0.00	-114.57	-2291	2291	2291
2	1168.0	1005.0	163.0	264.90	0.00	-264.90	-43179	45470	45470
3	1005.0	855.0	150.0	264.90	93.19	-171.71	-25757	71227	71227
4	855.0	551.0	304.0	264.90	218.30	-46.60	-14165	85391	85391
5	551.0	528.0	23.0	264.90	287.06	22.16	511	84881	84881
6	528.0	505.0	23.0	725.13	414.51	-310.62	-7144	92025	92025
7	505.0	501.1	3.9	725.13	429.23	-295.90	-1142	93167	93167
8	501.1	501.0	0.1	725.13	442763.73	442038.60	44204	48963	48963
9	501.0	464.9	36.2	725.13	463.34	-261.79	-9467	58430	58430
10	464.9	413.0	51.8	725.13	338.23	-386.90	-20054	78484	78484
11	413.0	395.0	18.0	1473.29	338.23	-1135.06	-20482	98967	98967
12	395.0	388.0	7.0	574.80	338.23	-236.57	-1656	100623	100623
13	388.0	379.6	8.4	460.23	338.23	-122.00	-1020	101643	101643
14	379.6	341.0	38.6	804.27	338.23	-466.04	-17994	119637	119637
15	341.0	331.0	10.0	804.27	210.78	-593.49	-5935	125572	125572
16	331.0	315.0	16.0	1141.70	210.78	-930.92	-14918	140490	140490
17	315.0	303.0	12.0	804.27	210.78	-593.49	-7122	147612	147612
18	303.0	298.0	5.0	804.27	117.59	-686.68	-3433	151045	151045
19	298.0	295.0	3.0	804.27	14.72	-789.55	-2369	153414	153414
20	295.0	293.7	1.3	0.00	14.72	14.72	19	153395	153395

Conventional steam reforming



Reforming with CO₂ addition

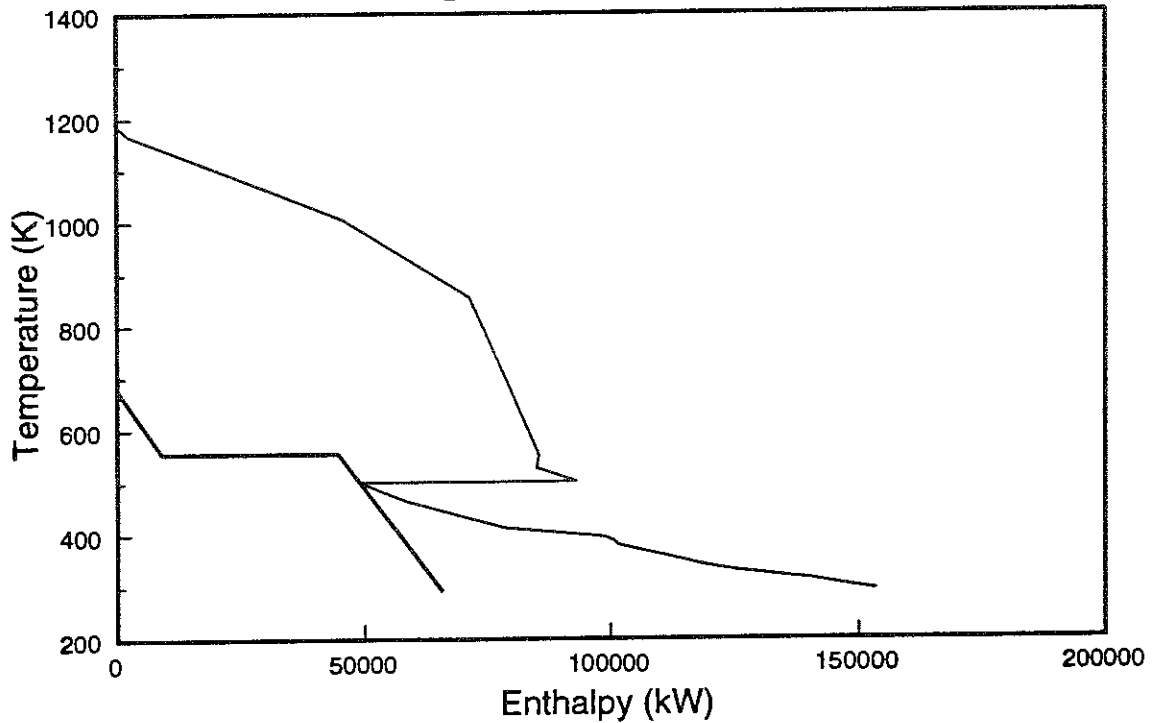


Figure 6A-3: Grand composite curves for methanol production from natural gas, showing how much steam can be raised from excess waste heat. The shaded region indicates process-to-process heat exchange.

Table 6A-5: Calculated material flows for hydrogen production from natural gas.

Name	Temp [K]	Pres. [bar]	Total Volume Flow [kmol/hr]	Molecular Weight [kg/kmol]	H ₂ O	Component Volume Flow Rates [kmol/hr]						
						H ₂	CO	CO ₂	CH ₄	C ₂ H ₆	O ₂	N ₂
1 Natural gas feed	293	25.00	3042	16.77	0	0	0	6	2881	85	0	70
2 Natural gas to reformer	500	24.50	2507	16.77	0	0	0	5	2374	70	0	58
3 Reformer feed	523	24.50	10051	17.70	7544	0	0	5	2374	70	0	58
4 Preheated reformer feed	850	24.00	10051	17.70	7544	0	0	5	2374	70	0	58
5 Reformer exit	1173	23.50	14495	12.28	4604	7314	1505	723	292	0	0	58
6 High temperature shift feed	623	23.00	14495	12.28	4604	7314	1505	723	292	0	0	58
7 High temperature shift exit	700	22.50	14495	12.28	3597	8320	498	1729	292	0	0	58
8 Low temperature shift feed	500	22.00	14495	12.28	3597	8320	498	1729	292	0	0	58
9 Low temperature shift exit	500	21.50	14495	12.28	3168	8750	69	2159	292	0	0	58
10 PSA makeup feed	313	21.00	11359	10.69	33	8750	69	2158	292	0	0	58
11 PSA-A feed	313	21.00	14137	11.08	33	9853	343	2158	1462	0	0	288
12 PSA-B feed	313	20.65	11946	5.11	0	9853	343	0	1462	0	0	288
13 Hydrogen compressor feed	313	20.30	8474	2.02	0	8474	0	0	0	0	0	0
14 Hydrogen compressor exit	383	75.00	8474	2.02	0	8474	0	0	0	0	0	0
15 Cooled Hydrogen product	313	75.00	8474	2.02	0	8474	0	0	0	0	0	0
16 PSA recycle stream	313	1.30	3472	12.65	0	1379	343	0	1462	0	0	288
17 Recycle compressor feed	313	1.30	2778	12.65	0	1104	274	0	1170	0	0	231
18 Recycle compressor exit	433	21.20	2778	12.65	0	1104	274	0	1170	0	0	231
19 PSA-A recycle feed	313	21.00	2778	12.65	0	1104	274	0	1170	0	0	231
20 Nat. gas to reformer furnace	293	25.00	535	16.77	0	0	0	1	506	15	0	12
21 Purge stream	313	1.30	694	12.65	0	276	69	0	292	0	0	58
22 Heated reformer furnace fuel	700	1.30	1229	14.44	0	276	69	1	799	15	0	70
23 Reformer furnace products	1193	1.00	11039	27.68	1918	0	0	898	0	0	272	7950
24 Stack gases	393	1.00	11039	27.68	1918	0	0	898	0	0	272	7950
25 Reformer furnace air	298	1.00	9975	28.85	0	0	0	0	0	0	2095	7880
26 Heated reformer furnace air	1000	1.00	9975	28.85	0	0	0	0	0	0	2095	7880
27 Reformer steam	546	24.50	7544	18.02	7544	0	0	0	0	0	0	0
28 Carbon dioxide removed	313	1.30	2191	43.62	33	0	0	2158	0	0	0	0
29 Condensate	313	21.00	3135	18.02	3135	0	0	0	0	0	0	0

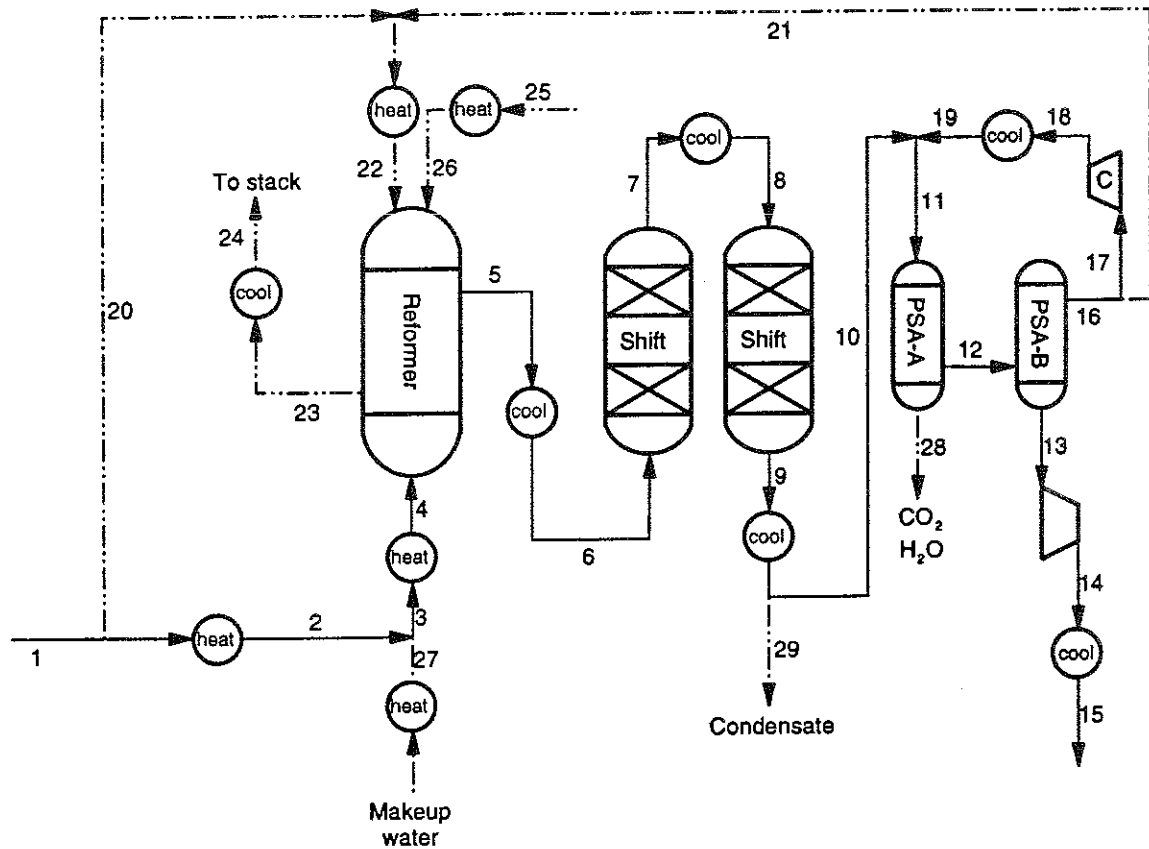


Figure 6A-4: Process configuration for the modeling of hydrogen production from natural gas using conventional steam reforming.

Table 6A-6: Pinch analysis for hydrogen production from natural gas using conventional steam reforming.

Stream Table

Streams	T source (K)	T target (K)	H in (GJ/hr)	H out (GJ/hr)	Delta T (K)	Delta H (kW)	CP (kW/K)	T source cor'ctd	T target cor'ctd
COMB1 (hot)	1193.0	393.0	-483.18	-785.70	-800.0	-84035	105.04	1188.0	388.0
REFPROD (h)	1173.0	623.0	-1153.98	-1437.21	-550.0	-78676	143.05	1168.0	618.0
SHIFT3 (h)	699.6	500.0	-1437.47	-1536.17	-199.6	-27415	137.38	694.6	495.0
LTS (hot)	500.1	500.0	-1536.17	-1553.08	-0.1	-4698	46983.61	495.1	495.0
SHIFT5-a (h)	500.0	421.6	0.00	-37.91	-78.4	-10530	134.28	495.0	416.6
SHIFTC3 (h)	432.8	313.0	-105.55	-116.86	-119.8	-3143	26.24	427.8	308.0
SHIFT5-b (h)	421.6	388.6	-37.91	-145.15	-32.9	-29788	904.13	416.6	383.6
H22 (hot)	382.6	313.0	21.41	4.36	-69.6	-4735	68.04	377.6	308.0
SHIFT5-c (h)	388.6	313.0	-145.15	-232.23	-75.6	-24191	319.84	383.6	308.0
AIR1 (cold)	298.0	1000.0	-0.04	216.92	702.0	60269	85.85	303.0	1005.0
REFFEED3 (c)	522.7	850.0	-1936.79	-1792.59	327.3	40055	122.39	527.7	855.0
FUEL2 (c)	298.1	700.0	-69.12	-48.71	401.9	5669	14.11	303.1	705.0
REFW2-c (c)	496.1	546.0	368.78	388.21	49.9	5397	108.16	501.1	551.0
REFFEED1 (c)	293.0	500.0	-187.3299	-165.0126	207.0	6199	29.95	298.0	505.0
REFW2-b (c)	496.0	496.1	118.27	368.78	0.1	69586	69585.56	501.0	501.1
REFW2-a (c)	293.0	496.0	0.00	118.27	203.0	32853	161.81	298.0	501.0
						-47185			

Problem Table

Interval	T(i) (K)	T(i+1) (K)	Ti-T(i+1) (K)	Sum CPhot (kW/K)	Sum CPcold (kW/K)	CPc-CPH (kW/K)	delta H (kW)	Cascade	Corrected Cascade
0		1188.0						0	0
1	1188.0	1168.0	20.0	105.04	0.00	-105.04	-2101	2101	2101
2	1168.0	1005.0	163.0	248.09	0.00	-248.09	-40439	42539	42539
3	1005.0	855.0	150.0	248.09	85.85	-162.24	-24336	66875	66875
4	855.0	705.0	150.0	248.09	208.24	-39.85	-5978	72853	72853
5	705.0	694.6	10.4	248.09	222.35	-25.74	-269	73122	73122
6	694.6	618.0	76.6	385.47	222.35	-163.12	-12488	85609	85609
7	618.0	551.0	67.0	242.42	222.35	-20.07	-1344	86953	86953
8	551.0	527.7	23.3	242.42	330.51	88.09	2053	84901	84901
9	527.7	505.0	22.7	242.42	208.12	-34.30	-780	85681	85681
10	505.0	501.1	3.9	242.42	238.07	-4.35	-17	85697	85697
11	501.1	501.0	0.1	242.42	695985.47	695743.05	69574	16123	16123
12	501.0	495.1	5.9	242.42	291.72	49.30	293	15830	15830
13	495.1	495.0	0.1	47226.03	291.72	-46934.31	-4693	20524	20524
14	495.0	427.8	67.2	239.32	291.72	52.40	3524	17000	17000
15	427.8	416.6	11.2	265.56	291.72	26.16	292	16708	16708
16	416.6	388.0	28.6	1035.41	291.72	-743.69	-21255	37963	37963
17	388.0	383.6	4.4	930.37	291.72	-638.65	-2788	40751	40751
18	383.6	377.6	6.0	346.08	291.72	-54.36	-328	41080	41080
19	377.6	308.0	69.6	414.12	291.72	-122.40	-8519	49598	49598
20	308.0	303.1	4.9	0.00	291.72	291.72	1424	48174	48174
21	303.1	303.0	0.1	0.00	277.61	277.61	33	48141	48141
22	303.0	298.0	5.0	0.00	191.76	191.76	959	47183	47183

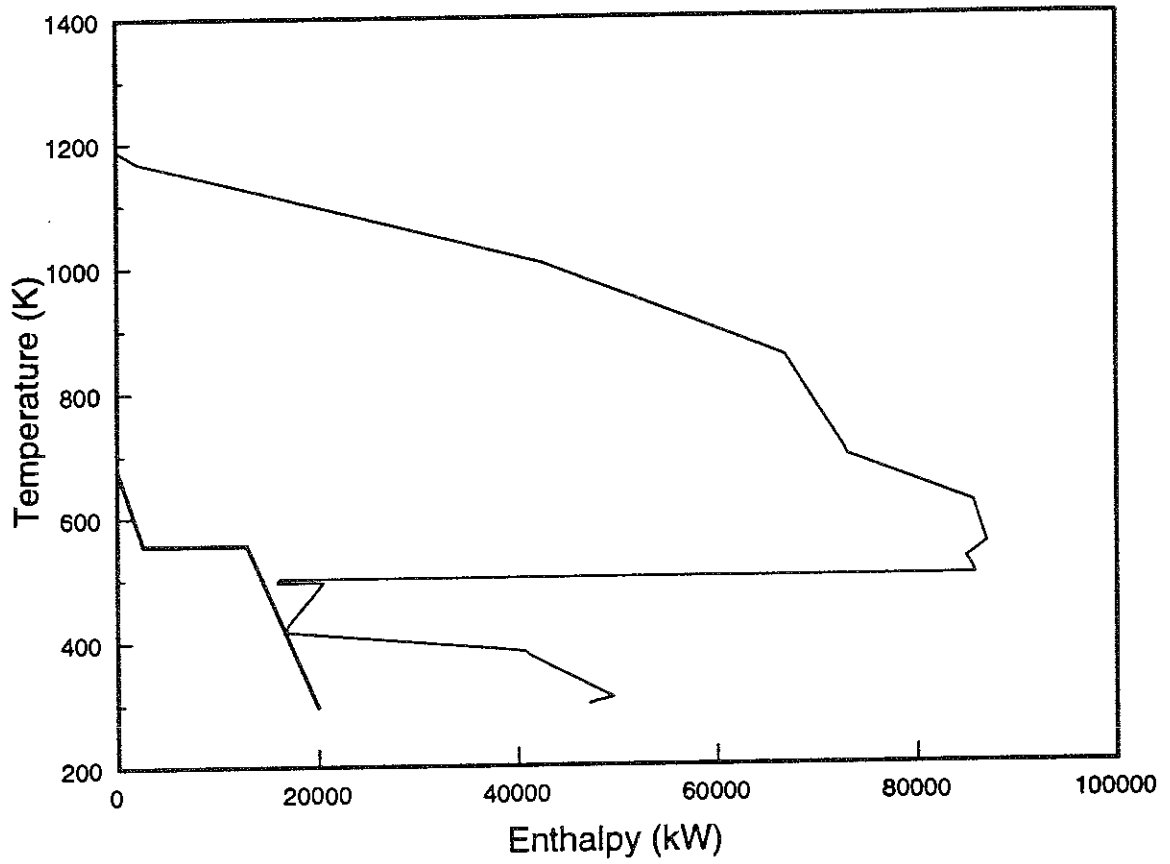


Figure 6A-5: Grand composite curve of hydrogen production from natural gas using conventional steam reforming.

Table 6A-7: Calculated material flows for methanol production from coal based on the Shell Gasifier.

Name	Temp [K]	Pres. Flow [bar]	Total Volume Flow [kmol/hr]	Molecular Weight [kg/kmol]	Component Volume Flow Rates [kmol/hr]									
					H ₂ O	H ₂	CO	CO ₂	CH ₄	H ₂ S	Ar	O ₂	N ₂	CH ₃ OH
1 Dried coal					1650 tonnes per day @ 5% moisture									
2 Dried, pressurized coal					1650 tonnes per day @ 5% moisture									
3 Gasifier inlet	1644	24.32	6353	20.49	127	1902	3841	103	5	75	73	0	227	0
4 Quench inlet	405	23.82	6353	20.49	127	1902	3841	103	5	75	73	0	227	0
5 Quench exit	369	23.32	6458	20.45	232	1902	3841	103	5	75	73	0	227	0
6 Gas Cleanup exit	369	23.32	6383	20.29	232	1902	3841	103	5	0	73	0	227	0
7 Shift feed	369	23.32	4058	20.29	148	1209	2442	65	3	0	46	0	144	0
8 Shift bypass	369	23.32	2325	20.29	85	693	1399	38	2	0	27	0	83	0
9 Heated Shift feed	623	22.82	4058	20.29	148	1209	2442	65	3	0	46	0	144	0
10 Shift exit	803	22.32	11235	18.84	5256	3278	372	2135	3	0	46	0	144	0
11 Cooled shift exit	400	21.82	6787	19.37	807	3278	372	2135	3	0	46	0	144	0
12 Selextol feed	395	21.82	9112	19.61	892	3971	1772	2172	5	0	73	0	227	0
13 Selextol exit	395	21.82	6171	11.73	0	3971	1772	123	5	0	73	0	227	0
14 Makeup compressor exit	393	105.88	6171	11.73	0	3971	1772	123	5	0	73	0	227	0
15 Hot synthesis feed 1	326	105.88	2558	17.51	0	1177	258	58	16	0	248	0	793	7
16 Hot synthesis feed 2	523	105.38	2558	17.51	0	1177	258	58	16	0	248	0	793	7
17 Synthesis product	533	97.28	27204	19.86	87	10460	1373	618	197	0	2997	0	9562	1910
18 Crude methanol product	300	96.28	1967	31.52	86	3	1	25	1	0	8	0	19	1825
19 Recycle stream	300	96.28	25237	18.95	1	10457	1372	594	196	0	2989	0	9544	85
20 Recycle compressor feed	300	96.28	24686	18.95	1	10228	1342	581	192	0	2924	0	9335	83
21 Recycle compressor exit	310	105.88	24686	18.95	1	10228	1342	581	192	0	2924	0	9335	83
22 Cold synthesis feed 1	326	105.88	28299	17.51	1	13022	2856	646	180	0	2749	0	8770	76
23 Cold synthesis feed 2	320	105.38	28299	17.51	1	13022	2856	646	180	0	2749	0	8770	76
24 Purge stream	300	96.28	551	18.95	0	228	30	13	4	0	65	0	209	2
25 Shift steam	623	22.82	7177	18.02	7177	0	0	0	0	0	0	0	0	0
26 Gasifier steam	500	24.50	115	18.02	115	0	0	0	0	0	0	0	0	0
27 Gasifier Oxygen	298	24.50	1804	32.00	0	0	0	0	0	0	73	1719	12	0
28 Carbon dioxide removed	395	21.82	2941	36.13	892	0	0	2049	0	0	0	0	0	0
29 Condensate	400	21.82	4448	18.02	4448	0	0	0	0	0	0	0	0	0
30 Quench feed water	294	25.00	704	18.02	704	0	0	0	0	0	0	0	0	0
31 Quench condensate	369	23.32	599	18.02	599	0	0	0	0	0	0	0	0	0

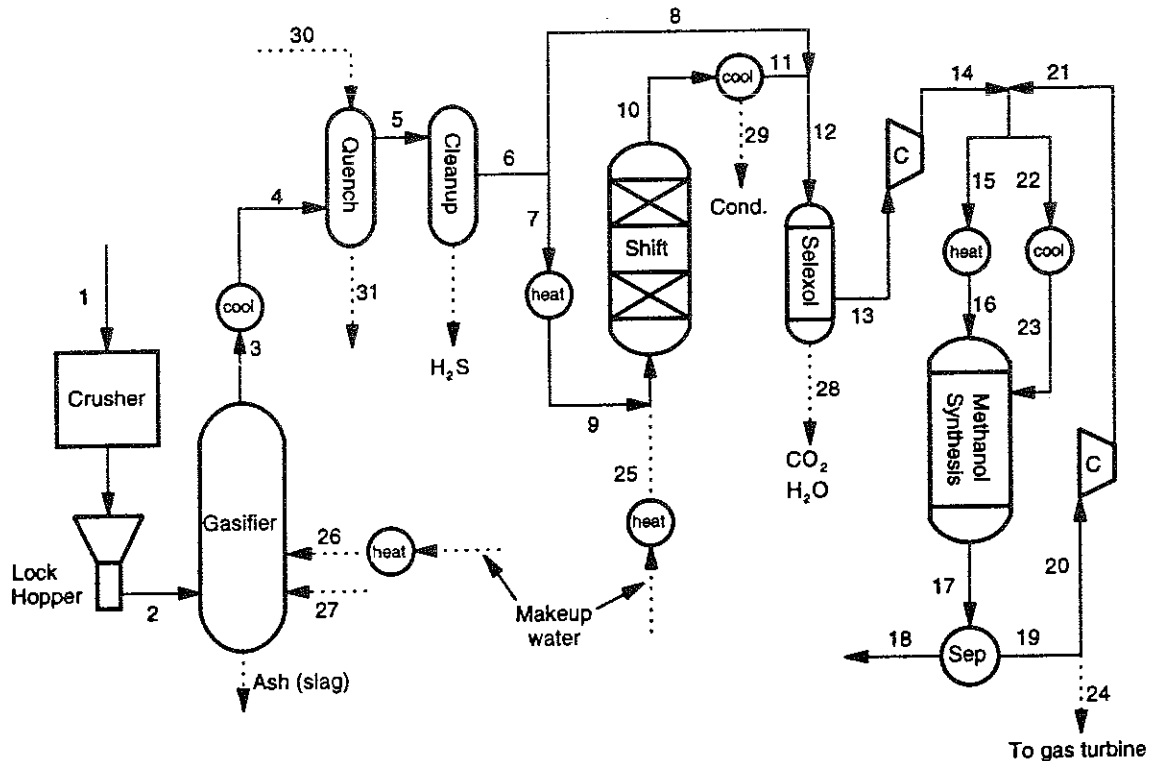


Figure 6A-6: Process configuration for the modeling of methanol production from coal based on the Shell entrained-bed gasifier.

Table 6A-8: Calculated material flows for hydrogen production from coal based on the Shell Gasifier.

Name	Temp [K]	Pres. [bar]	Total Volume Flow [kmol/hr]	Molecular Weight [kg/kmol]	H ₂ O	Component Volume Flow Rates [kmol/hr]												
						H ₂	CO	CO ₂	CH ₄	H ₂ S	Ar	O ₂	N ₂					
1 Dried coal			1737 tonnes per day	1737 tonnes per day	0	5% moisture												
2 Dried, pressurized coal			1737 tonnes per day	1737 tonnes per day	0	5% moisture												
3 Gasifier inlet	1644	24.32	6353	20.49	127	1902	3841	103	5	75	73	0	227					
4 Quench inlet	405	23.82	6353	20.49	127	1902	3841	103	5	75	73	0	227					
5 Quench exit	369	23.32	6462	20.45	236	1902	3841	103	5	75	73	0	227					
6 Gas Cleanup exit	369	23.32	6387	20.29	236	1902	3841	103	5	0	73	0	227					
7 High temperature shift feed	623	22.82	6387	20.29	236	1902	3841	103	5	0	73	0	227					
8 High temperature shift exit	804	22.32	17674	18.84	8271	5154	589	3355	5	0	73	0	227					
9 Low temperature shift feed	500	21.82	17674	18.84	8271	5154	589	3355	5	0	73	0	227					
10 Low temperature shift exit	500	21.32	17674	18.84	7716	5709	34	3910	5	0	73	0	227					
11 PSA makeup feed	313	20.82	9987	19.46	30	5709	34	3908	5	0	73	0	227					
12 PSA-A feed	313	20.80	12064	19.65	30	6429	172	3908	25	0	365	0	1135					
13 PSA-B feed	313	20.45	8125	7.94	0	6429	172	0	25	0	365	0	1135					
14 Hydrogen compressor feed	313	20.10	5529	2.02	0	5529	0	0	0	0	0	0	0					
15 Hydrogen compressor exit	383	75.00	5529	2.02	0	5529	0	0	0	0	0	0	0					
16 Cooled Hydrogen product	313	75.00	5529	2.02	0	5529	0	0	0	0	0	0	0					
17 PSA recycle stream	313	1.30	2597	20.56	0	900	172	0	25	0	365	0	1135					
18 Recycle compressor feed	313	1.30	2077	20.56	0	720	137	0	20	0	292	0	908					
19 Recycle compressor exit	456	21.00	2077	20.56	0	720	137	0	20	0	292	0	908					
20 PSA-A recycle feed	313	20.80	2077	20.56	0	720	137	0	20	0	292	0	908					
21 Purge stream	313	1.30	519	20.56	0	180	34	0	5	0	73	0	227					
22 Gasifier steam	500	24.50	115	18.02	115	0	0	0	0	0	0	0	0					
23 Gasifier oxygen	298	24.50	1804	32.00	0	0	0	0	0	0	73	1719	12					
24 Shift steam	623	22.82	11287	18.02	11287	0	0	0	0	0	0	0	0					
25 Carbon dioxide removed	313	1.30	3939	43.81	30	0	0	3908	0	0	0	0	0					
26 Condensate	313	20.82	7687	18.02	7686	0	0	1	0	0	0	0	0					
27 Quench feed water	294	25.00	316	18.02	316	0	0	0	0	0	0	0	0					
28 Quench condensate	369	23.32	207	18.02	207	0	0	0	0	0	0	0	0					

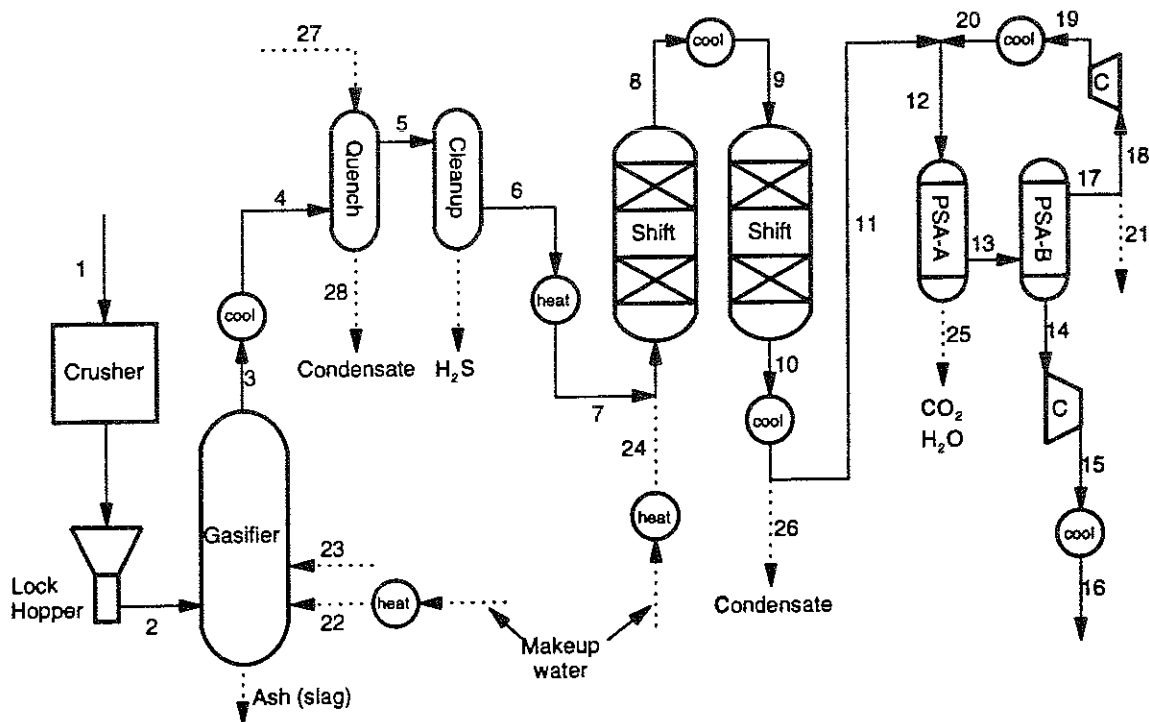


Figure 6A-7: Process configuration for the modeling of hydrogen production from coal based on the Shell entrained-bed gasifier.

Table 6A-9: Pinch analysis for methanol production from coal using the Shell entrained-bed gasifier.

Stream Table

Streams	T source (K)	T target (K)	H in (kW)	H out (kW)	Delta T (K)	Delta H (kW)	CP (kW/K)	T source cor'ctd	T target cor'ctd
GFRPROD (h)	1644.0	405.0	-61733	-132880	-1239.0	-71147	57.42	1639.0	400.0
SHIFT5-a (h)	803.1464	452.8	0	-40678	-350.3	-40678	116.12	798.1	447.8
COLD1 (h)	651.5	543.0	-161070	-162570	-108.5	-1500	13.82	646.5	538.0
SYNPROD (h)	533	300.0	-172930	-249420	-233.0	-76490	328.28	528.0	295.0
SHIFT5-b (h)	452.8	400.0	-40678	-94423	-52.8	-53745	1017.50	447.8	395.0
SHW1-c (c)	492.4	623.0	97437	109387	130.6	11950	91.50	497.4	628.0
SHIFT2 (c)	369.0	623.0	-89914	-81216	254.0	8698	34.25	374.0	628.0
HOTFEED1 (c)	326.0	523.0	-14558	-10367	197.0	4190	21.27	331.0	528.0
GFRW1-c (c)	496.1	500.0	1552	1559	3.9	7	1.86	501.1	505.0
GFRW1-b (c)	496.0	496.1	496	1552	0.1	1056	10583.11	501.0	501.1
GFRW1-a (c)	293.0	496.0	0	496	203.0	496	2.44	298.0	501.0
SHW1-b (c)	492.3	492.4	30645	97437	0.1	66792	667916.39	497.3	497.4
SHW1-a (c)	293.0	492.3	0	30645	199.3	30645	153.76	298.0	497.3
						-119725			

Problem Table

Interval	T(i) (K)	T(i+1) (K)	Ti-T(i+1) (K)	Sum CPhot (kW/K)	Sum CPcold (kW/K)	CPc-CPH (kW/K)	delta H (kW)	Cascade	Corrected Cascade
0		1639.0						0	0
1	1639.0	798.1	840.9	57.42	0	-57.42	-48282	48282	48282
2	798.1	646.5	151.6	173.54	0	-173.54	-26317	74599	74599
3	646.5	628.0	18.5	187.36	0	-187.36	-3466	78065	78065
4	628.0	538.0	90.0	187.36	125.75	-61.61	-5545	83610	83610
5	538.0	528.0	10.0	173.54	125.75	-47.79	-478	84087	84087
6	528.0	505.0	23.0	501.82	147.02	-354.80	-8160	92248	92248
7	505.0	501.1	3.9	501.82	148.88	-352.94	-1363	93610	93610
8	501.1	501.0	0.1	501.82	10730.13	10228.31	1021	92590	92590
9	501.0	497.4	3.6	501.82	149.46	-352.36	-1280	93869	93869
10	497.4	497.3	0.1	501.82	667974.35	667472.53	66747	27122	27122
11	497.3	447.8	49.5	501.82	211.72	-290.10	-14356	41478	41478
12	447.8	400.0	47.8	1403.2	211.72	-1191.48	-56977	98456	98456
13	400.0	395.0	5.0	1345.78	211.72	-1134.06	-5670	104126	104126
14	395.0	374.0	21.0	328.28	211.72	-116.56	-2448	106574	106574
15	374.0	331.0	43.0	328.28	177.47	-150.81	-6485	113058	113058
16	331.0	298.0	33.0	328.28	156.2	-172.08	-5679	118737	118737
17	298.0	295.0	3.0	328.28	0	-328.28	-985	119722	119722

Table 6A-10: Pinch analysis for hydrogen production from coal using the Shell entrained-bed gasifier.

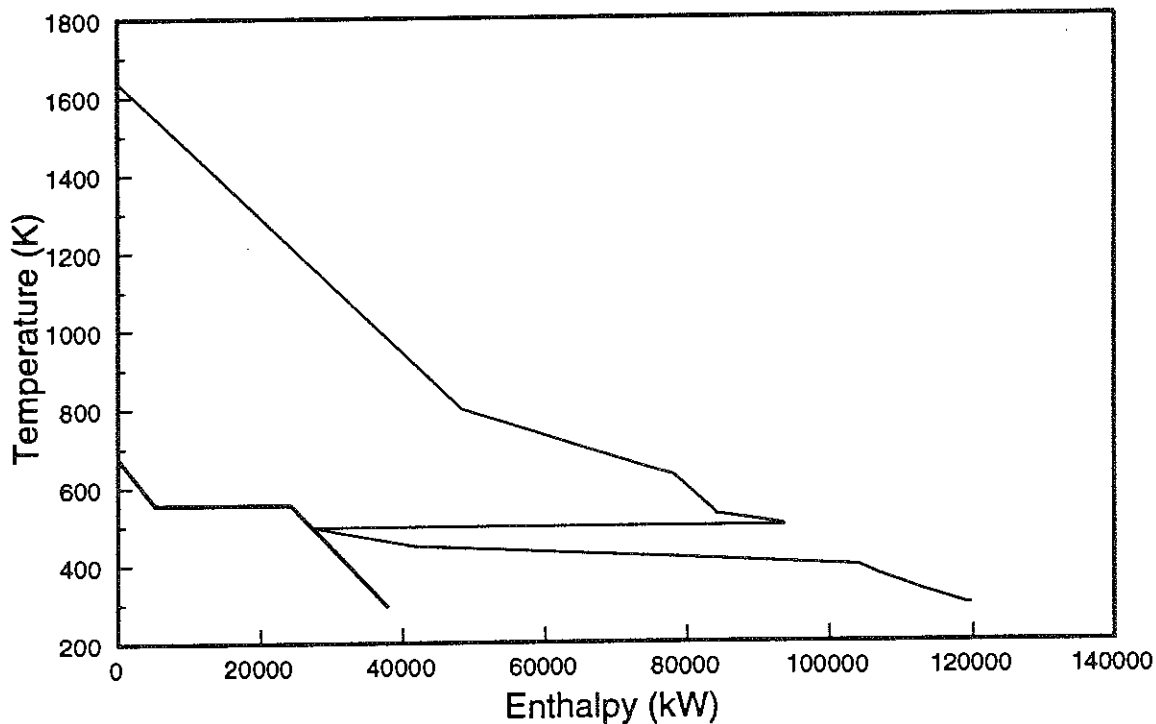
Stream Table

Streams	T source (K)	T target (K)	H in (kW)	H out (kW)	Delta T (K)	Delta H (kW)	CP (kW/K)	T source cor'ctd	T target cor'ctd
GFRPROD (hot)	1644.1	405.0	-61733	-132880	-1239.1	-71147	57.42	1639.1	400.0
SHIFT4 (hot)	804.0	500.0	-853460	-909310	-304.0	-55850	183.72	799.0	495.0
LTS (hot)	500.1	500.0	---	---	-0.1	-5996	59955.56	495.1	495.0
SHIFT6-a (hot)	500.0	447.6	0	-9305	-52.4	-9305	177.57	495.0	442.6
RECYC3 (hot)	456.0	313.0	-2085	-4421	-143.0	-2337	16.34	451.0	308.0
SHIFT6-b (hot)	447.6	410.1	-9305	-80804	-37.5	-71498	1906.74	442.6	405.1
SHIFT6-c (hot)	410.1	313.0	-80804	-129286	-97.1	-48482	499.30	405.1	308.0
H22 (hot)	383.0	313.0	3899	790	-70.0	-3109	44.41	378.0	308.0
SHIFT1 (cold)	369.0	623.0	-141690	-128010	254.0	13680	53.86	374.0	628.0
SHW1-c (c)	491.8	623.0	166535	182588	131.2	16054	122.40	496.8	628.0
GFRH2O1-c (c)	496.1	500.0	1552	1559	3.9	7	1.86	501.1	505.0
GFRH2O1-b (c)	496.0	496.1	496	1552	0.1	1056	10583.11	501.0	501.1
GFRH2O1-a (c)	293.0	496.0	0	496	203.0	496	2.44	298.0	501.0
SHW1-b (c)	491.7	491.8	56270	166535	0.1	110264	1102643.61	496.7	496.8
SHW1-a (c)	293.0	491.7	0	56270	198.7	56270	283.13	298.0	496.7
						-69896			

Problem Table

Interval	T(i) (K)	T(i+1) (K)	Ti-T(i+1) (K)	Sum CPhot (kW/K)	Sum CPcold (kW/K)	CPc-CPh (kW/K)	delta H (kW)	Cascade	Corrected Cascade
0		1639.1						0	13498
1	1639.1	799.0	840.1	57.4	0.0	-57.42	-48239	48239	61737
2	799.0	628.0	171.0	241.1	0.0	-241.14	-41235	89473	102972
3	628.0	505.0	123.0	241.1	176.3	-64.88	-7980	97454	110952
4	505.0	501.1	3.9	241.1	178.1	-63.02	-243	97697	111195
5	501.1	501.0	0.1	241.1	10759.4	10518.23	1050	96647	110145
6	501.0	496.8	4.2	241.1	178.7	-62.44	-262	96909	110407
7	496.8	496.7	0.1	241.1	1102699.9	1102458.77	110246	-13337	161
8	496.7	495.1	1.6	241.1	339.4	98.29	161	-13498	-0
9	495.1	495.0	0.1	60196.7	339.4	-59857.27	-5986	-7512	5986
10	495.0	451.0	44.0	235.0	339.4	104.44	4595	-12108	1390
11	451.0	442.6	8.4	251.3	339.4	88.10	740	-12848	650
12	442.6	405.1	37.5	1980.5	339.4	-1641.07	-61536	48688	62186
13	405.1	400.0	5.1	573.1	339.4	-233.63	-1191	49880	63378
14	400.0	378.0	22.0	515.6	339.4	-176.21	-3877	53756	67254
15	378.0	374.0	4.0	560.1	339.4	-220.62	-882	54639	68137
16	374.0	308.0	66.0	560.1	285.6	-274.48	-18116	72755	86253
17	308.0	298.0	10.0	0.0	285.6	285.57	2856	69899	83397

Methanol Production



Hydrogen production

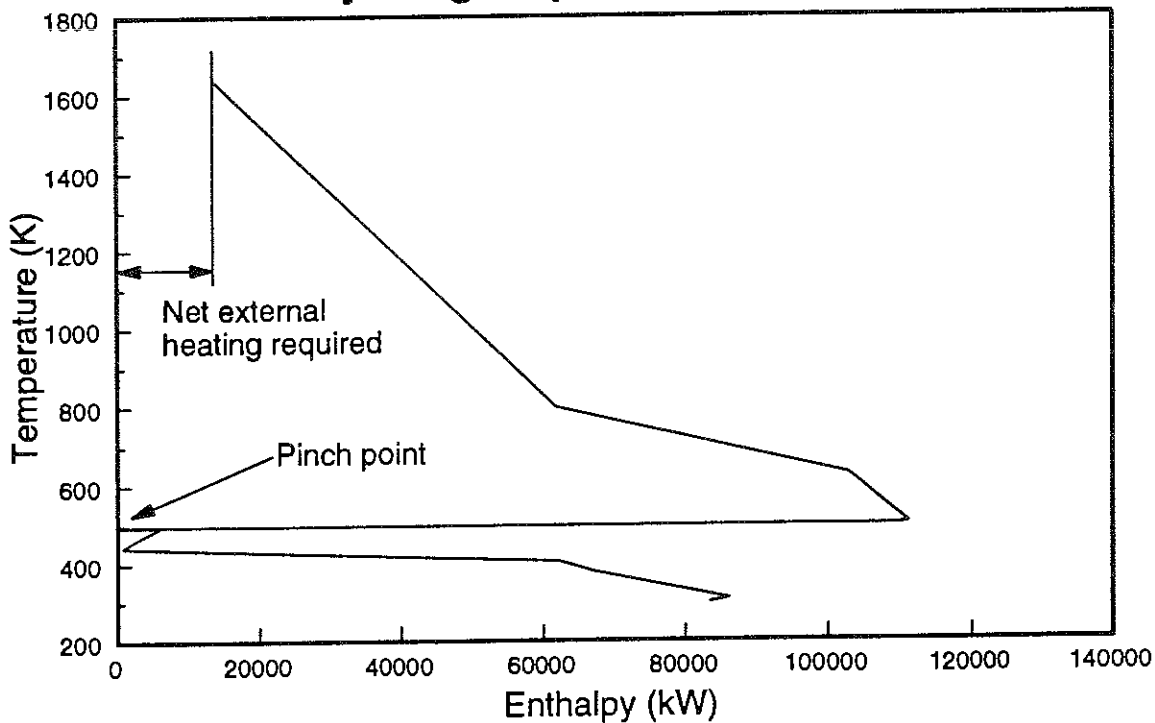


Figure 6A-8: Grand composite curves for methanol and hydrogen production from coal, showing the need for external heating in the hydrogen case.

Table 6A-11: Calculated material flows for methanol production from biomass based on the Shell Gasifier.

Name	Temp [K]	Pres. [bar]	Total Volume Flow [kmol/hr]	Molecular Weight [kg/kmol]	Component Volume Flow Rates [kmol/hr]							
					H ₂ O	H ₂	CO	CO ₂	CH ₄	O ₂	N ₂	CH ₃ OH
1 Raw Biomass			3000	tonnes per day	@ 45% moisture							
2 Dried, pressurized biomass			1854	tonnes per day	@ 10% moisture							
3 Gasifier inlet	1358	24.32	5453	20.07	1001	1672	2129	642	6	0	3	0
4 Quench inlet	465	23.82	5453	20.07	1001	1672	2129	642	6	0	3	0
5 Quench exit	373	23.32	4657	20.36	219	1671	2129	629	6	0	3	0
6 Shift feed	373	23.32	2565	20.36	121	920	1173	347	3	0	2	0
7 Shift bypass	373	23.32	2091	20.36	98	750	956	283	3	0	1	0
8 Heated Shift feed	623	22.82	2565	20.36	121	920	1173	347	3	0	2	0
9 Shift exit	778	22.32	5963	19.02	2566	1873	220	1299	3	0	2	0
10 Cooled shift exit	400	21.82	3843	19.58	446	1873	220	1299	3	0	2	0
11 Selexol feed	391	21.82	5934	19.86	544	2623	1176	1582	6	0	3	0
12 Selexol exit	391	21.82	3886	10.76	0	2623	1176	78	6	0	3	0
13 Makeup compressor exit	394	105.88	3886	10.76	0	2623	1176	78	6	0	3	0
14 Synthesis feed	356	105.88	9114	8.52	1	6897	1450	307	279	0	147	34
15 Preheated synthesis feed	523	105.38	9114	8.53	1	6897	1450	307	279	0	147	34
16 Synthesis product	533	97.28	6643	11.70	65	4361	279	242	279	0	147	1269
17 Crude methanol product	320	96.78	1308	31.42	65	0	0	8	0	0	0	1235
18 Recycle stream	320	96.78	5334	6.86	1	4361	279	234	279	0	147	35
19 Recycle compressor feed	320	96.78	5228	6.86	1	4274	273	229	273	0	144	34
20 Recycle compressor exit	330	105.88	5228	6.86	1	4274	273	229	273	0	144	34
21 Purge stream	320	96.78	107	6.86	0	87	6	5	6	0	3	1
22 Shift steam	623	22.82	3398	18.02	3398	0	0	0	0	0	0	0
23 Gasifier steam	500	24.50	115	18.02	115	0	0	0	0	0	0	0
24 Gasifier oxygen	298	24.50	967	32.00	0	0	0	0	0	967	0	0
25 Carbon dioxide removed	391	21.82	2048	37.11	544	0	0	1504	0	0	0	0
26 Quench feed water	293	25.00	13158	18.02	13158	0	0	0	0	0	0	0
27 Quench Condensate	373	23.32	13955	18.04	13941	2	0	13	0	0	0	0
28 Condensate	400	21.82	2120	18.02	2120	0	0	0	0	0	0	0

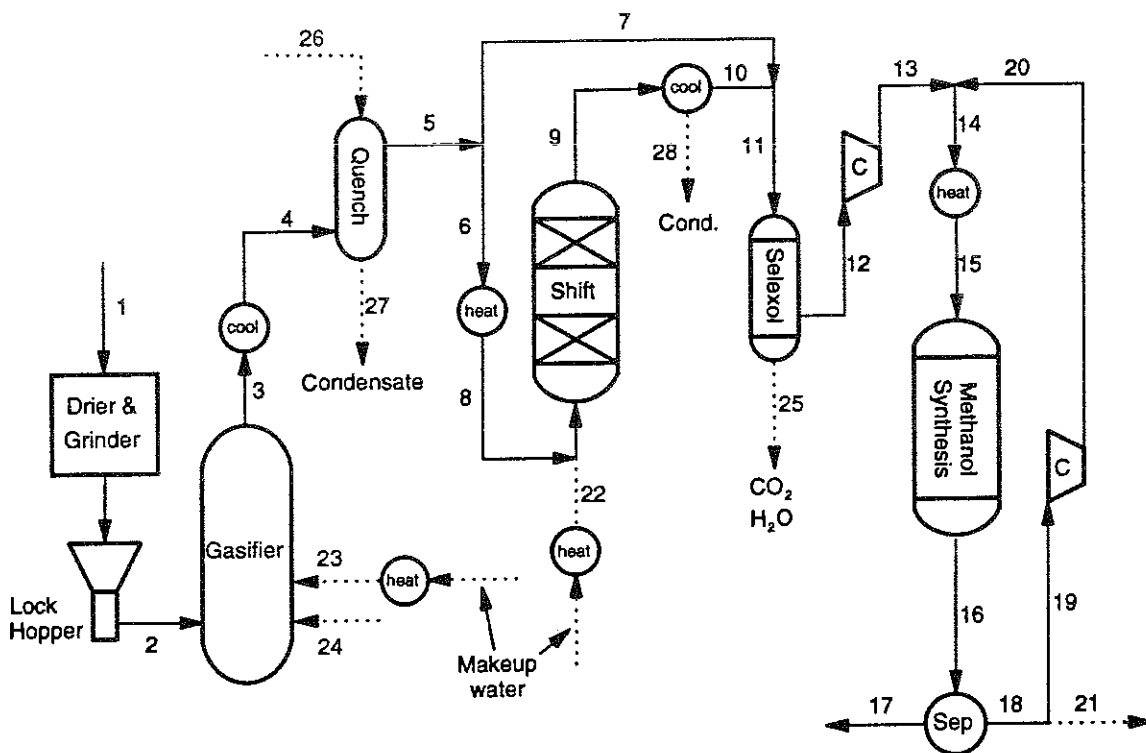


Figure 6A-9: Process configuration for the modeling of methanol production from biomass based on the Shell entrained-bed gasifier.

Table 6A-12: Calculated material flows for hydrogen production from biomass based on the Shell Gasifier.

Name	Temp [K]	Pres. [bar]	Total Volume Flow [kmol/hr]	Molecular Weight [kg/kmol]	Component Flow Rates [kmol/hr]						
					H ₂ O	H ₂	CO	CO ₂	CH ₄	O ₂	N ₂
1 Raw Biomass					3000 tonnes per day @ 45% moisture						
2 Dried, pressurized biomass					1854 tonnes per day @ 10% moisture						
3 Gasifier exit	1358	24.32	5453	20.07	1001	1672	2129	642	6	0	3
4 Quench inlet	465	23.82	5453	20.07	1001	1672	2129	642	6	0	3
5 Quench exit	373	23.32	4657	20.36	219	1671	2129	629	6	0	3
6 High temperature shift feed	623	22.82	4657	20.36	219	1671	2129	629	6	0	3
7 High temperature shift exit	778	22.32	10825	19.02	4658	3400	400	2359	6	0	3
8 Low temperature shift feed	500	21.82	10825	19.02	4658	3400	400	2359	6	0	3
9 Low temperature shift exit	500	21.32	10825	19.02	4285	3772	27	2731	6	0	3
10 PSA makeup feed	313	20.82	6551	19.64	22	3772	27	2721	6	0	3
11 PSA-A feed	313	20.80	7170	18.60	22	4248	136	2721	28	0	15
12 PSA-B feed	313	20.45	4427	2.99	0	4248	136	0	28	0	15
13 Hydrogen compressor feed	313	20.10	3653	2.02	0	3653	0	0	0	0	0
14 Hydrogen compressor exit	383	75.00	3653	2.02	0	3653	0	0	0	0	0
15 Cooled Hydrogen product	313	75.00	3653	2.02	0	3653	0	0	0	0	0
16 PSA recycle stream	313	1.30	774	7.60	0	595	136	0	28	0	15
17 Recycle compressor feed	313	1.30	619	7.60	0	476	109	0	23	0	12
18 Recycle compressor exit	450	21.00	619	7.60	0	476	109	0	23	0	12
19 PSA-A recycle feed	313	20.80	619	7.60	0	476	109	0	23	0	12
20 Purge stream	313	1.30	155	7.60	0	119	27	0	6	0	3
21 Gasifier steam	500	24.50	115	18.02	115	0	0	0	0	0	0
22 Gasifier oxygen	298	24.50	967	32.00	0	0	0	0	0	967	0
23 Shift steam	623	22.82	6168	18.02	6168	0	0	0	0	0	0
24 Carbon dioxide removed	313	1.30	2743	43.80	22	0	0	2721	0	0	0
25 Quench feed water	293	25.00	13158	18.02	13158	0	0	0	0	0	0
26 Quench Condensate	373	23.32	13955	18.04	13941	2	0	13	0	0	0
27 Condensate	313	20.82	4274	18.08	4263	0	0	10	0	0	0

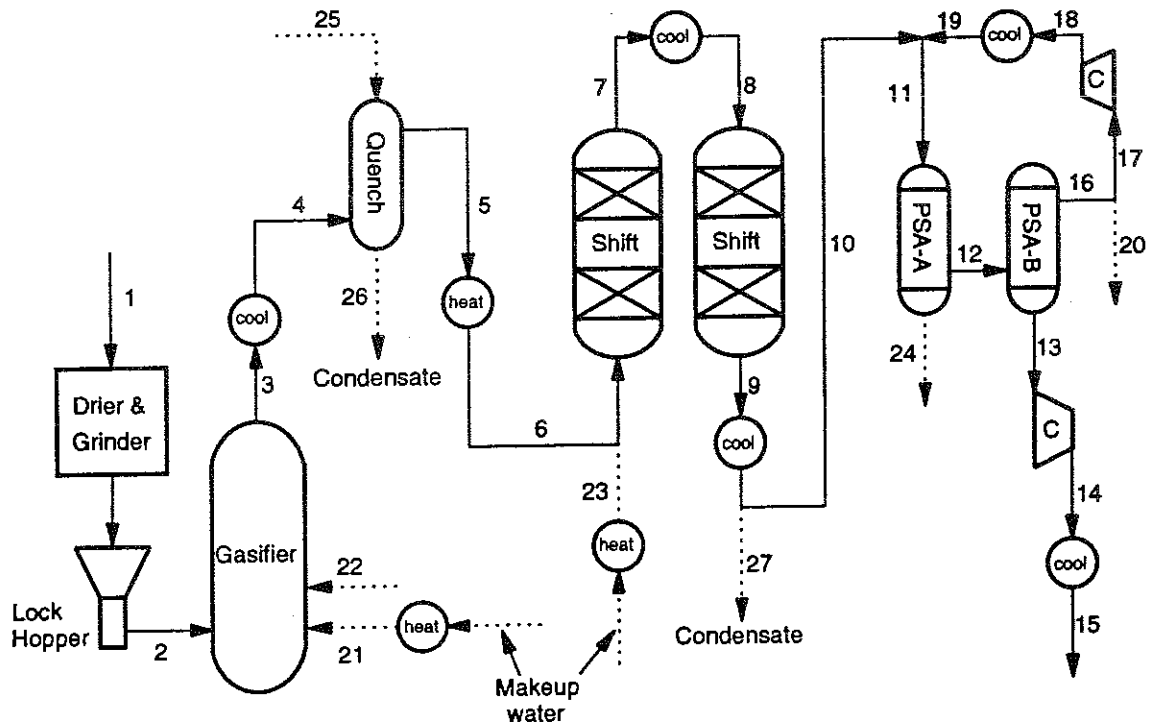


Figure 6A-10: Process configuration for the modeling of hydrogen production from biomass based on the Shell entrained-bed gasifier.

Table 6A-13: Pinch analysis for methanol production from biomass using the Shell entrained-bed gasifier.

Stream Table

Streams	T source (K)	T target (K)	H in (GJ/hr)	H out (GJ/hr)	Delta T (K)	Delta H (kW)	CP (kW/K)	T source cor'ctd	T target cor'ctd
GFRPROD (h)	1357.8	465.4	-529.42	-702.79	-892.5	-48158	53.96	1352.8	460.4
SHIFT4-a (h)	777.8	450.1	0.00	-72.26	-327.7	-20072	61.26	772.8	445.1
Synth (hot)	533.1	533.0	-245.84	-364.81	-0.1	-21856	218555.56	528.1	528.0
SYNPROD (h)	533.0	320.0	-364.81	-465.54	-213.0	-27980	131.36	528.0	315.0
SHIFT4-b (h)	450.1	433.5	-72.26	-120.55	-16.7	-13414	804.37	445.1	428.5
SHIFT4-c (h)	433.5	400.0	-120.55	-165.8	-33.5	-12557	375.34	428.5	395.0
SHIFT1 (c)	372.7	623.0	-289.97	-269.35	250.3	5727	22.88	377.7	628.0
SHW2-c (c)	492.4	623.0	166.05	186.41	130.6	5657	43.32	497.4	628.0
SYNFEED1 (c)	356.2	523.0	-292.36	-245.84	166.8	12923	77.49	361.2	528.0
GFRW2-c (c)	496.1	500.0	5.59	5.61	3.9	7	1.86	501.1	505.0
GFRW2-b (c)	496.0	496.1	1.79	5.59	0.1	1056	10561.94	501.0	501.1
GFRW2-a (c)	293.0	496.0	0.00	1.79	203.0	496	2.44	298.0	501.0
SHW2-b (c)	492.3	492.4	52.21	166.05	0.1	31621	316212.78	497.3	497.4
SHW2-a (c)	293.0	492.3	0.00	52.21	199.3	14503	72.76	298.0	497.3
Drier (cold)	293.0	393.0	---	---	100.0	46380	463.80	298.0	398.0
						-25666			

Problem Table

Interval	T(i) (K)	T(i+1) (K)	Ti-T(i+1) (K)	Sum CPhot (kW/K)	Sum CPCold (kW/K)	CPC-CPh (kW/K)	delta H (kW)	Cascade	Corrected Cascade
0		1352.8						0	0
1	1352.8	772.8	580.0	53.96	0.00	-53.96	-31298	31298	31298
2	772.8	628.0	144.8	115.22	0.00	-115.22	-16684	47982	47982
3	628.0	528.1	99.9	115.22	66.20	-49.02	-4897	52879	52879
4	528.1	528.0	0.1	218670.78	66.20	-218604.58	-21860	74740	74740
5	528.0	505.0	23.0	246.58	143.69	-102.89	-2366	77106	77106
6	505.0	501.1	3.9	246.58	145.55	-101.03	-390	77496	77496
7	501.1	501.0	0.1	246.58	10705.63	10459.05	1046	76450	76450
8	501.0	497.4	3.6	246.58	146.13	-100.45	-365	76815	76815
9	497.4	497.3	0.1	246.58	316315.59	316069.01	31607	45208	45208
10	497.3	460.4	36.9	246.58	175.57	-71.01	-2623	47831	47831
11	460.4	445.1	15.2	192.62	175.57	-17.05	-260	48091	48091
12	445.1	428.5	16.7	935.73	175.57	-760.16	-12677	60768	60768
13	428.5	398.0	30.5	506.70	175.57	-331.13	-10085	70853	70853
14	398.0	395.0	3.0	506.70	639.37	132.67	398	70455	70455
15	395.0	377.7	17.3	131.36	639.37	508.01	8804	61651	61651
16	377.7	361.2	16.4	131.36	616.49	485.13	7977	53673	53673
17	361.2	315.0	46.2	131.36	539.00	407.64	18843	34830	34830
18	315.0	298.0	17.0	0.00	539.00	539.00	9163	25667	25667

Table 6A-14: Pinch analysis for hydrogen production from biomass using the Shell entrained-bed gasifier.

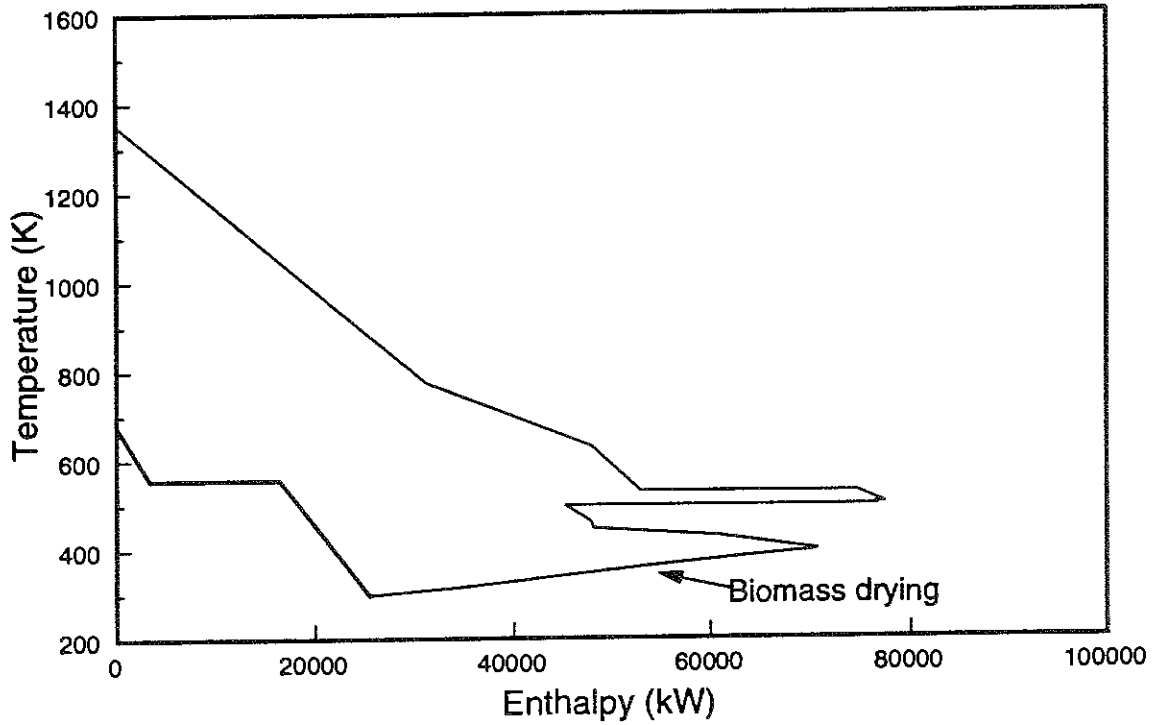
Stream Table

Stream	T source (K)	T target (K)	H in (GJ/hr)	H out (GJ/hr)	Delta T (K)	Delta H (kW)	CP (kW/K)	T source cor'ctd	T target cor'ctd
GFRPROD (h)	1357.8	465.4	-529.42	-702.79	-892.5	-48158	53.96	1352.8	460.4
SHIPT3 (h)	777.8	500.0	-1916.63	-2028.44	-277.8	-31059	111.79	772.8	495.0
LTS (hot)	500.1	500.0	-2028.44	-2043.15	-0.1	-4086	40859.44	495.1	495.0
SHIPT5-a (h)	500.0	439.2	0.00	-23.66	-60.8	-6573	108.03	495.0	434.2
RECYC3 (h)	449.5	313.0	-10.98	-13.47	-136.5	-692	5.07	444.5	308.0
SHIPT5-b (h)	439.2	402.5	-23.66	-167.07	-36.6	-39835	1088.14	434.2	397.5
SHIPT5-c (h)	402.5	313.0	-167.07	-267.31	-89.5	-27845	310.95	397.5	308.0
H22 (hot)	383.3	313.0	9.41	1.98	-70.3	-2063	29.34	378.3	308.0
QCHOUT (c)	372.7	623.0	-526.35	-488.93	250.3	10396	41.53	377.7	628.0
SHW2-c (c)	492.4	623.0	301.44	338.41	130.6	10269	78.64	497.4	628.0
GFRW2-c (c)	496.1	500.0	5.59	5.61	3.9	7	1.86	501.1	505.0
GFRW2-b (c)	496.0	496.1	1.79	5.59	0.1	1056	10561.94	501.0	501.1
GFRW2-a (c)	293.0	496.0	0.00	1.79	203.0	496	2.44	298.0	501.0
SHW2-b (c)	492.3	492.4	94.80	301.44	0.1	57398	573984.44	497.3	497.4
SHW2-a (c)	293.0	492.3	0.00	94.80	199.3	26334	132.13	298.0	497.3
Drier (cold)	293.0	393.0	---	---	100.0	46380	463.80	298.0	398.0
						-7973			

Problem Table

Interval	T(i) (K)	T(i+1) (K)	Ti-T(i+1) (K)	Sum CPhot (kW/K)	Sum CPcold (kW/K)	CPC-CPH (kW/K)	delta H (kW)	Cascade	Corrected Cascade
0		1352.8						0	0
1	1352.8	772.8	580.0	53.96	0.00	-53.96	-31296	31296	31296
2	772.8	628.0	144.8	165.75	0.00	-165.75	-24007	55303	55303
3	628.0	505.0	123.0	165.75	120.17	-45.58	-5606	60910	60910
4	505.0	501.1	3.9	165.75	122.03	-43.72	-169	61079	61079
5	501.1	501.0	0.1	165.75	10682.11	10516.36	1052	60027	60027
6	501.0	497.4	3.6	165.75	122.61	-43.14	-157	60184	60184
7	497.4	497.3	0.1	165.75	574028.41	573862.66	57386	2797	2797
8	497.3	495.1	2.2	165.75	176.09	10.34	23	2775	2775
9	495.1	495.0	0.1	41025.19	176.09	-40849.10	-4085	6859	6859
10	495.0	460.4	34.6	161.99	176.09	14.10	488	6371	6371
11	460.4	444.5	15.8	108.03	176.09	68.06	1077	5294	5294
12	444.5	434.2	10.4	113.10	176.09	62.99	654	4640	4640
13	434.2	398.0	36.2	1093.21	176.09	-917.12	-33158	37797	37797
14	398.0	397.5	0.5	1093.21	639.89	-453.32	-206	38003	38003
15	397.5	378.3	19.2	316.02	639.89	323.87	6233	31770	31770
16	378.3	377.7	0.6	345.36	639.89	294.53	186	31584	31584
17	377.7	308.0	69.7	345.36	598.36	253.00	17626	13958	13958
18	308.0	298.0	10.0	0.00	598.36	598.36	5984	7974	7974

Methanol production



Hydrogen production

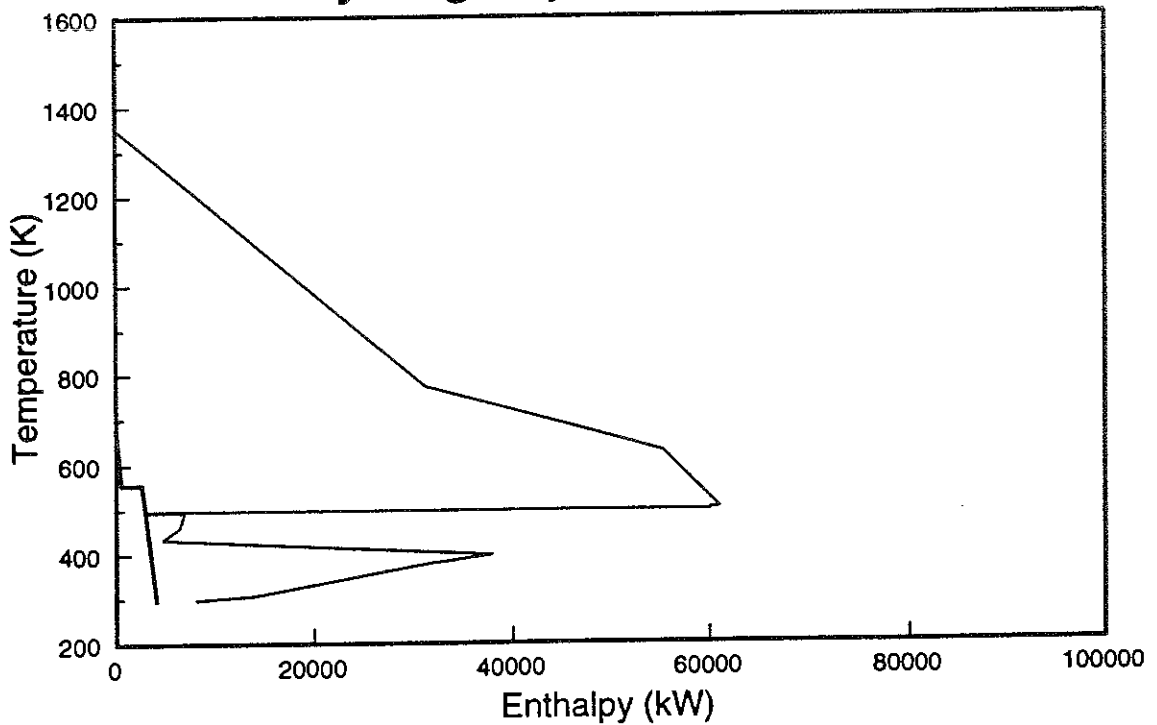


Figure 6A-11: Grand composite curves for methanol and hydrogen production from biomass using the Shell entrained-bed gasifier.

Table 6A-15: Calculated material flows for methanol production from biomass based on the IGT Gasifier.

Name	Temp [K]	Pres. [bar]	Total Volume Flow [kmol/hr]	Molecular Weight [kg/kmol]	Component Volume Flow Rates [kmol/hr]																
					H ₂ O	H ₂	CO	CO ₂	CH ₄	C ₂ H ₄	O ₂	N ₂	CH ₃ OH								
1 Raw Biomass	298	1.00	3000 tonnes per day @ 45% moisture																		
2 Dried, pressurized biomass	398	34.50	1941 tonnes per day @ 15% moisture																		
3 Gasifier inlet	1255	34.50	5635	22.27	1792	1172	845	1347	462	17	0	0	0								
4 Quench inlet	673	34.00	5635	22.27	1792	1172	845	1347	462	17	0	0	0								
5 Quench exit	372	33.50	3851	23.51	127	1167	845	1235	459	17	0	0	0								
6 Reformer feed	459	33.50	6196	21.43	2472	1167	845	1235	459	17	0	0	0								
7 Preheated reformer feed	850	33.00	6196	21.43	2472	1167	845	1235	459	17	0	0	0								
8 Reformer exit	1140	32.50	6808	19.50	2233	2000	1236	1159	180	0	0	0	0								
9 Cooled reformer exit	623	16.00	6808	19.50	2233	2000	1236	1159	180	0	0	0	0								
10 Shift feed	623	16.00	1804	19.50	592	530	328	307	48	0	0	0	0								
11 Shift bypass	623	16.00	5004	19.50	1641	1470	908	852	132	0	0	0	0								
12 Shift exit	729	31.50	2195	19.24	745	768	90	545	48	0	0	0	0								
13 Mixer exit	656	31.50	7199	19.42	2386	2238	998	1397	180	0	0	0	0								
14 Seloxel feed	400	31.00	5248	19.95	435	2238	998	1397	180	0	0	0	0								
15 Seloxel exit	400	31.00	3485	11.02	0	2238	998	70	180	0	0	0	0								
16 Makeup compressor exit	457	105.88	3485	11.02	0	2238	998	70	180	0	0	0	0								
17 Hot synthesis feed 1	331	105.88	6880	12.41	0	2798	684	207	3173	0	0	0	0								18
18 Hot synthesis feed 2	523	105.38	6880	12.41	0	2798	684	207	3173	0	0	0	0								18
19 Synthesis product	533	97.28	17102	13.91	55	5675	927	521	8840	0	0	0	0								1084
20 Crude methanol product	300	96.78	1092	31.39	54	0	0	5	0	0	0	0	0								1033
21 Recycle stream	300	96.78	16010	12.72	1	5675	927	517	8840	0	0	0	0								51
22 Recycle compressor feed	300	96.78	15684	12.72	1	5559	908	506	8660	0	0	0	0								50
23 Recycle compressor exit	308	105.88	15684	12.72	1	5559	908	506	8660	0	0	0	0								50
24 Cold synthesis feed 1	331	105.88	12290	12.41	0	4999	1222	369	5667	0	0	0	0								32
25 Cold synthesis feed 2	320	105.38	12290	12.41	0	4999	1222	369	5667	0	0	0	0								32
26 Purge stream	300	96.78	325	12.72	0	115	19	10	180	0	0	0	0								1
27 Heated purge stream	700	96.78	325	12.72	0	115	19	10	180	0	0	0	0								1
28 Reformer furnace products	1160	1.00	2592	27.57	475	0	0	209	0	0	64	1844	1								
29 Stack gases	393	1.00	2592	27.57	475	0	0	209	0	0	64	1844	1								
30 Reformer furnace air	298	1.00	2334	28.85	0	0	0	0	0	0	490	1844	0								
31 Heated reformer furnace air	910	1.00	2334	28.85	0	0	0	0	0	0	490	1844	0								
32 Reformer steam	613	33.50	2345	18.02	2345	0	0	0	0	0	0	0	0								
33 Shift steam	623	16.00	391	18.02	391	0	0	0	0	0	0	0	0								
34 Gasifier steam	535	34.50	1145	18.02	1145	0	0	0	0	0	0	0	0								
35 Gasifier oxygen	293	34.50	645	32.00	0	0	0	0	0	0	645	0	0								
36 Carbon dioxide removed	400	31.00	1763	37.59	435	0	0	1327	0	0	0	0	0								
37 Quench water inlet	293	34.50	35985	18.02	35985	0	0	0	0	0	0	0	0								
38 Quench water outlet	372	33.50	37770	18.09	37650	5	0	112	2	0	0	0	0								
39 Condensate	400	31.00	1951	18.02	1951	0	0	0	0	0	0	0	0								

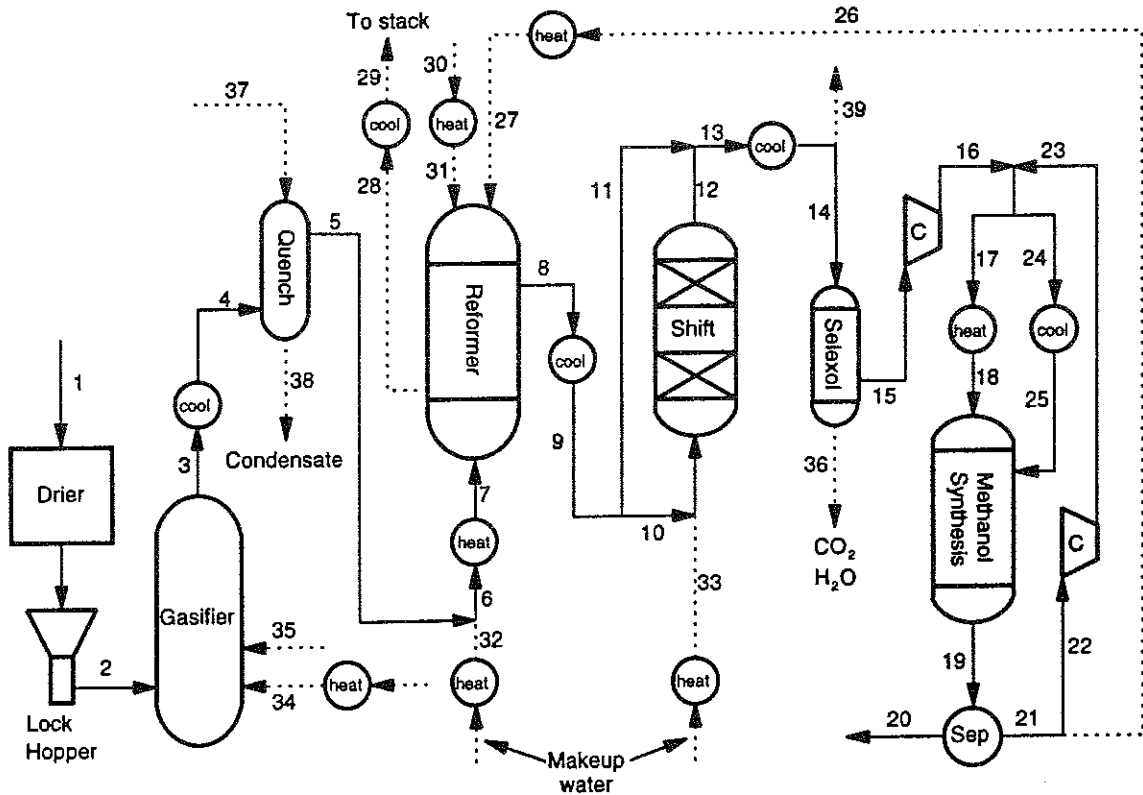


Figure 6A-12: Process configuration for the modeling of methanol production from biomass based on the IGT fluidized-bed gasifier.

Table 6A-16: Calculated material flows for hydrogen production from biomass based on the IGT Gasifier.

Name	Temp [K]	Pres. [bar]	Total Volume Flow [kmol/hr]	Molecular Weight [kg/kmol]	Component Volume Flow Rates [kmol/hr]								
					H ₂ O	H ₂	CO	CO ₂	CH ₄	C ₂ H ₄	O ₂	N ₂	
1 Raw Biomass	298	1.00	3000	tonnes per day @ 45% moisture									
2 Dried, pressurized biomass	398	34.50	1941	tonnes per day @ 15% moisture									
3 Gasifier exit	1255	34.50	5635	22.27	1792	1172	845	1347	462	17	0	0	
4 Quench inlet	673	34.00	5635	22.27	1792	1172	845	1347	462	17	0	0	
5 Quench exit	372	33.50	3851	23.51	127	1167	845	1235	459	17	0	0	
6 Reformer feed	459	33.50	6196	21.43	2472	1167	845	1235	459	17	0	0	
7 Preheated reformer feed	850	33.00	6196	21.43	2472	1167	845	1235	459	17	0	0	
8 Reformer exit	1140	32.50	6808	19.50	2233	2000	1236	1159	180	0	0	0	
9 High temperature shift feed	623	32.00	6808	19.50	2233	2000	1236	1159	180	0	0	0	
10 High temperature shift exit	729	31.50	8283	19.24	2811	2897	339	2056	180	0	0	0	
11 Low temperature shift feed	500	31.00	8283	19.24	2811	2897	339	2056	180	0	0	0	
12 Low temperature shift exit	500	30.50	8283	19.24	2506	3202	34	2361	180	0	0	0	
13 PSA make-up feed	313	30.00	5792	19.76	16	3202	34	2361	180	0	0	0	
14 PSA-A feed	313	29.65	7052	18.53	16	3606	171	2361	899	0	0	0	
15 PSA-B feed	313	29.65	4675	5.66	0	3606	171	0	899	0	0	0	
16 Hydrogen compressor feed	313	29.30	3101	2.02	0	3101	0	0	0	0	0	0	
17 Hydrogen compressor exit	367	75.00	3101	2.02	0	3101	0	0	0	0	0	0	
18 Cooled Hydrogen product	313	75.00	3101	2.02	0	3101	0	0	0	0	0	0	
19 PSA recycle stream	313	1.30	1574	12.85	0	505	171	0	899	0	0	0	
20 Recycle compressor feed	313	1.30	1260	12.85	0	404	137	0	719	0	0	0	
21 Recycle compressor exit	442	30.20	1260	12.85	0	404	137	0	719	0	0	0	
22 PSA-A recycle feed	313	30.00	1260	12.85	0	404	137	0	719	0	0	0	
23 Purge stream	313	1.30	315	12.85	0	101	34	0	180	0	0	0	
24 Heated purge stream	700	1.30	315	12.85	0	101	34	0	180	0	0	0	
25 Reformer furnace products	1160	1.00	2585	27.65	460	0	0	214	0	0	64	1847	
26 Stack gases	393	1.00	2585	27.65	460	0	0	214	0	0	64	1847	
27 Reformer furnace air	298	1.00	2338	28.85	0	0	0	0	0	0	491	1847	
28 Heated reformer furnace air	897	1.00	2338	28.85	0	0	0	0	0	0	491	1847	
29 Gasifier steam	535	34.50	1145	18.02	1145	0	0	0	0	0	0	0	
30 Gasifier oxygen	293	34.50	645	32.00	0	0	0	0	645	0	0	0	
31 Reformer steam	613	33.50	2345	18.02	2345	0	0	0	0	0	0	0	
32 Shift steam	623	16.00	1474	18.02	1474	0	0	0	0	0	0	0	
33 Carbon dioxide removed	313	1.30	2377	43.84	16	0	0	2361	0	0	0	0	
34 Condensate	313	30.00	2490	18.02	2490	0	0	0	0	0	0	0	
35 Quench feed water	293	35.00	35998	18.02	35998	0	0	0	0	0	0	0	
36 Quench condensate	372	33.50	37783	18.09	37663	5	0	112	2	0	0	0	

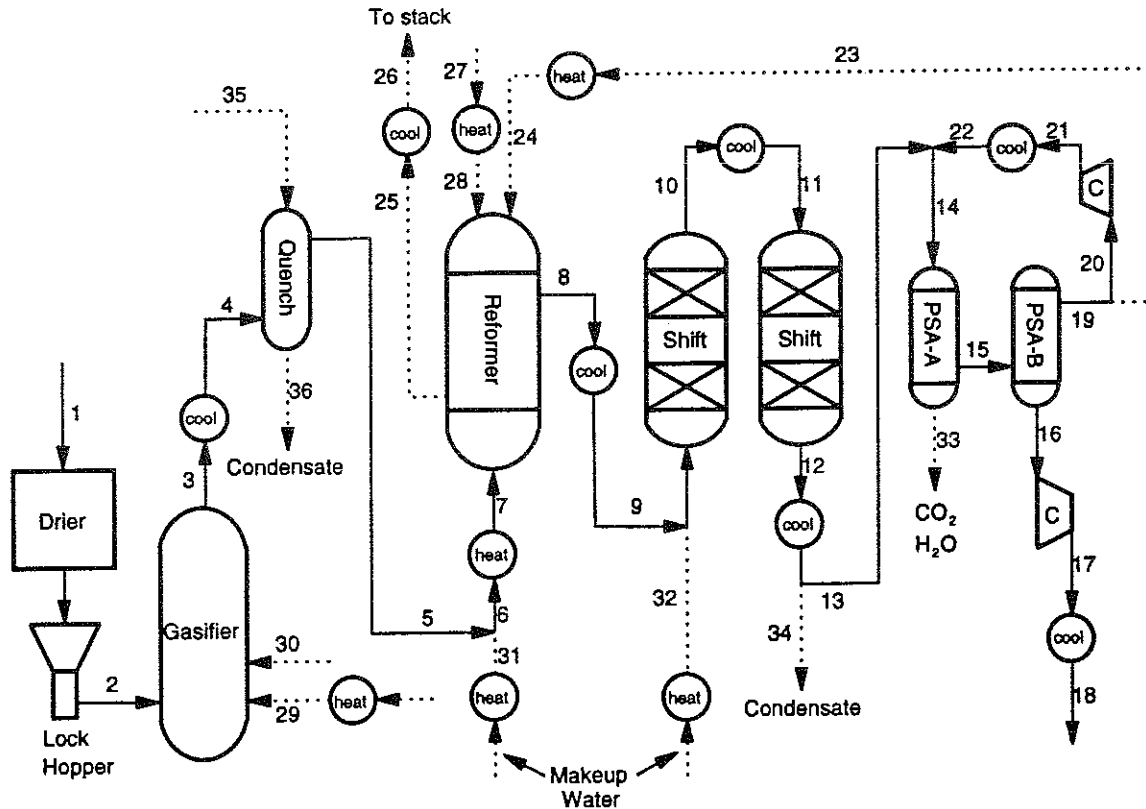


Figure 6A-13: Process configuration for the modeling of hydrogen production from biomass based on the IGT fluidized-bed gasifier.

Table 6A-17: Pinch analysis for methanol production from biomass using the IGT fluidized-bed gasifier.

Stream Table

Streams	T source (K)	T target (K)	H in (GJ/hr)	H out (GJ/hr)	Delta T (K)	Delta H (kW)	CP (kW/K)	T source cor'ctd	T target cor'ctd
GFRPROD (h)	1255.2	673.0	-873.59	-1015.41	-582.2	-39395	67.67	1250.2	668.0
COMB1 (h)	1160.0	393.0	-121.75	-189.78	-767.0	-18897	24.64	1155.0	388.0
REFPROD (h)	1140.0	623.0	-936.78	-1072.75	-517.0	-37771	73.06	1135.0	618.0
SHIF5-a (h)	656.3	453.9	0.00	-52.39	-202.4	-14553	71.89	651.3	448.9
SYNPROD-a (h)	533.0	381.0	0.00	-107.56	-152.0	-29877	196.57	528.0	376.0
SHIF5-b (h)	453.9	431.8	-52.39	-103.37	-22.1	-14161	641.96	448.9	426.8
SHIF5-c (h)	431.8	400.0	-103.37	-142.14	-31.8	-10768	338.23	426.8	395.0
SYNPROD-b (h)	381.0	300.0	-107.56	-203.75	-81.0	-26721	329.84	376.0	295.0
COLD1 (h)	330.6	320.0	-704.44	-709.22	-10.6	-1327	124.59	325.6	315.0
AIR1 (cold)	298.0	910.5	-0.00	43.87	612.5	12188	19.90	303.0	915.5
REFFEED1 (c)	459.1	850.0	-1180.17	-1084.73	390.9	26510	67.82	464.1	855.0
PURGE1 (c)	300.0	700.0	-20.09	-14.71	400.0	1495	3.74	305.0	705.0
SHW1-c (c)	510.7	623.0	19.08	21.26	112.3	607	5.40	515.7	628.0
REFW2-c (c)	513.3	613.2	114.63	126.60	99.9	3327	33.30	518.3	618.2
GFRW2-c (c)	515.0	534.9	53.62	54.94	19.9	369	18.53	520.0	539.9
HOTFEED1 (c)	330.6	523.0	-394.35	-344.19	192.4	13931	72.43	335.6	528.0
GFRW2-b (c)	514.9	515.0	18.90	53.62	0.1	9644	96435.83	519.9	520.0
GFRW2-a (c)	294.0	514.9	0.00	18.90	220.9	5250	23.77	299.0	519.9
REFW2-b (c)	513.2	513.3	40.10	114.63	0.1	20704	207035.56	518.2	518.3
REFW2-a (c)	294.0	513.2	0.00	40.10	219.2	11138	50.81	299.0	518.2
SHW1-b (c)	510.6	510.7	6.57	19.08	0.1	3474	34740.56	515.6	515.7
SHW1-a (c)	294.0	510.6	0.00	6.57	216.6	1825	8.43	299.0	515.6
Drier (cold)	293.0	393.0	---	---	100.0	42757	427.57	298.0	398.0
						-40253			

Problem Table

Interval	T(i) (K)	T(i+1) (K)	Ti-T(i+1) (K)	Sum CPhot (kW/K)	Sum CPcold (kW/K)	CPC-CPH (kW/K)	delta H (kW)	Cascade	Corrected Cascade
0		1250.2						0	0
1	1250.2	1155.0	95.2	67.67	0.00	-67.67	-6440	6440	6440
2	1155.0	1135.0	20.0	92.31	0.00	-92.31	-1849	8289	8289
3	1135.0	915.5	219.5	165.37	0.00	-165.37	-36303	44592	44592
4	915.5	855.0	60.5	165.37	19.90	-145.47	-8797	53389	53389
5	855.0	705.0	150.0	165.37	87.72	-77.65	-11648	65037	65037
6	705.0	668.0	37.0	165.37	91.46	-73.91	-2735	67771	67771
7	668.0	651.3	16.7	97.70	91.46	-6.24	-104	67875	67875
8	651.3	628.0	23.3	169.59	91.46	-78.13	-1823	69698	69698
9	628.0	618.2	9.8	169.59	96.86	-72.73	-712	70410	70410
10	618.2	618.0	0.2	169.59	130.16	-39.43	-9	70418	70418
11	618.0	539.9	78.1	96.53	130.16	33.63	2627	67791	67791
12	539.9	528.0	11.9	96.53	148.69	52.16	621	67171	67171
13	528.0	520.0	8.0	293.10	221.12	-71.98	-576	67747	67747
14	520.0	519.9	0.1	293.10	96638.42	96345.32	9635	58113	58113
15	519.9	518.3	1.6	293.10	226.36	-66.74	-105	58218	58218
16	518.3	518.2	0.1	293.10	207228.62	206935.52	20694	37524	37524
17	518.2	515.7	2.5	293.10	243.87	-49.23	-123	37647	37647
18	515.7	515.6	0.1	293.10	34979.03	34685.93	3469	34179	34179
19	515.6	464.1	51.5	293.10	246.90	-46.20	-2378	36557	36557
20	464.1	448.9	15.2	293.10	179.08	-114.02	-1738	38295	38295
21	448.9	426.8	22.1	863.17	179.08	-684.09	-15090	53385	53385
22	426.8	398.0	28.8	559.44	179.08	-380.36	-10968	64353	64353
23	398.0	395.0	3.0	559.44	606.65	47.21	142	64212	64212
24	395.0	388.0	7.0	221.21	606.65	385.44	2698	61514	61514
25	388.0	376.0	12.0	196.37	606.65	410.28	4918	56595	56595
26	376.0	335.6	40.4	329.84	606.65	276.81	11173	45422	45422
27	335.6	325.6	10.0	329.84	534.22	204.38	2044	43379	43379
28	325.6	315.0	10.6	454.43	534.22	79.79	850	42529	42529
29	315.0	305.0	10.0	329.84	534.22	204.38	2044	40485	40485
30	305.0	303.0	2.0	329.84	530.48	200.64	401	40084	40084
31	303.0	299.0	4.0	329.84	510.58	180.74	723	39361	39361
32	299.0	298.0	1.0	329.84	427.57	97.73	98	39263	39263
33	298.0	295.0	3.0	329.84	0.00	-329.84	-990	40253	40253

Table 6A-18: Pinch analysis for hydrogen production from biomass using the IGT fluidized-bed gasifier.

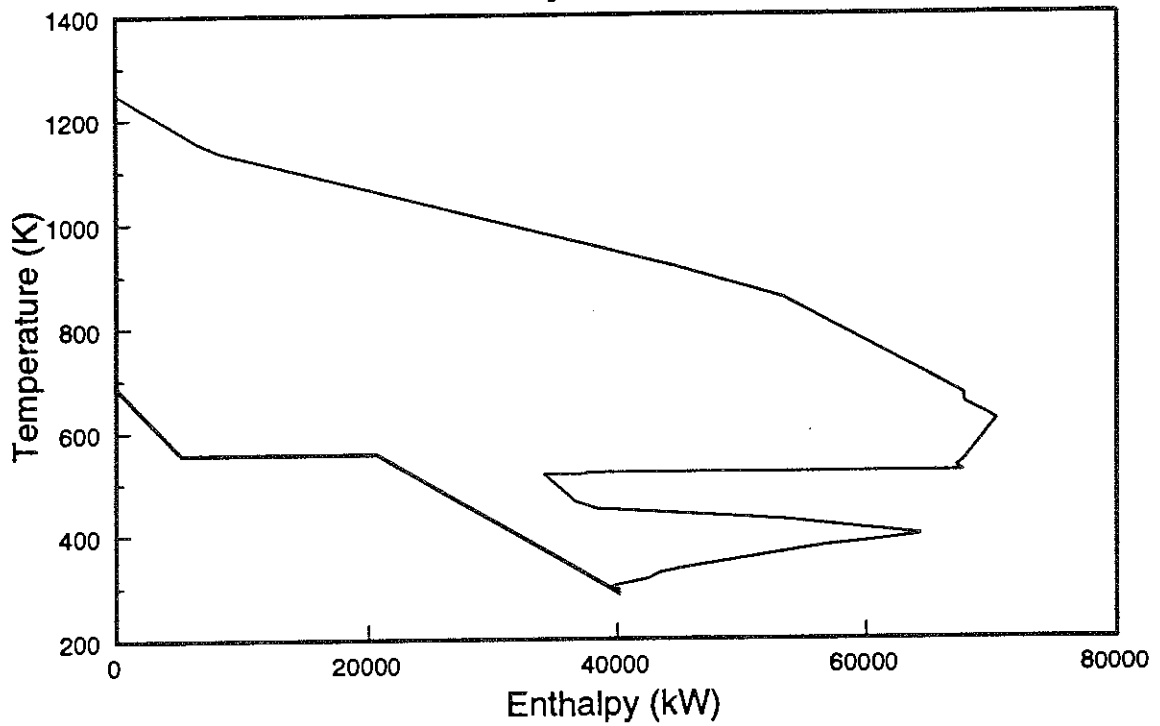
Stream Table

Streams	T source (K)	T target (K)	H in (GJ/hr)	H out (GJ/hr)	Delta T (K)	Delta H (kW)	CP (kW/K)	T source cor'ctd	T target cor'ctd
GFRPROD (h)	1255.2	673.0	-873.6	-1015.4	-582.2	-39395	67.67	1250.2	668.0
COMB1 (h)	1160.0	393.0	-120.3	-188.1	-767.0	-18837	24.56	1155.0	388.0
REFPROD (h)	1140.0	623.0	-936.8	-1072.7	-517.0	-37771	73.06	1135.0	618.0
SHIFT3 (h)	729.2	500.0	-1414.4	-1485.4	-229.2	-19731	86.07	724.2	495.0
LTS (hot)	500.1	500.0	-1485.4	-1497.5	-0.1	-3353	33532.78	495.1	495.0
SHIFT5-a (h)	500.0	448.2	0.0	-15.6	-51.8	-4326	83.50	495.0	443.2
SHIFT5-b (h)	448.2	403.7	-15.6	-102.4	-44.5	-24128	542.52	443.2	398.7
RECYC3 (hot)	441.6	313.0	-62.8	-68.6	-128.6	-1627	12.65	436.6	308.0
SHIFT5-c (h)	403.7	313.0	-102.4	-161.0	-90.7	-16259	179.21	398.7	308.0
H22 (hot)	367.4	313.0	6.6	1.7	-54.4	-1353	24.88	362.4	308.0
AIR1 (cold)	298.0	896.7	-0.0	42.9	598.7	11921	19.91	303.0	901.7
REFFEED1 (c)	459.1	850.0	-1180.2	-1084.7	390.9	26510	67.82	464.1	855.0
PURGE1 (c)	313.0	700.0	-17.1	-12.3	387.0	1339	3.46	318.0	705.0
SHW2-c (c)	510.7	623.0	72.1	80.3	112.3	2290	20.39	515.7	628.0
REFW2-c (c)	513.3	613.2	114.6	126.6	99.9	3327	33.30	518.3	618.2
GFRW2-c (c)	515.0	534.9	53.6	54.9	19.9	369	18.53	520.0	539.9
GFRW2-b (c)	514.9	515.0	18.9	53.6	0.1	9644	96435.83	519.9	520.0
GFRW2-a (c)	294.0	514.9	0.0	18.9	220.9	5250	23.77	299.0	519.9
REFW2-b (c)	513.2	513.3	40.1	114.6	0.1	20704	207036.67	518.2	518.3
REFW2-a (c)	294.0	513.2	0.0	40.1	219.2	11138	50.81	299.0	518.2
SHW2-b (c)	510.6	510.7	24.9	72.1	0.1	13107	131073.89	515.6	515.7
SHW2-a (c)	294.0	510.6	0.0	24.9	216.6	6909	31.89	299.0	515.6
Drier (cold)	293.0	393.0	---	---	100.0	42757	427.57	298.0	398.0
						-11515			

Problem Table

Interval	T(i) (K)	T(i+1) (K)	Ti-T(i+1) (K)	Sum CPhot (kW/K)	Sum CPcold (kW/K)	CPc-CPH (kW/K)	delta H (kW)	Cascade	Corrected Cascade
0		1250.2						0	0
1	1250.2	1155.0	95.2	67.67	0.00	-67.67	-6442	6442	6442
2	1155.0	1135.0	20.0	92.23	0.00	-92.23	-1846	8287	8287
3	1135.0	901.7	233.3	165.29	0.00	-165.29	-38567	46854	46854
4	901.7	855.0	46.7	165.29	19.91	-145.38	-6785	53639	53639
5	855.0	724.2	130.8	165.29	87.73	-77.56	-10142	63781	63781
6	724.2	705.0	19.2	251.36	87.73	-163.63	-3148	66929	66929
7	705.0	668.0	37.0	251.36	91.19	-160.17	-5926	72855	72855
8	668.0	628.0	40.0	183.69	91.19	-92.50	-3700	76555	76555
9	628.0	618.2	9.8	183.69	111.58	-72.11	-705	77261	77261
10	618.2	618.0	0.2	183.69	144.88	-38.81	-8	77269	77269
11	618.0	539.9	78.1	110.63	144.88	34.25	2675	74594	74594
12	539.9	520.0	19.9	110.63	163.41	52.78	1050	73544	73544
13	520.0	519.9	0.1	110.63	96580.71	96470.08	9647	63896	63896
14	519.9	518.3	1.6	110.63	168.65	58.02	92	63805	63805
15	518.3	518.2	0.1	110.63	207172.02	207061.39	20706	43099	43099
16	518.2	515.7	2.5	110.63	186.16	75.53	188	42910	42910
17	515.7	515.6	0.1	110.63	131239.66	131129.03	13113	29798	29798
18	515.6	495.1	20.5	110.63	197.66	87.03	1786	28011	28011
19	495.1	495.0	0.1	33643.41	197.66	-33445.75	-3345	31356	31356
20	495.0	464.1	30.9	108.06	197.66	89.60	2765	28591	28591
21	464.1	443.2	20.9	108.06	129.84	21.78	456	28135	28135
22	443.2	436.6	6.6	567.08	129.84	-437.24	-2880	31015	31015
23	436.6	398.7	37.9	579.73	129.84	-449.89	-17045	48060	48060
24	398.7	398.0	0.7	216.42	129.84	-86.58	-63	48123	48123
25	398.0	388.0	10.0	216.42	557.41	340.99	3410	44713	44713
26	388.0	362.4	25.6	191.86	557.41	365.55	9372	35341	35341
27	362.4	318.0	44.4	216.74	557.41	340.67	15113	20228	20228
28	318.0	308.0	10.0	216.74	553.95	337.21	3372	16856	16856
29	308.0	303.0	5.0	0.00	553.95	553.95	2770	14086	14086
30	303.0	299.0	4.0	0.00	534.04	534.04	2136	11950	11950
31	299.0	298.0	1.0	0.00	427.57	427.57	428	11522	11522

Methanol production



Hydrogen Production

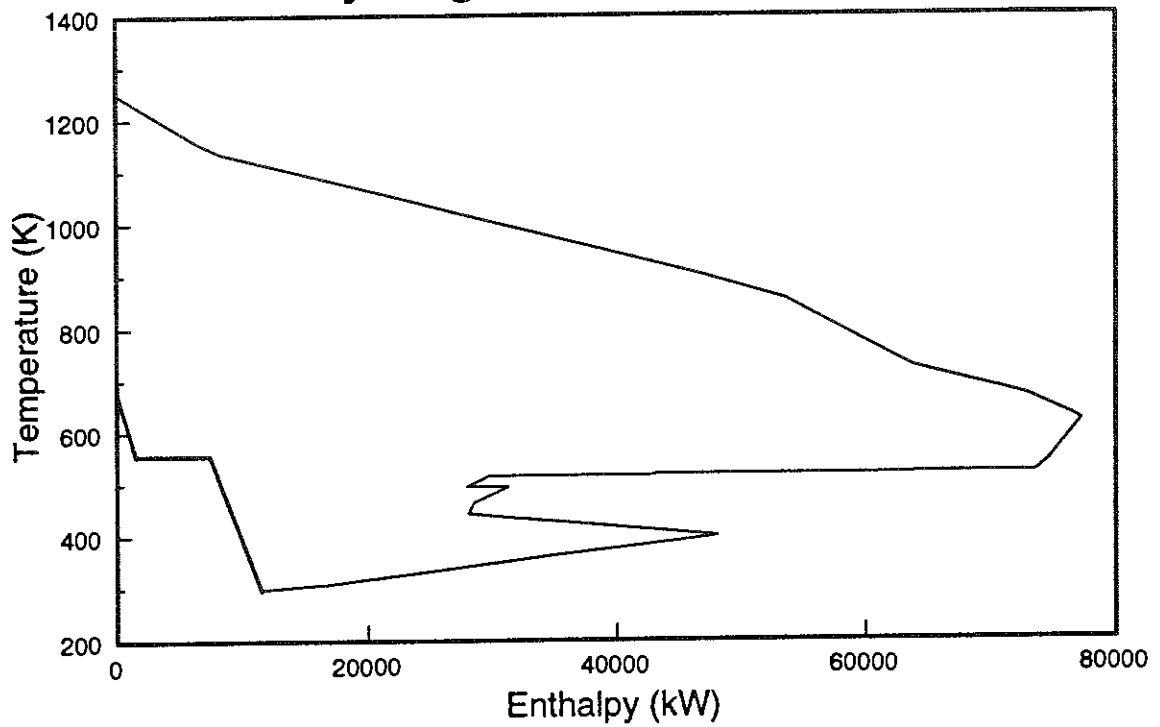


Figure 6A-14: Grand composite curves for methanol and hydrogen production from biomass using the IGT fluidized-bed, oxygen-blown gasifier.

Table 6A-19: Calculated material flows for methanol production from biomass based on the WM Gasifier.

Name	Temp [K]	Pres. [bar]	Total Volume Flow [kmol/hr]	Molecular Weight [kg/kmol]	Component Volume Flow Rates [kmol/hr]															
					H ₂ O	H ₂	CO	CO ₂	CH ₄	O ₂	N ₂	CH ₃ OH								
1 Raw Biomass				3000 tonnes per day @ 45% moisture																
2 Dried, pressurized biomass				3000 tonnes per day @ 45% moisture																
3 Gasifier exit	873	15.00	5644	21.82	2370	677	226	1242	1129	0	0	0	0	0	0	0	0	0	0	0
4 Quench inlet	423	14.50	5644	21.82	2370	677	226	1242	1129	0	0	0	0	0	0	0	0	0	0	0
5 Quench exit	373	14.00	3508	23.90	270	676	226	1209	1127	0	0	0	0	0	0	0	0	0	0	0
6 Reformer feed	373	14.00	3014	23.90	232	581	194	1039	969	0	0	0	0	0	0	0	0	0	0	0
7 Preheated reformer feed	850	13.50	5688	21.13	2906	581	194	1039	969	0	0	0	0	0	0	0	0	0	0	0
8 Reformer exit	1120	13.00	7392	16.26	2245	2946	1237	848	117	0	0	0	0	0	0	0	0	0	0	0
9 Selexol feed	400	12.50	6411	15.99	1265	2946	1237	848	117	0	0	0	0	0	0	0	0	0	0	0
10 Selexol exit	400	12.50	4387	10.56	0	2946	1237	88	117	0	0	0	0	0	0	0	0	0	0	0
11 Makeup compressor exit	504	105.88	4387	10.56	0	2946	1237	88	117	0	0	0	0	0	0	0	0	0	0	0
12 Hot synthesis feed 1	344	105.88	4394	8.07	0	2875	319	48	1143	0	0	0	0	0	0	0	0	0	0	9
13 Hot synthesis feed 2	523	105.68	4394	8.07	0	2875	319	48	1143	0	0	0	0	0	0	0	0	0	0	9
14 Synthesis product	533	97.58	19311	9.17	84	11643	365	156	5704	0	0	0	0	0	0	0	0	0	0	1358
15 Crude methanol product	300	97.08	1396	31.22	83	0	0	2	0	0	0	0	0	0	0	0	0	0	0	1311
16 Recycle stream	300	97.08	17914	7.45	1	11643	365	155	5704	0	0	0	0	0	0	0	0	0	0	47
17 Recycle compressor feed	300	97.08	17548	7.45	1	11405	357	151	5588	0	0	0	0	0	0	0	0	0	0	46
18 Recycle compressor exit	308	105.88	17548	7.45	1	11405	357	151	5588	0	0	0	0	0	0	0	0	0	0	46
19 Cold synthesis feed 1	344	105.88	17541	8.07	1	11476	1275	191	4562	0	0	0	0	0	0	0	0	0	0	37
20 Cold synthesis feed 2	320	105.68	17541	8.07	1	11476	1275	191	4562	0	0	0	0	0	0	0	0	0	0	37
21 Purge stream	300	97.08	366	7.45	0	238	7	3	117	0	0	0	0	0	0	0	0	0	0	1
22 Heated reformer fuel gas	700	1.00	860	16.89	38	333	39	173	275	0	0	0	0	0	0	0	0	0	0	1
23 Reformer furnace products	1140	1.00	4706	27.81	922	0	0	488	0	110	3186	0	0	0	0	0	0	0	0	1
24 Stack gases	393	1.00	4706	27.81	922	0	0	488	0	110	3186	0	0	0	0	0	0	0	0	1
25 Reformer furnace air	298	1.00	4032	28.85	0	0	0	0	0	847	3186	0	0	0	0	0	0	0	0	0
26 Heated reformer furnace air	1000	1.01	4032	28.85	0	0	0	0	0	847	3186	0	0	0	0	0	0	0	0	0
27 Fuel gas to reformer	373	14.00	494	23.90	38	95	32	170	159	0	0	0	0	0	0	0	0	0	0	0
28 Reformer steam	518	14.00	2674	18.02	2674	0	0	0	0	0	0	0	0	0	0	0	0	0	0	0
29 Carbon dioxide removed	400	12.50	2024	27.77	1265	0	0	760	0	0	0	0	0	0	0	0	0	0	0	0
30 Condensate	400	12.50	955	18.02	955	0	0	0	0	0	0	0	0	0	0	0	0	0	0	0
31 Quench feed water	293	15.00	21331	18.02	21331	0	0	0	0	0	0	0	0	0	0	0	0	0	0	0
32 Quench condensate	373	14.00	23468	18.05	23432	1	0	33	2	0	0	0	0	0	0	0	0	0	0	0

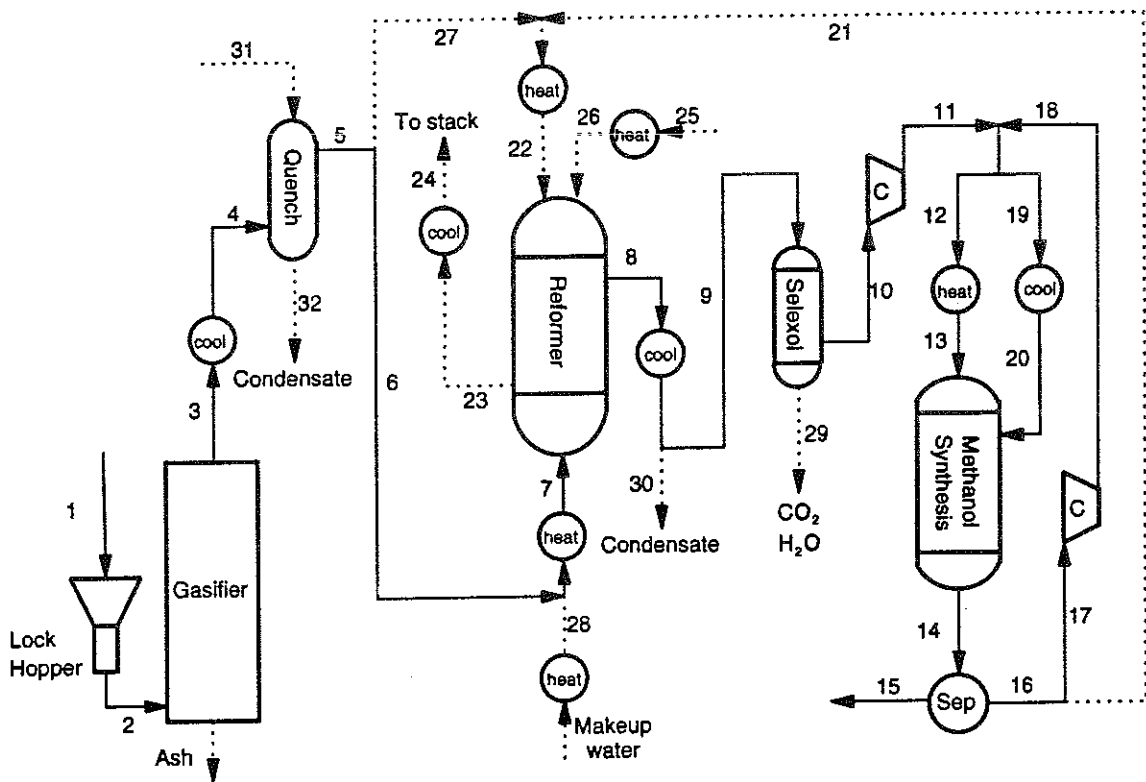


Figure 6A-15: Process configuration for the modeling of methanol production from biomass based on the Wright-Malta (WM) indirectly-heated gasifier.

Table 6A-20: Calculated material flows for hydrogen production from biomass based on the WM Gasifier.

Name	Temp [K]	Press. [bar]	Total Volume Flow [kmol/hr]	Molecular Weight [kg/kmol]	Component Volume Flow Rates [kmol/hr]						
					H ₂ O	H ₂	CO	CO ₂	CH ₄	O ₂	N ₂
1 Raw Biomass			3000	tonnes per day @ 45% moisture							
2 Dried, pressurized biomass			3000	tonnes per day @ 45% moisture							
3 Gasifier exit	873	15.00	5644	21.82	2370	677	226	1242	1129	0	0
4 Quench inlet	423	14.50	5644	21.82	2370	677	226	1242	1129	0	0
5 Quench exit	373	14.00	3524	23.97	272	677	226	1222	1128	0	0
6 Reformer feed	373	14.00	3103	23.97	239	596	199	1076	993	0	0
7 Preheated reformer feed	850	13.50	5843	21.18	2979	596	199	1076	993	0	0
8 Reformer exit	1120	13.00	7590	16.30	2306	3016	1273	875	119	0	0
9 High temperature shift feed	623	12.50	7590	16.30	2306	3016	1273	875	119	0	0
10 High temperature shift exit	727	12.00	9104	16.59	2919	3917	373	1776	119	0	0
11 Low temperature shift feed	500	11.50	9104	16.59	2919	3917	373	1776	119	0	0
12 Low temperature shift exit	500	11.00	9104	16.59	2586	4251	39	2110	119	0	0
13 PSA makeup feed	313	10.50	6566	16.03	47	4251	39	2110	119	0	0
14 PSA-A feed	313	10.50	7044	15.46	47	4571	78	2110	239	0	0
15 PSA-B feed	313	10.15	4887	3.11	0	4571	78	0	239	0	0
16 Hydrogen compressor feed	313	9.80	3931	2.02	0	3931	0	0	0	0	0
17 Hydrogen compressor exit	415	75.00	3931	2.02	0	3931	0	0	0	0	0
18 Cooled Hydrogen product	313	75.00	3931	2.02	0	3931	0	0	0	0	0
19 PSA recycle stream	313	1.30	956	7.62	0	640	78	0	239	0	0
20 Recycle compressor feed	313	1.30	478	7.62	0	320	39	0	119	0	0
21 Recycle compressor exit	411	10.70	478	7.62	0	320	39	0	119	0	0
22 PSA-A recycle feed	313	10.50	478	7.62	0	320	39	0	119	0	0
23 Purge stream	313	1.30	478	7.62	0	320	39	0	119	0	0
24 Fuel gas to reformer	373	14.00	421	23.97	32	81	27	146	135	0	0
25 Heated reformer fuel gas	700	1.30	899	15.28	32	401	66	146	254	0	0
26 Reformer furnace products	1140	1.01	4726	27.69	942	0	0	466	0	111	3207
27 Stack gases	393	1.01	4726	27.69	942	0	0	466	0	111	3207
28 Reformer furnace air	298	1.01	4060	28.85	0	0	0	0	0	853	3207
29 Heated reformer furnace air	1000	1.01	4060	28.85	0	0	0	0	0	853	3207
30 Reformer steam	537	14.00	2740	18.02	2740	0	0	0	0	0	0
31 Shift steam	623	12.50	1514	18.02	1514	0	0	0	0	0	0
32 Carbon dioxide removed	313	1.30	2157	43.44	47	0	0	2110	0	0	0
33 Condensate	313	10.50	2538	18.02	2538	0	0	0	0	0	0
34 Quench feed water	293	15.00	11434	18.02	11434	0	0	0	0	0	0
35 Quench condensate	373	14.00	13553	18.05	13533	1	0	19	1	0	0

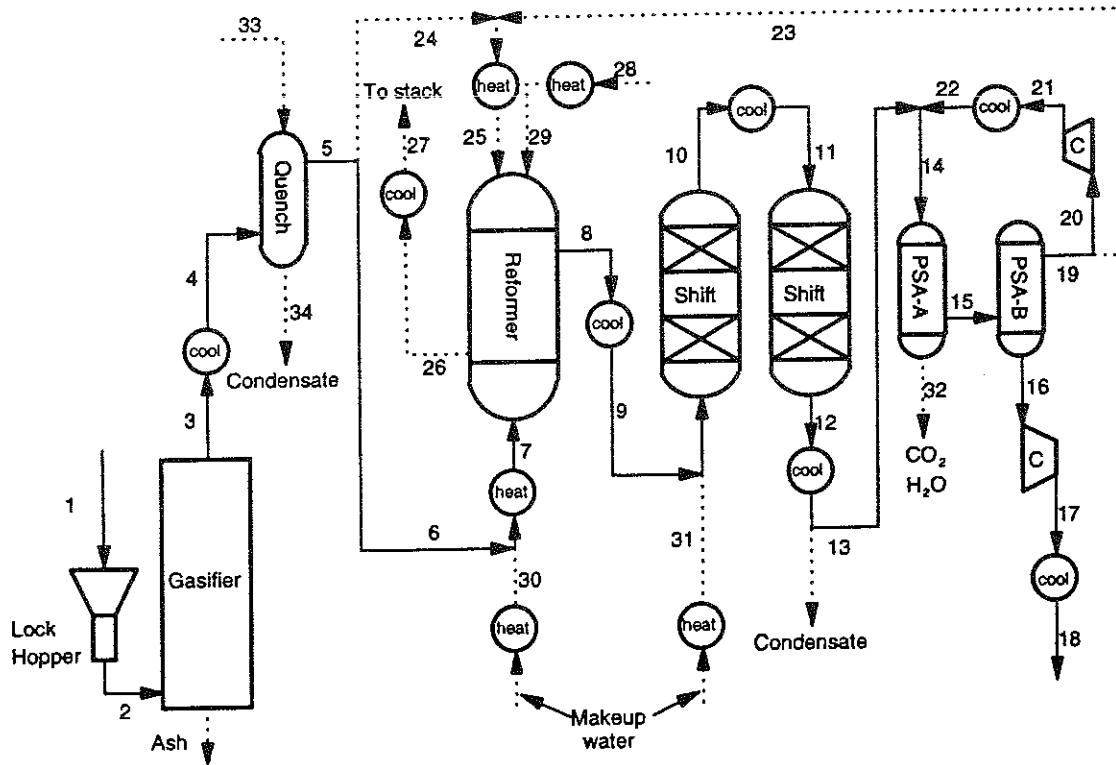


Figure 6A-16 Process configuration for the modeling of hydrogen production from biomass based on the Wright-Malta (WM) indirectly-heated gasifier.

Table 6A-21: Pinch analysis for methanol production from biomass based on the WM gasifier.

Stream Table

Streams	T source (K)	T target (K)	H in (GJ/hr)	H out (GJ/hr)	Delta T (K)	Delta H (kW)	CP (kW/K)	T source cor'ctd	T target cor'ctd
COMB1 (h)	1140.0	393.0	-290.39	-412.19	-747.0	-33834	45.29	1135.0	388.0
REFPROD-a (h)	1120.0	415.0	0.00	-180.80	-705.0	-50222	71.24	1115.0	410.0
GFRPROD-a (h)	873.0	428.0	0.00	-106.03	-445.0	-29453	66.18	868.0	423.0
SYNPROD (h)	533.0	300.0	-1106.34	-1336.97	-233.0	-64064	274.95	528.0	295.0
GFRPROD-b (h)	428.0	423.0	-106.03	-125.79	-5.0	-5489	1101.82	423.0	418.0
REFPROD-b (h)	415.0	400.0	-180.80	-222.03	-15.0	-11454	763.10	410.0	395.0
COLD1 (h)	341.7	320.0	-843.54	-855.92	-21.7	-3439	158.60	336.7	315.0
AIR1 (cold)	298.0	1000.0	-0.02	86.92	702.0	24150	34.40	303.0	1005.0
Gasifier (c)	298.0	873.0	---	---	575.0	78924	137.26	303.0	878.0
REFFEED2 (c)	433.9	850.0	-1149.49	-1053.49	416.1	26666	64.09	438.9	855.0
FUEL2 (c)	359.6	700.0	-118.61	-106.85	340.4	3267	9.60	364.6	705.0
HOTFEED1 (c)	341.7	523.0	-286.81	-250.41	181.3	10111	55.76	346.7	528.0
REFW2-c (c)	468.3	518.2	126.70	132.70	49.9	1666	33.39	473.3	523.2
REFW2-b (c)	468.2	468.3	34.91	126.70	0.1	25497	254970.56	473.2	473.3
REFW2-a (c)	293.0	468.2	0.00	34.91	175.2	9697	55.35	298.0	473.2
						-17975			

Problem Table

Interval	T(i) (K)	T(i+1) (K)	Ti-T(i+1) (K)	Sum CPhot (kW/K)	Sum CPcold (kW/K)	CPc-CPH (kW/K)	delta H (kW)	Cascade	Corrected Cascade
0		1135.0						0	13880
1	1135.0	1115.0	20.0	45.29	0.00	-45.29	-906	906	14786
2	1115.0	1005.0	110.0	116.53	0.00	-116.53	-12818	13724	27604
3	1005.0	878.0	127.0	116.53	34.40	-82.13	-10431	24155	38035
4	878.0	868.0	10.0	116.53	171.66	55.13	551	23603	37483
5	868.0	855.0	13.0	182.71	171.66	-11.05	-144	23747	37627
6	855.0	705.0	150.0	182.71	235.75	53.04	7956	15791	29671
7	705.0	528.0	177.0	182.71	245.35	62.64	11087	4704	18584
8	528.0	523.2	4.8	457.66	301.11	-156.55	-752	5456	19336
9	523.2	473.3	49.9	457.66	334.50	-123.16	-6146	11601	25481
10	473.3	473.2	0.1	457.66	255271.67	254814.01	25481	-13880	0
11	473.2	438.9	34.3	457.66	356.46	-101.20	-3467	-10413	3467
12	438.9	423.0	16.0	457.66	292.37	-165.29	-2638	-7775	6105
13	423.0	418.0	5.0	1493.30	292.37	-1200.93	-5982	-1793	12087
14	418.0	410.0	8.0	391.48	292.37	-99.11	-792	-1001	12879
15	410.0	395.0	15.0	1083.34	292.37	-790.97	-11873	10871	24751
16	395.0	388.0	7.0	320.24	292.37	-27.87	-195	11066	24946
17	388.0	364.6	23.4	274.95	292.37	17.42	408	10658	24538
18	364.6	346.7	17.9	274.95	282.77	7.82	140	10518	24398
19	346.7	336.7	10.0	274.95	227.01	-47.94	-479	10998	24878
20	336.7	315.0	21.7	433.55	227.01	-206.54	-4478	15476	29356
21	315.0	303.0	12.0	274.95	227.01	-47.94	-575	16051	29931
22	303.0	298.0	5.0	274.95	55.35	-219.60	-1098	17149	31029
23	298.0	295.0	3.0	274.95	0.00	-274.95	-825	17974	31854

Table 6A-22: Pinch analysis for hydrogen production from biomass using the WM indirectly-heated gasifier.

Stream Table

Streams	T source (K)	T target (K)	H in (GJ/hr)	H out (GJ/hr)	Delta T (K)	Delta H (kW)	CP (kW/K)	T source cor'ctd	T target cor'ctd
COMB1 (hot)	1140.0	393.0	-275.44	-397.52	-747.0	-33911	45.40	1135.0	388.0
REFPROD (h)	1120.0	623.0	-834.04	-971.84	-497.0	-38279	77.02	1115.0	618.0
GFRPROD-a (h)	873.0	428.0	0.00	-106.03	-445.0	-29453	66.18	868.0	423.0
SHIFT3 (h)	727.1	500.0	-1321.62	-1395.52	-227.1	-20528	90.40	722.1	495.0
LTS (hot)	500.1	500.0	---	---	-0.1	-3688	36880.56	495.1	495.0
SHIFT5-a (h)	500.0	406.5	0.00	-29.30	-93.5	-8138	87.00	495.0	401.5
GFRPROD-b (h)	428.0	423.0	-106.03	-125.79	-5.0	-5489	1101.82	423.0	418.0
H22 (hot)	415.4	313.0	13.79	2.13	-102.4	-3239	31.62	410.4	308.0
RECYC3 (h)	410.7	313.0	-11.55	-13.02	-97.7	-409	4.19	405.7	308.0
SHIFT5-b (h)	406.5	366.3	-29.30	-125.31	-40.1	-26669	665.00	401.5	361.3
SHIFT5-c (h)	366.3	313.0	-125.31	-167.08	-53.3	-11602	217.48	361.3	308.0
AIR1 (cold)	298.0	1000.0	-0.04	88.30	702.0	24539	34.96	303.0	1005.0
Gasifier (c)	298.0	873.0	---	---	575.0	78924	137.26	303.0	878.0
REFPEED2 (c)	443.0	850.0	-1212.30	-1113.76	407.0	27373	67.26	448.0	855.0
FUEL2 (c)	341.9	700.0	-90.46	-78.42	358.1	3345	9.34	346.9	705.0
SHW1-c (c)	457.5	623.0	79.15	88.76	165.5	2670	16.13	462.5	628.0
REFW1-c (c)	462.5	537.4	143.50	151.54	74.9	2232	29.80	467.5	542.4
REFW1-b (c)	462.4	462.5	43.27	143.50	0.1	27841	278414.72	467.4	467.5
REFW1-a (c)	293.0	462.4	0.00	43.27	169.4	12020	70.96	298.0	467.4
SHW1-b (c)	457.4	457.5	23.18	79.15	0.1	15546	155458.61	462.4	462.5
SHW1-a (c)	293.0	457.4	0.00	23.18	164.4	6440	39.18	298.0	462.4
						19524			

Problem Table

Interval	T(i) (K)	T(i+1) (K)	Ti-T(i+1) (K)	Sum CPhot (kW/K)	Sum CPcold (kW/K)	CPc-CPH (kW/K)	delta H (kW)	Cascade	Corrected Cascade
0		1135.0						0	35256
1	1135.0	1115.0	20.0	45.4	0	-45.40	-908	908	36164
2	1115.0	1005.0	110.0	122.42	0	-122.42	-13466	14374	49630
3	1005.0	878.0	127.0	122.42	34.96	-87.46	-11107	25482	60737
4	878.0	868.0	10.0	122.42	172.22	49.80	498	24984	60239
5	868.0	855.0	13.0	188.6	172.22	-16.38	-213	25197	60452
6	855.0	722.1	132.9	188.6	239.48	50.88	6763	18433	53689
7	722.1	705.0	17.1	279	239.48	-39.52	-675	19108	54364
8	705.0	628.0	77.0	279	248.82	-30.18	-2324	21432	56688
9	628.0	618.0	10.0	279	264.95	-14.05	-140	21573	56828
10	618.0	542.4	75.6	201.98	264.95	62.97	4761	16812	52067
11	542.4	495.1	47.3	201.98	294.75	92.77	4387	12424	47680
12	495.1	495.0	0.1	37082.54	294.75	-36787.79	-3679	16103	51359
13	495.0	467.5	27.5	198.58	294.75	96.17	2645	13458	48713
14	467.5	467.4	0.1	198.58	278679.67	278481.09	27848	-14390	20865
15	467.4	462.5	4.9	198.58	335.91	137.33	676	-15066	20189
16	462.5	462.4	0.1	198.58	155778.39	155579.81	15558	-30624	4631
17	462.4	448.0	14.3	198.58	358.96	160.38	2297	-32921	2334
18	448.0	423.0	25.1	198.58	291.7	93.12	2334	-35256	-0
19	423.0	418.0	5.0	1234.22	291.7	-942.52	-4695	-30560	4695
20	418.0	410.4	7.6	132.4	291.7	159.30	1209	-31769	3486
21	410.4	405.7	4.7	164.02	291.7	127.68	601	-32371	2885
22	405.7	401.5	4.2	168.21	291.7	123.49	525	-32895	2360
23	401.5	388.0	13.5	746.21	291.7	-454.51	-6115	-26781	8475
24	388.0	361.3	26.7	700.81	291.7	-409.11	-10903	-15877	19378
25	361.3	346.9	14.5	253.29	291.7	38.41	555	-16433	18823
26	346.9	308.0	38.9	253.29	282.36	29.07	1131	-17563	17692
27	308.0	303.0	5.0	0	282.36	282.36	1412	-18975	16280
28	303.0	298.0	5.0	0	110.14	110.14	551	-19526	15730

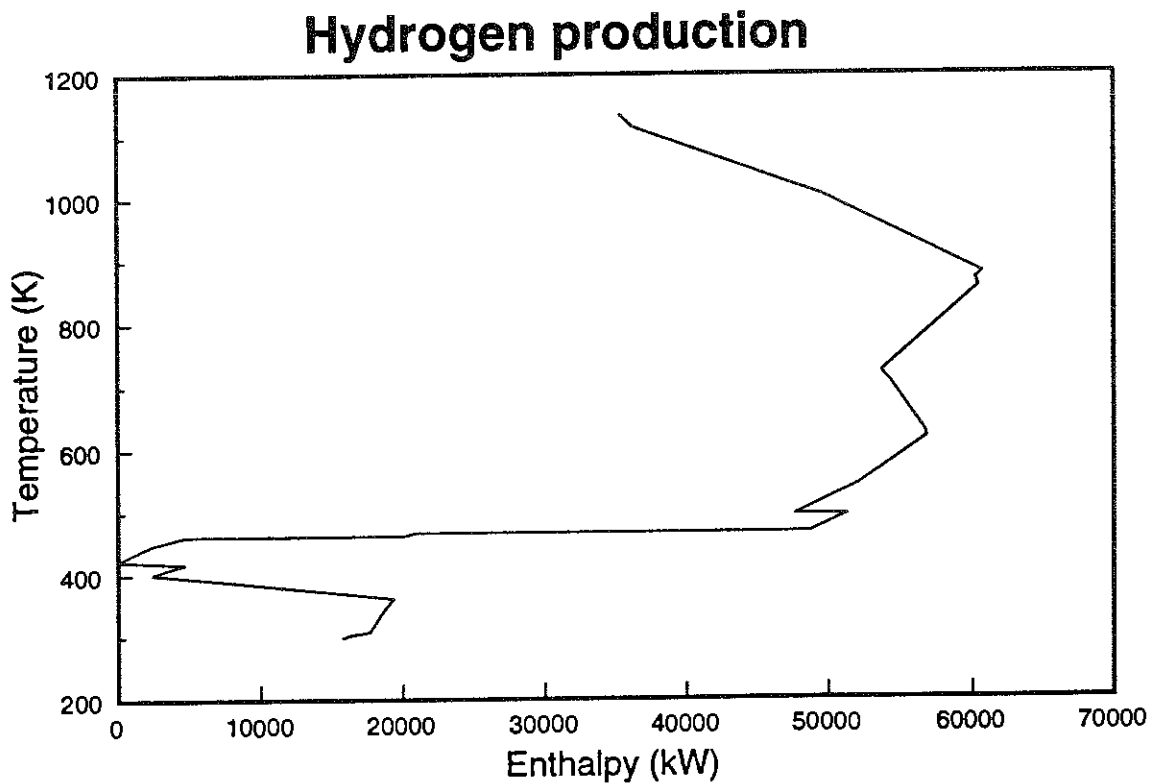
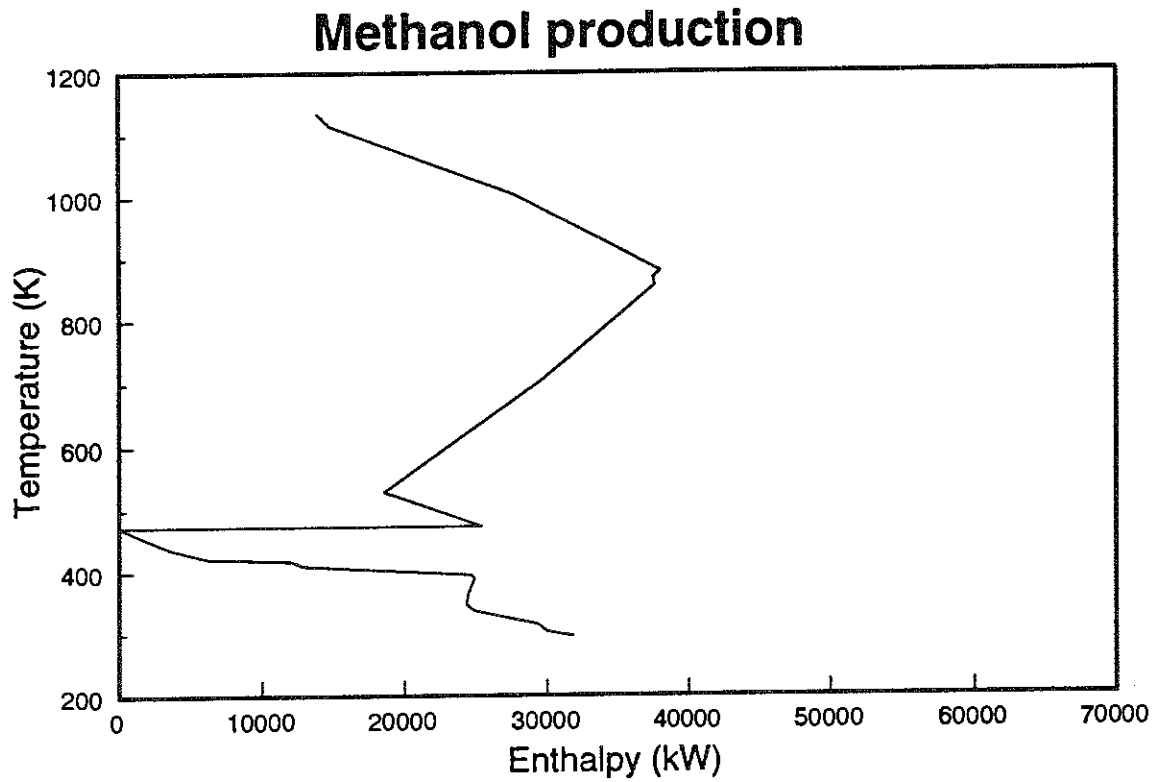


Figure 6A-17: Grand composite curves for methanol and hydrogen production from biomass using the WM indirectly-heated gasifier. Note the large external heating requirements.

Table 6A-23: Calculated material flows for methanol production from biomass based on the MTCI Gasifier.

Name	Temp [K]	Pres. [bar]	Total Volume Flow [kmol/hr]	Molecular Weight [kg/kmol]	Component Volume Flow Rates [kmol/hr]									
					H ₂ O	H ₂	CO	CO ₂	CH ₄	C ₂ +	O ₂	N ₂	CH ₃ OH	
1 Raw Biomass					3000 tonnes per day @ 45% moisture									
2 Dried biomass					2126 tonnes per day @ 22% moisture									
3 Gasifier exit	970	1.50	10093	17.65	4997	2550	1125	987	408	24	0	2	0	
4 Quench inlet	673	1.50	10093	17.65	4997	2550	1125	987	408	24	0	2	0	
5 Quench exit	370	1.50	11092	17.69	5996	2550	1125	987	408	24	0	2	0	
6 Selexol feed	400	15.00	5203	17.31	107	2550	1125	987	408	24	0	2	0	
7 Selexol exit	400	15.00	4197	11.58	0	2550	1125	88	408	24	0	2	0	
8 Makeup compressor exit	489	105.88	4197	11.58	0	2550	1125	88	408	24	0	2	0	
9 Hot synthesis feed 1	338	105.88	7665	12.93	0	3044	805	200	3492	76	0	21	26	
10 Hot synthesis feed 2	523	105.38	7665	12.93	0	3044	805	200	3492	76	0	21	26	
11 Synthesis product	533	97.28	18721	14.50	52	6019	1122	497	9560	209	0	58	1202	
12 Crude methanol product	300	96.78	1251	31.57	51	2	1	18	35	16	0	0	1128	
13 Recycle stream	300	96.78	17469	13.27	1	6017	1122	479	9525	193	0	58	74	
14 Recycle compressor feed	300	96.78	16787	13.27	1	5782	1078	460	9153	186	0	56	71	
15 Recycle compressor exit	308	105.88	16787	13.27	1	5783	1078	460	9152	186	0	56	71	
16 Cold synthesis feed 1	338	105.88	13318	12.93	1	5289	1398	348	6068	133	0	37	45	
17 Cold synthesis feed 2	320	105.38	13318	12.93	1	5289	1398	348	6068	133	0	37	45	
18 Purge stream	300	96.78	683	13.27	0	235	44	19	372	8	0	2	3	
19 Heated purge stream	533	96.78	683	13.27	0	235	44	19	372	8	0	2	3	
20 Char to pulse combustor	500	1.00			2542 kg per hour									
21 Pulse combustor flue gases	1000	1.00	6254	28.15	1019	0	0	678	0	0	52	4506	0	
22 Stack gases	393	1.00	6254	28.15	1019	0	0	678	0	0	52	4506	0	
23 Pulse combustor air	298	1.00	5700	28.85	0	0	0	0	0	0	1197	4503	0	
24 Heated pulse combustor air	615	1.00	5700	28.85	0	0	0	0	0	0	1197	4503	0	
25 Gasifier steam	430	1.30	5228	18.02	5228	0	0	0	0	0	0	0	0	
26 Carbon dioxide removed	400	15.00	1007	41.23	107	0	0	899	0	0	0	0	0	
27 Quench feed water	293	1.50	18652	18.02	18652	0	0	0	0	0	0	0	0	
28 Quench condensate	370	1.50	17654	18.02	17654	0	0	0	0	0	0	0	0	
29 Stage 1 condensate	330	3.23	5763	18.02	5763	0	0	0	0	0	0	0	0	
30 Stage 2 condensate	330	6.96	125	18.02	125	0	0	0	0	0	0	0	0	

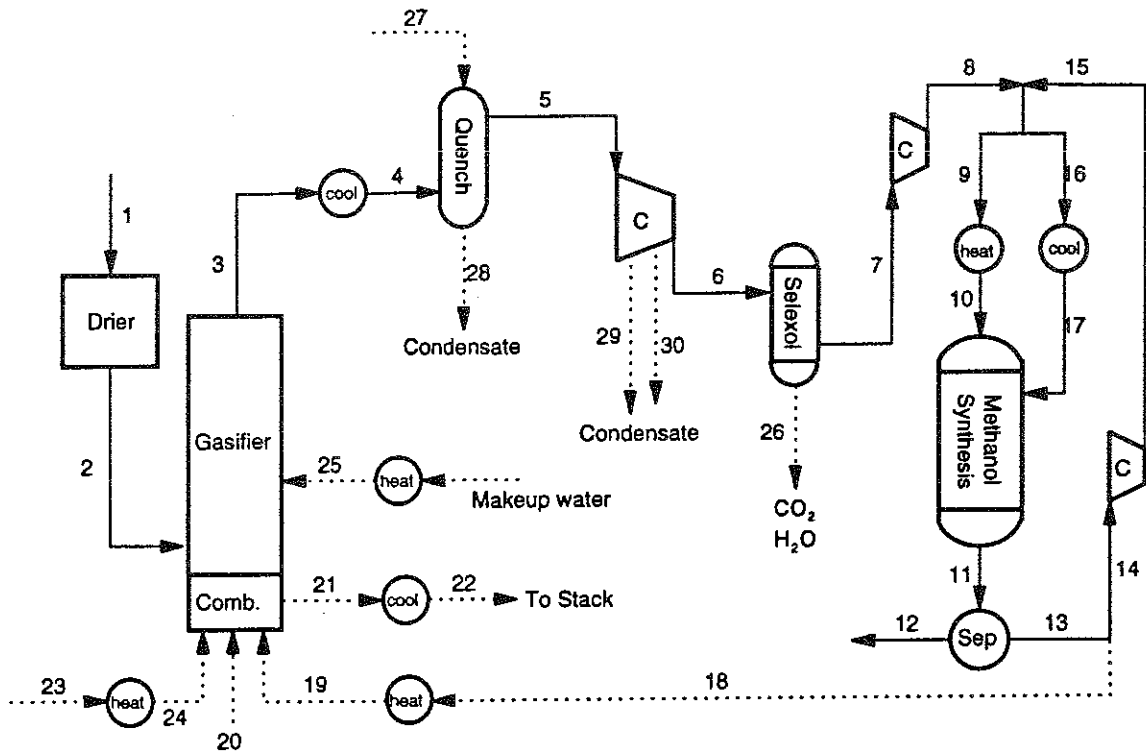


Figure 6A-18: Process configuration for the modeling of methanol production from biomass based on the MTCI indirectly-heated gasifier.

Table 6A-24: Calculated material flows for hydrogen production from biomass based on the MTCI Gasifier.

Name	Temp [K]	Pres. [bar]	Total Volume Flow [kmol/hr]	Molecular Weight [kg/kmol]	Component Volume Flow Rates [kmol/hr]							
					H ₂ O	H ₂	CO	CO ₂	CH ₄	C ₂ +	O ₂	N ₂
1 Raw Biomass					3000 tonnes per day @ 45% moisture							
2 Dried, pressurized biomass					2126 tonnes per day @ 22% moisture							
3 Gasifier exit	970	1.50	10093	17.65	4997	2550	1125	987	408	24	0	2
4 Quench inlet	673	1.50	10093	17.65	4997	2550	1125	987	408	24	0	2
5 Quench exit	370	1.50	11091	17.69	5996	2550	1125	987	408	24	0	2
6 High temperature shift feed	623	1.50	11091	17.69	5996	2550	1125	987	408	24	0	2
7 High temperature shift exit	710	1.50	11091	17.69	5051	3494	181	1931	408	24	0	2
8 Low temperature shift feed	500	1.50	11091	17.69	5051	3494	181	1931	408	24	0	2
9 Low temperature shift exit	500	1.50	11091	17.69	4888	3658	18	2095	408	24	0	2
10 Compressor feed	313	1.50	6446	17.45	242	3658	18	2095	408	24	0	2
11 Compressor exit	436	15.00	6446	17.45	242	3658	18	2095	408	24	0	2
12 PSA make-up feed	313	14.50	6446	17.45	242	3658	18	2095	408	24	0	2
13 PSA-A feed	313	14.50	8711	16.94	242	4119	88	2095	2038	118	0	12
14 PSA-B feed	312	14.15	6374	8.01	0	4119	88	0	2038	118	0	12
15 Hydrogen compressor feed	312	13.80	3542	2.02	0	3542	0	0	0	0	0	0
16 Hydrogen compressor exit	400	75.00	3542	2.02	0	3542	0	0	0	0	0	0
17 Cooled Hydrogen product	313	75.00	3542	2.02	0	3542	0	0	0	0	0	0
18 PSA recycle stream	312	1.30	2832	15.50	0	577	88	0	2038	118	0	12
19 Recycle compressor feed	312	1.30	2266	15.50	0	461	70	0	1631	94	0	10
20 Recycle compressor exit	402	14.70	2266	15.50	0	461	70	0	1631	94	0	10
21 PSA-A recycle feed	313	14.50	2266	15.50	0	461	70	0	1631	94	0	10
22 Purge stream	312	1.30	566	15.50	0	115	18	0	408	24	0	2
23 Heated purge stream	533	1.30	566	15.50	0	115	18	0	408	24	0	2
24 Char to pulse combustor	500	1.00			2542 kg per hour							
25 Pulse combustor flue gas	1000	1.00	6589	28.22	1050	0	0	737	0	0	17	4784
26 Stack gas	393	1.00	6589	28.22	1050	0	0	737	0	0	17	4784
27 Pulse combustor air	298	1.00	6052	28.85	0	0	0	0	0	0	1271	4781
28 Heated pulse combustor air	437	1.00	6052	28.85	0	0	0	0	0	0	1271	4781
29 Gasifier steam	430	1.30	5228	18.02	5228	0	0	0	0	0	0	0
30 Carbon dioxide removed	312	1.30	2337	41.32	242	0	0	2095	0	0	0	0
31 Condensate	313	1.50	4646	18.02	4646	0	0	0	0	0	0	0
32 Quench feed water	293	1.50	18657	18.02	18657	0	0	0	0	0	0	0
33 Quench condensate	370	1.50	17658	18.02	17658	0	0	0	0	0	0	0

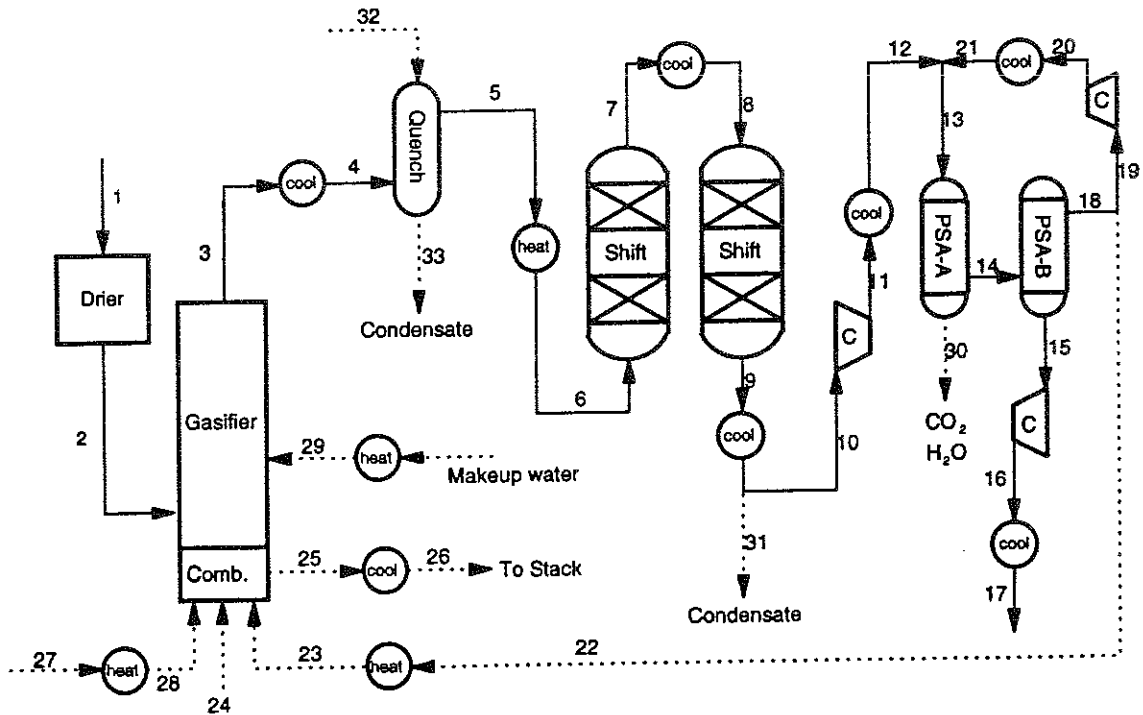


Figure 6A-19: Process configuration for the modeling of hydrogen production from biomass based on the MTCI indirectly-heated gasifier.

Table 6A-25: Pinch analysis for methanol production from biomass using the MTCI gasifier.

Stream Table

Streams	T source (K)	T target (K)	H in (kW)	H out (kW)	Delta T (K)	Delta H (kW)	CP (kW/K)	T source cor'ctd	T target cor'ctd
COMB1 (h)	1000.0	393.0	-366.23	-494.93	-607.0	-35748	58.89	995.0	388.0
GFRPROD (h)	970.0	673.0	-1508.99	-1624.67	-297.0	-32134	108.20	965.0	668.0
SYNPROD (h)	533.0	300.0	-1141.58	-1366.74	-233.0	-62543	268.43	528.0	295.0
QCHOUT (h)	462.2	330.0	---	---	-132.2	-86389	653.47	457.2	325.0
COLD1 (h)	338.3	320.0	-753.49	-762.60	-18.3	-2531	138.28	333.3	315.0
AIR1 (c)	293.0	614.7	-0.02	53.74	321.7	14934	46.42	298.0	619.7
PURGE1 (c)	300.0	533.0	-41.67	-35.27	233.0	1778	7.63	305.0	538.0
HOTFEED1 (c)	338.3	523.0	-433.64	-378.59	184.7	15291	82.79	343.3	528.0
GFRW1-c (c)	380.4	430.3	245.17	254.71	49.9	2651	53.12	385.4	435.3
Drier (c)	293.0	393.0	---	---	100.0	37376	373.76	298.0	398.0
GFRW1-b (c)	380.3	380.4	34.44	245.17	0.1	58535	585353.06	385.3	385.4
GFRW1-a (c)	293.0	380.3	0.00	34.44	87.3	9567	109.62	298.0	385.3
						-79213			

Problem Table

Interval	T(i) (K)	T(i+1) (K)	Ti-T(i+1) (K)	Sum CPhot (kW/K)	Sum CPcold (kW/K)	Cpc-CPh (kW/K)	delta H (kW)	Cascade	Corrected Cascade
0		995.0						0	0
1	995.0	965.0	30.0	58.89	0.00	-58.89	-1767	1767	1767
2	965.0	668.0	297.0	167.09	0.00	-167.09	-49626	51392	51392
3	668.0	619.7	48.3	58.89	0.00	-58.89	-2844	54236	54236
4	619.7	538.0	81.7	58.89	46.42	-12.47	-1019	55255	55255
5	538.0	528.0	10.0	58.89	54.05	-4.84	-48	55304	55304
6	528.0	457.2	70.8	327.32	136.84	-190.48	-13486	68790	68790
7	457.2	435.3	21.9	980.79	136.84	-843.95	-18505	87295	87295
8	435.3	398.0	37.3	980.79	189.96	-790.83	-29477	116772	116772
9	398.0	388.0	10.0	980.79	563.72	-417.07	-4171	120942	120942
10	388.0	385.4	2.6	921.90	563.72	-358.18	-941	121883	121883
11	385.4	385.3	0.1	921.90	585863.66	584941.76	58494	63389	63389
12	385.3	343.3	42.0	921.90	620.22	-301.68	-12662	76051	76051
13	343.3	333.3	10.0	921.90	537.43	-384.47	-3845	79896	79896
14	333.3	325.0	8.3	1060.18	537.43	-522.75	-4339	84235	84235
15	325.0	315.0	10.0	406.71	537.43	130.72	1307	82928	82928
16	315.0	305.0	10.0	268.43	537.43	269.00	2690	80238	80238
17	305.0	298.0	7.0	268.43	529.80	261.37	1830	78409	78409
18	298.0	295.0	3.0	268.43	0.00	-268.43	-805	79214	79214

Table 6A-26: Pinch analysis for hydrogen production from biomass using the MTCI gasifier.

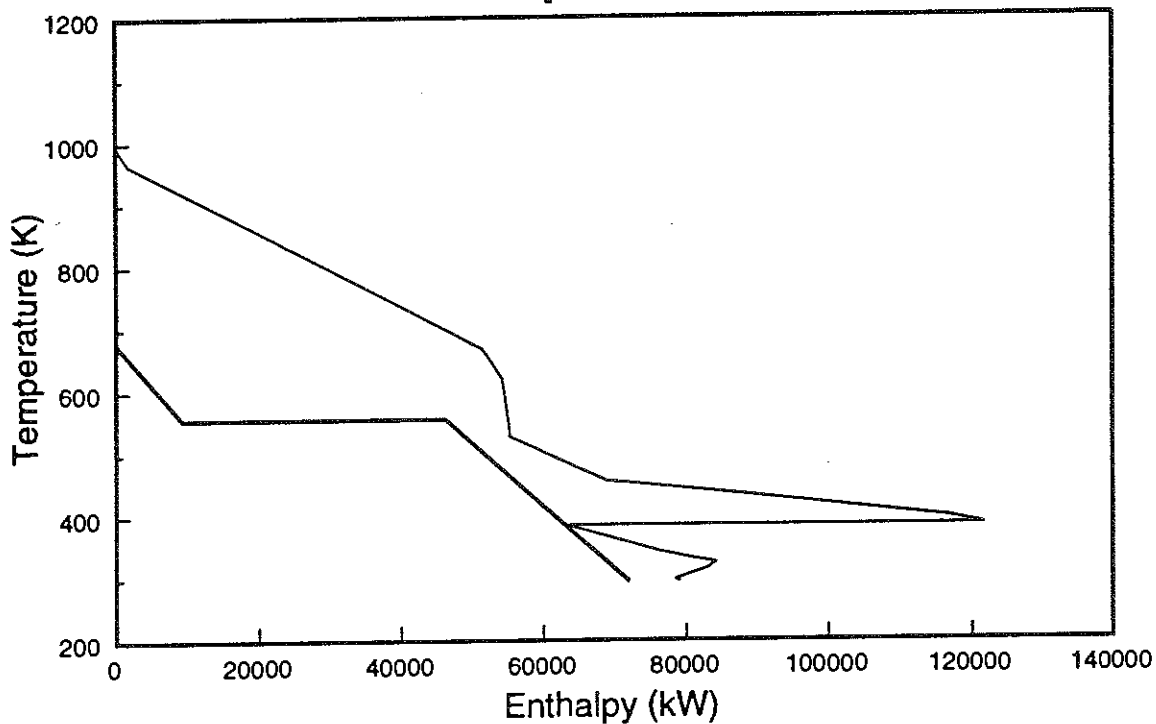
Stream Table

Streams	T source (K)	T target (K)	H in (GJ/hr)	H out (GJ/hr)	Delta T (K)	Delta H (kW)	CP (kW/K)	T source cor'ctd	T target cor'ctd
PPROD1 (h)	1000.0	393.0	-389.36	-525.11	-607.0	-37709	62.12	995.0	388.0
GFRPROD (hot)	970.0	673.0	-1508.99	-1624.67	-297.0	-32134	108.20	965.0	668.0
SHIPT3 (hot)	710.3	500.0	-1873.45	-1959.65	-210.3	-23946	113.89	705.3	495.0
LTS (hot)	500.1	500.0	-1959.65	-1966.16	-0.1	-1807	18073.61	495.1	495.0
SHIPT5-a (hot)	500.0	364.7	0.00	-52.31	-135.3	-14532	107.44	495.0	359.7
PSA2 (h)	436.3	313.0	-888.72	-925.88	-123.3	-10323	83.71	431.3	308.0
RECYC3 (hot)	402.4	313.0	-130.84	-139.07	-89.4	-2284	25.56	397.4	308.0
H22 (hot)	399.5	313.0	10.69	1.82	-86.5	-2463	28.46	394.5	308.0
SHIPT5-b (hot)	364.7	351.6	-52.31	-179.30	-13.1	-35274	2683.16	359.7	346.6
SHIPT5-c (hot)	351.6	313.0	-179.30	-286.88	-38.6	-29883	774.21	346.6	308.0
QCHOUT (cold)	370.0	623.0	-1971.34	-1873.44	253.0	27194	107.49	375.0	628.0
PURGE1 (c)	313.0	533.0	-34.71	-29.29	220.0	1505	6.84	318.0	538.0
PAIR1 (c)	298.0	436.6	-0.03	24.63	138.6	6848	49.40	303.0	441.6
GFRW1-c (c)	380.4	430.3	245.17	254.71	49.9	2651	53.12	385.4	435.3
Drier (c)	293.0	393.0	---	---	100.0	37376	373.76	298.0	398.0
GFRW1-b (c)	380.3	380.4	34.44	245.17	0.1	58535	585353.06	385.3	385.4
GFRW1-a (c)	293.0	380.3	0.00	34.44	87.3	9567	109.62	298.0	385.3
						-46679			

Problem Table

Interval	T(i) (K)	T(i+1) (K)	Ti-T(i+1) (K)	Sum CPhot (kW/K)	Sum CPcold (kW/K)	CPc-CPH (kW/K)	delta H (kW)	Cascade	Corrected Cascade
0		995.0						0	0
1	995.0	965.0	30.0	62.12	0.00	-62.12	-1864	1864	1864
2	965.0	705.3	259.7	170.32	0.00	-170.32	-44238	46101	46101
3	705.3	668.0	37.3	284.21	0.00	-284.21	-10592	56693	56693
4	668.0	628.0	40.0	176.01	0.00	-176.01	-7040	63733	63733
5	628.0	538.0	90.0	176.01	107.49	-68.52	-6167	69900	69900
6	538.0	495.1	42.9	176.01	114.33	-61.68	-2646	72546	72546
7	495.1	495.0	0.1	18249.62	114.33	-18135.29	-1814	74360	74360
8	495.0	441.6	53.4	169.56	114.33	-55.23	-2948	77308	77308
9	441.6	435.3	6.4	169.56	163.73	-5.83	-37	77345	77345
10	435.3	431.3	3.9	169.56	216.85	47.29	187	77158	77158
11	431.3	398.0	33.3	253.27	216.85	-36.42	-1214	78372	78372
12	398.0	397.4	0.6	253.27	590.61	337.34	207	78164	78164
13	397.4	394.5	2.8	278.83	590.61	311.78	888	77276	77276
14	394.5	388.0	6.5	307.29	590.61	283.32	1852	75424	75424
15	388.0	385.4	2.6	245.17	590.61	345.44	907	74517	74517
16	385.4	385.3	0.1	245.17	585890.55	585645.38	58565	15952	15952
17	385.3	375.0	10.3	245.17	647.11	401.94	4129	11823	11823
18	375.0	359.7	15.3	245.17	539.62	294.45	4492	7331	7331
19	359.7	346.6	13.1	2820.89	539.62	-2281.27	-29990	37321	37321
20	346.6	318.0	28.6	911.94	539.62	-372.32	-10648	47969	47969
21	318.0	308.0	10.0	911.94	532.78	-379.16	-3792	51761	51761
22	308.0	303.0	5.0	0.00	532.78	532.78	2664	49097	49097
23	303.0	298.0	5.0	0.00	483.38	483.38	2417	46680	46680

Methanol production



Hydrogen production

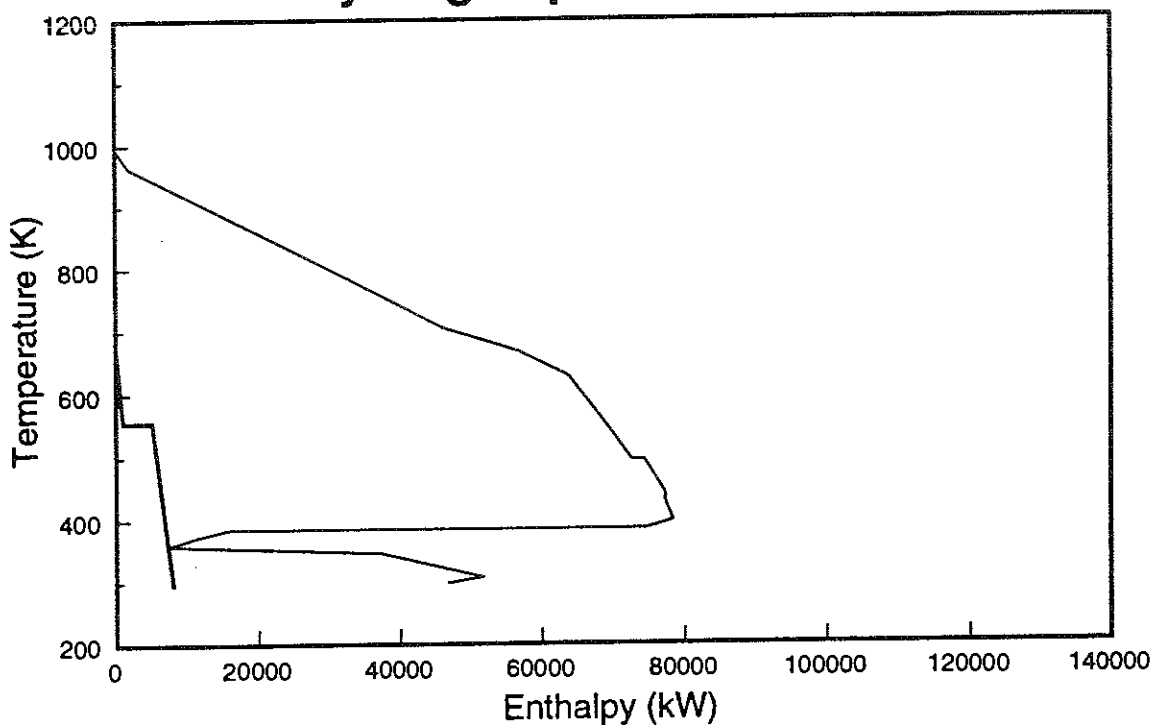


Figure 6A-20: Grand composite curves of methanol and hydrogen production from biomass using the MTCI indirectly-heated gasifier.

Table 6A-27: Calculated material flows for methanol production from biomass based on the BCL Gasifier.

Name	Temp [K]	Pres. Flow [bar]	Total Volume Flow [kmol/hr]	Molecular Weight [kg/kmol]	Component Volumes Flow Rates [kmol/hr]															
					H ₂ O	H ₂	CO	CO ₂	CH ₄	C ₂ H ₄	C ₂ H ₆	O ₂	N ₂	CH ₃ OH						
1 Raw Biomass				3000 tonnes per day	8 45%	moisture														
2 Dried biomass				1673 tonnes per day	8 10%	moisture														
3 Gasifier exit	1200	1.01	4005	21.15	1223	577	1283	309	437	144	20	0	12	0						
4 Quench inlet	673	1.01	4005	21.15	1223	577	1283	309	437	144	20	0	12	0						
5 Quench exit	355	1.01	4974	20.54	2192	577	1283	309	437	144	20	0	12	0						
6 Splitter exit to compressor	355	1.01	4667	20.54	2057	542	1204	290	410	135	19	0	11	0						
7 Compressor exit	577	15.50	4667	20.54	2057	542	1204	290	410	135	19	0	11	0						
8 Reformer feed	850	15.00	5125	20.31	2514	542	1204	290	410	135	19	0	11	0						
9 Reformer exit	1140	14.50	6172	16.87	1502	2447	1373	711	127	0	0	0	11	0						
10 Shift feed	623	14.00	1170	16.87	285	464	260	135	24	0	0	0	2	0						
11 Shift bypass	623	14.00	5002	16.87	1217	1983	1113	576	103	0	0	0	9	0						
12 Shift exit	743	13.50	1666	17.21	587	658	66	329	24	0	0	0	2	0						
13 Mixer exit	655	13.50	6668	16.95	1804	2641	1179	905	127	0	0	0	11	0						
14 Selextol feed	400	13.00	5959	16.83	1095	2641	1179	905	127	0	0	0	11	0						
15 Selextol exit	400	13.00	4040	10.96	0	2641	1179	81	127	0	0	0	11	0						
16 Makeup compressor exit	502	105.88	4040	10.96	0	2641	1179	81	127	0	0	0	11	0						
17 Hot synthesis feed 1	344	105.88	2991	10.98	0	1537	290	59	999	0	0	0	97	8						
18 Hot synthesis feed 2	523	105.38	2991	10.98	0	1537	290	59	999	0	0	0	97	8						
19 Synthesis product	533	97.28	16579	12.61	63	7261	680	311	6362	0	0	0	620	1283						
20 Crude methanol product	300	96.78	1336	31.34	62	2	1	14	26	0	0	0	1	1229						
21 Recycle stream	300	96.78	15244	10.98	1	7258	679	297	6336	0	0	0	619	54						
22 Recycle compressor feed	300	96.78	15000	10.98	1	7142	669	292	6234	0	0	0	609	53						
23 Recycle compressor exit	308	105.88	15000	10.98	1	7142	669	292	6234	0	0	0	609	53						
24 Cold synthesis feed 1	344	105.88	16048	10.98	1	8246	1557	315	5362	0	0	0	523	45						
25 Cold synthesis feed 2	320	105.38	16048	10.98	1	8246	1557	315	5362	0	0	0	523	45						
26 Purge stream	300	96.78	244	10.98	0	116	11	5	101	0	0	0	10	1						
27 Fuel gas to reformer	355	1.01	307	20.54	135	36	79	19	27	9	1	0	1	0						
28 Heated reformer fuel gas	700	1.01	550	16.31	135	152	90	24	128	9	1	0	11	1						
29 Reformer furnace products	1160	1.00	2666	27.56	565	0	0	262	0	0	0	0	61	1776						
30 Stack gases	393	1.00	2666	27.56	565	0	0	262	0	0	0	0	61	1776						
31 Reformer furnace air	298	1.00	2235	28.85	0	0	0	0	0	0	0	0	469	1766						
32 Heated reformer furnace air	1000	1.00	2235	28.85	0	0	0	0	0	0	0	0	469	1766						
33 Reformer steam	523	15.50	458	18.02	458	0	0	0	0	0	0	0	0	0						
34 Shift steam	623	14.00	496	18.02	496	0	0	0	0	0	0	0	0	0						
35 Gasifier steam	430	1.30	1098	18.02	1098	0	0	0	0	0	0	0	0	0						
36 Carbon dioxide removed	400	13.00	1919	29.18	1095	0	0	0	0	0	0	0	0	0						
37 Condensate	400	13.00	709	18.02	709	0	0	0	0	0	0	0	0	0						
38 Quench feed water	293	1.50	1500	18.02	1500	0	0	0	0	0	0	0	0	0						
39 Quench condensate	355	1.01	531	18.02	531	0	0	0	0	0	0	0	0	0						
40 Combustor air	298	1.00	6492	28.85	0	0	0	0	0	0	0	0	1364	5128						
41 Preheated combustor air	866	1.00	6492	28.85	0	0	0	0	0	0	0	0	1364	5128						

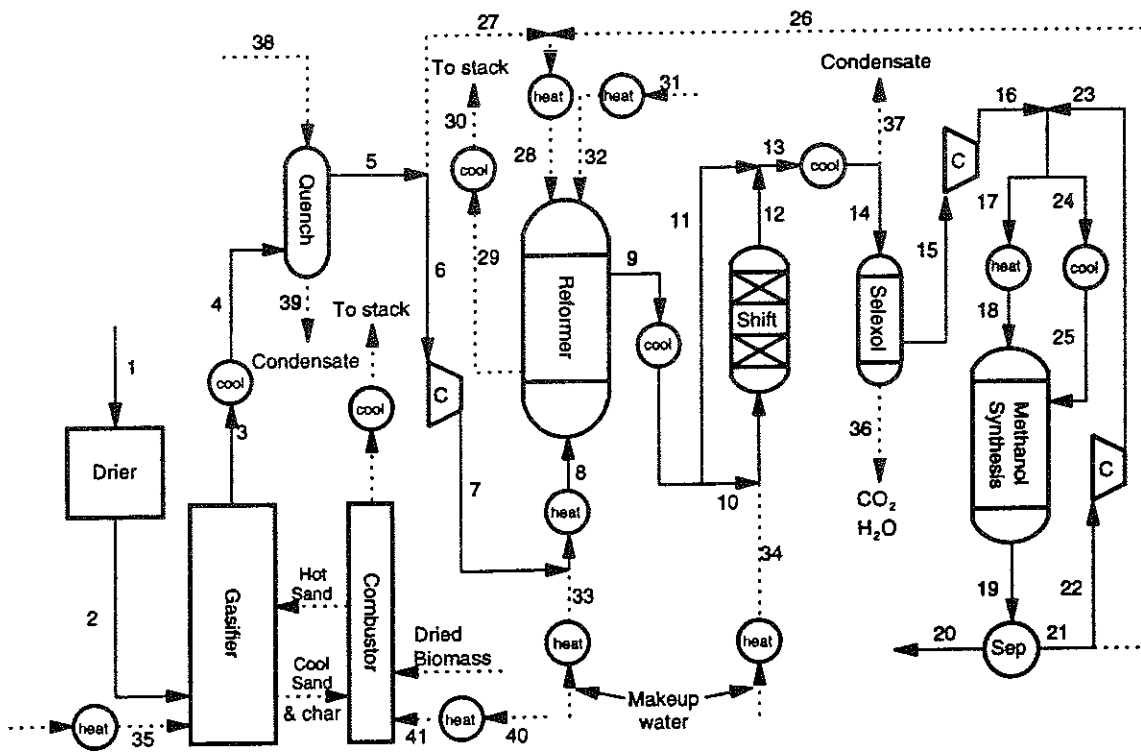


Figure 6A-21: Process configuration for the modeling of methanol production from biomass based on the Battelle Columbus Laboratory indirectly-heated gasifier.

Table 6A-28: Calculated material flows for hydrogen production from biomass based on the BCL Gasifier.

Name	Temp [K]	Pres. Flow [bar]	Total Volume Flow [kmol/hr]	Molecular Weight [kg/kmol]	Component Volume Flow Rates [kmol/hr]									
					H ₂ O	H ₂	CO	CO ₂	CH ₄	C ₂ H ₄	C ₂ H ₆	O ₂	N ₂	
1 Raw Biomass			3000 tonnes per day		% 45% moisture									
2 Dried biomass			1673 tonnes per day		% 45% moisture									
3 Gasifier exit	1200	1.01	4005	21.15	1223	577	1283	309	437	144	20	0	12	
4 Quench inlet	673	1.01	4005	21.15	1223	577	1283	309	437	144	20	0	12	
5 Quench exit	355	1.01	4974	20.54	2192	577	1283	309	437	144	20	0	12	
6 Splitter exit to compressor	355	1.01	4933	20.54	2174	573	1272	306	433	143	20	0	12	
7 Compressor exit	577	15.50	4933	20.54	2174	573	1272	306	433	143	20	0	12	
8 Reformer feed	850	15.00	5037	20.49	2278	573	1272	306	433	143	20	0	12	
9 Reformer exit	1140	14.50	6091	16.94	1307	2434	1498	679	161	0	0	0	12	
10 High temperature shift feed	623	14.00	6091	16.94	1307	2434	1498	679	161	0	0	0	12	
11 High temperature shift exit	748	13.50	9278	17.31	3357	3571	361	1816	161	0	0	0	12	
12 Low temperature shift feed	500	13.00	9278	17.31	3357	3571	361	1816	161	0	0	0	12	
13 Low temperature shift exit	500	12.50	9278	17.31	3028	3901	32	2145	161	0	0	0	12	
14 PSA makeup feed	313	12.00	6281	16.98	31	3901	32	2145	161	0	0	0	12	
15 PSA-A feed	313	12.00	7592	16.18	31	4393	158	2145	805	0	0	0	60	
16 PSA-B feed	313	11.65	5416	5.15	0	4393	158	0	805	0	0	0	60	
17 Hydrogen compressor feed	313	11.30	3778	2.02	0	3778	0	0	0	0	0	0	0	
18 Hydrogen compressor exit	409	75.00	3778	2.02	0	3778	0	0	0	0	0	0	0	
19 Cooled Hydrogen product	313	75.00	3778	2.02	0	3778	0	0	0	0	0	0	0	
20 PSA recycle stream	313	1.30	1638	12.37	0	615	158	805	0	0	0	0	60	
21 Recycle compressor feed	313	1.30	1310	12.37	0	492	127	644	0	0	0	0	48	
22 Recycle compressor exit	409	12.20	1310	12.37	0	492	127	644	0	0	0	0	48	
23 PSA-A recycle feed	313	12.00	1310	12.37	0	492	127	644	0	0	0	0	48	
24 Purge stream	313	1.30	328	12.37	0	123	32	161	0	0	0	0	12	
25 Fuel gas to reformer	355	1.01	40	20.54	18	5	10	3	1	0	0	0	0	
26 Heated purge stream	700	1.01	368	13.27	18	128	42	165	1	0	0	0	12	
27 Reformer furnace products	1160	1.00	2572	27.57	477	0	0	212	0	0	0	63	1820	
28 Stack gases	393	1.00	2572	27.57	477	0	0	212	0	0	0	63	1820	
29 Reformer furnace air	298	1.00	2289	28.85	0	0	0	0	0	0	0	481	1808	
30 Heated reformer furnace air	1000	1.00	2289	28.85	0	0	0	0	0	0	0	481	1808	
31 Gasifier steam	430	1.30	1098	18.02	1098	0	0	0	0	0	0	0	0	
32 Reformer steam	523	15.50	104	18.02	104	0	0	0	0	0	0	0	0	
33 Shift steam	623	14.00	3187	18.02	3187	0	0	0	0	0	0	0	0	
34 Carbon dioxide removed	313	1.30	2176	43.64	31	0	0	2145	0	0	0	0	0	
35 Condensate	313	12.00	2997	18.02	2996	0	0	0	0	0	0	0	0	
36 Quench feed water	293	1.50	1500	18.02	1500	0	0	0	0	0	0	0	0	
37 Quench condensate	355	1.01	531	18.02	531	0	0	0	0	0	0	0	0	
38 Combustor air	298	1.00	6492	28.85	0	0	0	0	0	0	0	1364	5128	
39 Preheated combustor air	866	1.00	6492	28.85	0	0	0	0	0	0	0	1364	5128	

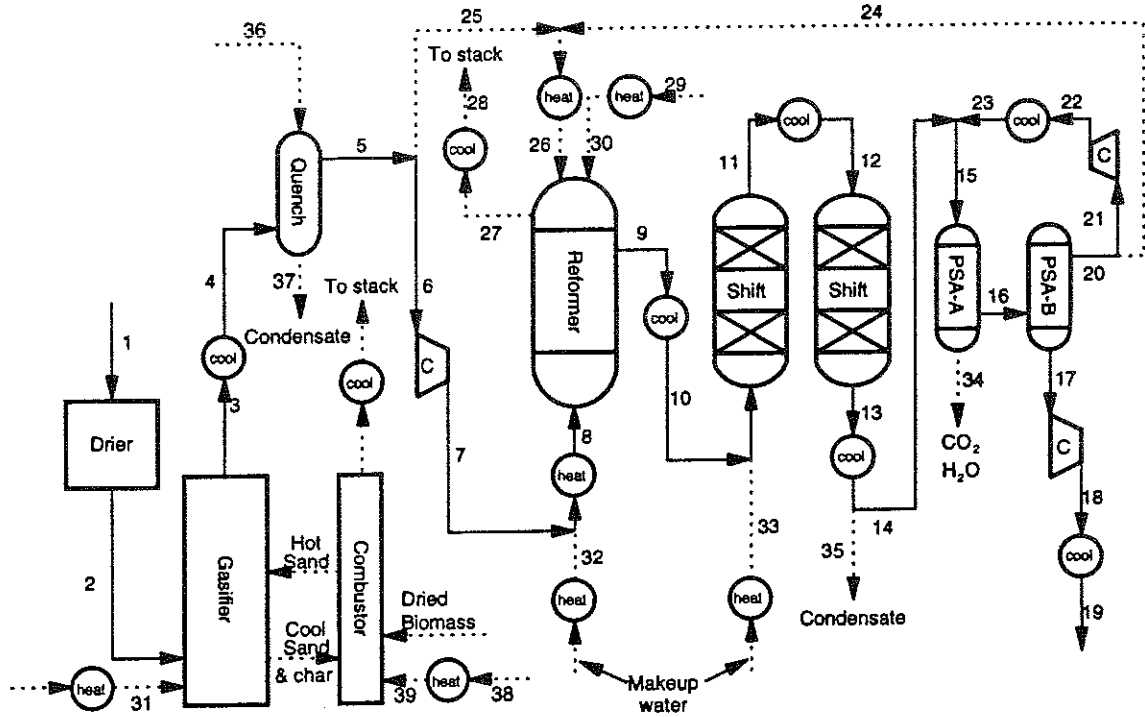


Figure 6A-22: Process configuration for the modeling of hydrogen production from biomass based on the Battelle Columbus Laboratory indirectly-heated gasifier.

Table 6A-29: Pinch analysis for methanol production from biomass using the BCL indirectly-heated gasifier.

Stream Table

Streams	T source (K)	T target (K)	H in (GJ/hr)	H out (GJ/hr)	Delta T (K)	Delta H (kW)	CP (kW/K)	T source cor'ctd	T target cor'ctd
Flue (hot)	1366.3	393.0	-71.12	-295.56	-973.3	-62343	64.05	1361.3	388.0
GFRPROD (hot)	1199.7	673.0	-422.59	-532.76	-526.7	-30601	58.10	1194.7	668.0
COMB1 (h)	1160.2	393.0	-161.22	-232.25	-767.2	-19732	25.72	1155.2	388.0
REFPROD (h)	1140.0	623.0	-623.70	-739.77	-517.0	-32242	62.36	1135.0	618.0
SHIFT6-a (h)	654.5	412.7	0.00	-54.95	-241.8	-15263	63.13	649.5	407.7
SYNPROD (h)	533.0	320.0	-808.69	-1005.44	-213.0	-54654	256.59	528.0	315.0
SHIFT6-b (h)	412.7	400.0	-54.95	-86.96	-12.7	-8893	701.21	407.7	395.0
COLD1 (h)	344.4	320.0	-686.28	-699.75	-24.4	-3743	153.26	339.4	315.0
AIR1 (cold)	298.0	1000.0	-0.01	48.61	702.0	13505	19.24	303.0	1005.0
C. Air (cold)	298.0	866.3	-0.02	112.72	568.3	31316	55.10	303.0	871.3
REFFEED3 (c)	571.3	850.0	-833.34	-777.07	278.7	15632	56.08	576.3	855.0
FUEL2 (c)	341.2	700.0	-60.65	-53.43	358.8	2007	5.59	346.2	705.0
SHW2-c (c)	468.3	623.0	24.14	27.38	154.7	900	5.82	473.3	628.0
REFW2-c (c)	473.1	523.0	22.28	23.36	49.9	298	5.98	478.1	528.0
HOTFEED1 (c)	344.4	523.0	-127.91	-108.93	178.6	5271	29.52	349.4	528.0
REFW2-b (c)	473.0	473.1	6.30	22.28	0.1	4440	44396.67	478.0	478.1
REFW2-a (c)	293.0	473.0	0.00	6.30	180.0	1750	9.72	298.0	478.0
SHW2-b (c)	468.2	468.3	6.64	24.14	0.1	4861	48606.11	473.2	473.3
SHW2-a (c)	293.0	468.2	0.00	6.64	175.2	1846	10.54	298.0	473.2
GFRW2-c (c)	380.4	430.3	51.47	53.47	49.9	557	11.15	385.4	435.3
Drier (cold)	293.0	393.0	---	---	100.0	47112	471.12	298.0	398.0
GFRW2-b (c)	380.3	380.4	7.23	51.47	0.1	12288	122881.67	385.3	385.4
GFRW2-a (c)	293.0	380.3	0.00	7.23	87.3	2008	23.01	298.0	385.3
						-83680			

Problem Table

Interval	T(i) (K)	T(i+1) (K)	Ti-T(i+1) (K)	Sum CPhot (kW/K)	Sum CPcold (kW/K)	CPc-CPH (kW/K)	delta H (kW)	Cascade	Corrected Cascade
0		1361.3						0	0
1	1361.3	1194.7	166.6	64.05	0.00	-64.05	-10671	10671	10671
2	1194.7	1155.2	39.5	122.15	0.00	-122.15	-4821	15492	15492
3	1155.2	1135.0	20.2	147.87	0.00	-147.87	-2991	18483	18483
4	1135.0	1005.0	130.0	210.23	0.00	-210.23	-27330	45813	45813
5	1005.0	871.3	133.7	210.23	19.24	-190.99	-25535	71349	71349
6	871.3	855.0	16.3	210.23	74.34	-135.89	-2215	73564	73564
7	855.0	705.0	150.0	210.23	130.42	-79.81	-11972	85535	85535
8	705.0	668.0	37.0	210.23	136.01	-74.22	-2746	88281	88281
9	668.0	649.5	18.5	152.13	136.01	-16.12	-299	88580	88580
10	649.5	628.0	21.5	215.26	136.01	-79.25	-1702	90282	90282
11	628.0	618.0	10.0	215.26	141.83	-73.43	-734	91016	91016
12	618.0	576.3	41.7	152.90	141.83	-11.07	-462	91478	91478
13	576.3	528.0	48.3	152.90	85.75	-67.15	-3241	94719	94719
14	528.0	478.1	49.9	409.49	121.25	-288.24	-14383	109102	109102
15	478.1	478.0	0.1	409.49	44511.94	44102.45	4410	104692	104692
16	478.0	473.3	4.7	409.49	124.99	-284.50	-1340	106032	106032
17	473.3	473.2	0.1	409.49	48725.28	48315.79	4832	101200	101200
18	473.2	435.3	37.9	409.49	129.71	-279.78	-10610	111810	111810
19	435.3	407.7	27.6	409.49	140.86	-268.63	-7412	119222	119222
20	407.7	398.0	9.7	1047.57	140.86	-906.71	-8779	128001	128001
21	398.0	395.0	3.0	1047.57	611.98	-435.59	-1307	129308	129308
22	395.0	388.0	7.0	346.36	611.98	265.62	1859	127448	127448
23	388.0	385.4	2.6	256.59	611.98	355.39	934	126515	126515
24	385.4	385.3	0.1	256.59	123482.50	123225.91	12323	114192	114192
25	385.3	349.4	35.9	256.59	623.84	367.25	13167	101026	101026
26	349.4	346.2	3.2	256.59	594.32	337.73	1085	99940	99940
27	346.2	339.4	6.8	256.59	588.73	332.14	2254	97686	97686
28	339.4	315.0	24.4	409.85	588.73	178.88	4369	93318	93318
29	315.0	303.0	12.0	0.00	588.73	588.73	7065	86253	86253
30	303.0	298.0	5.0	0.00	514.79	514.79	2574	83679	83679

Table 6A-30: Pinch analysis for hydrogen production from biomass using the BCL indirectly-heated gasifier.

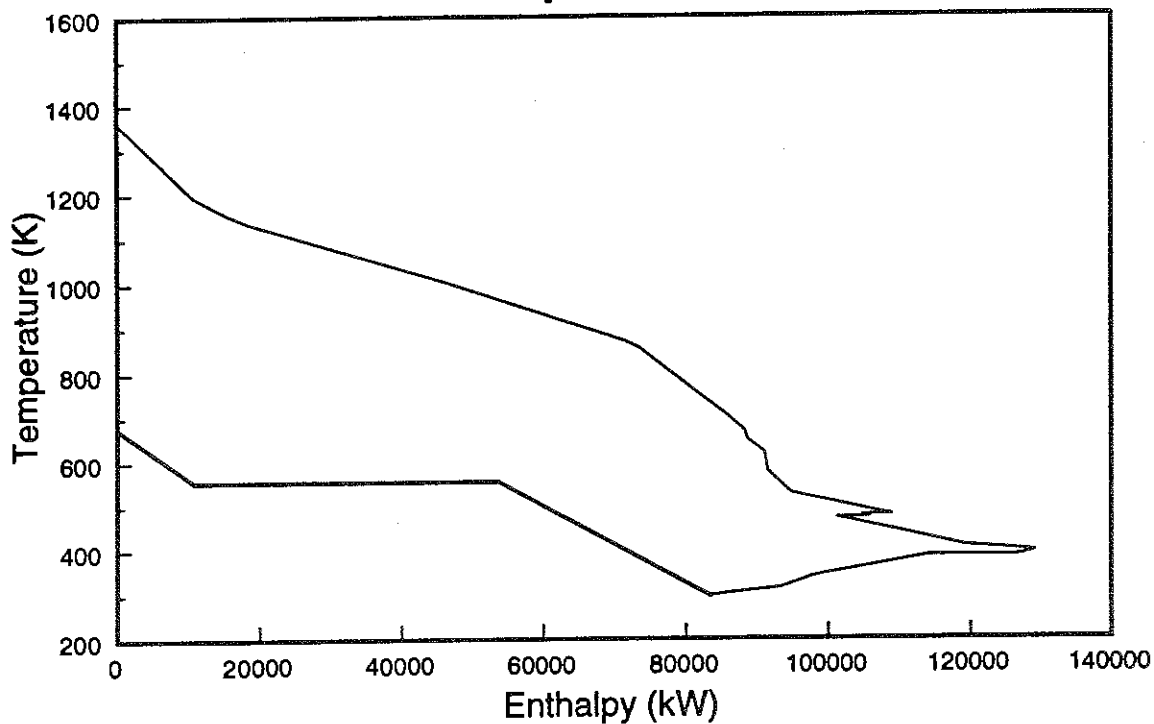
Stream Table

Streams	T source (K)	T target (K)	H in (GJ/hr)	H out (GJ/hr)	Delta T (K)	Delta H (kW)	CP (kW/K)	T source cor'ctd	T target cor'ctd
Flue (hot)	1366.3	393.0	-71.12	-295.56	-973.3	-62343	64.05	1361.3	388.0
GFRPROD (hot)	1199.7	673.0	-422.59	-532.76	-526.7	-30601	58.10	1194.7	668.0
COMB1 (hot)	1160.0	393.0	-123.88	-191.43	-767.0	-18763	24.46	1155.0	388.0
REFPROD (hot)	1140.0	623.0	-583.10	-697.31	-517.0	-31726	61.37	1135.0	618.0
SHIFT3 (hot)	748.3	500.0	-1433.85	-1517.85	-248.3	-23332	93.98	743.3	495.0
LTS (hot)	500.1	500.0	---	---	-0.1	-3604	36036.11	495.1	495.0
SHIFT5-a (hot)	500.0	416.4	0.00	-27.21	-83.6	-7558	90.42	495.0	411.4
SHIFT5-b (hot)	416.4	372.7	-27.21	-147.86	-43.7	-33515	767.51	411.4	367.7
RECYC3 (hot)	409.0	313.0	-57.39	-61.70	-96.0	-1196	12.46	404.0	308.0
H22 (hot)	408.6	313.0	12.39	1.94	-95.6	-2903	30.37	403.6	308.0
SHIFT5-c (hot)	372.7	313.0	-147.86	-197.15	-59.7	-13691	229.14	367.7	308.0
AIR1 (cold)	298.0	1000.0	-0.01	49.77	702.0	13829	19.70	303.0	1005.0
C. Air (cold)	298.0	866.3	-0.02	112.72	568.3	31316	55.10	303.0	871.3
REFFEED3 (c)	575.8	850.0	-791.56	-737.01	274.2	15152	55.26	580.8	855.0
FUEL2 (c)	317.6	700.0	-22.01	-16.67	382.4	1484	3.88	322.6	705.0
SHW2-c (c)	468.3	623.0	155.12	175.93	154.7	5781	37.37	473.3	628.0
REFW2-c (c)	473.1	523.0	5.07	5.31	49.9	68	1.36	478.1	528.0
REFW2-b (c)	473.0	473.1	1.43	5.07	0.1	1010	10098.89	478.0	478.1
REFW2-a (c)	293.0	473.0	0.00	1.43	180.0	398	2.21	298.0	478.0
SHW2-b (c)	468.2	468.3	42.74	155.12	0.1	31215	312146.67	473.2	473.3
SHW2-a (c)	293.0	468.2	0.00	42.74	175.2	11873	67.77	298.0	473.2
GFRW2-c (c)	380.4	430.3	51.47	53.47	49.9	557	11.15	385.4	435.3
Drier (cold)	293.0	393.0	---	---	100.0	47112	47112	298.0	398.0
GFRW2-b (c)	380.3	380.4	7.23	51.47	0.1	12288	122881.67	385.3	385.4
GFRW2-a (c)	293.0	380.3	0.00	7.23	87.3	2008	23.01	298.0	385.3
						-55141			

Problem Table

Interval	T(i) (K)	T(i+1) (K)	Ti-T(i+1) (K)	Sum CPhot (kW/K)	Sum CPcold (kW/K)	CPC-CPh (kW/K)	delta H (kW)	Cascade	Corrected Cascade
0		1361.3						0	0
1	1361.3	1194.7	166.6	64.05	0	-64.05	-10671	10671	10671
2	1194.7	1155.0	39.7	122.15	0	-122.15	-4849	15520	15520
3	1155.0	1135.0	20.0	146.61	0	-146.61	-2932	18452	18452
4	1135.0	1005.0	130.0	207.98	0	-207.98	-27037	45490	45490
5	1005.0	871.3	133.7	207.98	19.7	-188.28	-25173	70663	70663
6	871.3	855.0	16.3	207.98	74.8	-133.18	-2171	72834	72834
7	855.0	743.3	111.7	207.98	130.06	-77.92	-8706	81540	81540
8	743.3	705.0	38.3	301.96	130.06	-171.90	-6578	88118	88118
9	705.0	668.0	37.0	301.96	133.94	-168.02	-6217	94335	94335
10	668.0	628.0	40.0	243.86	133.94	-109.92	-4397	98731	98731
11	628.0	618.0	10.0	243.86	171.31	-72.55	-726	99457	99457
12	618.0	580.8	37.2	182.49	171.31	-11.18	-416	99873	99873
13	580.8	528.0	52.8	182.49	116.05	-66.44	-3507	103380	103380
14	528.0	495.1	32.9	182.49	117.41	-65.08	-2141	105521	105521
15	495.1	495.0	0.1	36218.6	117.41	-36101.19	-3610	109132	109132
16	495.0	478.1	16.9	178.93	117.41	-61.52	-1039	110171	110171
17	478.1	478.0	0.1	178.93	10214.94	10036.01	1004	109167	109167
18	478.0	473.3	4.7	178.93	118.26	-60.67	-286	109453	109453
19	473.3	473.2	0.1	178.93	312227.56	312048.63	31205	78248	78248
20	473.2	435.3	37.9	178.93	148.66	-30.27	-1148	79396	79396
21	435.3	411.4	23.9	178.93	159.81	-19.12	-456	79852	79852
22	411.4	404.0	7.4	856.02	159.81	-696.21	-5163	85015	85015
23	404.0	403.6	0.4	868.48	159.81	-708.67	-293	85308	85308
24	403.6	398.0	5.6	898.85	159.81	-739.04	-4129	89436	89436
25	398.0	388.0	10.0	898.85	630.93	-267.92	-2679	92116	92116
26	388.0	385.4	2.6	810.34	630.93	-179.41	-471	92587	92587
27	385.4	385.3	0.1	810.34	123501.45	122691.11	12269	80318	80318
28	385.3	367.7	17.5	810.34	642.79	-167.55	-2936	83254	83254
29	367.7	322.6	45.2	271.97	642.79	370.82	16753	66501	66501
30	322.6	308.0	14.6	271.97	638.91	366.94	5346	61155	61155
31	308.0	303.0	5.0	0.00	638.91	638.91	3195	57960	57960
32	303.0	298.0	5.0	0.00	564.11	564.11	2821	55140	55140

Methanol production



Hydrogen production

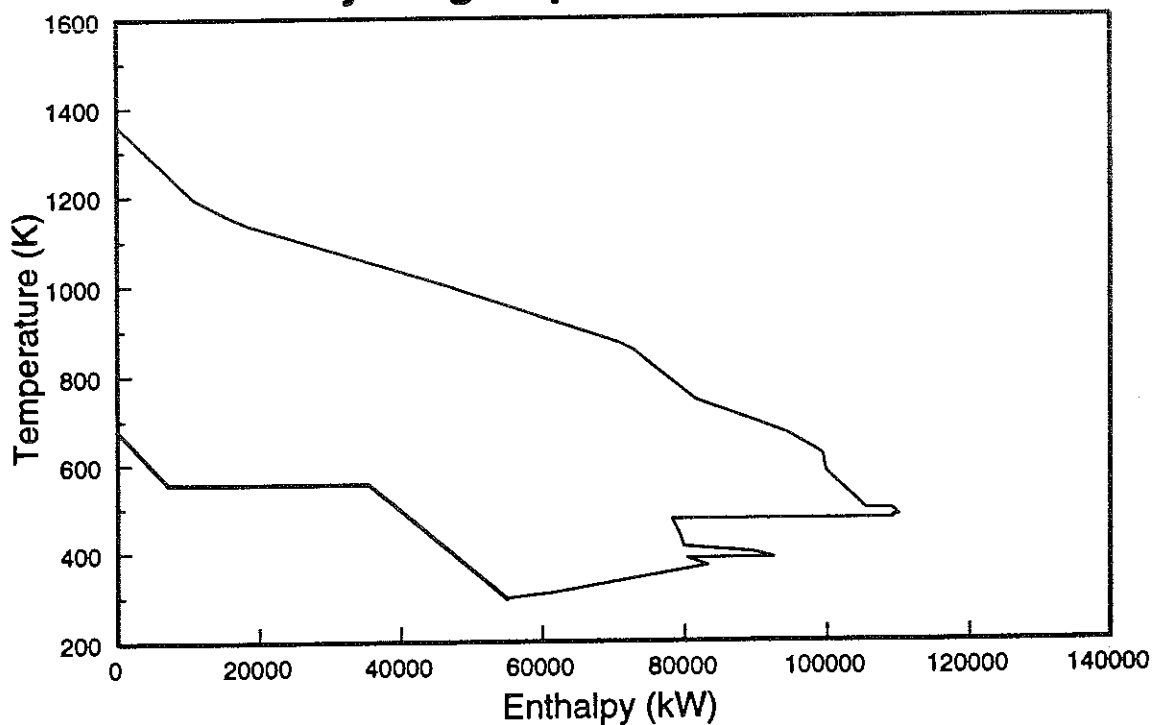
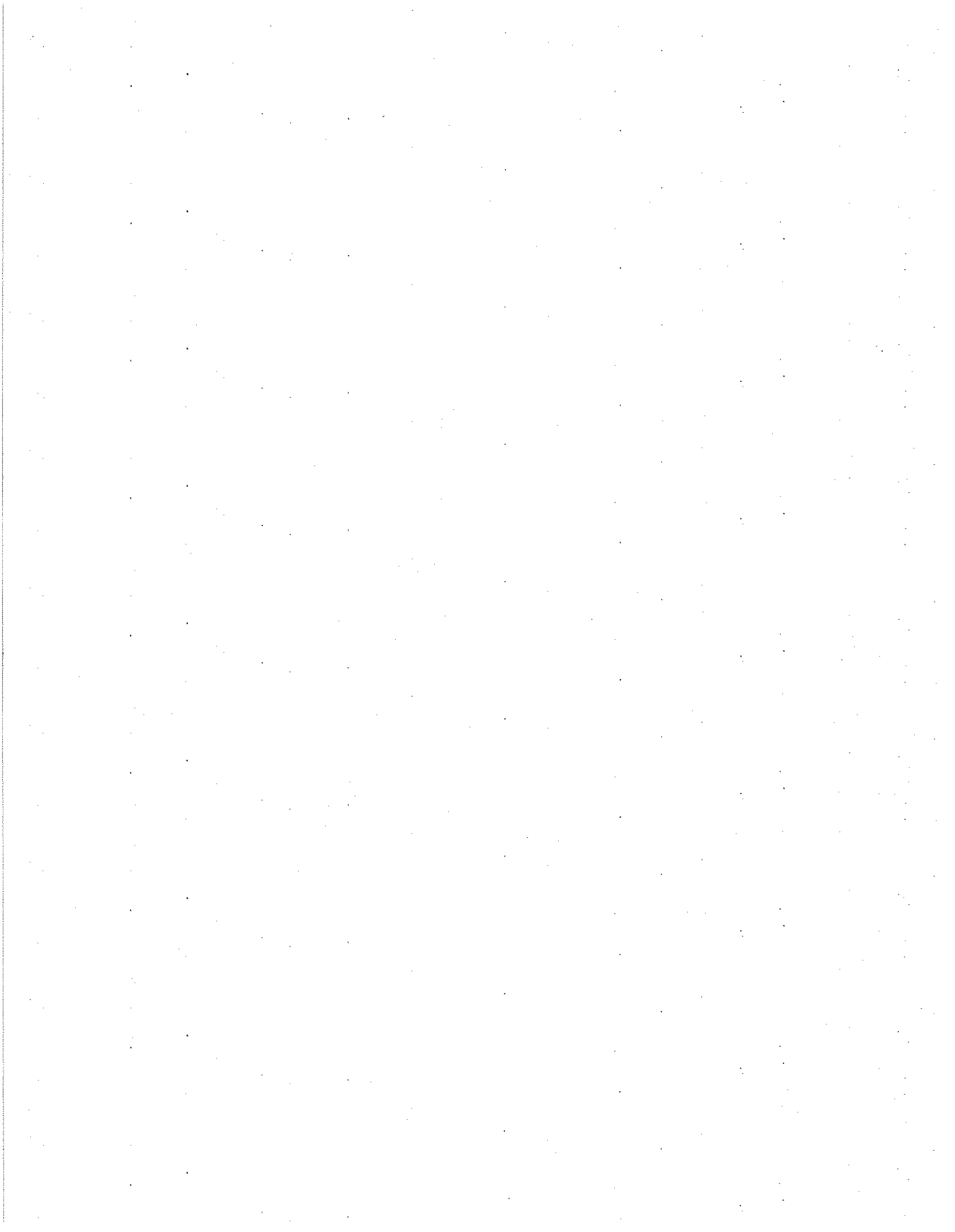


Figure 6A-23: Grand composite curves of methanol and hydrogen production from biomass using the Battelle-Columbus Laboratory (BCL) indirectly-heated gasifier.



Chapter 7: The Economics of Methanol and Hydrogen Production

7.1 Introduction

In Chapter 6 it was shown that by using advanced indirect gasification technology, methanol and hydrogen could be produced more efficiently from biomass than from coal, but less efficiently than from natural gas. Nevertheless, efficiency is not the only criterion to use when selecting an energy source. This chapter builds upon the results of Chapter 6 and addresses the economic aspects of methanol and hydrogen production. There are two basic questions that must be answered. The first is whether or not biomass will be considered seriously as a feedstock for methanol and hydrogen production, given that these fuels can also be manufactured from coal and natural gas. The economics of biomass energy will have to be attractive enough such that people will be willing to risk the shift from well established, conventional energy sources to an entirely new one. To answer this question, economic estimates of the cost of production (COP) of methanol and hydrogen from biomass, coal, and natural gas are made, drawing upon previous studies where necessary. The second question is, assuming that biomass is used as a feedstock for transportation fuels, can these fuels compete with gasoline when crude oil costs \$20-25 per barrel, the price of crude oil today. In answering these two questions, this chapter seeks to evaluate the prospects for using methanol and hydrogen produced from biomass, and how they might be integrated into an overall strategy to supply clean fuels to a transportation sector that will be significantly different in the future than it is today. This chapter will show that methanol and hydrogen produced from biomass have the potential become highly competitive in the medium- to long-term, even if coal and crude oil prices remain at or near current levels, and if natural gas prices rise as expected in current projections.

50% of the total cost of production at today's gas prices, and will account for an even higher percentage in the future.

7.2.1 Natural Gas Costs

The cost of natural gas has varied considerably over the last 25 years. In 1970 the delivered cost of natural gas in the US was approximately \$0.80/GJ, whereas in 1985 it was as high as \$3.75/GJ (DOE, 1991). Today, the cost of natural gas in the United States is approximately \$2/GJ, reflecting a relatively low demand for this resource when compared with projections made in the 1980s.

According to the USDOE's *National Energy Strategy*, the delivered price of natural gas will increase steadily over the next 40 years, reaching \$8.50-8.80/GJ by the year 2030 (DOE, 1991).¹ This corresponds to a well-head natural gas price of \$7.25-7.35/GJ in the year 2030. A more recent estimate of the world natural gas price (CEC, 1992) is in close agreement with this projection. That study assumed the following prices: \$2.56/GJ in 1995, \$3.07/GJ in 2000, and \$3.58/GJ in 2005, equivalent to an average growth rate 3.42% per year. If this growth rate persists beyond 2005, the price of natural gas will reach \$8.30/GJ by the year 2030.

It is difficult to assess the accuracy of these projections. However, the use of natural gas is expected to increase significantly in the future, as the demand grows for lower polluting fuels. Currently, natural gas is used at roughly half the rate of oil, as measured by the ratio of the total estimated resources to the annual production (Williams, 1992). Total natural gas resources are estimated to be roughly equal to oil resources (~9000 EJ). If the rate of use of natural gas becomes comparable to that of crude oil,

¹ This is the delivered cost to the industrial sector. The delivered cost to the utility sector is slightly lower.

technologies, these estimates are probably high (Johansson, et al., 1992a). Therefore, for the subsequent analysis, it is assumed that the world oil price remains in the \$20-25/bbl range for the time period considered for natural gas and coal above. This corresponds to a retail gasoline price (without taxes) of \$8.5-9.5/GJ (\$0.30-0.33/liter, \$1.12-1.25/gallon), as calculated using the following formula from Johansson, et al. (1992a), and assuming gasoline has a HHV of 34.8 MJ/liter.

$$P_{gasoline} = 0.00699 * P_{crude} + 0.156 \text{ \$/liter} \quad (7-1)$$

where $P_{gasoline}$ is in \$/liter and P_{crude} is in \$/barrel.

This gasoline price includes the cost of refining, the added costs of producing reformulated gasoline, storage and distribution, and the markup at the retail level. Taxes are not included.

7.2.4 Biomass Costs

Since low cost biomass residues are a limited resource, the analysis here focusses on the use of biomass grown on dedicated energy plantations. Biomass must be collected over a wide area, making its cultivation a labor intensive activity. Therefore, the cost of biomass should be lower in countries with lower wages. Some recent costs estimates for biomass grown on plantations are summarized in Table 7-1, along with the current and projected prices of fossil fuels. Estimates for the delivered cost of biomass range from \$1.40/GJ for *Eucalyptus* grown on a large scale in northeast Brazil to \$4/GJ for *Switchgrass* grown in the United States. The Brazilian estimates are based on actual experience with commercial plantations, and are indicative of average costs that would

Table 7-1 Levelized costs of production for plantation biomass grown in the United States and Brazil, and current and projected fossil fuel prices. n/a = not available.

Location and Type	Levelized Cost of Production (\$/GJ)	
	1990	2010
Brazil^a		
Eucalyptus	1.41	n/a
U.S. Midwest^b		
Hybrid poplar	3.61	2.59
Switchgrass	4.00	2.83
Sorghum	2.83	1.94
U.S. Southeast		
Energy cane	3.08	1.93
Switchgrass	3.65	2.27
Crude oil ^c	3.61	3.61-5.42
Natural Gas ^d	2.11	4.24-5.94
Coal ^d	1.50	1.91

(a) Based on actual experience with commercial *Eucalyptus* plantations (Carpentieri, et al., 1992).

(b) Based on a 6% discount rate, 6 months of storage and an average transportation distance of 40 km (Hall, et al., 1992).

(c) The 1990 cost assumes a crude oil cost of \$22/bbl and a higher heating value of 145 MJ/gallon. The 2010 cost assumes oil will cost anywhere from \$22-33/bbl, the higher estimate being based on the projections of the National Energy Strategy (DOE, 1991).

(d) The 1990 cost is the delivered cost to the industrial sector in the United States (DOE, 1991). Projections for 2010 are based on DOE (1991) and CEC (1992), the latter providing estimates for world energy prices.

extent to which it will be necessary to quantify environmental externalities in order to make biomass derived fuels cost competitive with gasoline and with methanol and hydrogen produced from coal or natural gas.

7.3 Baseline Production Cost Estimates

Economic estimates for methanol and hydrogen production from biomass that were developed previously (Larson and Katofsky, 1992) were used to estimate the total

Table 7-2: Estimated production costs for methanol from natural gas, coal and biomass. All energy quantities are on a higher heating value basis. All costs are in 1991 U.S. Dollars.

Conversion technology	SMR	SMR-CO ₂	Shell-coal	Shell-bio	IGT	WM	MTCI	BCL
Feedstock throughput capacity^a								
Dry tonnes per day	1224	1224	5000	1650	1650	1650	1650	1650
GJ per hour	2700	2700	6188	1325	1325	1439	1334	1383
Output production capacity^a								
Tonnes per day	2012	2114	4252	950	794	1012	868	945
GJ per hour	1903	1999	4023	898	751	957	821	894
Annual feed and output^b								
Feed (10 ⁶ GJ per year)	21.30	21.30	48.82	10.46	10.46	11.35	10.52	10.91
Product output (10 ⁶ GJ per year)	15.01	15.77	31.74	7.09	5.93	7.55	6.48	7.06
CAPITAL COSTS (10⁶ \$)								
Hardware (installed cost)								
Feed preparation ^c	0.00	0.00	64.52	36.83	16.44	7.40	13.69	19.74
Gasifier ^d	0.00	0.00	113.97	28.23	28.23	64.00	15.16	7.23
High temperature gas cooling ^e	0.00	0.00	133.18	0.00	0.00	0.00	0.00	0.00
Oxygen plant ^f	0.00	0.00	107.52	55.35	41.67	0.00	0.00	0.00
Sulfur recovery ^g	0.00	0.00	34.41	0.00	0.00	0.00	0.00	0.00
Reformer feed compressor ^h	0.00	0.00	0.00	0.00	0.00	0.00	12.40	11.04
Reformer ⁱ	28.43	23.87	0.00	0.00	17.70	16.36	0.00	15.50
Vessels/exchangers/pumps/filters ^j	9.40	9.40	20.43	9.40	9.40	9.40	9.40	9.40
CO ₂ removal ^k	0.00	21.89	59.50	22.05	20.20	12.72	15.38	14.47
Methanol synthesis & purification ^l	76.51	79.05	125.39	46.60	41.42	48.62	43.93	46.47
Utilities/auxiliaries ^m	28.59	33.55	164.73	49.61	43.77	39.62	27.49	30.96
Subtotal	142.93	167.75	823.64	248.07	218.84	198.11	137.46	154.81
Contingencies ⁿ	28.59	33.55	164.73	49.61	43.77	39.62	27.49	30.96
Owners costs, fees, profits ^p	14.29	16.78	82.36	24.81	21.88	19.81	13.75	15.48
Startup ^q	6.91	6.91	23.92	6.91	6.91	6.91	6.91	6.91
Total capital requirement	192.71	224.99	1094.66	329.41	291.40	264.46	185.61	208.16
Working capital ^p	14.29	16.78	82.36	24.81	21.88	19.81	13.75	15.48
Land ^q	2.30	2.30	6.97	2.30	2.30	2.30	2.30	2.30
OPERATING COSTS (10⁶ \$ per year)								
Variable costs								
Feed ^r	42.60	42.60	73.23	20.91	20.91	22.70	21.05	21.82
Catalysts and chemicals ^s	2.54	2.54	8.80	0.49	1.73	1.73	0.49	2.59
Purchased energy ^t	5.45	3.19	11.45	3.96	2.15	7.00	3.53	1.63
Subtotal	50.59	48.33	93.47	25.37	24.79	31.43	25.08	26.04
Fixed costs ^t								
Labor	0.70	0.70	3.30	0.99	0.99	1.18	1.18	1.18
Maintenance	4.29	5.03	24.71	7.44	6.57	5.94	4.12	4.64
General Overhead	3.25	3.73	18.21	5.48	4.91	4.63	3.45	3.79
Direct Overhead	0.32	0.32	1.49	0.45	0.45	0.53	0.53	0.53
Subtotal	8.56	9.78	47.71	14.36	12.91	12.28	9.28	10.14
Total operating costs	59.14	58.11	141.18	39.73	37.70	43.72	34.36	36.19
LEVELIZED COSTS (\$ per GJ)								
Capital ^u	2.05	2.27	5.48	7.39	7.82	5.58	4.57	4.70
Labor & maintenance	0.74	0.78	1.78	2.10	2.47	1.86	1.51	1.80
Purchased energy	0.36	0.20	0.36	0.56	0.36	0.93	0.55	0.23
Feedstock	2.84	2.70	2.31	2.95	3.53	3.01	3.25	3.09
Total	5.99	5.96	9.93	13.00	14.18	11.37	9.88	9.83
Total (\$/liter)	0.11	0.11	0.18	0.24	0.26	0.21	0.18	0.18

Notes to Table 7-2 and Table 7-3

- (a) Based on the *Energy Ratios* presented in Chapter 6.
- (b) Assuming a 90% capacity factor.
- (c) Based on Wyman, et al. (1992) and OPPA (1990). The Shell-biomass case includes the cost of sizing. The WM case does not include any drying. The MTCI cost is assumed to be proportionately lower because less drying is needed.
- (d) The Shell-coal cost is scaled from OPPA (1989), which estimated the cost for a "second generation" entrained-bed coal gasifier similar to the Shell gasifier. The IGT and BCL gasifier costs are scaled from Wyman, et al. (1992). Scaling is based on the ratio of the dry feed rates raised to the 0.7 power. Since no cost estimates are available for the Shell gasifier operating on biomass, the cost of this gasifier was assumed to be the same as the IGT gasifier: both gasifiers are pressurized, and the lower cost associated with the higher throughput of the entrained-bed gasifier was assumed to be offset by the higher cost associated with higher temperature operation. The WM costs are for 10 gasifiers that would operate in parallel (Coffman, 1991). The MTCI gasifier cost is scaled linearly from a baseline cost of \$1 million for a 4.5 tonnes/hour black liquor gasifier (Steedman, 1993).
- (e) Gas cooling costs are based on OPPA (1989) scaled to the 0.7 power.
- (f) Oxygen plant costs for the biomass cases are scaled from the estimate in Wyman, et al. (1992) according to the O₂ production rate raised to the 0.7 power. For the coal case, the estimate is based on OPPA (1989) scaled to the 0.7 power.
- (g) Based on OPPA (1989) using a 0.7 scale power factor.
- (h) Compressor cost is assumed to be \$700 per kW of compressor capacity required. In the MTCI case the reformer feed compressor refers to the feed compressor used prior to CO₂ removal (methanol production) or H₂ separation (hydrogen production).
- (i) Reformer cost is scaled according to feed rate raised to the 0.7 power, based on an estimate from Kessler (1991) of \$16.9 million for a feed rate of 5800 kmol/hour.
- (j) This includes shift reactors, heat exchangers, pumps, filters, etc. (Kessler, 1991) and is assumed to be the same for all biomass and natural gas cases, and is scaled according to throughput raised to the 0.7 power for the coal cases.
- (k) Using Union Carbide's SELEXOL[®] process, leaving approximately 2% CO₂ in the exit gas. Costs are scaled according to the volume of CO₂ removed raised to the 0.7 power. The baseline cost estimate is \$14.3 million for 810 kmol/hour of CO₂ removed (Epps, 1991). Includes the cost of compressing recycled CO₂ in the SMR-CO₂ case.
- (l) Using the ICI low-pressure methanol synthesis process. Baseline costs are \$50 million for a plant with a methanol production capacity of 1056 tonnes/day. A scale power factor of 0.66 is used (Mansfield, 1991). The cost estimates assume synthesis gas available at suction of makeup gas compressor at 1.5 MPa, the synthesis loop is operated at 10 MPa, single column distillation producing fuel grade methanol, equipment and erection in a developed location (e.g. U.S. Gulf Coast). Equipment included in the costs are the make-up compressor, recycle compressor, synthesis loop equipment, distillation column and shift tanks for intermediate storage.
- (m) Using the "Gemini-9" pressure swing adsorption system from Air Products, which removes CO₂ and H₂O in the first bed and produces a fuel gas and 99.999% purity H₂ in the second bed. Baseline costs are \$23 million for a feed rate of 9600 kmol/hour including the recycle feed (Solomon, 1991). Costs are scaled according to the feed rate using a scaling power factor of 0.7. The cost excludes the recycle compressor.
- (n) Assumed to be 25% of the sum of all other hardware costs (Wyman, et al., 1992).
- (o) Assumed to be 20% of installed hardware costs (Wyman, et al., 1992).
- (p) Assumed to be 10% of installed hardware costs (Wyman, et al., 1992).
- (q) From Wyman, et al. (1992). Assumed to be the same for both methanol and hydrogen production. The MTCI "catalyst and chemicals" costs were assumed to be the same as the Shell-biomass case since no reformer was required.
- (r) Assuming a feedstock cost of \$2/GJ for biomass and natural gas. Coal is assumed to cost \$1.50/GJ. (HHV basis).
- (s) Assuming electricity costs 5 cents/kWh and heat costs \$4/GJ. See Chapter 6 for the quantities of purchase energy required.
- (t) Fixed costs are based on Wyman, et al. (1992). Labor costs for the biomass cases are assumed to be the same as those estimated for a slightly larger methanol production facility (1983 dry tonnes biomass per day). The coal and natural gas costs are scaled using the feed rate raised to the 0.7 power. Maintenance cost is assumed to be 3% of the hardware subtotal, general overhead is assumed to be 65% of labor and maintenance, and direct overhead is assumed to be 45% of labor.
- (u) The annual capital charge rate for plant and equipment is assumed to be 15.1% per year, which is based on average financial parameters for major U.S. corporations over the period 1984-88 (9.91% real rate of return on equity, 6.2% real rate of return on debt, a 30% debt fraction, a 44% corporate income tax rate), a property and insurance rate of 1.5% per year, and a 25 year plant life. For land and working capital, the annual capital charge rate is taken to be 9.91% per year, the corporate discount rate.

7.3.2 Hydrogen Costs from Biomass

In all cases, hydrogen production costs are significantly lower than methanol production costs. This is due to both lower capital costs and higher efficiencies. Pressure swing adsorption costs about as much as a SELEXOL unit, but replaces both the SELEXOL unit and methanol synthesis, which is a large capital cost item (approximately the same cost as oxygen separation). As in the methanol cases, the indirectly heated gasifiers produce the least costly hydrogen at this scale. The costs are \$7.6/GJ for the BCL system, \$7.9/GJ for the MTCI system, and \$8.9/GJ for the WM system. Hydrogen produced using the entrained-bed gasifier would cost \$10.1/GJ, and \$11.3/GJ if produced using the IGT gasifier.

7.3.3 Methanol and Hydrogen Production Using Other Feedstocks

Figure 7-1 shows that both methanol and hydrogen can be produced at substantially lower costs from natural gas costing \$2/GJ. This is partly due to the fact that the scale considered for natural gas was roughly double that used for the biomass cases (in terms of output capacity). Nevertheless, the capital costs are so much lower for natural gas processes, that even if the scales were comparable, natural gas would still produce less costly fuels.⁸ The higher efficiencies of the natural gas processes also contribute to the lower levelized costs. For the scale considered here it is estimated that methanol from natural gas would cost \$6.0/GJ using either conventional steam reforming or CO₂ augmented reforming.⁹ Hydrogen would cost \$4.2/GJ.

⁸ Wyman, et al. (1992) estimated that methanol from a large biomass facility (5550 tonnes/day of methanol) using the BCL gasifier would have roughly the same levelized cost as methanol produced using steam reforming of natural gas in a facility with a 2500 tonnes/day capacity (see Table 7-4 and Figure 7-2).

⁹ Since the efficiency of producing methanol is higher for the SMR-CO₂ case, it would probably be favored at higher natural gas prices. Alternatively, if CO₂ contaminated natural gas were available, it would be possible to eliminate the CO₂ removal and recycling equipment, so that for a natural gas cost of \$2/GJ, methanol would

Table 7-4, along with similar cost functions for the estimates made here. For the same feedstock costs used above (\$2/GJ for biomass and natural gas, and \$1.50/GJ for coal), the levelized costs of producing methanol from biomass, coal and natural gas are plotted as a function of scale in Figure 7-2. Figure 7-3 shows a similar plot for hydrogen production. The costs of hydrogen from renewable resources other than biomass (wind and solar-photovoltaic) are also included, and have been calculated based on post-2000 commercial cost estimates (Ogden and DeLuchi, 1992; Ogden and Nitsch, 1992).

Figure 7-2, Figure 7-3, and Table 7-4 show that with the exception of the coal-methanol and natural gas-methanol cases, the estimates made here for coal and natural gas are in good agreement with other studies. With these two cases, the main difference is the higher efficiency estimates made in Chapter 6, which lowers levelized costs. This effect can also be seen with some of the other estimates made here. Nevertheless, all of the studies cited confirm that neither methanol nor hydrogen from biomass would be cost competitive with natural gas at today's prices, even if the scales were comparable. The other cost estimates for coal-based systems also support the finding that methanol and hydrogen produced from biomass and coal would have roughly the same costs, provided that the scale of the coal facility were considerably larger than the biomass facility and that the cost of coal was lower than the cost of biomass.

Hydrogen produced from the electrolysis of water using electricity generated from other renewable resources would be considerably more expensive than hydrogen produced thermochemically from biomass. One reason is that the cost of electricity from wind and solar energy is characterized by very moderate economies of scale due to the modular designs of these systems. Therefore, at large scales, hydrogen would be significantly less costly if produced from biomass.

7.4 Hydrogen and Methanol Use in the Transportation Sector

In light of the cost estimates made above, there are two basic questions that arise. The first question deals with the competition between the three feedstocks: Assuming that methanol and hydrogen will be used instead of gasoline in the transportation sector, will biomass ever be considered seriously as an alternative to natural gas or coal? Because biomass is not commonly used for energy today in the US, the ability to use it on a large scale would involve significant infrastructure changes and large capital investments, which will only be possible with the combined support of the existing energy and automotive industries, and the agricultural sector. The general public would also have to be educated about the benefits of biomass derived fuels so that they would be willing to accept a radically new technology (i.e. fuel cell vehicles) on a large scale. This suggests that there is a role for government policy, if the environmental and societal benefits of biomass energy are seen as important, but economic or other barriers are preventing it from entering the marketplace.¹¹

The second question, which is related to the first, is whether or not methanol and hydrogen produced from biomass will be able to compete with gasoline in the transportation sector. Although environmental quality and energy security both favor the use of domestically produced methanol and hydrogen in fuel cell vehicles over the use of gasoline in internal combustion engine vehicles, economics will again play a major role in determining the speed and degree of penetration biofuels will have in the market. As above, this implies that there may be a role for public policy, if it is deemed that biofuels offer important societal benefits.

¹¹ The case of ethanol in Brazil is a good example where the government helped develop an indigenous resource that could not compete economically with gasoline, in order to derive other benefits such as energy security, technological development and rural employment (Goldemberg, et al., 1992).

As for natural gas, Figure 7-4 and Figure 7-5 show that \$2/GJ biomass will be able to compete with natural gas costing approximately \$4.50-5.50/GJ, whereas the range of breakeven prices for \$3/GJ biomass is roughly \$5.5-6.5/GJ. These are probably not unrealistic prices for natural gas, given the anticipated increase in demand for natural gas in the coming decades. If we assume that the NES projections for natural gas prices are accurate, it is conceivable that biomass could begin replacing natural gas early in the next century, provided that plantations were capable of delivering a steady supply of biomass fuel by that time. The ability to use CO₂ contaminated natural gas (which presumably will not increase in price as rapidly as higher quality gas since demand for it will be lower) and the possibility of improved economics with large facilities using advanced partial oxidation schemes will tend to delay the use of biomass. As well, the direct partial oxidation of methane to methanol may significantly reduce the cost of methanol if this technology can be commercialized (see Chapter 4). Nevertheless, biomass would almost certainly become economically competitive with natural gas early in the next century, again, provided that the technology was ready at that time. For example, even methanol produced in a very large scale facility using advanced partial oxidation technology (10,000 tonnes methanol/day capacity) would become more costly than methanol derived from biomass when biomass costs \$3/GJ and natural gas approximately \$6.40/GJ, the well-head price predicted in the NES by the year 2020.

Another factor to consider is that natural gas is fairly limited when compared to the abundance of coal, and the fact that biomass can be used indefinitely. Thus, natural gas has an important role to play as a transition fuel. The precise timetable is a secondary concern.

Table 7-5 shows a more precise comparison, including the *breakeven* natural gas and coal prices for some of the cost functions reported in Table 7-4. According to

Table 7-5: Comparison of cost estimates for methanol and hydrogen production showing the fossil fuels prices and time frame required for biomass to be cost competitive.

Biomass cost function ^a	Fossil fuel cost function ^a	Breakeven fossil fuel price (\$/GJ) ^b			
		\$2/GJ biomass	Year	\$3/GJ biomass	Year
METHANOL					
6.73 + 1.54·P _b	<u>Natural Gas</u>				
	3.15 + 1.42·P _{ng}	4.69	1998	5.77	2007
	2.47 + 1.39·P _{ng} ^c	5.28	2002	6.39	2010
	<u>Coal</u>				
	7.62 + 1.54·P _c	1.42	d	2.42	2030
HYDROGEN					
5.07 + 1.28·P _b	<u>Natural Gas</u>				
	1.98 + 1.11·P _{ng}	5.09	2000	6.24	2009
	<u>Coal</u>				
	6.65 + 1.28·P _c	0.76	e	1.76	2010

- (a) These are selected cost functions from Table 7-4. Unless otherwise noted, they are the estimates made in this study (the BCL gasifier is used for biomass). P_x is the price of the feedstock in \$/GJ. b = biomass, c = coal, and ng = natural gas.
- (b) The *breakeven* price is that delivered price of the fossil fuel such that the cost of producing methanol or hydrogen from fossil fuels equals the cost of producing methanol or hydrogen from biomass. *Year* is the year in which the U.S. Department of Energy *National Energy Strategy* estimates that the fossil fuel will reach the breakeven price.
- (c) This is the cost estimate from OPPA (1989) for a 10,000 tonnes/day methanol facility using advanced partial oxidation instead of steam-methane reforming.
- (d) This is roughly the price for steam coal in the US today.
- (e) This is actually below the mine-mouth coal price in the US today.

(DeLuchi, 1992; Ogden and DeLuchi, 1992; Ogden and Nitsch, 1992). Table 7-6 shows the basic vehicle characteristics and costs used in these studies.¹² FCEVs will be characterized by higher purchase prices than ICEVs, which will be offset by a longer expected lifetime range, significantly higher fuel economies, and lower annual maintenance costs. The assumptions of a longer life and lower maintenance costs are based on experience with existing electric vehicles, which are mechanically simpler than

¹² The values used here are based largely on DeLuchi (1992) with some minor modifications by DeLuchi, as documented in Williams (1993).

(\$9.5/GJ), the expected retail price (without taxes) of reformulated gasoline in the United States when crude oil costs \$25/barrel (Johansson, et al., 1992a). The *breakeven gasoline price* is the gasoline price (without taxes) at which the lifecycle cost of the baseline gasoline powered ICEV is equal to the lifecycle cost of the alternative vehicle. Fuel taxes are assumed to be the same for all cases on a per kilometer basis.

If FCEVs perform as indicated in Table 7-6, Table 7-7 shows that on a lifecycle cost basis, FCEVs fueled with methanol and hydrogen derived from biomass will be less expensive to own than gasoline powered ICEVs even if biomass costs \$3/GJ. For methanol FCEVs, the breakeven prices of gasoline are \$0.09 and \$0.12 per liter for biomass costing \$2/GJ and \$3/GJ respectively. For hydrogen FCEVs, the corresponding breakeven gasoline prices are \$0.16/liter and \$0.17/liter. Applying Equation (7-1) to these gasoline prices gives crude oil prices of -\$9/barrel and -\$5/barrel for methanol FCEVs, and \$1/barrel and \$2/barrel for hydrogen FCEVs. Of course, negative crude oil prices are not indicative of real prices, but of the methodology of calculating crude oil prices from gasoline prices. Nevertheless, these calculations do indicate that biomass/FCEVs would be cost competitive at any reasonable crude oil price. Of course, the key uncertainty is whether FCEVs will perform as indicated in Table 7-6. However, as can be seen by the very low breakeven prices for biomass/FCEVs, there is some room for poorer performance than is indicated here. It should also be noted that a second independent evaluation of the costs of FCEVs relative to ICEVs conducted for the Ford Motor Company (Kuhn, 1992) concluded that the cost of FCEVs would only be up to \$1000 more than a comparable ICEV (for a FCEV production rate of 100,000 vehicles per year), which is significantly less than the incremental costs assumed here (\$5000-7000). Another important result is that battery powered electric vehicles will probably be significantly more expensive than either FCEVs or ICEVs, largely due to the high cost of batteries needed to provide an adequate range. Therefore, a significant improvement

expensive than ICEVs, and FCEVs fueled with PV-hydrogen would cost about 5% more than ICEVs on a lifecycle basis.

7.5 A Scenario for Using Biomass Derived Fuels

This section briefly outlines a possible scenario for introducing biofuels into the US transportation sector. For the sake of this discussion, the NES energy price projection are used for natural gas and coal, while the crude oil price is assumed to remain near current levels. The following assumptions are also required:

- A commitment to developing and using fuel cell vehicles.
- The FCEV performance as outlined above is technically feasible.
- A biomass price of \$2-3/GJ in the US early in the next century.

Between now and the first decade of the 21st century, fuel cells and fuel cell vehicles would be demonstrated commercially and the major automobile manufacturers would prepare to produce them on a larger scale, first for centrally fueled test fleets (e.g. government fleets), and then for the general public. At the same time, the use of methanol in ICEVs would increase, and the use of compressed natural gas (CNG) in ICEVs would familiarize consumers with the use of gaseous transportation fuels and facilitate the shift to hydrogen. The increased use of methanol and CNG would help develop the infrastructure for delivering large quantities of methanol and hydrogen. During this period, plantations would also be established on excess cropland and advanced biomass gasification technologies would be demonstrated at large scales.

When FCEVs first enter the commercial market around the turn of the century, natural gas would still be the preferred feedstock. However, by approximately 2010, biomass and coal could start to become economically attractive alternatives. The use of

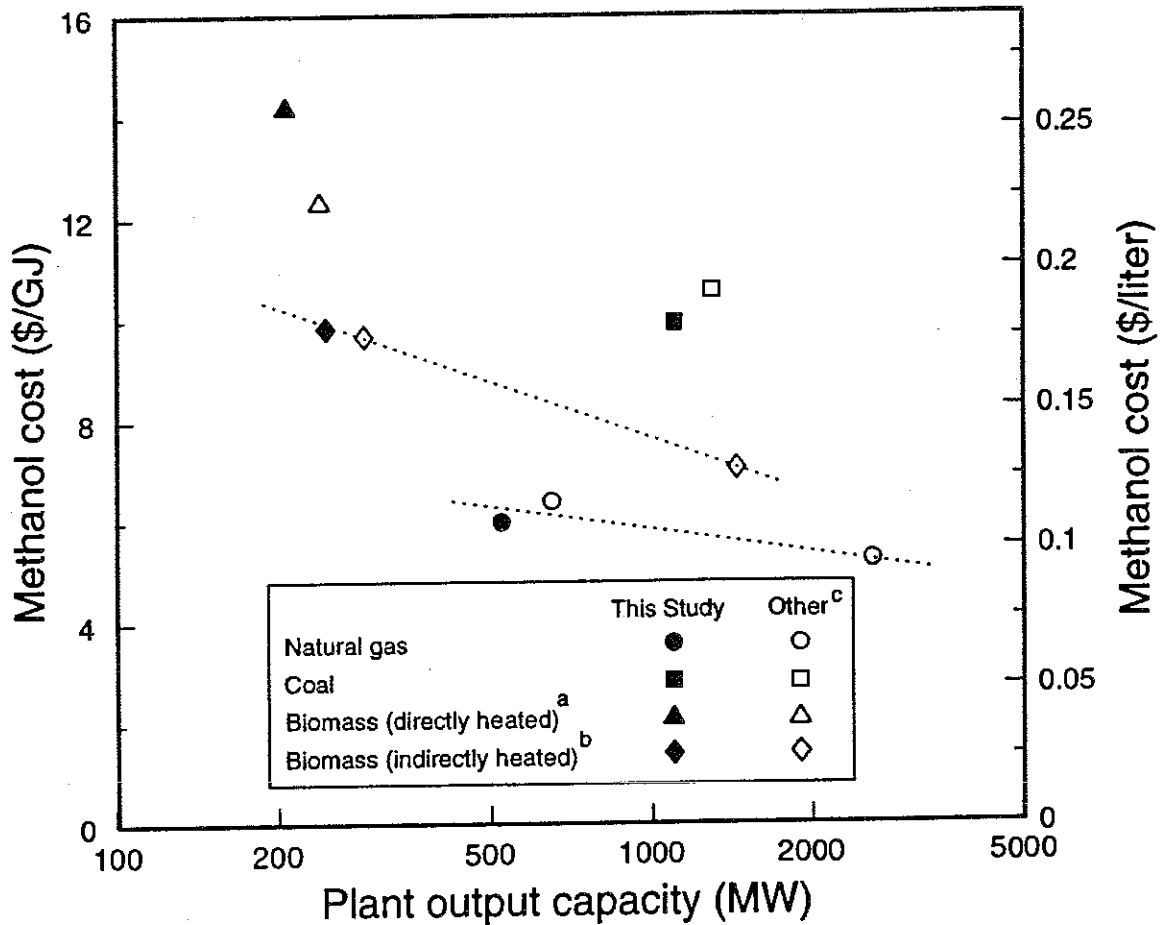
private sector to take a leading role in developing these technologies, especially when the *business as usual* approach is profitable. If the world were to rely purely on market forces to commercialize the fuel cell vehicle and simultaneously to develop a biomass energy industry, it would either not happen at all or proceed much too slowly to capture the all potential benefits. However, with appropriate policies and incentives, a transition could be made to biomass energy and fuel cell vehicles, in which the competitive marketplace could be used to stimulate innovation and product development by the private sector. Specifically, governments should consider taking the following actions:

- Promote commercial demonstrations of advanced biomass gasification technologies.
- Promote the establishment of biomass energy plantations on excess agricultural land and degraded land.
- Promote commercial demonstrations of fuel cell vehicles and research and development into several fuel cell and fuel storage technologies. Governments could help build markets for FCEVs and related technologies by requiring the use of FCEVs in government fleets.
- Promote the use of alternative fuels in ICEVs in the near term, which would help build the necessary infrastructure to support a FCEV based transportation sector. Specifically, encouraging the use of methanol and compressed natural gas (CNG) in ICEVs would be very helpful in establishing the needed infrastructure for distributing fuels for FCEVs as well as increasing the production capacity of alternative fuels. Using CNG in automobiles would facilitate the switch to hydrogen.

biomass is crucial. When oxygen blown biomass gasifiers are used, methanol and hydrogen costs are significantly higher than the production costs using coal.

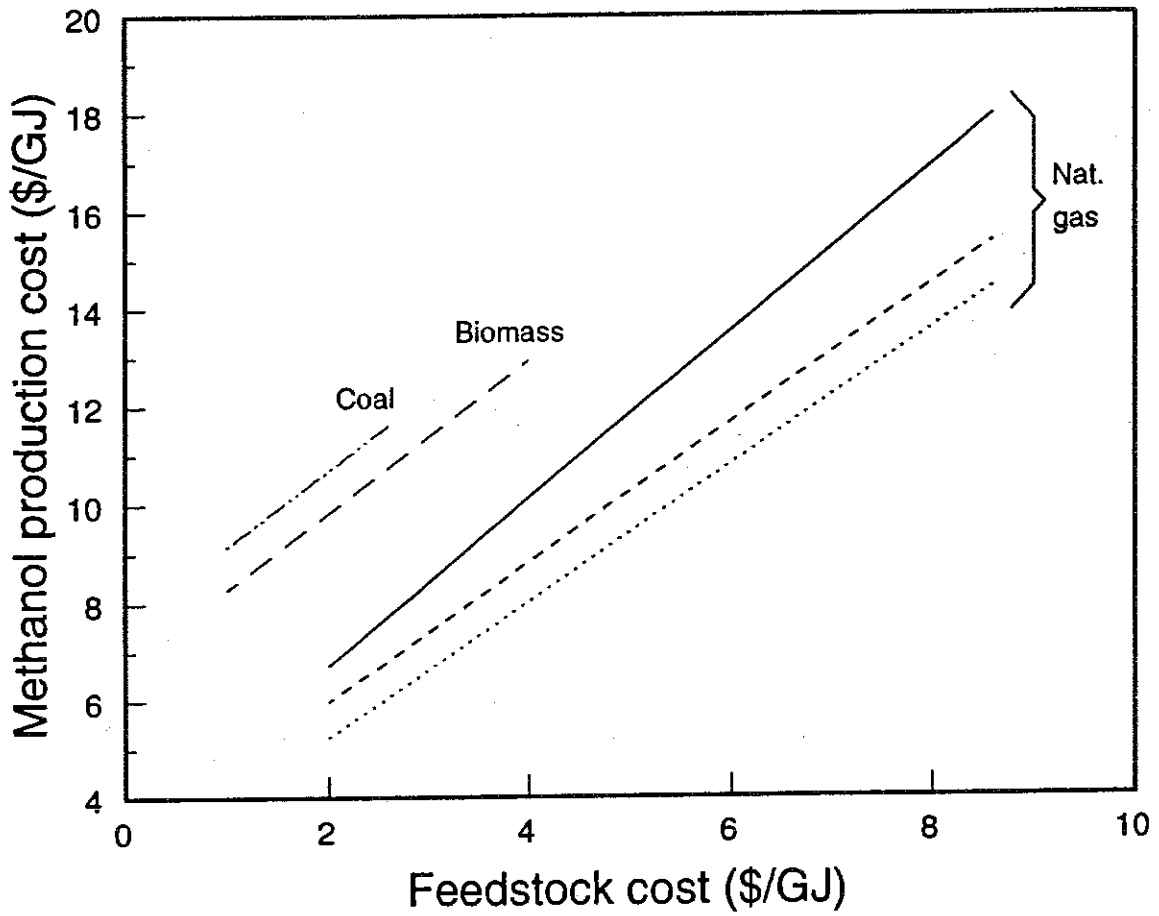
Natural gas will play an important role as a transition fuel, because methanol and hydrogen production from natural gas are commercial processes and because in the near term, these processes will produce the least costly fuels. Biomass and coal could gradually replace natural gas during the first quarter of the next century.

One important element in this analysis is that there would be relatively long lead times associated with the establishment of plantations and the commercialization of large scale biomass gasification technologies. Therefore, if the timetable outlined above is to be met, a commitment to bioenergy needs to be made in the very near future. Given the embryonic state of fuel cell vehicles and commercial biofuels technology in the US, the government would need to take an active role in supporting the transition to biomass powered fuel cell vehicles.



- (a) Based on the IGT gasifier.
- (b) Based on the BCL gasifier.
- (c) All estimates are from Wyman, et al. (1992) except for the large natural gas-methanol plant, which is the estimate from OPPA (1989).

Figure 7-2: Comparison of different cost estimates for methanol production from natural gas, coal and biomass. Biomass and natural gas costs are \$2/GJ and coal costs \$1.50/GJ. The same capital charge rate has been applied in all cases.



Natural gas - Wyman et al. (1992)	Natural gas - this study	Natural Gas - OPPA (1989) ^b
Biomass - this study ^a	Coal - this study	

(a) Using the BCL gasifier

(b) For a very large facility using advanced partial oxidation instead of steam reforming (10,000 tonnes/day of methanol).

Figure 7-4: Effect of feedstock price on the total cost of production for methanol from biomass, coal, and natural gas.

References

- Blok, K., Hendriks, C.A., Turkenburg, W.C., and Williams, R.H. *Producing Fuel and Electricity from Coal with Low Carbon Dioxide Emissions*. Draft manuscript, University of Utrecht, June 1991.
- Carpentieri, A.E., Larson, E.D., and Woods, J. *Prospects for Sustainable Utility-Scale Biomass-Based Electricity Supply in Northeast Brazil*. PU/CEES Report No. 270, Center for Energy and Environmental Studies, Princeton University, Princeton, New Jersey, 1992.
- CEC (Commission of the European Communities). *Energy in Europe: A View to the Future*. Brussels: Directorate General for Energy (DG XVII), September 1992.
- Coffman, J. Wright-Malta Corp. Ballston Spa, NY. Personal communication, June 1991.
- Council of Economic Advisors. *Economic Indicators*. Prepared for the Joint Economic Committee. Washington DC: US Government Printing Office, June 1992.
- DeLuchi, Mark A. *Hydrogen Fuel-Cell Vehicles*. Research Report ECD-ITS-RR-92-14 (Draft), Institute of Transportation Studies, University of California, Davis, September 1, 1992.
- DOE (Department of Energy). *National Energy Strategy, Technical Annex 2: Integrated Analysis Supporting the National Energy Strategy: Methodology, Assumptions and Results*. (DOE/S-0086P) Washington DC: US Department of Energy, 1991.
- Epps, R. (Technical Service Engineer). Union Carbide Chemicals and Plastics, Specialty Chemical Division. Houston, TX. Personal communication. June and December 1991.
- Goldemberg, José, Monaco, Lourival C., and Macedo, Isaias C. "The Brazilian Fuel-Alcohol Program." *Renewable Energy: Sources for Fuels and Electricity*. Ed. T.B. Johansson, H. Kelly, A.K.N. Reddy, and R.H. Williams. Washington DC: Island Press, 1992.
- Hall, David O., Rosillo-Calle, Frank, Williams, Robert H., and Woods, Jeremy. "Biomass for Energy: Supply Prospects." *Renewable Energy: Sources for Fuels and Electricity*. Ed. T.B. Johansson, H. Kelly, A.K.N. Reddy, and R.H. Williams. Washington DC: Island Press, 1992.
- Johansson, Thomas B., Kelly, Henry, Reddy, Amulya K.N., and Williams, Robert H. "A Renewables-Intensive Global Energy Scenario (Appendix to Chapter 1)." *Renewable Energy: Sources for Fuels and Electricity*. Ed. T.B. Johansson, H. Kelly, A.K.N. Reddy, and R.H. Williams. Washington DC: Island Press, 1992a.

Ryan E. Katofsky

Steinberg, M. and Cheng, H.C. *Assessment of Hydrogen Production by Conventional and Advanced Processes*. Prepared at Brookhaven National Laboratory. Washington DC: US Department of Energy, 1988.

White House Fact Sheet. Fact sheet on the proposed energy tax. February 22, 1993.

Williams, Robert H. "A Strategic Approach for Coping with Unsafe Nuclear Plants in the Former Soviet Union and Eastern Europe." *Perspectives in Energy*. Vol. 2, 1992, pp. 13-18.

Williams, Robert H. (Senior Research Scientist). Center for Energy and Environmental Studies, Princeton University. Princeton, NJ. Personal communication. April 1993.

Wyman, Charles E., Bain, Richard L., Hinman, Norman D., and Stevens, Don J. "Ethanol and Methanol from Cellulosic Biomass." *Renewable Energy: Sources for Fuels and Electricity*. Ed. T.B. Johansson, H. Kelly, A.K.N. Reddy, and R.H. Williams. Washington DC: Island Press, 1992.

vehicles would emit water and only minute quantities of carbon monoxide, NO_x, and unburned hydrocarbons when compared to gasoline ICEVs or even alcohol ICEVs.

There are synergistic effects from coupling biomass energy and fuel cell vehicles. Methanol and hydrogen are relatively easy to produce from biomass, and are the leading candidate fuels for FCEVs. However, land and water constraints will limit the amount of biomass that can be grown sustainably in the US for energy purposes. Nevertheless, since FCEVs would be 2.4-2.8 times as efficient as gasoline ICEVs with comparable range and performance characteristics, FCEVs would make much better use of biomass energy, allowing it to become a significant resource. For example, by using FCEVs instead of ICEVs it would be possible to grow more than enough biomass to meet the energy needs of the entire US light duty vehicle, just by using excess cropland to establish energy plantations. Therefore, large scale biomass use in the US could reduce oil imports by several million barrels per day without contributing to deforestation. In fact, biomass plantations could actually restore degraded and deforested lands and help create a new domestic energy industry, which would generate new economic and employment opportunities.

The high efficiency of FCEVs would also make methanol and hydrogen derived from biomass cost competitive with gasoline (on a lifecycle cost basis) even if the initial cost of a FCEV is nearly 40% higher than that of an ICEV and the delivered costs of methanol or hydrogen produced from biomass are significantly higher than gasoline prices. Previously, transportation fuels from biomass were always considered to be uneconomical because it was assumed that they could be used only in ICEVs.

Because of the tremendous potential and multiple benefits of combining biomass derived fuels with fuel cell vehicles, this thesis has carefully evaluated the technology and

at much milder conditions than entrained-bed gasifiers. By comparing optimal coal gasifiers to what can be considered optimal biomass gasifiers, this thesis has shown that biomass systems can be competitive with coal systems, even though coal would be less expensive than biomass and coal conversion facilities would be much larger than biomass facilities.

8.2 Summary of Specific Results

The specific thermodynamic and economic results of this thesis are summarized in Table 8-1. The major conclusions of my research are:

1. Natural gas processes are by far the most efficient, because there is no need for an energy intensive gasification step. Exergy analysis shows that gasification is the single largest source of thermodynamic losses, and that these losses are greater than the losses associated with steam reforming of natural gas. The relatively larger external energy requirements (electricity and heat that cannot be supplied using process waste heat) for gasification systems also contribute to lower efficiencies than for natural gas processes.
2. For a given feedstock, hydrogen production is characterized by higher thermal efficiencies and lower production costs than methanol production. More external energy would be required for hydrogen production.
3. Depending on the gasification technology, biomass-based systems can be more or less efficient than coal-based systems. The BCL indirectly heated gasifier is the most efficient gasification process studied in this thesis, for both methanol and hydrogen production.

\$0.17/liter for an ICEV to be cost competitive with a methanol and hydrogen FCEV respectively. However, the lowest possible cost of reformulated gasoline, assuming that crude oil is free, would be \$0.156/liter.¹ \$0.17/liter for reformulated gasoline corresponds to a crude oil price of \$2/barrel, which is well below the current price of approximately \$21/barrel. If biomass cost \$2/GJ, gasoline would have to cost as little as \$0.09/liter for the ICEV to compete with the methanol FCEV, and \$0.12/liter to compete with the hydrogen FCEV. Therefore, FCEVs can be cost competitive with ICEVs even if the delivered costs of the fuels are much higher than the delivered cost of gasoline. For a biomass cost of \$3/GJ the delivered costs of methanol and hydrogen would be \$14.2/GJ and \$14.6/GJ respectively, whereas \$0.12/liter for gasoline corresponds to a delivered price of \$3.4/GJ.

8. Biomass is by far the least expensive renewable energy source for transportation fuels produced on a large scale.
9. In spite of its high equivalent fuel economy, on a lifecycle cost basis the battery powered electric vehicle would be much less economical than either the fuel cell vehicle or the gasoline powered internal combustion engine vehicle, because of its very high purchase price (about \$10,000 more than a comparable ICEV).
10. There is a strong role for government policy in "jump starting" a modern biofuels industry, because the initial infrastructure costs are not easily borne by the private

¹ Recall that the formula used to calculate the cost of gasoline from crude oil as taken from Johansson, et al. (1992a) is: $P_{\text{gasoline}} = 0.00699 \times P_{\text{crude}} + 0.156$, where P_{crude} is in \$/barrel and P_{gasoline} is in \$/liter. Gasoline is assumed to have a higher heating value of 34.8 MJ/liter. This includes the cost of the feedstock, refining, distribution and storage, and the markup at the gas station. Taxes are excluded. Thus, even if crude oil were free, gasoline would cost at least \$0.156/liter.

Table 8-1: Summary of thermodynamic and economic results.

	Feedstock Throughput (MW)	Thermal Efficiency (%)		Feedstock Price (\$/GJ)	Production Cost (\$/GJ)	
		Methanol	Hydrogen		Methanol	Hydrogen
Natural gas						
Conventional	750	67.5	84.8	2	6.0	4.2
				8	14.5	10.9
with CO ₂ addition	750	72.1	---	2	6.0	---
				8	14.0	
Shell-coal	1720	61.8	63.0	1.5	9.9	8.6
				2.5	11.5	9.9
Shell-biomass	368	62.0	65.7	2	13.0	10.1
				3	14.5	11.4
IGT-biomass	368	54.5	57.2	2	14.2	11.3
				3	15.9	12.8
WM-biomass	399	58.6	63.4	2	11.3	8.9
				3	12.9	10.1
MTCI-biomass	370	57.8	61.7	2	9.9	7.9
				3	11.5	9.2
BCL-biomass	384	62.8	68.6	2	9.8	7.6
				3	11.4	8.9

Lifecycle Costs of Different Vehicle/Feedstock/Fuel Combinations^a

Vehicle type	BPEV	FCEV	FCEV	FCEV	FCEV	ICEV
Energy source	US avg mix	\$2/GJ (\$3/GJ) biomass	\$2/GJ (\$3/GJ) biomass	Wind	PV	Petroleum
Energy carrier	Elec.	MeOH	H ₂	H ₂	H ₂	Gasoline
Lifecycle Cost (cents/km)	21.50	18.33 (18.54)	18.91 (19.06)	20.77	21.63	20.49
Delivered price of energy carrier (\$/GJ)	22.0	12.6 (14.2)	13.3 (14.6)	31.3	37.4	9.5
(\$/gallon gas. equiv.)	2.90	1.66	1.75	4.12	4.93	1.25
Breakeven gasoline price (\$/liter)	0.44	0.09 (0.12)	0.16 (0.17)	0.36	0.46	0.33
(\$/gallon)	1.67	0.34 (0.45)	0.60 (0.64)	1.36	1.72	1.25
Crude oil price (\$/bbl)	41	-9 (-5)	1 (2)	29	44	25

(a) BPEV = battery powered electric vehicle, FCEV = fuel cell electric vehicle, ICEV = internal combustion engine vehicle.

References

Johansson, Thomas B., Kelly, Henry, Reddy, Amulya K.N., and Williams, Robert H. "A Renewables-Intensive Global Energy Scenario (Appendix to Chapter 1)." *Renewable Energy: Sources for Fuels and Electricity*. Ed. T.B. Johansson, H. Kelly, A.K.N. Reddy, and R.H. Williams. Washington DC: Island Press, 1992a.